National Library of Canada
Canadian Theses Service
Ottawa, Canada
K1A 0N4

Bibliothèque nationale du Canada
Service des thèses canadiennes

## NOTICE

The quality of this microform is heavily dependent upon the quality of the original thesis submitted for microfilming. Every effort has been made to ensure the highest quality of reproduction possible.

If pages are missing, contact the university which granted the degree.

Some pages may have indistinct print especially if the original pages were typed with a poor typewriter ribbon or if the university sent us an inferior photocopy.

Reproduction in full or in part of this microform is governed by the Canadian Copyright Act, R.S.C. 1970, c. C-30, and subsequent amendments.

## AVIS

La qualité de cette microforme dépend grandement de la qualité de la thèse soumise au microfilmage. Nous avons tout fait pour assurer une qualité supérieure de reproduction.

S'il manque des pages, veuillez communiquer avec l'université qui a conféré le grade.

La qualité d'impression de certaines pages peut laisser à désirer, surtout si les pages originales ont été dactylographiées à l'aide d'un ruban usé ou si l'université nous a fait parvenir une photocopie de qualité inférieure.

La reproduction, même partielle, de cette microforme est soumise à la Loi canadienne sur le droit d'auteur, SRC 1970, c. C-30, et ses amendements subséquents.

NL-339 (r. 88/04) c

Canada

National Library of Canada
Bibliothèque nationale du Canada

Canadian Theses Service
Service des thèses canadiennes

Ottawa Canada
K1A 0N4

The author has granted an irrevocable non-exclusive licence allowing the National Library of Canada to reproduce, loan, distribute or sell copies of his/her thesis by any means and in any form or format, making this thesis available to interested persons.

L'auteur a accordé une licence irrévocable et non exclusive permettant à la Bibliothèque nationale du Canada de reproduire, prêter, distribuer ou vendre des copies de sa thèse de quelque manière et sous quelque forme que ce soit pour mettre des exemplaires de cette thèse à la disposition des personnes intéressées.

The author retains ownership of the copyright in his/her thesis. Neither the thesis nor substantial extracts from it may be printed or otherwise reproduced without his/her permission.

L'auteur conserve la propriété du droit d'auteur qui protège sa thèse. Ni la thèse ni des extraits substantiels de celle-ci ne doivent être imprimés ou autrement reproduits sans son autorisation.

ISBN 0-315-55542-4

Canada

THE UNIVERSITY OF ALBERTA

# WEAK HADRONIC DECAYS OF HEAVY FLAVOR MESONS

BY

NITA SINHA (C)

A THESIS

SUBMITTED TO THE FACULTY OF GRADUATE STUDIES AND RESEARCH

IN PARTIAL FULFILMENT OF THE REQUIREMENTS FOR THE DEGREE

OF DOCTOR OF PHILOSOPHY

IN

THEORETICAL PHYSICS

DEPARTMENT OF PHYSICS

EDMONTON, ALBERTA

FALL, 1989

THE UNIVERSITY OF ALBERTA

RELEASE FORM

NAME OF AUTHOR: NITA SINHA

TITLE OF THESIS: WEAK HADRONIC DECAYS OF HEAVY FLAVOR MESONS

DEGREE: DOCTOR OF PHILOSOPHY

YEAR THIS DEGREE WAS GRANTED: FALL 1989

Permission is hereby granted to THE UNIVERSITY OF ALBERTA LIBRARY to reproduce single copies of this thesis and to lend or sell such copies for private, scholarly or scientific research purposes only.

The author reserves other publication rights, and neither the thesis nor extensive extracts from it may be printed or otherwise reproduced without the author's written permission.

Nita Sinha

.....

(Student's Signature)

Permanent address:

8/17 Old Rajinder Nagar
New Delhi-110060
INDIA

Date: 28th August 1989.

THE UNIVERSITY OF ALBERTA

FACULTY OF GRADUATE STUDIES AND RESEARCH

The undersigned certify that they have read, and recommend to the Faculty of Graduate Studies and Research for acceptance, a thesis entitled WEAK HADRONIC DEACYS OF HEAVY FLAVORED MESONS submitted by NITA SINHA in partial fulfilment of the requirements for the degree of DOCTOR OF PHILOSOPHY in THEORETICAL PHYSICS

Supervisor

Date: Aug 24, 1989

This work is dedicated to the author's parents

for their constant encouragement,

sacrifice and support.

## ABSTRACT

We have performed a coupled multichannel calculation for various two-body hadronic decays of charmed mesons. Particular attention is paid to the role of weak annihilation term in these decays. A two channel calculation of Cabibbo-angle favored $D_s^+ \to VP$ results in a satisfactory fit to $D_s^+ \to \phi\pi^+$, $\rho^0\pi^+$ and $K^+\bar{K}^{*0}$ data from ARGUS and E-691. An extension of this to include the $\omega\pi^+$ mode, whose un-unitarized amplitude is zero, also satisfies the recent experimental limit. For Cabibbo angle-favored $D \to VP$ decays, we perform a three channel calculation, coupling the $K^*\pi$, $K\rho$ and $\bar{K}^0\phi$ states in isospin 1/2. In isospin 3/2 only the two channels $K^*\pi$ and $K\rho$ are coupled. It is possible to generate enough $B(D^0 \to \bar{K}^0\phi)$ without a weak annihilation term, though a finite annihilation term, about (15-20)% of the spectator term in $D^0 \to K^-\rho^+$, is not ruled out by data. For the Cabibbo-angle favored $D/D_s \to VV$ decay modes, a similar treatment is followed. Cabibbo-angle suppressed modes are also studied in a coupled channel formalism. The $D^+ \to \rho^0\pi^+$ branching ratio can be fitted in this approach, whereas its un-unitarized amplitude yields a very small value. Some of the other models proposed to study heavy flavor decays are also discussed. We attempt to incorporate the effect of final state interactions, through introduction of phases in the amplitudes given by the QCD sum rule approach.

The possibility of large $D_s^+ \to \eta\pi^+$, $\eta'\pi^+$ branching ratios

is investigated in a theoretical framework. A factorization model with orthogonal mixing scheme fails to satisfy the Mark II results. These values can be accommodated in a nonet symmetry breaking model, where the coupling to the singlet is large. Finally, the effect of final state scattering phases on two-body B decays are studied, in view of a possible measurement of the mixing angle $V_{ub}$ from the noncharmed, nonstrange hadronic decays of the bottom mesons.

**ACKNOWLEDGEMENTS**

I am extremely grateful to my supervisor, Prof. Kamal, for his continuous guidance and encouragement throughout the period during which this work was performed.

I would also like to thank the rest of my committee, Prof. Khanna, Prof. Weichmann and Prof. Ludwig, for the help and comments they provided during the course of this work. I would like to express sincere thanks to Prof. Kernahan, for his help and interest in my graduate studies. I extend my appreciation to the office staff, for providing all those little things that made life in the Physics Department, enjoyable and comfortable.

Lastly, I would like to thank my husband, without whose love and support, this work could not have been accomplished.

## TABLE OF CONTENTS


| CHAPTER | | PAGE |
|---|---|---|
| I. | Introduction | 1 |
| II. | Review of basic ideas in Heavy Quark Physics | 6 |
| | 1. The Standard Model | 6 |
| | 2. Weak Current and Hamiltonian | 9 |
| | 3. Strong Interaction Effects | 11 |
| | 4. Valence Quark Approximation | 16 |
| III. | Final State Interactions | 30 |
| | 1. Analytic Properties of the Scattering Matrix | 31 |
| | 2. Muskhelishivili Omnes Equation for Multichannel Case | 34 |
| | 3. A K-matrix Model | 37 |
| IV. | A Coupled Channel Treatment of Charmed Meson Hadronic Decays | 41 |
| | 1. K-matrix Parametrization | 43 |
| | 2. Calculation of Un-unitarized Amplitudes | 46 |
| | 3. Cabibbo-angle favored $D_s^+ \to VP$ decays | 55 |
| | 4. Cabibbo-angle favored $D \to VP$ decays | 70 |
| | 5. Cabibbo-angle favored $D, D_s^+ \to VV$ decays | 78 |
| | 6. Cabibbo-suppressed $D \to VP$ decays | 88 |
| V. | Other Approaches to study Heavy Flavor Decays | 102 |
| | 1. $1/N_c$ Approach | 102 |
| | 2. QCD Sum Rules | 108 |
| VI. | The Decay Modes $D_s^+ \to \eta\pi^+$ and $D_s^+ \to \eta'\pi^+$ | 128 |
| | 1. $\eta$-$\eta'$ mixing | 128 |

2. Factorization Approach.....130

3. A Nonet Symmetry Beaking Model.....137

VII. Final State Interactions in Two-Body B Decays.....149

1. Phases from Isospin relations.....150

2. Theoretical Amplitudes and the Resulting Phases.....153

VIII. Summary and Conclusions.....165

References.....169

Appendix A.....176

Appendix B.....178

## LIST OF FIGURES


FIGURE PAGE

1. Decay mechanisms in Valence Quark Approximation.....17
2. Interference in $D^+$ decays.....21
3. $D^{-1}(s)$ in presence of a resonance.....39
4. Fits to ARGUS data for Cabibbo-angle favored $D_s^+ \to VP$ decays.....59
5. Fits to E-691 data for Cabibbo-angle favored $D_s^+ \to VP$ decays.....63
6. Fits to Cabibbo-suppressed $D \to VP$ decays.....100
7. 1/N Rules.....104
8. Two-body decays in 1/N approach.....105
9. Diagrammatic relations which follow from Fierz identity.....106
10. Four point correlator.....110
11. Skeleton Diagrams in QCD sum rules.....111

12(a). $R_{00}(K^*\pi)$ and $R_{0+}(K^*\pi)$ plots.....116

12(b). $R_{00}(K\rho)$ and $R_{0+}(K\rho)$ plots.....118

12(c). $R_{00}(K\pi)$ and $R_{0+}(K\pi)$ plots.....120

12(d). $R_{00}(\pi\pi)$ and $R_{0+}(\pi\pi)$ plots.....122

12(e). $R_{00}(KK)$ and $R_{0+}(KK)$ plots.....124

13(a). $B(D_s^+ \to \eta'\pi)$ vs. $B(D_s^+ \to \eta\pi)$ for solution set I.....146

13(b). $B(D_s^+ \to \eta'\pi)$ vs. $B(D_s^+ \to \eta\pi)$ for solution set II.....147

14(a). $R_{0-}(D\pi)$ vs. $r^{D\pi}$.....151

14(b) $R_{00}(D\rho)$ vs. $r^{D\rho}$.....152

14(c) $R_{0-}(D\rho)$ vs. $r^{D\rho}$.....152

## LIST OF TABLES


TABLE PAGE

1. Un-unitarized amplitudes for Cabibbo-angle favored $D, D_s \to VP$ decays.....52
2. NLL estimates for $a_1/a_2$ values.....54
3. Fits to ARGUS data for Cabibbo-angle favored $D_s^+ \to VP$ decays.....60
4. Fits to E-691 data for Cabibbo-angle favored $D_s^+ \to VP$ decays.....62
5. Range of R allowed by Cabibbo-angle favored $D_s^+ \to VP$ data.....65
6. Fits to ARGUS data for $D_s^+ \to VP$ decays for parameters maximizing $B(D_s^+ \to \omega\pi^+)$.....69
7. Fits to E-691 data for $D_s^+ \to VP$ decays for parameters maximizing $B(D_s^+ \to \omega\pi^+)$.....69
8. Fits to Mark III data for Cabibbo-angle favored $D \to VP$ decays.....75
9. Theoretical branching ratios for Cabibbo-angle favored $D \to VV$ decays, with resonant coupling in isospin 1/2, P-wave amplitude.....81
10. Theoretical branching ratios for Cabibbo-angle favored $D \to VV$ decays, with a phase in the D-wave amplitude.....83
11. Fits to Cabibbo-angle favored $D_s^+ \to VV$ decays.....88
12. Fits to data for Cabibbo-suppressed $D \to VP$ decays.....99
13. Range of R allowed in Cabibbo-suppressed $D \to VP$

decays.....101
14. Allowed range of phase for amplitudes in QCD sum rule approach.....125
15. Factorizable and non-factorizable parts of amplitudes in Sum-rule approach,.....126
16. Decay rates of $D_s^+ \to \eta\pi^+, \eta'\pi^+$ in KS and BSW models.....132
17. Branching ratios of $D_s^+ \to \eta\pi^+, \eta'\pi^+$ in KS and BSW models.....133
18. Effect of Final state interactions on $D_s^+ \to \eta\pi^+$, $\eta'\pi^+$ and $\bar{K}^0K^+$ modes.....137
19. Un-unitarized amplitudes of $D, D_s \to PP$ in a nonet symmetry breaking model.....141
20. Solutions in a nonet symmetry breaking model satisfying Mark III data.....144
21. Solutions in a nonet symmetry breaking model satisfying Mark II data.....145
22. NLL estimates of QCD coefficients at bottom mass scale.....154
23(a). Branching ratios for $B \to D\pi$ modes for various phase values.....159
23(b). Branching ratios for $B \to D\rho$ modes for various phase values.....160
23(c). Branching ratios for $B \to D^*\pi$ modes for various phase values.....161
24(a). $|V_{ub}|$ limits from $B \to \pi\pi$ modes.....162
24(b). $|V_{ub}|$ limits from $B \to \rho\pi$ modes.....163

# I. INTRODUCTION

The interactions of the fundamental constituents of matter, quarks and leptons, are believed to be given by the so called Standard model.[1] In this model the electromagnetic and weak interactions are unified into the electroweak gauge theory,[2] with the gauge bosons- photon and the $W^{\pm}$, Z vector bosons. The strong interactions are also described by a gauge theory known as Quantum Chromodynamics[3] (QCD), where the gauge bosons are the gluons. It is currently believed[1] that there exist six flavors of quarks- up, down, strange, charm, bottom and top and six leptons- electron, muon, tau and their neutrinos. These quarks and leptons belong to three generations. Members of the different generations have identical quantum numbers and differ only in their masses. Each generation consists of a doublet whose members differ in their charge.

Quarks as well as leptons, participate in electroweak interactions. Strong interactions on the other hand involve only the quarks, which carry an additional color quantum number. The quarks remain confined[3] to color singlet bound states called hadrons. There are two kinds of hadrons, the quark-antiquark ($q\bar{q}$) states called mesons and the three quark states (qqq) called baryons. The interactions of hadrons have proved very difficult to understand, as it is not possible to solve QCD at low energies. QCD is a non-

abelian gauge theory which has the feature of asymptotic freedom,[4] i.e., the effective coupling constant $\alpha_s$ is small at short distances (or large momentum). Hence, in the deep inelastic region, perturbative solutions can be obtained reliably. However, at low momentum, the coupling constant is large and a perturbative theory is not applicable. It is therefore hoped that hadrons carrying heavy quarks, will be better described.

The heavy quarks decay into the lighter ones, through weak interactions. A wealth of experimental data[5,6] on the decays of the heavy mesons (Charmed and Bottom) has emerged in the last decade. Since the decaying heavy quarks are within the bounds of a hadron, the effects of QCD play an important role. Hence, the heavy flavor systems are regarded as a laboratory for the study, not only of weak interactions, but also of strong interactions. Much theoretical attention[7,8] has therefore been devoted to understanding the weak decays of the heavy open flavor mesons. Open flavor mesons $Q\bar{q}$ with Q(q) denoting a heavy (light) flavor can perhaps shed some light on the dynamics of light mesons $q\bar{q}$, where our understanding is rather unsatisfactory.[8] The quarkonia states $Q\bar{Q}$ are understood quite well in the framework of potential models.[9]

Open flavor pseudoscalar mesons can decay only through weak interactions. In the charm sector there exist[10] three such mesons, the $(D^0(c\bar{u}), D^+(c\bar{d}))$ isodoublet and the $D_s^+(c\bar{s})$ isosinglet. There are[10] four pseudoscalar B mesons, the $(B_d^0,$

$B_u^-$) isodoublet and the $B_s^0$, $B_c^-$ isosinglets. Apart from providing valuable information on weak/strong interaction physics, weak decays of the D and B mesons will also provide an estimation of certain fundamental parameters unknown within the standard model. The weak eigenstates of the quarks are related to the strong eigenstates through the Kobayashi-Maskawa[11] (KM) mixing matrix. The elements of the KM matrix can therefore be extracted from the weak decays of the heavy flavor mesons. By establishing the structure of these decays, one may also hope for clues to the physics beyond the Standard model.

The short time-scale of the weak decays allows one to separate the possible corrections from strong interactions into short and long distance contributions. The short distance corrections can be calculated perturbatively[12,13] and modify the structure of the weak interaction Hamiltonian. The long distance effects are harder to estimate. Our theoretical understanding of the strange quark decays is unsatisfactory[8] essentially due to the lack of understanding of these long distance corrections. It is hoped that in charm and bottom decays, the mass of the decaying quark is large enough that long distance corrections become less important. However, experimental data[5,6] on the exclusive two body decays of charmed (and bottom) mesons, indicate that hadronization does play an important role.

Although the gross features of charm and bottom decays

can be reproduced from fairly simple quark level calculations,[14] the light quark and gluon content of the hadronic bound states have a greater influence than anticipated. A detailed understanding cannot be achieved just at the quark level, but has to be at the hadronic level, where the appropriate formfactors are included.[15-17] In addition, one needs to consider[18-22] the role of strong interactions of the final states produced in a weak decay, the importance of which has been established[6] experimentally. Also, there could be effects such as annihilation,[23] a reliable estimate of which is still unavailable.

In the next chapter, we start with a brief review of the standard model. The short-distance QCD corrected Hamiltonian[12,13] for the decays of charmed and bottom mesons is presented. We describe the so-called valence quark approximation,[24] for estimation of two-body nonleptonic decays, employing the assumption of factorization.[25] We point out the theoretical uncertainties in this simple picture.

In chapter III, we discuss the theory of final state interactions and propose a model to incorporate these effects.

Hadronic two-body decays of the charmed mesons are discussed in chapter IV. We parameterize the **K**-matrix[26] model for final state interactions, obtained in chapter III and apply it to the different decay modes of the D mesons. In particular, we study the Cabibbo-allowed D, $D_s$ decays to

a vector (V) and pseudoscalar (P) and also to two vector (VV) mesons. A similar treatment is also carried out for Cabibbo-suppressed D→VP decays. In all the decay modes we introduce weak annihilation contribution as a parameter.

In chapter V we describe some of the other theoretical models[27-29] proposed to study the weak decays of heavy mesons. We point out that none of these include a satisfactory treatment of final state interactions. To some of the amplitudes obtained from the the QCD sum rule approach,[29] we have attempted to introduce corrections due to final state interactions.

In chapter VI, we have examined the decay modes $D_s^+ \to \eta\pi^+$, $\eta'\pi^+$. Experimental[30-32] data on these modes are not yet conclusive; surprisingly large branching ratios have been observed by the Mark II[32] collaboration. We have explored the possibility of accommodating such large values in a theoretical framework.

Chapter VII considers the effects of final state interactions in B-decays. These are expected to be small, yet if the nonleptonic B-decays are used to extract the Kobayashi-Maskawa matrix element $V_{bu}$, it will be important to know the magnitude of such effects.

Finally, in chapter VIII, we present our conclusions.

## II. REVIEW OF BASIC IDEAS IN HEAVY QUARK DECAYS

The understanding of heavy open flavor mesons containing one charm or bottom quark, has progressed rapidly in recent years through steady improvements[33] in experimental techniques for production and detection of their decays. On the theoretical side, heavy quark systems are simpler to analyze than systems involving light quarks. It was believed[14] that non-perturbative effects would be unimportant in the decays of these charmed ($D^0, D^+, D_s^+$) and bottom ($B_u^+, B_d^0, B_s^0$) mesons. In the case of charm, experimental data[5,6] indicates, that the light antiquark and gluon content of the hadronic bound states have a greater impact than originally anticipated.

In this chapter, we start with a brief review of the gauge theory of electroweak interactions. We then add the corrections due to strong interaction effects and apply these quark level calculations to actual hadrons, assuming a simple model. Finally we point out the need for refining this simple theoretical picture.

### II.1 The Standard Model

The theoretical framework for weak decays of heavy quarks is provided by the standard $SU(3)\otimes SU(2)\otimes U(1)$ model[1] of strong and electroweak interactions. In the electroweak sector, the left-handed fermion fields form doublets of weak

isospin, whereas the right-handed components are kept as singlets. There are three generations of quark and lepton doublets:

$$\underset{\text{Leptons}}{\begin{pmatrix}\nu_e\\ e\end{pmatrix}}\ \begin{pmatrix}\nu_\mu\\ \mu\end{pmatrix}\ \begin{pmatrix}\nu_\tau\\ \tau\end{pmatrix}\ \underset{\text{Charge}}{\begin{pmatrix}0\\ -1\end{pmatrix}}\qquad \underset{\text{Quarks}}{\begin{pmatrix}u\\ d'\end{pmatrix}}\ \begin{pmatrix}c\\ s'\end{pmatrix}\ \begin{pmatrix}t\\ b'\end{pmatrix}\ \underset{\text{Charge}}{\begin{pmatrix}2/3\\ -1/3\end{pmatrix}} \qquad \text{(II.1)}$$

The charge -1/3 weak interaction eigenstates d',s',b' are mixtures of the strong interaction (or mass) eigenstates d,s,b. Hence, decays caused by transitions between the generations of quarks can occur. The weak eigenstates are related to the mass eigenstates by the unitary Kobayashi-Maskawa[11] (KM) matrix,

$$\begin{pmatrix}d'\\ s'\\ b'\end{pmatrix} = \begin{pmatrix}V_{ud} & V_{us} & V_{ub}\\ V_{cd} & V_{cs} & V_{cb}\\ V_{td} & V_{ts} & V_{tb}\end{pmatrix}\begin{pmatrix}d\\ s\\ b\end{pmatrix}. \qquad \text{(II.2)}$$

This matrix is the generalization of the Cabibbo matrix[34] relevant for two generations of quarks. Whereas the Cabibbo matrix depends on a single mixing parameter $\theta_1 \simeq \theta_c$ (the Cabibbo angle), the matrix in eq.(II.2) can be parameterized in terms of three mixing angles $\theta_1, \theta_2, \theta_3$ and one complex phase $\delta$ as follows:[35]

$$\begin{pmatrix} c_1 & s_1c_3 & s_1s_3\\ -s_1c_2 & c_1c_2c_3-s_2s_3e^{i\delta} & c_1c_2s_3+s_2c_3e^{i\delta}\\ -s_1s_2 & c_1s_2c_3+c_2s_3e^{i\delta} & c_1s_2s_3-c_2c_3e^{i\delta}\end{pmatrix}, \qquad \text{(II.3)}$$

where $c_i = \cos\theta_i$, $s_i = \sin\theta_i$ (i=1,2,3). The phenomenological success of the 4-quark scheme with $\sin\theta_c \simeq 0.221 \pm 0.002$[10], implies that the angles $\theta_2$ and $\theta_3$ must be small. In the case

of leptons, no such flavor mixing has been established. A massless neutrino would rule out[36] mixing in the lepton sector.

There are four gauge bosons corresponding to the four generators of the $SU(2)\otimes U(1)$. These vector bosons must be massless for the theory to be renormalizable.[37] However, 't Hooft[38] showed that renormalizability can be maintained in a theory with spontaneous symmetry breaking,[39] where three of the bosons acquire mass through the Higgs mechanism.[40] These massive bosons are the mediators of the weak interaction, which has a short range. The fourth boson remains massless and corresponds to the photon of electromagnetism, which is a long range force. The couplings in the model are the fine structure constant $\alpha$=1/137.03599 and g, g'. The coupling constants g and g' are related through the electroweak mixing angle $\theta_W$ to $\alpha$ through:

$$g\sin\theta_W = \sqrt{4\pi\alpha} \quad \text{and} \quad g'\cos\theta_W = \sqrt{4\pi\alpha}. \qquad \text{(II.4)}$$

$\sin^2\theta_W$ is measured in deep inelastic neutrino scattering to have the value[10] 0.230±0.005. The masses of the weak gauge bosons can be expressed in terms of the coupling constants and the mixing angle,

$$M_Z = \frac{M_W}{\cos\theta_W} \approx 90 \text{ GeV}, \quad M_W = \left(\frac{\pi\alpha}{\sqrt{2}G_F\sin^2\theta_W}\right)^{1/2} \approx 80 \text{ GeV}. \qquad \text{(II.5)}$$

These predictions are in excellent agreement with the experimental values:[10] (92.4±1.8) GeV and (81.0± 1.3) GeV respectively.

Flavor changing neutral currents have not been observed.[10] The charm quark was postulated to guarantee the absence of flavor changing neutral currents in lowest order perturbation theory via the GIM mechanism.[41] In the six-quark model this feature is incorporated through the unitarity of the KM mixing matrix (eq.II.3). The parameters of the KM matrix are not determined within the standard model.

## II.2 Weak Currents and Hamiltonian

Flavor changing weak decays thus proceed only via charged current interactions, i.e., through exchange or emission of a W boson. The Lagrangian for flavor changing interaction is given by,[8]

$$L = \frac{g}{2\sqrt{2}} \{J^{\mu}_{-} W_{\mu}^{+} + h.c.\}, \qquad (II.6)$$

where the charged currents are,

$$J^{\mu}_{-} = (\bar{u}\ \bar{c}\ \bar{t})\gamma^{\mu}(1-\gamma^5)V\begin{pmatrix} d \\ s \\ b \end{pmatrix} + (\bar{\nu}_e \bar{\nu}_{\mu} \bar{\nu}_{\tau})\gamma^{\mu}(1-\gamma^5)\begin{pmatrix} e^{-} \\ \mu^{-} \\ \tau^{-} \end{pmatrix} \qquad (II.7)$$

and $J^{\mu}_{+} = (J^{\mu}_{-})^{\dagger}$; V is the KM matrix (eqs. (II.2), (II.3)). Since $M_W >> m_{quark}$ , $m_{lepton}$ , the $q^2$ dependence of the W propagator can be neglected. Hence, in the absence of QCD effects the effective Hamiltonian for the charged weak interaction of quarks (and leptons) has the current×current form:

$$H^{0}_{eff} = \frac{G_F}{\sqrt{2}} (J_\mu^{+}(0) J^{\mu-}(0) + \text{h.c.}), \text{ where } \frac{G_F}{\sqrt{2}} = \frac{g^2}{8m_W^2}, \qquad \text{(II.8)}$$

$G_F = (1.16637 \pm 0.00002) \times 10^{-5} \text{GeV}^{-2}$, is the Fermi coupling constant.[10] The charm lowering part is obtained from eqs. (II.7) and (II.8) as,

$$H^{0}_{eff}(\Delta C=-1) = \frac{G_F}{\sqrt{2}} \{ (\bar{s}'c)(\bar{u}d') + (\bar{s}'c)(\bar{\nu}_l l) \}, \qquad \text{(II.9)}$$

where, $d' = d \cos\theta_c + s \sin\theta_c$, $s' = -d \sin\theta_c + s \cos\theta_c$ and mixing in the third generation has been neglected. Also, in writing the above we have used the following notation,

$$(\bar{q}_2 q_1) = \sum_i \bar{q}_{2i} \gamma^\mu (1-\gamma^5) q_{1i}, \qquad \text{(II.10)}$$

where i is the color index, summation over i implying that the charged currents must be color singlets. The nonleptonic part may be explicitly written as,

$$H^{0}_{NL}(\Delta C=-1) = \frac{G_F}{\sqrt{2}} \{ (\bar{s}c)(\bar{u}d)\cos^2\theta_c + (\bar{s}c)(\bar{u}s)\cos\theta_c \sin\theta_c - (\bar{d}c)(\bar{u}d)\sin\theta_c \cos\theta_c - (\bar{d}c)(\bar{u}s)\sin^2\theta_c \}. \qquad \text{...(II.11)}$$

The terms proportional to $\cos^2\theta_c$ are referred to as Cabibbo-allowed, those with $\cos\theta_c \sin\theta_c$ and $\sin^2\theta_c$ as Cabibbo-suppressed and doubly-suppressed respectively. For the semileptonic part we have,

$$H^{0}_{SL}(\Delta C=-1) = \frac{G_F}{\sqrt{2}} \{ (\bar{s}c)(\bar{e}\nu_e)\cos\theta_c + (\bar{s}c)(\bar{\mu}\nu_\mu)\cos\theta_c - (\bar{d}c)(\bar{e}\nu_e)\sin\theta_c - (\bar{d}c)(\bar{\mu}\nu_\mu)\sin\theta_c \}. \qquad \text{...(II.12)}$$

The Hamiltonian for bottom decays can be obtained similarly.

For the rest of this chapter, we will concentrate on charm decays to demonstrate the ideas involved in weak decays of heavy flavor mesons. The generalization to bottom decays will be obvious.

## II.3 Strong Interaction Effects

The theory of weak processes is, in essence, a theory of strong interactions. The decaying heavy quarks are necessarily confined inside hadronic bound states. The force responsible for the binding of quarks and gluons is described by Quantum Chromodynamics[3] (QCD). The confinement mechanism is still not understood completely and weak decays of quarks thus offer a chance of achieving a deeper insight into strong interaction dynamics.

QCD involves an unbroken $SU(3)_c$ gauge group. Each quark flavor exists in three colors, while the leptons are color neutral. The eight generators of $SU(3)_c$ correspond to an octet of massless gauge bosons-the gluons, which are flavor neutral. The nonabelian structure of QCD leads to self-interaction of gluons. This results in the property of asymptotic freedom[4], i.e., at small distances or equivalently, at large momentum transfers the effective strong coupling constant is small.

Thus for sufficiently small distances, the effects of strong interactions can be calculated[3] in a perturbation theory with $\alpha_s(Q^2)$ being the expansion parameter. As the distance scale increases, non-perturbative effects will

become important. Both short range effects and long range effects of QCD will come into play in the decay of a heavy meson. Heavy flavor decays thus present an opportunity to learn about QCD on the interface between the perturbative and the non-perturbative regimes. In the weak decays of a hadron, the heavy quark decays at a time-scale given by $\tau \simeq 1/M_W$. The spectator quarks, sea quarks and gluons, go along unaffected until the confinement forces become important after the much longer time-scale $\tau \simeq 1/\Lambda$, where $\Lambda$ is the scale parameter[3] of QCD. Due to these differing time-scales it is assumed[8] that the short and long distance contributions of the strong interaction effects can be separated. The long distance effects including bound state wavefunctions, soft gluon radiation and final state interactions are absorbed into the initial and final state hadronic wave functions. The short distance effects originating in hard gluon interactions are calculated perturbatively and included in the effective weak Hamiltonian. The above assumption then implies that the amplitude for a meson M decaying into a final state b, c, is determined by the matrix element of the effective weak Hamiltonian between asymptotic initial and final states,

$$A(M \to bc) = \langle bc|H_{eff}|M\rangle \qquad \text{(II.13)}$$

$H_{eff}$ includes the hard gluon corrections and is calculated from perturbative QCD. The non-perturbative phenomena cannot be calculated from first principles in QCD. Hence the matrix elements have to be evaluated from physically motivated

models and are discussed in section II.4.

*Hard Gluon Effects*

In the absence of QCD effects, the hadronic part of the weak Hamiltonian has the form,

$$H^0_{eff} = \frac{G_F}{\sqrt{2}}(\bar{q}_2 q_1)(\bar{q}_4 q_3). \qquad \text{(II.14)}$$

Corrections to the above four-quark operator come from one-loop diagrams in the lowest order. The vertex and self energy corrections are absorbed in the physical coupling constant, $G_F$. The gluon exchange diagrams result in the following corrected Hamiltonian:

$$H^1 = H^0 - \frac{G_F}{\sqrt{2}}\frac{3\alpha_s}{8\pi}\ln\frac{M_W^2}{\mu^2}(\bar{q}_2\lambda^a q_1)(\bar{q}_4\lambda^a q_3). \qquad \text{(II.15)}$$

The hard gluon exchange induces an additional four-quark operator, having the same chiral and flavor structure as the uncorrected $H^0$, but involves a product of color octet currents. Using a Fierz transformation[42] and the properties of SU(3) algebra one has the relation:

$$[(\bar{q}_2\lambda^a q_1)(\bar{q}_4\lambda^a q_3)] = \frac{-2}{3}(\bar{q}_2 q_1)(\bar{q}_4 q_3) + 2(\bar{q}_2 q_3)(\bar{q}_4 q_1). \qquad \text{(II.16)}$$

Hence,

$$H^1 = \frac{G_F}{\sqrt{2}}\left\{\left(1 + \frac{\alpha_s}{4\pi}\ln\frac{M_W^2}{\mu^2}\right)(\bar{q}_2 q_1)(\bar{q}_4 q_3) - \frac{3\alpha_s}{4\pi}\ln\frac{M_W^2}{\mu^2}(\bar{q}_2 q_3)(\bar{q}_4 q_1)\right\}. \qquad \text{...(II.17)}$$

From the above one can see that the hard gluon exchange renormalizes the original four-quark operators and introduces an additional effective neutral current interaction.

The four quark interaction has the color structure $3\otimes 3 = \bar{3} + 6$. The operators corresponding to the sextet and

anti-triplet are:

$$O_{\pm} = \frac{1}{2}\{(\bar{q}_2 q_1)(\bar{q}_4 q_3) \pm (\bar{q}_2 q_3)(\bar{q}_4 q_1)\} \qquad \text{(II.18)}$$

The Hamiltonian without QCD corrections can then be written in the form,

$$H^0 = \frac{G_F}{\sqrt{2}}[c_+ O_+ + c_- O_-], \qquad \text{(II.19)}$$

where $c_+ = c_- = 1$. The first order corrected Hamiltonian may be similarly decomposed,

$$H^1 = \frac{G_F}{\sqrt{2}}[c_+^1 O_+ + c_-^1 O_-], \qquad \text{(II.20)}$$

where,

$$c_+^1 = 1 - \frac{\alpha_s}{2\pi}\ln\frac{M_W^2}{\mu^2} \quad \text{and} \quad c_-^1 = 1 + \frac{\alpha_s}{\pi}\ln\frac{M_W^2}{\mu^2}\,. \qquad \text{(II.21)}$$

The strong interaction effects modify the coefficients $c_+$ and $c_-$, but do not mix the operators $O_+$ and $O_-$, which are even and odd under interchange of color indices respectively. Note that QCD corrections increase $c_-$ but decrease $c_+$.

The hard gluon corrections can be summed up to all orders in $\alpha_s$ using the techniques of operator product expansion[43] and renormalization group.[44] The time ordered product of weak currents is expanded in terms of local operators,

$$T[J^{\rho}(x) J^{\dagger\sigma}(0)] = \sum_k c_k(x; g_s, m_q, \ldots \mu)\ O_k^{\rho\sigma}(0). \qquad \text{(II.21)}$$

In the limit of massless quarks, the short distance expansion of the time-ordered product of weak currents consists of only two operators,[12] leading to the following Hamiltonian:

$$H^{eff} = c_+(g_s, M_W/\mu)\ O_+(0) + c_-(g_s, M_W/\mu)\ O_-(0) \qquad \text{(II.22)}$$

with

$$O_\pm = \tfrac{1}{2}\{[\bar{q}_{2/3}\gamma^\nu q_{1/3}]_L[\bar{q}_{1/3}\gamma^\dagger_\nu q_{2/3}]_L \pm [\bar{q}_{2/3}\gamma^\nu q_{2/3}]_L[\bar{q}_{1/3}\gamma_\nu q_{1/3}]_L\} \qquad \text{...(II.23)}$$

with $q_{2/3} = \begin{pmatrix} u \\ c \\ t \end{pmatrix}$ and $q_{1/3} = \begin{pmatrix} d \\ s \\ b \end{pmatrix}$.

The coefficients $c_\pm$, must compensate the dependence of the matrix elements $\langle f|O_k(0)|i\rangle$ on the normalization point $\mu$ and hence are obtained as the solutions of the renormalization group equation. In the leading log approximation[12]

$$c_\pm(g_s, \frac{M_W}{\mu}) = c_\pm(0, \frac{M_W}{\mu}) \left[\frac{\alpha_s(\mu^2)}{\alpha_s(M_W^2)}\right]^{\frac{d_\pm}{b}}, \qquad \text{(II.24)}$$

where $$\alpha_s(Q^2) = \frac{4\pi}{b\ln(Q^2/\Lambda^2)},$$

$g_s$ is the effective coupling constant, $d_\pm$ are the anomalous dimensions and $b=11-2N_f/3$, $N_f$ being the number of flavors. Since $d_-=2d_+$, we have the relation $c_-=1/c_+^2$. The calculation has also been done in the next to leading log (NLL) approximation.[13] These NLL corrections are small and reinforce the leading log shift of $c_\pm$ w.r.t. their free quark values:

$$c_\pm(g_s, \frac{M_W}{\mu}) = \left[\frac{\alpha_s(\mu^2)}{\alpha_s(M_W^2)}\right]^{\frac{d_\pm}{b}} \left[1 + \frac{\alpha_s(\mu^2) - \alpha_s(M_W^2)}{\pi}\rho_\pm(N_f)\right], \qquad \text{(II.25)}$$

where,

$$\alpha_s(Q^2) \equiv \alpha_s^{NLL}(Q^2) = \alpha_s^{LL}(Q^2)\left\{1 - [102 - \tfrac{38}{3}N_f]\frac{1}{b^2}\frac{\ln[\ln(Q^2/\Lambda^2)}{\ln(Q^2/\Lambda^2)}\right\}$$

$$\rho_+(N_f) = \frac{1}{b}\left[\frac{-221}{24} + \frac{5}{9}N_f\right] + \frac{1}{b^2}\left[51 - \frac{19}{3}N_f\right]$$

and $\rho_-(N_f) = \frac{1}{b}\left[\frac{263}{12} - \frac{10}{9} N_f\right] + \frac{1}{b^2}\left[-102 + \frac{38}{3} N_f\right]$.

The corrected Cabibbo allowed charm lowering Hamiltonian may now be rewritten in terms of the coefficients,

$$C_1 = \frac{C_+ + C_-}{2} \quad \text{and} \quad C_2 = \frac{C_+ - C_-}{2}$$

as,

$$H_{NL}(\Delta C=-1) = \frac{G_F}{\sqrt{2}} \cos^2\theta_c \left[ C_1 (\bar{s}c)(\bar{u}d) + C_2 (\bar{s}d)(\bar{u}c) \right]. \quad \ldots(II.26)$$

**II.4** Valence Quark Approximation

The short distance QCD corrections to the Hamiltonian of weak interaction were calculated using perturbation theory. Now, to determine the amplitude for any weak decay, one needs to calculate the matrix element of this Hamiltonian. One thus has to deal with non-perturbative bound state effects, and an approximate model is required. The simplest approach[8] is that of the valence quark approximation. The calculations are done at the quark level. The initial state meson is represented by its valence quark configuration, and the final state quarks represent the inclusive hadronic final state. Soft gluon interactions accompanying the weak process are neglected. The decay mechanisms[8] possible are shown in Fig. 1. The diagram in 1(a) represents flavor decay, while 1(b) and 1(c) are flavor annihilation via W-exchange and W-annihilation respectively.

In the flavor decay mechanism (also referred to as the spectator diagram), the spectator quark remains passive. The semileptonic width from flavor decay should thus be

identical to the μ-decay amplitude:[35]

$$\Gamma_D(P\to l\nu_1 X) \propto \Gamma(Q\to q l\nu_1) = \Gamma(\mu\to\nu_\mu e\nu_e)\,(m_Q/m_\mu)^5$$

$$= \frac{G_F^2 m_Q^5}{192\,\pi^3} . \qquad \text{(II.27)}$$

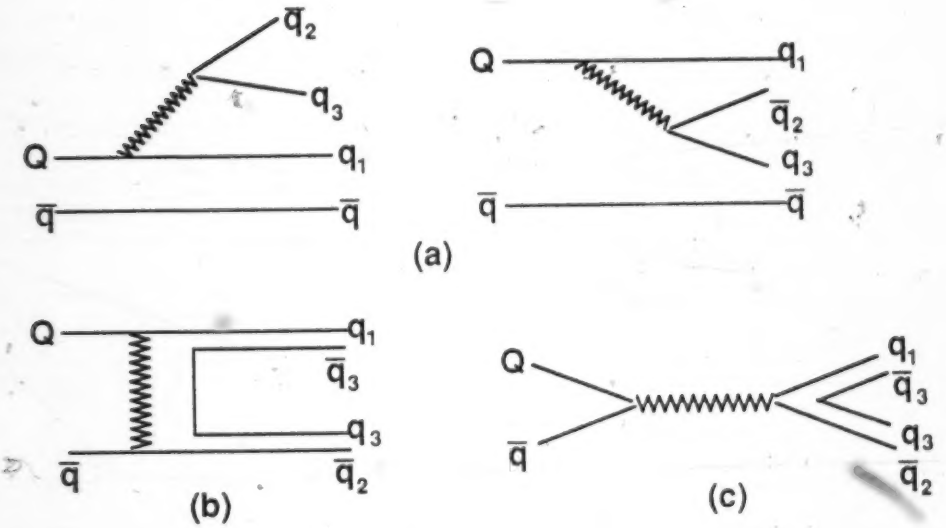


**Fig. 1** Decay mechanisms in valence quark approximation: (a) flavor decay, (b) flavor annihilation via W-exchange and (c) W-annihilation.

For light final state quarks, the hadronic width would also be the same, apart from a color factor, which accounts for three color states in which $\bar{q}_2 q_3$ can be produced, i.e.,

$$\Gamma_D(P\to X_H) \propto \Gamma(Q\to q_1\bar{q}_2 q_3) = \frac{3G_F^2 m_Q^5}{192\,\pi^3} . \qquad \text{(II.28)}$$

In the case of flavor annihilation the light antiquark has an active role. Since weak interactions are point-like the heavy quark and the light antiquark have to overlap for the annihilation process to occur. Thus, the meson decay

constant $f_p$ defined by $\langle 0|J^\mu|P\rangle = if_p p^\mu$, comes into the picture. The annihilation width is given by:[8]

$$\Gamma_{Ann}(P\to X_H) = C\,\frac{G_F^2}{8\pi}\,f_p^2\,M_p(m_1^2 + m_2^2) \times \text{phase space}, \qquad \text{(II.29)}$$

where C is the color factor, $M_p$ the initial meson mass and $m_i$ are the final state quark masses. The dependence of the width on the light quark masses implies that the annihilation process is helicity suppressed. This is analogous to the suppression of $\pi\to e\bar{\nu}_e$ versus $\pi\to\mu\bar{\nu}_\mu$. A pseudoscalar meson cannot decay into a massless fermion-antifermion pair if only left-handed fermions participate in weak interactions.

*Spectator Model*

In the so called spectator model[14], the light constituents of the decaying heavy meson are assumed to be inert. Thus the annihilation process is neglected and the decay assumed to occur via spectator diagram only. Thus, in this model the lifetimes of $D^+$, $D^0$, $D_s^+$ mesons should all be equal and essentially determined by the lifetime $\tau_c$ of the charm quark:

$$\tau(D^\pm) \simeq \tau(D^0) \simeq \tau(D_s^+) = \tau_c.$$

In the charm quark decay, at the Cabibbo-allowed level, only two leptonic modes and one hadronic mode is possible. Hence, using eqs.(II.27) and (II.28), we have

$$\tau_c = \frac{1}{\Gamma_c} \simeq \frac{1}{5}\left(\frac{m_\mu}{m_c}\right)^5 \tau_\mu \approx 7\times10^{-13}\text{s}, \quad \text{for } m_c \simeq 1.5\text{GeV}. \qquad \text{(II.30)}$$

The experimental values[6] of the lifetimes of $D^0$, $D^+$ and $D_s^+$ are:

$$\tau(D^0) = (4.27 \pm 0.10) \times 10^{-13} s,$$

$$\tau(D^+) = (10.45 \pm^{0.31}_{0.29}) \times 10^{-13} s$$

and $$\tau(D_s^+) = (4.31 \pm^{0.36}_{0.32}) \times 10^{-13} s. \qquad \text{(II.31)}$$

The naive prediction of the spectator model is quite close to the experimental values. Thus the spectator model does provide a very useful qualitative basis for calculating the weak decay of heavy quarks. However, one notes that the lifetimes of $D^+$ and $D^0$ are not equal. Thus we need to look beyond the spectator model and include the effects of the other quarks and gluons present in the initial or final state. Note that the short distance QCD corrections were ignored in the above. However, within the spectator model framework, their inclusion still results in equal lifetimes for all the charm particles. The nonleptonic rate, including QCD corrections is given by,

$$\Gamma(c \to s\bar{d}u) = (2c_+^2 + c_-^2) \frac{G_F^2 m_c^5}{192\pi^3} . \qquad \text{(II.32)}$$

Thus, the hard gluon corrections enhance the non-leptonic rate by a factor $(2c_+^2+c_-^2)/3$ w.r.t. the rate obtained using the uncorrected Hamiltonian.

In the spectator model, the semileptonic branching ratios of all weakly decaying states with the same heavy flavors will also be the same. For charm quark decay, one out of five decays leads to a particular lepton in the final state, therefore,

$$B(c \to l\nu_l X) = 1/5 = 20\% . \qquad \text{(II.33)}$$

The nonleptonic QCD enhancement would lead to,

$$B(c\to l\nu_l X) = \frac{1}{2 + 2c_+^2 + c_-^2} \simeq 16\% \ . \qquad \text{(II.34)}$$

Again, this result is in variance with the observed[6] semileptonic branching ratios:

$$B(D^+\to e^+X) = (17.0\pm1.9\pm0.7)\%$$

and $$B(D^0\to e^+X) = (7.5\pm1.1\pm0.4)\% . \qquad \text{(II.35)}$$

Since the electroweak sector is well understood, it may be expected that the reason for the lifetime difference must be hidden in the purely hadronic sector.

Now, $$\frac{B(D^+\to e^+X)}{B(D^0\to e^+X)} = \frac{\Gamma(D^+\to e^+X)}{\Gamma(D^0\to e^+X)}\,\frac{\tau(D^+)}{\tau(D^0)} \ . \qquad \text{(II.36)}$$

If $\Gamma(D^+\to e^+X) = \Gamma(D^0\to e^+X)$, then the ratios of the semileptonic branching ratios should be equal to the lifetime ratios. This is indeed the case.

Thus, the spectator model, which only incorporates the short distance structure of heavy flavor decays, is not able to reproduce the detailed pattern of charmed particle decays. Long distance phenomena, involving the light constituents appear to play a significant role. Two such effects have been proposed to resolve the lifetime difference: quark interference[45] and flavor annihilation.[23]

*Interference*

From the Cabibbo-allowed nonleptonic charm changing Hamiltonian given in eq.(II.26), one can see that the two terms with coefficients $C_1$ and $C_2$, both give rise to the same final states in $D^+$ decay, whereas the final states are

distinct in $D^0$ decay (see Fig. 2). Thus, one can expect

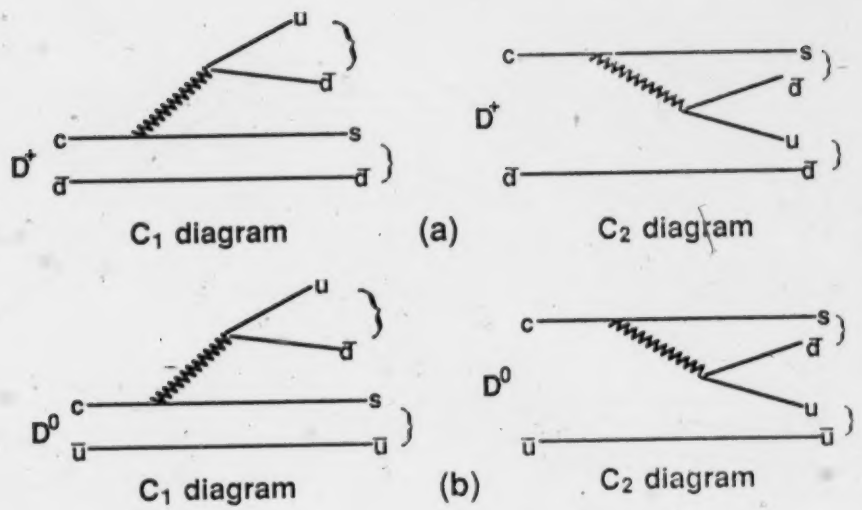


**Fig 2.** Amplitudes for (a) $D^+$ and (b) $D^0$ decays arising from the $C_1$ and $C_2$ terms. Brackets denote color singlet final states.

interference between the two amplitudes in $D^+$ case. Further, if this interference is destructive then it could account for the higher $D^+$ lifetime. The amount of interference can be accounted for by a parameter $\alpha$, where $0 \leq \alpha \leq 1$. The nonleptonic width for $D^+$ (neglecting Cabibbo suppressed terms), then becomes:[8]

$$\Gamma_{NL}(D^+) = [2(1+\alpha)c_+^2 + (1-\alpha)c_-^2]\frac{G_F^2 m_c^5}{192\pi^3} . \qquad \text{(II.37)}$$

Since, the interference would be absent in $D^0$ decay, we have,

$$\frac{\tau(D^+)}{\tau(D^0)} = \frac{2 + 2c_+^2 + c_-^2}{2 + 2(1+\alpha)c_+^2 + (1-\alpha)c_-^2} \quad . \qquad \text{(II.38)}$$

Even for maximal destructive interference, i.e. $\alpha = 1$, the above ratio is 1.5. Hence, this mechanism is probably present at some level, but not enough of an effect by itself to be consistent with the observed $D^+$ and $D^0$ lifetimes.

The interference can also arise at the quark level before hadronization, from the presence of two identical $\bar{d}$ quarks in the final state. If a $\bar{d}$ quark spectator is present in the initial hadron, the newly produced $\bar{d}$ cannot occupy the whole phase space; according to Pauli principle, the part of the phase space already occupied by the $\bar{d}$ spectator is inaccessible to the new $\bar{d}$. A calculation of the $D^+$ hadronic width including this Pauli interference leads to,[8]

$$\Gamma_D(D^+ \to X_H) = (2c_+^2 + c_-^2) \frac{G_F^2 M^5}{192\pi^3} - (c_-^2 - 2c_+^2) \frac{G_F^2 M^2}{\pi} |\Phi(0)|^2 . \qquad \text{...(II.39)}$$

The correction to the original width is seen to depend on $\Phi(0)$, the bound state wavefunction at the origin, since an overlap of identical quarks in space leads to the Pauli interference. Note that since $c_-^2 > 2c_+^2$, the interference does decrease the $D^+$ width. Estimates[7] using simple quark models for the $D^+$ meson, indicate that the interference effect probably does not exceed 20%.

*Annihilation*

The W-exchange and W-annihilation diagrams can contri-

bute to $D^0$ and $D_s^+$ nonleptonic decays at the Cabibbo-allowed level. The annihilation graph is present only at the Cabibbo-suppressed level for $D^+$. Thus non-vanishing annihilation contributions could be responsible for the lifetime differences in charm particles. The helicity suppression of these diagrams could be lifted by the presence of gluons in the decaying meson. The $c\bar{q}$ pair can then be in a spin one configuration and thus annihilation into a pair of light fermions will not be impeded by small mass ratios.

A perturbative QCD calculation[23] of the effect of single gluon emission from the light quark line yields:

$$\frac{\Gamma_{Ann}}{\Gamma_D} = \frac{2\pi\alpha_s}{27(2c_+^2 + c_-^2)} (c_+ + c_-)^2 \left(\frac{f_D}{m_u}\right)^2 \quad \text{for } D^0 \to X_H \qquad \text{(II.40)}$$

$$\approx 6\times10^{-2}.$$

However, perturbation theory may not be relevant in estimating the annihilation contributions. Non-perturbative approaches such as QCD sum rules[29] and QCD multipole expansion[46] give much larger values. Thus, precise quantitative predictions are very difficult due to the lack of understanding of hadronic bound states and the role of soft gluon interactions. We thus need to determine them phenomenologically.

*Nonleptonic Two-Body Decays*

Since the discovery of charmed mesons, many exclusive decay channels of these particles have been measured[5,6] by various collaborations. Two-body and quasi-two-body modes seem to dominate[6] the nonleptonic D decays. The hadronic

matrix elements are simple to calculate for these modes. Some two-body decay channels of B mesons have been measured as well.[47] Of course two-body decays of B mesons are not expected to be as dominant as in the case of D decays, due to the larger phase space.

Neglecting soft gluon interactions, the two-body decay amplitudes are determined as follows. First, the quark currents in the effective Hamiltonian are replaced by the corresponding hadronic currents $J_H$. For two body final states consisting of two pseudoscalars, a pseudoscalar and a vector or two vectors, henceforth denoted by PP, PV and VV respectively, one employs the factorization ansatz[15]

$$\langle f|J_H \cdot J_H|D\rangle \simeq \langle P \text{ or } V|J_H|0\rangle\langle P \text{ or } V|J_H|D\rangle. \qquad \text{(II.41)}$$

Thus, the matrix element of the $H_{NL}^{eff}$ can be written in terms of simpler matrix elements of single currents and thus are determined in terms of meson decay constants and hadron current matrix elements.

Let us consider the decay $D^+ \to \bar{K}^0\pi^+$. Using eqs.(II.26) and (II.41) we have :

$$\begin{aligned} A(D^+ \to \bar{K}^0\pi^+) = \frac{G_F}{\sqrt{2}}\cos^2\theta_c \{ & C_1\langle\pi^+|\bar{u}^i d_i|0\rangle\langle\bar{K}^0|\bar{s}^j c_j|D^+\rangle \\ & + C_1\langle\bar{K}^0|\bar{s}^j d_i|0\rangle\langle\pi^+|\bar{u}^i c_j|D^+\rangle \\ & + C_2\langle\pi^+|\bar{u}^j d_i|0\rangle\langle\bar{K}^0|\bar{s}^i c_j|D^+\rangle \\ & + C_2\langle\bar{K}^0|\bar{s}^i d_i|0\rangle\langle\pi^+|\bar{u}^j c_j|D^+\rangle \} \end{aligned} \qquad \text{(II.42)}$$

Using,

$$\langle\pi^+|\bar{u}^i d_j|0\rangle = \frac{1}{N_c}\,\delta^i_j\langle\pi^+|\bar{u}d|0\rangle$$

and

$$\langle\bar{K}^0|\bar{s}^i c_j|0\rangle = \frac{1}{N_c}\,\delta^i_j\langle\bar{K}^0|\bar{s}c|D^+\rangle \qquad \text{(II.43)}$$

we get,

$$A(D^+\to \bar{K}^0\pi^+) = \frac{G_F}{\sqrt{2}}\cos^2\theta_c\Big\{\Big(C_1 + \frac{C_2}{N_c}\Big)\langle\pi^+|\bar{u}d|0\rangle\langle\bar{K}^0|\bar{s}c|D^+\rangle + \Big(C_2 + \frac{C_1}{N_c}\Big)\langle\bar{K}^0|\bar{s}d|0\rangle\langle\pi^+|\bar{u}c|D^+\rangle\Big\}. \qquad \text{...(II.44)}$$

In general the transition amplitude may be written in the form:

$$T(D\to f) = \frac{G_F\cos^2\theta_c}{\sqrt{2}}\{\,a_1\langle f|(\bar{s}c)_{L,H}(\bar{u}d)_{L,H}|D\rangle + a_2\langle f|(\bar{u}c)_{L,H}(\bar{s}d)_{L,H}|D\rangle\}, \qquad \text{(II.45)}$$

where, $a_1 = C_1 + \xi C_2$ and $a_2 = C_2 + \xi C_1$. (II.46)

Both charged and effective neutral current receive contributions from a term where the color indices are automatically matched to form color singlet hadrons and a second term where the color indices are mismatched. $\xi$ is the color mismatch factor, and we expect $\xi=1/N_c$ for $N_c$ colors.

In the absence of QCD corrections,

$C_1\to 1$ implying that $a_1\to 1$

$C_2\to 0$ $a_2\to\xi=1/N_c$

Thus the amplitudes with coefficient $a_2$ are then color suppressed w.r.t. those with coefficient $a_1$. In the presence of QCD corrections, an additional neutral current interaction with coefficient $C_2$ is introduced, the hadronic amplitudes then have the full coefficients $a_1$ and $a_2$,

defined in eq.(II.46). Thus both $a_1$ and $a_2$ have color allowed and color suppressed parts.

In the case of $D^0$ decay the charged current operator with coefficient $a_1$ results in charged final states (referred[27] to as class I transitions by Bauer et. al.) while the effective neutral current operator with coefficient $a_2$ results in neutral final states (called class II transitions). As a consequence of QCD corrections ($c_->1$, $c_+<1$) $|a_2|<|a_1|$, leading to class II amplitudes being smaller than class I amplitudes. Thus for example:

$\Gamma(D^0\to K^-\pi^+,\ K^-\rho^+,\ \text{etc.}) \propto a_1^2, \quad \Gamma(D^0\to \bar{K}^0\pi^0,\ \bar{K}^0\rho^0,\ \text{etc}) \propto a_2^2$ .

In the absence of QCD effects one expects that the ratio:

$$R = \frac{\Gamma(D^0 \to \bar{K}^0\pi^0)}{\Gamma(D^0 \to K^-\pi^+)} = \frac{1}{2N_c^2} = \frac{1}{18}, \quad \text{for } N_c=3, \qquad \text{(II.47)}$$

the 1/2 factor comes from the square of the $\pi^0$ wave function $(u\bar{u}-d\bar{d})/\sqrt{2}$. QCD corrections require that:

$$R = \frac{\Gamma(D^0 \to \bar{K}^0\pi^0)}{\Gamma(D^0 \to K^-\pi^+)} = \frac{1}{2}\left(\frac{C_2+\xi C_1}{C_1+\xi C_2}\right)^2 \qquad \text{(II.48)}$$

$$= \frac{1}{2}\left(\frac{2C_+ - C_-}{2C_+ + C_-}\right)^2 \approx \frac{1}{50} \quad \text{for } \xi = \frac{1}{3} ,$$

reducing it even further. This is in gross disagreement with the experimental branching ratios:[6]

$$B(D^0\to \bar{K}^0\pi^0) = (1.9\pm0.4\pm0.2)\%, \qquad \text{(II.49)}$$

and $$B(D^0\to K^-\pi^+) = (4.2\pm0.4\pm0.4)\% .$$

In the naive quark model the parameter $\xi$ has the value 1/3. However, in the presence of soft gluons i.e. nonperturbative effects, this may not be justified. The discrepancy between

the above theoretical value (see eq.(II.48)) and the experimental prediction was used by Buras et al,[28] to be an indication of the absence of color suppressed diagrams, i.e. $\xi=0$. For $\xi=0$ the above ratio is,

$$R = \frac{1}{2}\left(\frac{C_+ - C_-}{C_+ + C_-}\right)^2 \approx 0.1 \qquad \text{(II.50)}$$

in better agreement with the values of eq.(II.49). Similar absence of color suppressed contributions was also shown to give better agreement for the neutral and charged $K\rho$ and $K^*\pi$ modes.

Before making any conclusive statements about the factor $\xi$ from the above data, one needs to consider two effects. The first important effect[18] is that of final state interactions. The three $D\to K\pi$ amplitudes, $D^0\to K^-\pi^+$, $\bar{K}^0\pi^0$ and $D^+\to\bar{K}^0\pi^+$ can be expressed in terms of two isospin amplitudes with isospin 1/2 and 3/2 in the final state as,

$$\begin{aligned} A(D^0\to K^-\pi^+) &= \frac{1}{\sqrt{3}}(\sqrt{2}A_{1/2} + A_{3/2}) \\ A(D^0\to \bar{K}^0\pi^0) &= \frac{1}{\sqrt{3}}(-A_{1/2} + \sqrt{2}A_{3/2}) \qquad \text{(II.51)} \\ A(D^+\to \bar{K}^0\pi^+) &= \sqrt{3}A_{3/2}\ . \end{aligned}$$

Without final state interactions the amplitudes $A_{1/2}$ and $A_{3/2}$ would be real. Mark III measurements[6] however indicate that they need to be complex and that the phase shift between the two isospin amplitudes $\delta_{1/2}-\delta_{3/2}\approx 77^\circ$. Thus, final state interactions could account[48,22] for the discrepancy between theory and experiment for the neutral to charged ratios of $D^0$ decay modes. Note that there is not

complete agreement between theory and experiment for these ratios even for $\xi=0$, in the absence of final state interactions.

The other effect which also needs to be considered is that of annihilation. It was pointed out earlier that in the presence of gluons in the meson wave function there is no helicity suppression for the annihilation process. Alternately, there could be a dynamical mechanism[49,22] such as the presence of a resonance, with quantum numbers equal to that of a $\bar{K}^0$ with mass close to $D^0$ and a $\pi^+$ close to $D_s^+$, which could also enhance the annihilation contribution in $D^0$ and $D_s^+$ decays respectively.

There are some special decay modes that can be generated only via annihilation. The valence quark structure of these final states cannot be produced via spectator decays in a direct way. $D^0 \to \bar{K}^0\phi$ [50] and $\bar{K}^0K^{*0}$ should be clear signatures for W-exchange. Here the $\bar{u}$ quark of the initial state is absent in the final state meson. For the $D_s^+$ meson, final states with no net strangeness and no $s\bar{s}$ content (such as $\rho\pi$) could be characteristic of W-annihilation. Final state interactions could however confuse the picture. The difficulty in calculating weak annihilation diagrams lies in the fact that form factors at large $q^2$ are involved, where the simple pole type form factors cannot be trusted.[16] Thus at present one cannot predict the strength of annihilation. We adopt the following strategy: we treat annihilation as a parameter and predict the rates for various decay modes.

Comparison with the experimental values can then give some idea about annihilation.

In addition to the spectator and annihilation graphs, there are the so-called Penguin diagrams,[8] which can also contribute to the decay processes. Here, a quark of flavor $q_1$ is transformed to a quark of flavor $q_2$ via a virtual quark loop, carrying flavor $q_f$. This effective flavor changing neutral current interacts with a flavor diagonal current via gluon exchange. The contribution of these diagrams to charm decays is small, being at the $|V_{ub}|$ level. In B-decays, these contributions may not be negligible. We will ignore the Penguin contributions in our discussions.

In the next chapter we will discuss the theory of final state interactions. In chapter IV final state interactions and annihilation will be incorporated in a model calculation for various D, $D_s$ decay modes.

## III. FINAL STATE INTERACTIONS

Charmed mesons can decay nonleptonically into a variety of hadronic channels. As charmed meson masses lie in the resonance region, strong interaction final state rescattering effects[18] can modify the naive expectations for exclusive two body D, $D_s$ decays substantially.

If the pair of hadrons produced in a weak decay has an energy which is below the inelastic threshold, the amplitude can still develop a phase from elastic scattering. For example, consider a process 'X', in which the final state is composed of two possible isospins. The corresponding portions of the weak amplitude, each pick up a phase that is appropriate to scattering in that particular isospin state. Depending on the phase difference of the two isospin states, the net amplitude for the physical process 'X' can be very different from that predicted from the weak decay alone.

When one is above inelastic threshold, it is also possible to produce the final state through scattering of other channels.[20,22] Thus, the amplitudes of the different coupled channels can feed into each other, resulting in enhancement or depletion of the weak amplitudes. A coupled multichannel scattering calculation needs to be done for such a case.

The problem at hand is thus the following: Given a set of n strongly interacting channels which can communicate, we

want to determine the amplitudes for a weakly interacting system to go into each of these channels. The technique for handling this problem consists of writing the unitarity relations and solving the resulting coupled integral equations, the so called Muskhelishvili-Omnes (MO) equations.[51]

In the literature the MO equation has been discussed[52] quite extensively, particularly for purely elastic single channel scattering. Charmed meson decays mainly involve inelastic multichannel final state interactions. We will therefore review the inelastic multichannel case[53] (in section III.2), mentioning the elastic case very briefly. In the following section we first consider the analytic properties of the scattering matrix.

**III.1** Analytic properties of the Scattering matrix

The strong interaction **S** matrix can be expressed in terms of the scattering **T** matrix as,

$$\mathbf{S}(s) = 1+2i\mathbf{T}(s) \qquad \text{(III.1)}$$

where s is the center of mass energy squared of the two-body subsystem. For n coupled channels **S** and **T** are n-dimensional matrices. The property of causality requires that **T**(s) be an analytic function of s, except for certain poles and branch cuts in the complex s plane. These branch cuts[26] may be separated into two classes: right-hand cut associated with the unitarity condition and left-hand cuts associated with the physical mechanisms which generate the reactions

considered.

For s above threshold, the unitarity of the **S** matrix, i.e. the condition $\mathbf{S}^\dagger\mathbf{S}=\mathbf{1}$ reduces to the following for the **T** matrix:

$$2i(\mathbf{T}_{ij}(s)-\mathbf{T}^\dagger_{ij}(s)) = -4\sum_k \mathbf{T}^\dagger_{ik}(s)\theta(s-s_k)\mathbf{T}_{kj}(s)$$

or,
$$\mathrm{Im}\mathbf{T}_{ij}(s) = \sum_k \mathbf{T}^\dagger_{ik}(s)\theta(s-s_k)\mathbf{T}_{kj}(s) \qquad \text{(III.2)}$$

where $s_k$ is the threshold for the channel k and $\theta(s-s_k)$ is the step function. Below the threshold energy, since there are no final states energetically available, $\mathrm{Im}\mathbf{T}(s)=0$. Once above threshold $\mathrm{Im}\mathbf{T}\neq 0$. Writing, $\mathbf{T}(s+i\varepsilon)=\mathrm{Re}\mathbf{T}+i\mathrm{Im}\mathbf{T}$ and $\mathbf{T}(s-i\varepsilon)=\mathrm{Re}\mathbf{T}-i\mathrm{Im}\mathbf{T}$ we have,

$$\mathrm{Im}\mathbf{T}(s) = \frac{\mathbf{T}(s+i\varepsilon)-\mathbf{T}(s-i\varepsilon)}{2i}.$$

A non-vanishing $\mathrm{Im}\mathbf{T}$ thus implies that $\mathbf{T}(s+i\varepsilon)$ and $\mathbf{T}(s-i\varepsilon)$ do not approach equal values as $\varepsilon\to 0$. This implies that there must be a branch cut on the real axis above the threshold, referred to as the right-hand cut.

The left-hand cuts on the other hand are provided by the production model. Thus, they depend on the dynamical details of the interaction, for e.g.,[54] they arise from the $\rho$-exchange graphs in the two channel problem involving $\pi\pi \leftrightarrow \pi\pi$, $\pi\pi \leftrightarrow \pi\omega$.

The scattering matrix **T**(s) for a partial wave of given angular momentum and isospin can be expressed as,

$$\mathbf{T}(s) = \mathbf{N}(s)\mathbf{D}^{-1}(s). \qquad \text{(III.3)}$$

This formalism, known as the N/D method,[55] guarantees the unitarity and analyticity properties of the scattering

matrix mentioned above. For an n channel system, $\mathbf{N}(s)$ and $\mathbf{D}(s)$ are nxn matrices, $\mathbf{D}(s)$ carries the physical unitarity cut, while $\mathbf{N}(s)$ carries the unphysical left-hand cuts. Note that time reversal invariance requires that $\mathbf{T}(s)$ be a symmetric matrix. $\mathbf{T}(s)$ given by eq.(III.3) satisfies this condition, provided[56] $\mathrm{Im}\mathbf{T}(s)$ is a symmetric matrix on the left-hand cuts.

Above the threshold, since $\mathbf{N}(s)$ is real, we have,

$$\mathrm{Im}\mathbf{D}_{ij}(s) = \mathrm{Im}[\mathbf{T}^{-1}(s)]_{ik}\mathbf{N}_{kj}(s) \qquad s>s_R \tag{III.4}$$

where, $s_R$ is the threshold energy appropriate to each element of $\mathbf{T}(s)$. Using eq.(III.1), we have,

$$\mathbf{T}^{-1}(s) = \left(\frac{\mathbf{S}-\mathbf{1}}{2i}\right)^{-1}. \tag{III.5}$$

Eq.(III.5) and a similar relation for $(\mathbf{T}^{-1})^{\dagger}$ may be used to obtain,

$$\mathrm{Im}\mathbf{T}^{-1}_{ij}(s) = -\delta_{ij}\theta(s-s_j). \tag{III.6}$$

Using (III.6) in (III.4), we have,

$$\mathrm{Im}\mathbf{D}_{ij}(s) = -\mathbf{N}_{ij}(s)\theta(s-s_i). \tag{III.7}$$

If we choose a normalization of $\mathbf{D}(s)$, such that $\mathrm{Re}\mathbf{D}(s)$ approaches the unit matrix as $s\to\infty$, then the analytic expression for $\mathbf{D}(s)$ in the complex plane is,

$$\mathbf{D}_{ij}(s) = \delta_{ij} - \frac{1}{\pi}\int_0^{\infty} \frac{\mathbf{N}_{ij}(s')\theta(s'-s_i)}{s'-s-i\varepsilon}\, ds'. \tag{III.8}$$

The physical value of $\mathbf{D}(s)$ is obtained by approaching the real s-axis from the upper half plane.

Since $\mathbf{D}(s)$ is real on the left-hand cuts, the imaginary part of $\mathbf{N}(s)$ may be similarly computed as,

$$\mathrm{Im}\mathbf{N}(s) = \mathrm{Im}\mathbf{T}(s)\mathbf{D}(s) \qquad s<s_L \tag{III.9}$$

where $s_L$ denotes the end point of the branch cut appropriate to each element of $\mathbf{T}(s)$. The function $\mathbf{N}(s)$ is therefore given by,

$$\mathbf{N}(s) = \frac{1}{\pi}\int_{-\infty}^{s_L} \frac{\mathrm{Im}\mathbf{T}(s')\mathbf{D}(s')}{s'-s-i\varepsilon}\, ds'. \qquad \text{(III.10)}$$

Note that $\mathbf{N}(s)\to 0$ as $s\to\infty$ to satisfy $\mathbf{T}(s)\to 0$ in the same limit.

**III.2** Muskhelishvili-Omnes Equation for multichannel case[53]

For n communicating intermediate states, we introduce the n-dimensional column vector $\mathbf{A}(s) \equiv (\mathbf{A}_i(s),\ i=1,\ldots n)$, formed of the n amplitudes for producing these states. In the following discussion, for convenience, we define a matrix $\hat{\theta}$, whose components are given by,

$$\hat{\theta}_{ij}(s) = \delta_{ij}\theta(s-s_i)$$

where $s_i$ denotes the threshold for the $i^{th}$ channel. The unitarity condition for the amplitudes $\mathbf{A}(s)$, takes the form,[57]

$$\mathrm{Im}\mathbf{A}(s) = \mathbf{T}^{\dagger}(s)\hat{\theta}(s)\mathbf{A}(s). \qquad \text{(III.11)}$$

As an example, consider two coupled channels, denoted by 1 and 2. The imaginary part of the amplitude of channel 1 will be given by,

$$\mathrm{Im}\mathbf{A}_1(s) = \mathbf{T}^{*}_{11}(s)\theta(s-s_1)\mathbf{A}_1(s)+\mathbf{T}^{*}_{12}(s)\theta(s-s_2)\mathbf{A}_2(s).$$

Using eq.(III.11), the unitarized (i.e. final state interactions corrected) amplitudes may be related to the ununitarized (uncorrected, weak) amplitudes through the following MO equations:

$$\mathbf{A}(s) = \mathbf{A}^{o}(s) + \frac{1}{\pi}\int_{0}^{\infty} \frac{\mathbf{T}^{\dagger}(s')\hat{\theta}(s')\mathbf{A}(s')}{s'-s-i\varepsilon}\, ds' \qquad \text{(III.12)}$$

$\mathbf{A}^{o}(s)$ are the real ununitarized amplitudes.

For single-channel elastic scattering this takes the simple form

$$\mathbf{A}(s) = \mathbf{A}^{o}(s) + \frac{1}{\pi}\int_{s_R}^{\infty} \frac{\mathbf{h}^{*}(s')\mathbf{A}(s')ds'}{s'-s-i\varepsilon} \qquad \text{(III.13)}$$

where, $\mathbf{h}(s)=e^{i\delta(s)}\sin\delta(s)$ for rescattering in the L=0 partial wave. The solution to the above is,

$$\mathbf{A}(s)=e^{i\delta(s)}\left[\mathbf{A}^{o}(s)\cos\delta(s) + \frac{e^{\sigma(s)}}{\pi}P\int_{s_R}^{\infty}\mathbf{A}^{o}(s')\frac{\sin\delta(s')e^{-\sigma(s')}}{s'-s}ds'\right] \qquad \text{(III.14)}$$

where, $$\sigma(s) = \frac{P}{\pi}\int_{s_R}^{\infty}\frac{\delta(s')ds'}{s'-s}\ .$$

The solution of the homogeneous equation (when allowed) can be added to the above. For small phase shifts, eq.(III.14) has the simple approximate form :

$$\mathbf{A}(s) \approx e^{i\delta(s)}\mathbf{A}^{o}(s). \qquad \text{(III.15)}$$

In the case of inelastic n-coupled channels, we seek a solution to eq.(III.12), in the region of energy, such that the two body channels of interest are all open. The parameter s must thus be greater than the maximum threshold. We define an n-dimensional column vector

$$\mathbf{F}(z) = \frac{1}{\pi}\int_{0}^{\infty}\frac{ds'}{s'-z}\mathbf{T}^{\dagger}(s')\hat{\theta}(s')\mathbf{A}(s'). \qquad \text{(III.16)}$$

Thus, we have,

$$\mathbf{A}(s) = \mathbf{A}^{o}(s) + \mathbf{F}(s+) \qquad \text{(III.17)}$$

where, $\mathbf{F}(s\pm) = \lim_{\varepsilon \to +0} \mathbf{F}(s\pm i\varepsilon)$ on the unitarity cuts. The discontinuity equation for $\mathbf{F}(z)$ can be written from eq.(III.16) as,

$$\mathbf{F}(s+) - \mathbf{F}(s-) = 2i\mathbf{T}^{\dagger}(s)\hat{\theta}(s)\mathbf{A}(s).$$

Using eqs.(III.3) & (III.17), we have,

$$\mathbf{F}(s+) - \mathbf{F}(s-) = 2i\tilde{\mathbf{D}}^{-1}(s-)\tilde{\mathbf{N}}(s+)\hat{\theta}(s)(\mathbf{A}^{\circ}(s)+\mathbf{F}(s+))$$

since, on the right-hand cut, $\mathbf{N}(s)$ is real and $\mathbf{D}^{*}(s)=\mathbf{D}(s-)$; $\tilde{\mathbf{D}}$, $\tilde{\mathbf{N}}$ denote the transpose of $\mathbf{D}$ and $\mathbf{N}$ respectively. Using eq.(III.7), this implies that,

$$\mathbf{F}(s+) - \mathbf{F}(s-) = 2i\tilde{\mathbf{D}}^{-1}(s-)(-\mathrm{Im}\tilde{\mathbf{D}}(s))(\mathbf{A}^{\circ}(s)+\mathbf{F}(s+)).$$

Rewriting this relation we have,

$$[\tilde{\mathbf{D}}(s-)+2i\mathrm{Im}\tilde{\mathbf{D}}(s)]\mathbf{F}(s+) - \tilde{\mathbf{D}}(s-)\mathbf{F}(s-) = -2i\mathrm{Im}\tilde{\mathbf{D}}(s)\mathbf{A}^{\circ}(s)$$

or,
$$\tilde{\mathbf{D}}(s+)\mathbf{F}(s+) - \tilde{\mathbf{D}}(s-)\mathbf{F}(s-) = -2i\mathrm{Im}\tilde{\mathbf{D}}(s)\mathbf{A}^{\circ}(s). \qquad \text{(III.18)}$$

A function of z which satisfies eq.(III.18) may be given by,

$$\tilde{\mathbf{D}}(z)\mathbf{F}(z) = -\frac{1}{\pi}\int_{0}^{\infty}\frac{\mathrm{Im}\tilde{\mathbf{D}}(s')\mathbf{A}^{\circ}(s')ds'}{s'-z} + \mathbf{P}(z) \qquad \text{(III.19)}$$

$\mathbf{P}(z)$ is a column vector of arbitrary polynomials. Eqs.(III.17) & (III.19) imply,

$$\mathbf{A}(s) = \mathbf{A}^{\circ}(s) - \frac{\tilde{\mathbf{D}}^{-1}(s)}{\pi}\int_{0}^{\infty}\frac{\mathrm{Im}\tilde{\mathbf{D}}(s')\mathbf{A}^{\circ}(s')ds'}{s'-z} + \tilde{\mathbf{D}}^{-1}\mathbf{P}(z). \qquad \text{...(III.20)}$$

We shall hereafter omit the polynomial term which gives a solution of the homogeneous equation[51] and restrict ourselves to the main term of the solution.

In the case of point interactions (eg. weak decays), the amplitudes $\mathbf{A}^{\circ}(s)$ are energy independent, hence,

eq.(III.20) reduces to,

$$\mathbf{A}(s) = \left[ 1 - \frac{\tilde{\mathbf{D}}^{-1}(s)}{\pi} \int_0^\infty \frac{\mathrm{Im}\tilde{\mathbf{D}}(s')ds'}{s'-s-i\varepsilon} \right] \mathbf{A}^0(s)$$

$$= \tilde{\mathbf{D}}^{-1}(s) \left[ \tilde{\mathbf{D}}(s) - \frac{1}{\pi} \int_0^\infty \frac{\mathrm{Im}\tilde{\mathbf{D}}(s')ds'}{s'-s-i\varepsilon} \right] \mathbf{A}^0(s).$$

Using eq.(III.8) in the above we get,

$$\mathbf{A}(s) = \tilde{\mathbf{D}}^{-1}(s)\mathbf{A}^0(s). \qquad \text{(III.21)}$$

Further, for a symmetric **D** matrix, we may write,

$$\mathbf{A}(s) = \mathbf{D}^{-1}(s)\mathbf{A}^0(s). \qquad \text{(III.22)}$$

It may be noted that this solution has several ambiguities. They come in the form of: (i)Polynomial ambiguity (see eq.(III.19)). (ii)Ambiguities arising from the presence of simple poles in **D**(s) (CDD[58] ambiguity). (iii) The normalization of the amplitude **A**(s).

III.3 A K-Matrix model.

The prescription in eq.(III.22) to determine the unitarized amplitudes in a multi-channel scattering problem requires the evaluation of the **D** matrix. At the mass scale of heavy flavor decays, there is as yet very little experimental information available regarding hadron-hadron scattering. Hence the **D** matrix is completely unknown. A simple approach is to write the **D** matrix in terms of the **K** matrix formalism.[26] In terms of the **K** matrix **S** is written as,

$$\mathbf{S}(s) = (1-i\mathbf{K}(s))^{-1}(1+i\mathbf{K}(s)) \qquad \text{(III.23)}$$

**K** must be hermitian to ensure the unitarity of **S**. Now, since

$$\mathbf{T}(s) = \left(\frac{\mathbf{S}(s)-1}{2i}\right),$$

using, eq.(III.23) in the above we get,

$$\mathbf{T}(s) = \mathbf{K}(s)(1-i\mathbf{K}(s))^{-1}. \qquad \text{(III.24)}$$

Time reversal invariance requires that $\mathbf{T}(s)$ be symmetric, hence $\mathbf{K}(s)$ must also be symmetric. Further, since $\mathbf{K}(s)$ is hermitian this implies that $\mathbf{K}(s)$ is a real symmetric matrix. For a system with n channels, whereas the $\mathbf{T}$ matrix would have $n(n+1)/2$ complex elements, the $\mathbf{K}$ matrix has the same number of independent real elements. The $\mathbf{K}$ matrix formalism therefore provides an economical parameterization method.

It can easily be shown that eq.(III.24) can also be written in the form,

$$\mathbf{T}(s) = (1-i\mathbf{K}(s))^{-1}\mathbf{K}(s) .$$

Using eq.(III.3) and the above relation we have

$$\mathbf{K}(s) = (1-i\mathbf{K}(s))\mathbf{N}(s)\mathbf{D}^{-1}(s)$$

which may be rewritten as

$$\mathbf{K}(s)[1+i\mathbf{N}(s)\mathbf{D}^{-1}(s)] = \mathbf{N}(s)\mathbf{D}^{-1}(s).$$

Hence,
$$\mathbf{K}(s) = \mathbf{N}(s)\mathbf{D}^{-1}(s)[1+i\mathbf{N}(s)\mathbf{D}^{-1}(s)]^{-1}$$
$$= \mathbf{N}(s)[(1+i\mathbf{N}(s)\mathbf{D}^{-1}(s))\mathbf{D}(s)]^{-1}.$$

Using eq.(III.7) in the above gives the following form for $\mathbf{K}(s)$.

$$\mathbf{K}(s) = \mathbf{N}(s)[\mathrm{Re}\mathbf{D}(s)]^{-1}. \qquad \text{(III.25)}$$

Note that since $\mathbf{N}(s)$ is real in the physical region, the above implies that $\mathbf{K}(s)$ is real, as desired.

By comparing eqs.(III.3) & (III.24) one also finds that a simple choice[22] for the $\mathbf{D}$ function is

$$\mathbf{D}(s) = \mathbf{1} - i\mathbf{K}(s). \qquad \text{(III.26)}$$

In this model, the unitarized amplitude will then be given by,

$$\mathbf{A}^{u}(s) = (\mathbf{1} - i\mathbf{K}(s))^{-1}\mathbf{A}^{o}(s) \qquad \text{(III.27)}$$

where we have introduced the superscript u to denote unitarized amplitude for clarity. The above choice of the **D** function is not unique, though it has the property, that in the limit the strong interactions are turned off, i.e., $\mathbf{K}(s)\to 0$, $\mathbf{D}(s)\to \mathbf{1}$, one recovers the un-unitarized amplitude. The enhancement factor $(\mathbf{D}^{-1}(s))$ in eq.(III.27) has the virtue of yielding the behavior expected[19] in the presence of a resonance that couples to the two-body channels under consideration. If such a state is represented by a pole in the **K**-matrix, then the form $(\mathbf{1}-i\mathbf{K})^{-1}$ corresponds to summing the geometric series shown in Fig. 3.

**Fig. 3** The geometric series that sums to $\mathbf{D}^{-1}(s)$. The broken line represents the decaying heavy meson, thin solid lines represent final state hadrons, which are assumed to scatter via a resonance (thick solid line).

The unitarization prescription of eq.(III.27) requires a suitable parameterization of the **K** matrix. In the next

chapter, we give the form of the **K** matrix and use this model to evaluate the unitarized amplitudes for various D, $D_s$ decay modes.

## IV. A COUPLED CHANNEL TREATMENT OF CHARMED MESON HADRONIC DECAYS

Considerable progress[7,8] has been made in our understanding of charmed meson decays in recent years. An economical model[27] which uses factorization, $\xi=0$ ($\xi=1/N_c$ for $N_c$ colors) and no weak (or direct) annihilation has been able to explain most of the two-body data with a consistent set of parameters. Although this description is quite successful in reproducing the data, the chapter on heavy flavor decays is far from closed. Relevant questions, like the real strength of weak annihilation and the role of final state interactions are still unanswered.

In the above, by 'weak annihilation' or 'direct annihilation', we mean W-annihilation, or flavor annihilation through W-exchange (see Fig.1), at the quark level. Annihilation type graphs also emerge through final state interactions, where a single resonance may couple to various hadronic channels. In these rescattering diagrams, the annihilation occurs due to the strong interactions with a typical range of one fermi and not due to the point-like weak interactions, thus it is clearly distinct from weak annihilation.

A search for the process $D^0 \to \bar{K}^0 \phi$ was originally proposed by Bigi and Fukugita[50] as a 'smoking gun' test of the existence of exclusive non-spectator processes (one needs to

get rid of both the c and $\bar{u}$ quarks in the initial state, since neither appears in the final hadrons). It is now believed,[20] however, that such a final state can be generated without W exchange, through rescattering effects. Another decay mode which cannot arise through a spectator process is that of $D_s^+ \to \rho^0 \pi^+$. In ref.[27] it was argued that any weak annihilation contribution would conflict with the low decay rate for $D_s^+ \to \rho^0 \pi^+$. We wish to point out that final state interactions could conceivably conspire with weak annihilation in such a way that the transition $D_s^+ \to \rho^0 \pi^+$ is interfered away. Thus direct annihilation processes could occur, though possibly at a reduced rate. However, no quantitative conclusions regarding it can be made without the simultaneous inclusion of final state rescattering effects.

In the following we perform a coupled channel final state interaction calculation for various D, $D_s$ decays. The annihilation contribution to the weak amplitude is taken as a parameter, since a reliable estimate for it is not possible. The layout of this chapter is as follows. In sect.IV.1, we describe the **K**-matrix parameterization[22] used for unitarizing the weak decay amplitudes. In sect.IV.2 we show the calculation of un-unitarized amplitudes. A coupled channel treatment[22] of Cabibbo-angle favored $D_s^+ \to VP$ decays is presented in sect.IV.3. Sect.IV.4 discusses the coupled channel treatment[22] for $D \to VP$ decays. Sect. IV.5 deals with the $D, D_s \to VV$ modes, while IV.6 treats the Cabibbo-suppressed

D→VP decays.

## IV.1 K-Matrix Parameterization

As discussed in the last chapter, we unitarize the weak decay amplitudes $\mathbf{A}^0(s)$ ($\sqrt{s}$ is finally set equal to the charmed meson mass) through,

$$\mathbf{A}^U(s)=(\mathbf{1}-i\mathbf{K}(s))^{-1}\mathbf{A}^0(s) \qquad \text{(IV.1)}$$

Since strong interactions conserve isospin and G-parity, the above equation has to be written for each isospin and G-parity (where it can be defined), separately.

In the case of a single channel, we choose

$$\mathbf{K}(s)=ka \qquad \text{(IV.2)}$$

where, k is the center of mass (c.m.) momentum in the channel and $a$ is a constant. Using eq.(III.23), the **S** matrix, then has the form,

$$\mathbf{S}(s) = (1-ika)^{-1}(1+ika) \qquad \text{(IV.3)}$$

Also,

$$\mathbf{S}(s) = e^{2i\delta}, \qquad \text{(IV.4)}$$

where $\delta$ is the phase shift. Equating eqs.(IV.3) & (IV.4), we have the following zero range formula,[59]

$$k\cot\delta = 1/a. \qquad \text{(IV.5)}$$

The parameter $a$, thus represents the scattering length. For a two-channel problem we generalize the **K**-matrix in eq.(IV.2) to have the real symmetric form

$$\mathbf{K}(s) = \begin{bmatrix} k_1 b & \sqrt{k_1 k_2}\,c \\ \sqrt{k_2 k_1}\,c & k_2 a \end{bmatrix} \qquad \text{(IV.6)}$$

where $a$, $b$ and $c$ are real functions of the energy. Again, if they are energy independent one is led to the zero-range

approximation;[60] $k_1$ and $k_2$ are the c.m. momenta in the two open channels. In channels that do not resonate we shall use the parameterization of eq.(IV.6) with energy independent parameters *a*, *b* and *c*.

For two coupled channels that resonate, we employ a single resonance approximation for the **K**-matrix,

$$\mathbf{K}(s) = \frac{1}{m_R^2 - s} \begin{bmatrix} k_1\Gamma_{11} & \sqrt{k_1 k_2}\Gamma_{12} \\ \sqrt{k_2 k_1}\Gamma_{21} & k_2\Gamma_{22} \end{bmatrix} \qquad \text{(IV.7)}$$

where $m_R$ is the mass of the resonance and s the c.m. $(\text{energy})^2$ of the two-body system. $\Gamma_{ij}$ are related to the coupling of the resonance to the channels i and j as will become clear in the following.

Eq. (IV.7) involves three parameters, assuming that $m_R$ is known. From the **K**-matrix parameterization in eq.(IV.7) one can construct the **T**-matrix using eq.(III.24). For example, the diagonal element $T_{11}$ is given by,

$$T_{11}(s) = \left( -i\det\mathbf{K} + \frac{k_1\Gamma_{11}}{m_R^2 - s} \right) \left(1 - \det\mathbf{K} - i\,\mathrm{Tr}\mathbf{K}\right)^{-1}. \qquad \text{(IV.8)}$$

If we set det **K**=0, i.e., $\Gamma_{11}\Gamma_{22}=\Gamma_{12}^2$, eq.(IV.8) takes on a simple factorized form[61] (by a factorized form we mean $T_{ij} \propto \Gamma_{ij}$)

$$T_{11} = \left( \frac{k_1\Gamma_{11}}{m_R^2 - s} \right) \left(1 - i\ \mathrm{Tr}\mathbf{K}\right)^{-1}. \qquad \text{(IV.9)}$$

On comparing eq.(IV.9) with the Breit-Wigner form, it is clear that Tr**K** is related to the total width of the resonance and $\Gamma_{11}$ to the partial width in channel 1. The

total width of the resonance, $\Gamma_R$ is given by

$$m_R\Gamma_R = k_1\Gamma_{11}+k_2\Gamma_{22} \qquad \text{(IV.10)}$$

Thus for a resonant parameterization, the condition $\Gamma_{11}\Gamma_{22}=\Gamma_{12}^2$, reduces the number of parameters from three to two. Finally, fixing the total width of the resonance reduces the number of free parameters to one.

For a three channel problem, the **K**-matrix of eq.(IV.6) or (IV.7) is extended to a real symmetric 3×3 form. We discuss here in some detail how we reduce the number of free parameters in the case of a resonant parameterization of the **K**-matrix. The real symmetric **K**-matrix we choose is given by,

$$\mathbf{K}(s) = \frac{1}{m_R^2-s}\begin{bmatrix} k_1\Gamma_{11} & \sqrt{k_1k_2}\Gamma_{12} & \sqrt{k_1k_3}\Gamma_{13} \\ \sqrt{k_2k_1}\Gamma_{21} & k_2\Gamma_{22} & \sqrt{k_2k_3}\Gamma_{23} \\ \sqrt{k_3k_1}\Gamma_{31} & \sqrt{k_3k_2}\Gamma_{32} & k_3\Gamma_{33} \end{bmatrix} \qquad \text{(IV.11)}$$

$k_i$ is the magnitude of the c.m. momentum of channel i. There are 6 independent parameters $\Gamma_{ij}$, assuming that $m_R$ is known. To reduce the independent parameters to a manageable number we generalize the factorization condition of the two-channel case by requiring that the diagonal factors of eq.(IV.11) vanish. This leads us to three conditions.

$$\Gamma_{11}\Gamma_{22}=\Gamma_{12}^2, \qquad \Gamma_{11}\Gamma_{33}=\Gamma_{13}^2, \qquad \Gamma_{22}\Gamma_{33}=\Gamma_{23}^2 . \qquad \text{(IV.12)}$$

In addition we impose the condition det **K**=0 which together with eq.(IV.12) implies,

$$\Gamma_{11}\Gamma_{22}\Gamma_{33}=\Gamma_{12}\Gamma_{13}\Gamma_{23}. \qquad \text{(IV.13)}$$

Eq.(IV.13) restricts the choice of the sign of $\Gamma_{12}$, $\Gamma_{13}$ and

$\Gamma_{23}$ obtained from eq.(IV.12). Eqs.(IV.12) and (IV.13) factorize the diagonal elements of the **T**-matrix but not the off diagonal ones. A condition similar to eq.(IV.10) is imposed on the diagonal $\Gamma_{ii}$ for the three channel case,

$$m_R\Gamma_R = \sum_{i=1}^{3} k_i \Gamma_{ii} \qquad \text{(IV.14)}$$

where $\Gamma_R$ is the total width of the resonance and $m_R$ its mass. Conditions (IV.12) & (IV.14) provide us with four constraints on six parameters. Note that the eq.(IV.13) is consistent with eq.(IV.12) and restricts only the sign of $\Gamma_{ij}$. Thus we have reduced the number of independent parameters to two.

**IV.2** Calculation of Un-unitarized Amplitudes

For Cabibbo-angle favored decays, the un-unitarized amplitudes $\mathbf{A}^{O}(s)$ are generated through the following Hamiltonian:

$$H_{NL}^{eff}(\Delta C=-1) = \frac{G_F}{\sqrt{2}}\cos^2\theta_c [a_1(\bar{s}c)_{L,H}(\bar{u}d)_{L,H} + a_2(\bar{s}d)_{L,H}(\bar{u}c)_{L,H}] \qquad \text{...(IV.15)}$$

The corresponding Hamiltonian for Cabibbo-suppressed decays is given by,

$$H_{NL}^{eff}(\Delta C=-1) = \frac{G_F}{\sqrt{2}}\cos\theta_c \sin\theta_c \Big\{a_1[(\bar{s}c)_{L,H}(\bar{u}s)_{L,H} - (\bar{d}c)_{L,H}(\bar{u}d)_{L,H}] + a_2[(\bar{s}s)_{L,H}(\bar{u}c)_{L,H} - (\bar{d}d)_{L,H}(\bar{u}c)_{L,H}]\Big\} \qquad \text{...(IV.16)}$$

For two-body decays of the type I→PP, PV or VV (I is the initial state pseudoscalar meson), the factorization

assumption (see sect II.4), allows the matrix elements of $H_{NL}^{eff}$ to be written in terms of the meson decay constants and hadron matrix elements. The decay constants are defined through,

$$\langle P|J_\mu|0\rangle = -if_P k_\mu \quad \text{and} \quad \langle V|J_\mu|0\rangle = \varepsilon_\mu f_V m_V \qquad \text{(IV.17)}$$

From Lorentz invariance, Bauer, Stech and Wirbel[17] write down the following form factor decomposition for the hadron matrix elements,

$$\langle P|J_\mu|I\rangle = (P_I+P_P - \frac{m_I^2-m_P^2}{q^2} q)_\mu F_1(q^2) + \frac{m_I^2-m_P^2}{q^2} q_\mu F_0(q^2) \qquad \text{...(IV.18)}$$

with $q_\mu = (P_I-P_P)_\mu$ and $F_1(0) = F_0(0)$. $F_0(q^2)$ and $F_1(q^2)$ denote longitudinal and transverse formfactors respectively; in the case of I decaying into a vector meson, four form factors appear, and the decomposition is written in the form,[17]

$$\langle V|J_\mu|I\rangle = \frac{2}{m_I+m_V} \varepsilon_{\mu\nu\rho\sigma} \varepsilon^\nu P_I^\rho P_V^\sigma V(q^2)$$
$$+ i\Big\{\varepsilon_\mu (m_I+m_V) A_1(q^2) - \frac{\varepsilon\cdot q}{(m_I+m_V)} (P_I+P_V)_\mu A_2(q^2)$$
$$- \frac{\varepsilon\cdot q}{q^2} 2m_V q_\mu A_3(q^2)\Big\} + i\frac{\varepsilon\cdot q}{q^2} 2m_V q_\mu A_0(q^2) \qquad \text{...(IV.19)}$$

where $A_3(0)=A_0(0)$, $A_3(q^2)$ denotes,

$$A_3(q^2) = \frac{(m_I+m_V)}{2m_V} A_1(q^2) - \frac{(m_I-m_V)}{2m_V} A_2(q^2),$$

$\varepsilon_\mu$ denotes the polarization vector of the outgoing vector meson and here, $q_\mu=(P_I-P_V)_\mu$.

The $q^2$ dependence of the various form factors $F_i(q^2)$, $A_i(q^2)$ and $V(q^2)$ is assumed[17] to be dominated by the nearest pole (of mass m), i.e., they have the form

$$\simeq \frac{h}{1-q^2/m^2} .$$

This ansatz ensures asymptotic ($q^2 \to \infty$) current conservation. In the limit of exact SU(3) symmetry, h's are unity; h's are therefore a measure of SU(3) breaking. The form factor decomposition in eqs.(IV.18) & (IV.19) has been done in such a way that each formfactor is dominated by one pole only: the vector formfactors $F_0$ and $(F_1,V)$ by the $0^+$ and $1^-$ poles and the axial vector formfactors $A_0$ and $(A_1,A)_2$ by the $0^-$ and $1^+$ poles, respectively. Although the precise positions of most poles are not known, however, approximate values are sufficient in most cases. For numerical calculations we use the mass values as given by Wirbel et. al.[17] (see Appendix A). The residues of the pole terms, h's are determined by the overlap integral of the appropriate hadronic wave function as obtained in a relativistic harmonic oscillator model. These have been evaluated in ref.[17] (Appendix A).

The spectator part of the PV decay amplitudes involve the following type of terms:

(i). $$A_{PV}(I\to P) \equiv \langle V|J_\mu|0\rangle\langle P|J_\mu|I\rangle.$$

Using eqs. (IV.17) & (IV.18), we get

$$A_{PV}(I\to P)=\left[\left(P_I+P_P-\frac{m_I^2-m_P^2}{q^2}\,q\right)_\mu F_1(q^2) + \frac{m_I^2-m_P^2}{q^2}\,q_\mu F_0(q^2)\right]\varepsilon^\mu m_V f_V.$$

Since, $q_\mu=(P_I-P_P)_\mu=P_{V_\mu}$, $q\cdot\varepsilon=0$. Hence, we have

$$A_{PV}(I\to P) = (P_I+P_P)\cdot\varepsilon\ m_V f_V F_1(q^2)$$
$$= 2m_V f_V F_1(q^2)\ \varepsilon\cdot k \qquad \text{(IV.20)}$$

where k is the momentum of the pseudoscalar meson and

$$F_1(q^2) = \frac{h_{F1}}{1-q^2/m_1^2}$$

$m_1$- is the vector pole for the appropriate current $J_\mu$.

(ii). $A_{PV}(I\to V) \equiv \langle P|J_\mu|0\rangle\langle V|J_\mu|I\rangle$.

Eqs. (IV.17) & (IV.19), imply that

$$A_{VP}(I\to V) = (-if_P P_P^\mu)\left[\frac{2}{m_I+m_V}\varepsilon_{\mu\nu\rho\sigma}\,\varepsilon^\nu\,P_I^\rho\,P_V^\sigma\,V(q^2)\right.$$
$$+ i\left\{\varepsilon_\mu(m_I+m_V)A_1(q^2) - \frac{\varepsilon\cdot q}{(m_I+m_V)}(P_I+P_V)_\mu A_2(q^2)\right.$$
$$\left.\left. - \frac{\varepsilon\cdot q}{q^2}\,2m_V q_\mu A_3(q^2)\right\} + i\frac{\varepsilon\cdot q}{q^2}\,2m_V q_\mu A_0(q^2)\right]$$

or,

$$A_{VP}(I\to V) = f_P\left\{\varepsilon\cdot P_P(m_I+m_V)A_1(q^2) - \frac{\varepsilon\cdot q}{(m_I+m_V)}(P_I+P_V)\cdot P_P A_2(q^2)\right.$$
$$\left. - \frac{\varepsilon\cdot q}{q^2}\,2m_V q\cdot P_P A_3(q^2) + \frac{\varepsilon\cdot q}{q^2}\,2m_V q\cdot P_P A_0(q^2)\right\}.$$

Here, $P_{P\mu}=(P_I-P_V)_\mu=q_\mu$, therefore, $(P_I+P_V)\cdot P_P=m_I^2-m_V^2$ and we have,

$$A_{VP}(I\to V) = f_P\left\{\varepsilon\cdot q(m_I+m_V)A_1(q^2) - \varepsilon\cdot q(m_I-m_V)A_2(q^2)\right.$$
$$- \varepsilon\cdot q 2m_V\left[\frac{m_I+m_V}{2m_V}A_1(q^2) - \frac{m_I-m_V}{2m_V}A_2(q^2)\right]$$
$$\left. + (\varepsilon.q)\,2m_V A_0(q^2)\right\}$$
$$= 2m_V f_P(\varepsilon\cdot k)A_0(q^2). \qquad \text{(IV.21)}$$

where, $$A_0(q^2) = \frac{h_{A0}}{1- q^2/m_{0^-}^2}$$

and $m_{0^-}$ is the pseudoscalar pole of the appropriate current.

For VV decays, the spectator contribution to the amplitude will only involve the following type of term,

$$A_{VV}(I\to V_1) \equiv \langle V_2|J^\mu|0\rangle\langle V_1|J_\mu|I\rangle$$

$$= \varepsilon_2^\mu m_{V2} f_{V2}\left[ \frac{2}{m_I+m_{V1}} \varepsilon_{\mu\nu\rho\sigma}\, \varepsilon_1^\nu\, P_I^\rho\, P_{V1}^\sigma V(q^2) \right.$$

$$+ i\left\{\varepsilon_{1\mu}(m_I+m_{V1})A_1(q^2) - \frac{\varepsilon_1\cdot q}{(m_I+m_{V1})}(P_I+P_{V1})_\mu A_2(q^2)\right.$$

$$\left.\left. - \frac{\varepsilon_1\cdot q}{q^2}\, 2m_{V1} q_\mu A_3(q^2)\right\} + i\frac{\varepsilon_1\cdot q}{q^2}\, 2m_{V1} q_\mu A_0(q^2)\right]$$

Since, $q_\mu = P_I - P_{V1} = P_{V2}$, $\varepsilon_2\cdot q = 0$, therefore we have,

$$A_{VV}(I\to V_1) = \frac{2m_{V2} f_{V2}}{m_I+m_{V1}} \varepsilon_{\mu\nu\rho\sigma}\, \varepsilon_1^\nu\, \varepsilon_2^\mu\, P_I^\rho\, P_{V1}^\sigma V(q^2)$$

$$+ i m_{V2} f_{V2}\left\{\varepsilon_1\cdot\varepsilon_2 (m_I+m_{V1})A_1(q^2)\right.$$

$$\left. - \frac{\varepsilon_1\cdot q}{(m_I+m_{V1})}(P_I+P_{V1})\cdot\varepsilon_2 A_2(q^2)\right\} \qquad \text{(IV.22)}$$

where,

$$V(q^2) = \frac{h_V}{1-q^2/m_{1^-}^2}, \quad A_1(q^2) = \frac{h_{A1}}{1-q^2/m_{1^+}^2} \quad \& \quad A_2(q^2) = \frac{h_{A2}}{1-q^2/m_{1^+}^2},$$

and $m_{1^-}$, $m_{1^+}$ are the vector and axial vector poles of the appropriate currents respectively. Eqs.(IV.20)-(IV.22) can be used to determine the un-unitarized amplitudes for all the decay modes which are listed in Table 1 (where the annihilation contribution is left as a parameter).

The un-unitarized amplitudes depend on the parameters $a_1$ and $a_2$. We evaluate $a_2$ for a chosen value of the ratio $a_1/a_2$ and $\xi$, as follows. Recall that (see eqs.(II.26) & (II.47)),

$$a_{1,2} = \frac{1}{2}\,[(c_+ \pm c_-) + \xi(c_+ \mp c_-)]. \qquad \text{(IV.23)}$$

Rewriting the above we have,

$$a_{1,2} = \frac{1}{2}\,[(1+\xi)c_+ \pm (1-\xi)c_-],$$

which gives the following relation for $c_-/c_+$,

$$\frac{c_-}{c_+} = \left(\frac{1+\xi}{1-\xi}\right)\left(\frac{a_1/a_2-1}{a_1/a_2+1}\right) \qquad \text{(IV.24)}$$

Also, using eq.(IV.23), we have

$$(a_1+a_2)(a_1-a_2) = (1-\xi^2)c_+c_-$$

Therefore,

$$c_+c_- = \frac{a_1^2-a_2^2}{1-\xi^2} = \frac{a_2^2[(a_1/a_2)^2-1]}{1-\xi^2}$$

or,
$$c_+^3\, c_-^3 = \left\{\frac{a_2^2[(a_1/a_2)^2-1]}{1-\xi^2}\right\}^3 = \frac{c_-}{c_+}\,, \qquad \text{(IV.25)}$$

where we have used the perturbative constraint,[62] $c_+^2 c_- = 1$. Equating (IV.24) & (IV.25), we get

$$a_2^6 = \frac{(1+\xi)^4(1-\xi)^2}{(a_1/a_2-1)^2(a_1/a_2+1)^4}\,.$$

Hence,

$$a_2 = \frac{(1+\xi)^{2/3}(1-\xi)^{1/3}}{(a_1/a_2-1)^{1/3}(a_1/a_2+1)^{2/3}}\,. \qquad \text{(IV.26)}$$

Once the ratio $a_1/a_2$ and $\xi$ are chosen, $a_2$ is calculated through the above equation, to be used in the un-unitarized amplitudes $\mathbf{A}^o(s)$ shown in Table 1. The unitarized amplitudes $\mathbf{A}^u(s)$ are then generated through eq. (IV.1).. Finally, the

**Table 1.** Un-unitarized amplitudes for D, $D_s \to VP$ decays. Multiply each amplitude by $G_F \cos^2\theta_c/\sqrt{2}a_2$. R, $R_s$ are the annihilation terms.

| Mode | Un-unitarized Amplitudes |
|---|---|
| $D_s^+ \to \rho^0\pi^+, \rho^+\pi^0$ | $-\frac{R_s}{\sqrt{2}}, \frac{R_s}{\sqrt{2}}$ |
| $D_s^+ \to K^{*+}\bar{K}^0$ | $2f_K m_{K^*}\frac{h_{A0}(D_s\to K)}{1-q^2/m_D^2} - \frac{R_s}{2}$ |
| $D_s^+ \to K^+\bar{K}^{*0}$ | $2f_{K^*}m_{K^*}\frac{h_{F1}(D_s\to K)}{1-q^2/m_{D^*}^2} + \frac{R_s}{2}$ |
| $D_s^+ \to \phi\pi^+$ | $(a_1/a_2)2f_\pi m_\phi \frac{h_{A0}(D_s\to\phi)}{1-q^2/m_{D_s}^2}$ |
| $D_s^+ \to \omega\pi^+$ | 0 |
| $D^0 \to \bar{K}^0\rho^0$ | $\sqrt{2}f_K m_\rho \frac{h_{A0}(D\to\rho)}{1-q^2/m_D^2} - \frac{R}{\sqrt{2}}$ |
| $D^0 \to K^-\rho^+$ | $(a_1/a_2)2f_\rho m_\rho \frac{h_{F1}(D\to K)}{1-q^2/m_{D_s}^2} + R$ |
| $D^0 \to \bar{K}^{*0}\pi^0$ | $\sqrt{2}f_{K^*}m_{K^*}\frac{h_{F1}(D\to\pi)}{1-q^2/m_{D^*}^2} + \frac{R}{\sqrt{2}}$ |
| $D^0 \to K^{*-}\pi^+$ | $(a_1/a_2)2f_\pi m_{K^*}\frac{h_{A0}(D\to K^*)}{1-q^2/m_{D_s}^2} - R$ |
| $D^0 \to \bar{K}^0\phi$ | R |
| $D^0 \to \bar{K}^{*0}\eta$ | $\frac{1}{\sqrt{6}}\left\{ 2f_{K^*}m_{K^*}\frac{h_{F1}(D\to\eta)}{1-q^2/m_{D^*}^2} - 3R \right\}$ |
| $D^0 \to \bar{K}^0\omega$ | $\frac{1}{\sqrt{2}}\left\{ 2f_K m_\omega \frac{h_{A0}(D\to\omega)}{1-q^2/m_D^2} + R \right\}$ |
| $D^+ \to \bar{K}^{*0}\pi^+$ | $(a_1/a_2)2f_\pi m_{K^*}\frac{h_{A0}(D\to K^*)}{1-q^2/m_{D_s}^2} + 2f_{K^*}m_{K^*}\frac{h_{F1}(D\to\pi)}{1-q^2/m_{D^*}^2}$ |
| $D^+ \to \bar{K}^0\rho^+$ | $(a_1/a_2)2f_\rho m_\rho \frac{h_{F1}(D\to K)}{1-q^2/m_{D_s}^2} + 2f_K m_\rho \frac{h_{A0}(D\to\rho)}{1-q^2/m_D^2}$ |

branching ratios are calculated as follows,

$$B(I\to VP) = \tau_I \frac{|A^u(I\to VP)|^2\ k^3}{8\pi m_v^2} \qquad \text{(IV.27)}$$

Note that in VP decays all amplitudes have the $(\varepsilon\cdot k)$ form, i.e., they involve P-waves (L=1) only, giving rise to the above $k^3$ form in the decay rate. VV decays, on the other hand involve more than one partial wave and hence a simple form for it's decay rate is not possible. For details see Appendix B.

We wish to make the following remarks regarding the ratio $a_1/a_2$. It was argued in ref.[27] from a fit to $D\to K\pi$ that the ratio $a_1/a_2$ lies roughly in the range $-3.3 \lesssim a_1/a_2 \lesssim -2.0$. In ref.[21] the branching ratios $B(D^0\to\bar{K}^0K^+)$ and $B(D^0\to\bar{K}^0\pi^+)$, neither of which involve annihilation process, were used to limit $a_1/a_2$ to be in the range $-4.1 \lesssim a_1/a_2 \lesssim -2.4$. These two observations are mutually consistent.

To evaluate the values of $c_+$, $c_-$ and the ratio $a_1/a_2$ we use the next to leading log (NLL) formula (eq.(II.25)), scaled down to the charm mass scale, as follows,

$$\begin{aligned} c_\pm^{NLL} = &\left(\frac{\alpha_s(\mu^2)}{\alpha_s(m_b^2)}\right)^{d_\pm/2b_4}\left\{1+\frac{\alpha_s(\mu^2)-\alpha_s(m_b^2)}{\pi}\rho_\pm(4)\right\} \\ &\times\left(\frac{\alpha_s(m_b^2)}{\alpha_s(m_t^2)}\right)^{d_\pm/2b_5}\left\{1+\frac{\alpha_s(m_b^2)-\alpha_s(m_t^2)}{\pi}\rho_\pm(5)\right\} \\ &\times\left(\frac{\alpha_s(m_t^2)}{\alpha_s(m_W^2)}\right)^{d_\pm/2b_6}\left\{1+\frac{\alpha_s(m_t^2)-\alpha_s(M_W^2)}{\pi}\rho_\pm(6)\right\}. \end{aligned} \qquad \text{...(IV.28)}$$

For reasonable values of the Q.C.D parameters $\mu$ and $\Lambda$ we

**Table 2.** Next to leading log estimates of Q.C.D. coefficients with $m_t$=50GeV.

| | | | | $a_1/a_2$ | |
|---|---|---|---|---|---|
| $\Lambda$(GeV) | $\mu$(GeV) | $C_+$ | $C_-$ | $\xi$=0 | $\xi$=1/3 |
| | 1.2 | 0.787 | 1.636 | -2.854 | -55.77 |
| 0.1 | 1.5 | 0.803 | 1.570 | -3.094 | +88.22 |
| | 1.8 | 0.815 | 1.523 | -3.302 | +29.47 |
| | 1.2 | 0.753 | 1.793 | -2.448 | -11.49 |
| 0.2 | 1.5 | 0.775 | 1.688 | -2.697 | -23.46 |
| | 1.8 | 0.791 | 1.617 | -2.915 | -91.40 |
| | 1.2 | 0.713 | 2.010 | -2.099 | -5.88 |
| 0.3 | 1.5 | 0.742 | 1.848 | -2.342 | -9.15 |
| | 1.8 | 0.762 | 1.745 | -2.550 | -14.79 |
| | 1.2 | 0.661 | 2.363 | -1.777 | -3.540 |
| 0.4 | 1.5 | 0.699 | 2.102 | -1.996 | -4.971 |
| | 1.8 | 0.724 | 1.950 | -2.181 | -6.769 |
| | 1.2 | 0.614 | 2.752 | -1.574 | -2.611 |
| 0.5 | 1.5 | 0.665 | 2.332 | -1.798 | -3.655 |
| | 1.8 | 0.697 | 2.113 | -1.984 | -4.877 |

determine $c_+$, $c_-$ and $a_1/a_2$ and list these values in Table 2 for both $\xi$=0 and $\xi$=1/3. It is clear from this tabulation that for $\xi$=0, a value of $a_1/a_2$ in the interval required by data is easily secured perturbatively with $\Lambda \leq 0.3$ GeV and reasonable values of $\mu$. Deep inelastic data require[10] 0.1 GeV $\leq \Lambda \leq$ 0.3 GeV. For $\xi$=1/3, a value of $a_1/a_2$ in the desired range can be secured in an NLL calculation, only by raising $\Lambda$ to about 0.5 GeV (or by lowering $\mu$ below the range shown in table 2). An alternate way to secure the desired value of $a_1/a_2$ would be if $c_+$ and $c_-$ were to receive significant nonperturbative corrections. Since in deriving the relation (IV.26) between $a_2$ and $a_1/a_2$ for a given value

of $\xi$ we have used the perturbative constraint $c_+^2\, c_- \approx 1$, we shall have no more to say about the possibility that $c_+$ and $c_-$ have significant non perturbative contributions.

**IV.3** Cabibbo-angle favored $D_s^+ \to VP$ decays

We shall consider the following Cabibbo-angle favored decays: $D_s^+ \to \rho^0\pi^+$, $\rho^+\pi^0$, $\phi\pi^+$, $K^+\bar{K}^{*0}$ and $K^{*+}\bar{K}^0$. Using eqs.(IV.20) & (IV.21) the weak amplitudes for these decays are evaluated as follows:

$$A(D_s^+\to K^+\bar{K}^{*0}) = \frac{G_F}{\sqrt{2}}\cos^2\theta_c\{a_1\langle K^+\bar{K}^{*0}|\bar{u}d|0\rangle\langle 0|\bar{s}c|D_s^+\rangle + a_2\langle\bar{K}^{*0}|\bar{s}d|0\rangle\langle K^+|\bar{u}c|D_s^+\rangle\}$$

$$= \frac{G_F}{\sqrt{2}}\cos^2\theta_c\left\{\frac{-a_1 r}{2} + a_2 2f_{K^*} m_{K^*}\frac{h_{F1}(D_s\to K)}{1-q^2/m_{D_s^*}^2}\right\}(\varepsilon\cdot k)$$

where r is the annihilation parameter,

$$A(D_s^+\to K^{*+}\bar{K}^0) = \frac{G_F}{\sqrt{2}}\cos^2\theta_c\{a_1\langle K^{*+}\bar{K}^0|\bar{u}d|0\rangle\langle 0|\bar{s}c|D_s^+\rangle + a_2\langle\bar{K}^0|\bar{s}d|0\rangle\langle K^{*+}|\bar{u}c|D_s^+\rangle\}$$

$$= \frac{G_F}{\sqrt{2}}\cos^2\theta_c\left\{\frac{a_1 r}{2} + a_2 2f_K m_{K^*}\frac{h_{A0}(D_s\to K^*)}{1-q^2/m_{D_s}^2}\right\}(\varepsilon\cdot k)$$

$$A(D_s^+\to\rho^0\pi^+) = \frac{G_F}{\sqrt{2}}\cos^2\theta_c\{a_1\langle\rho^0\pi^+|\bar{u}d|0\rangle\langle 0|\bar{s}c|D_s^+\rangle\}$$

$$= \frac{G_F}{\sqrt{2}}\cos^2\theta_c\frac{a_1 r}{\sqrt{2}}(\varepsilon\cdot k)$$

$$A(D_s^+\to\rho^+\pi^0) = \frac{G_F}{\sqrt{2}}\cos^2\theta_c\{a_1\langle\rho^+\pi^0|\bar{u}d|0\rangle\langle 0|\bar{s}c|D_s^+\rangle\}$$

$$= \frac{G_F}{\sqrt{2}}\cos^2\theta_c\frac{-a_1 r}{\sqrt{2}}(\varepsilon\cdot k)$$

$$A(D_s^+\to\phi\pi^+) = \frac{G_F}{\sqrt{2}}\cos^2\theta_c\{a_1\langle\pi^+|\bar{u}d|0\rangle\langle\phi|\bar{s}c|D_s^+\rangle\}$$

$$= \frac{G_F}{\sqrt{2}} \cos^2\theta_c \left\{ a_1 2 f_\pi m_\phi \frac{h_{A0}(D_s \to \phi)}{1 - q^2/m_{D_s}^2} \right\} (\varepsilon \cdot k) .$$

...(IV.29)

In the above we assume the annihilation to proceed through a $\pi^+$ like resonance and use SU(3) to relate the annihilation contributions of the various channels. Note that in Table 1 we have redefined the annihilation parameter as $R_s \equiv -a_1/a_2 r$. All the final states mentioned above are produced with I=1, since the weak spurion changes isospin by one unit. $\rho^0\pi^+$ (and $\rho^+\pi^0$) system has an odd G-parity while $\phi\pi^+$ system has an even G-parity. $K^+\bar{K}^{*0}$ and $K^{*+}\bar{K}^0$ can have either G-parity. Under G-parity the pseudoscalar particle and antiparticle K doublets transform as follows:

$$\begin{pmatrix} K^+ \\ K^0 \end{pmatrix} \xrightarrow{G} \begin{pmatrix} \bar{K}^0 \\ -K^- \end{pmatrix} \quad \text{and} \quad \begin{pmatrix} \bar{K}^0 \\ -K^- \end{pmatrix} \xrightarrow{G} -\begin{pmatrix} K^+ \\ K^0 \end{pmatrix} ,$$

the vector $K^*$ states transform similarly. Hence, the two eigenstates of G-parity are (note that the orbital angular momentum is required to be unity),

$$|K^*\bar{K}\rangle_{S,A} = \frac{1}{\sqrt{2}} (|K^{*+}\bar{K}^0\rangle \pm |K^+\bar{K}^{*0}\rangle) \qquad \text{(IV.30)}$$

The symmetric (antisymmetric) combination is G-even (odd). In the G even state, $|K^*\bar{K}\rangle_S$ will mix with $\phi\pi^+$, while in the G-odd state, $|K^*\bar{K}\rangle_A$ will mix with $\rho\pi^+$ final state. Thus our mixing problem reduces to a pair of coupled two-channel problems. Note that $\rho^+\pi^0$ and $\rho^0\pi^+$ states can have I=1 or 2,

$$\begin{aligned} |I=2, I_3=1\rangle &= \frac{1}{\sqrt{2}} (|\rho^+\pi^0\rangle + |\rho^0\pi^+\rangle) \\ |I=1, I_3=1\rangle &= \frac{1}{\sqrt{2}} (|\rho^+\pi^0\rangle - |\rho^0\pi^+\rangle) \end{aligned} \qquad \text{(IV.31)}$$

Since the weak spurion cannot excite I=2 final state, one finds that the quark amplitudes for $D_S^+ \to \rho^+\pi^0$ and $D_S^+ \to \rho^0\pi^+$ are equal in magnitude and opposite in sign.

In parameterizing the **K**-matrix we postulate that a resonance with allowed quantum numbers lying close to the $D_S^+$ mass will dominate the **K**-matrix. In G odd states, a resonance coupling the different channels, must have G=-1, I=1 and J=0, i.e., it must have $\pi$-like quantum numbers. An unconfirmed $\pi$-like resonance exists[10] close to the $D_S$ mass at 1770MeV. We therefore parameterize the **K**-matrix in G-odd state with the resonant form of eq.(IV.7) with $m_R$=1770MeV. In G=+1 channel there appears to be no confirmed or unconfirmed resonance with I=1 and J=0. We therefore, parameterize the **K**-matrix in G-even state as in eq.(IV.6) with energy independent parameters *a*, *b* and *c*. Due to the Okubo-Zweig-Izuka (OZI) rule,[63] we disallow $\pi\phi \nleftrightarrow \pi\phi$ transition by setting *b*=0 in the **K**-matrix. This approximation does not forbid $\pi\phi \nleftrightarrow \pi\phi$ scattering, since the reaction can proceed as a two-step process, $\pi\phi \to |K^*\bar{K}\rangle_S \to \pi\phi$. Hence our model **K**-matrix has two parameters, *a* and *c*, in G-even state and one parameter, $\Gamma_{11}$, in G-odd state. We choose $\Gamma_R$=300MeV.

Once the isospin one, G-even and G-odd unitarized amplitudes are determined, the unitarized observable amplitudes are evaluated as follows,

$$A^u(D_S^+ \to \rho^0\pi^+) = -\frac{1}{\sqrt{2}} A_1^{u,\rho\pi}$$

$$A^u(D_S^+ \to \rho^+\pi^0) = \frac{1}{\sqrt{2}} A_1^{u,\rho\pi}$$

$$A^u(D_s^+ \to \phi\pi^+) = A^{u,\phi\pi}$$
$$A^u(D^+ \to K^{*+}\bar{K}^0) = \frac{1}{\sqrt{2}}\{ A^{u,K^*K}_{G=1} + A^{u,K^*K}_{G=-1} \}$$
$$A^u(D^+ \to K^+\bar{K}^{*0}) = \frac{1}{\sqrt{2}}\{ A^{u,K^*K}_{G=1} - A^{u,K^*K}_{G=-1} \}$$

...(IV.32)

*Fit to Argus Data*[64]

First we set $\xi=0$ and the annihilation parameter $R_s=0$, as do the authors of ref.[27], and searched for a fit to ARGUS data[64] shown in the last column of Table 3 . We found none. As $R_s$ was made nonzero we started seeing solutions which, in the ratio $a_1/a_2$, appeared in the range $-2.3 \le a_1/a_2 \le -1.8$. In Fig. 4, we have shown the range of parameters $a$ and $\Gamma_{11}$ for which we could fit ARGUS data. In this figure we have used $a_1/a_2=-2.0$, $\xi=0$ and constrained the parameter $c$ through $c=a/4$. We see from Fig. 4(a) that for a small annihilation parameter $R_s=0.05\text{GeV}^2$ (to put this number in perspective, a typical spectator term is of the order 0.4-0.8 $\text{GeV}^2$), solutions appear for a limited range of $a$ and $\Gamma_{11}$. As $R_s$ is raised to 0.12 $\text{GeV}^2$, data can be fit with a wider range of parameters as seen from Fig.4(b). As $R_s$ is raised further, it gets harder to find solutions as seen from Fig.4(c). The small branching ratio for $D_s^+ \to \rho^0\pi^+$ is a strong constraint. For values of $R_s$ larger than 0.17 $\text{GeV}^2$, we did not find a solution to ARGUS data with $a_1/a_2=-2.0$ and $\xi=0$. In general the trend was that a larger annihilation term was needed as the magnitude of $a_1/a_2$ was increased, keeping the ratio negative.

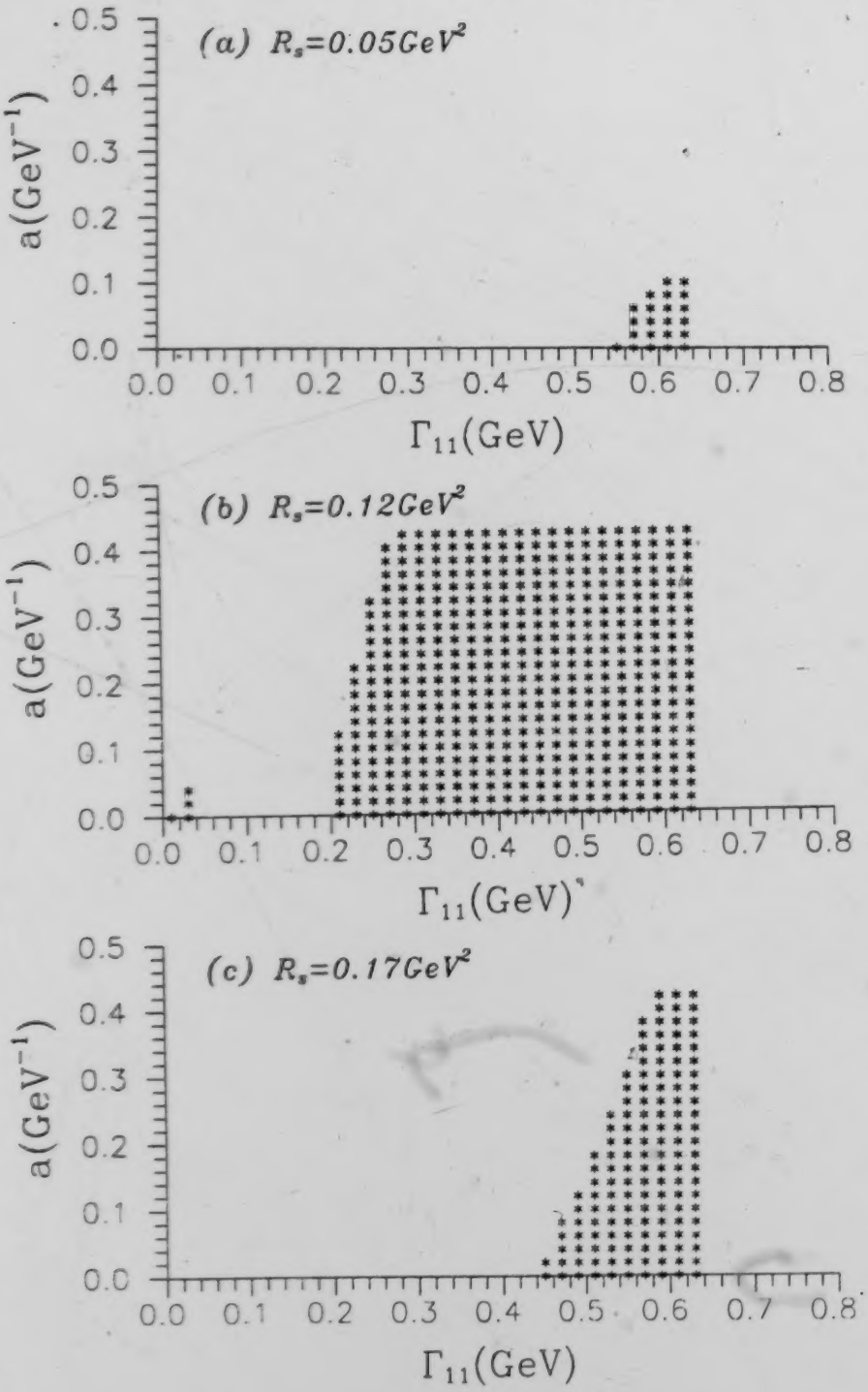


**Fig. 4** Fits to ARGUS data[64] for $D_s^+ \to VP$. Allowed region is marked in $a$-$\Gamma_{11}$ space for different values of the annihilation parameters $R_s$. We have used $a_1/a_2$=-2.0, $\xi$=0 and constrained $c=a/4$.

**Table 3.** Fits to ARGUS data (ref.64) for Cabibbo-angle favored $D_s^+ \to VP$ decays in a two-channel model. Theory column with $\xi=0$, $R_s=0.12\text{GeV}^2$ uses $a_1/a_2=-2.0$, $\Gamma_{11}=0.41\text{GeV}$, $\Gamma_{22}=0.279$ GeV, $a=0.2\text{GeV}^{-1}$, $c=0.05\text{GeV}^{-1}$. Theory column with $\xi=1/3$, $R_s=0.19\text{GeV}^2$ uses $a_1/a_2=-2.4$, $\Gamma_{11}=0.61\text{GeV}$, $\Gamma_{22}=0.037$ GeV, $a=0.0\text{GeV}^{-1}$, $c=0.0\text{GeV}^{-1}$.

| Branching ratio | Theory $\xi=0$ $R_s=0.12\text{GeV}^2$ | Theory $\xi=1/3$ $R_s=0.19\text{GeV}^2$ | ARGUS data |
|---|---|---|---|
| $B(D_s^+ \to K^+ \bar{K}^{*0})$ | 4.85 | 4.00 | 5.0±1.3 |
| $B(D_s^+ \to \rho^0 \pi^+)$ | 0.57 | 0.61 | <0.77 |
| $B(D_s^+ \to \phi \pi^+)$ | 3.90 | 3.66 | 3.2±0.7±0.5 |
| $\frac{B(D_s^+ \to K^+ \bar{K}^{*0})}{B(D_s^+ \to \phi \pi^+)}$ | 1.24 | 1.09 | 1.44±0.37 |
| $\frac{B(D_s^+ \to \rho^0 \pi^+)}{B(D_s^+ \to \phi \pi^+)}$ | 0.15 | 0.17 | <0.22 |
| $\frac{B(D_s^+ \to \bar{K}^0 K^{*+})}{B(D_s^+ \to K^+ \bar{K}^{*0})}$ | 0.12 | 0.05 | - |
| $\frac{B(D_s^+ \to \rho^+ \pi^0)}{B(D_s^+ \to \rho^0 \pi^+)}$ | 1.0 | 1.0 | - |
| $\frac{B(D_s^+ \to K^+ \bar{K}^{*0})}{B(D_s^+ \to \rho^0 \pi^+)}$ | 8.51 | 6.5 | - |

In column 2 of Table 3 we have shown the best fit, with $\xi=0$, to ARGUS data. Within the constraints of our model we require an annihilation term of the size of (15-30)% of the spectator term, depending on the decay mode, for the best fit. For $\xi=0$ we found no fits to ARGUS data for $a_1/a_2<-2.3$.

At $a_1/a_2$=-2.3 an annihilation term in the range (0.16-0.19) $GeV^2$ was allowed.

Next we chose $\xi$=1/3 and repeated the above procedure. This tacitly assumes that the range of $a_1/a_2$ in the interval (-3.0 to -2.0) is achievable in perturbative QCD. From Table 2 it is clear that in an NLL calculation, it would require $\Lambda$ to be close to 0.5 GeV and $\mu$ in the neighborhood of 1 GeV. We found fits to ARGUS data for $-2.2 \geq a_1/a_2 \geq -2.4$. The annihilation parameter was now somewhat larger; for example, in the limiting case of $a_1/a_2$=-2.4, $R_s$ was 0.19 $GeV^2$. One such fit to ARGUS data for $\xi$=1/3 has been shown in column 3 of Table 3, using $a_1/a_2$=-2.4. Again, we note that as $a_1/a_2$ was allowed to increase, keeping it negative, we needed a larger annihilation to fit data. We return to a discussion of allowed values of $R_s$ for different values of $a_1/a_2$ later.

*Fit to E-691 data*[65]

We followed the same procedure as above, to fit E-691 data.[65] Since the E-691 upper limit on $B(D_s^+ \to \rho^0\pi^+)$ is considerably lower than the ARGUS limit and also since the E-691 value for $B(D_s^+ \to K^+\bar{K}^{*0})$ is roughly a half of that from ARGUS (note that $\rho^0\pi^+$ and $K^+\bar{K}^{*0}$ channels couple in our formalism), it becomes easier to fit E-691 data with a smaller, indeed zero, annihilation term for both $\xi$=0 and 1/3. In Table 4 we have shown fits to E-691 data with $\xi$=0 and different values of the annihilation parameter, $R_s$. As $R_s$ increases beyond 0.1 $GeV^2$, theoretical values of $B(D_s^+ \to \rho^0\pi^+)$ and $B(D_s^+ \to K^+\bar{K}^{*0})$ begin to violate data for

$a_1/a_2$=-2.0 and $\xi$=0.

**Table 4.** Fits to E-691 data (ref.65) for Cabibbo-angle favored $D_s^+ \to VP$ decays in a two-channel model. Theory columns with $\xi$=0, use $a_1/a_2$=-2.0, $\Gamma_{11}$=0.31GeV, $\Gamma_{22}$=0.399GeV; column 1 with $R_s$=0, uses $a$= 0.4 $GeV^{-1}$, $c$=0.1$GeV^{-1}$, column 2 with $R_s$=0.1$GeV^2$ uses $a$=0.8$GeV^{-1}$ and $c$=0.2$GeV^{-1}$. Theory column with $\xi$=1/3, uses $a_1/a_2$= -2.4, $\Gamma_{11}$=0.41GeV, $\Gamma_{22}$=0.28GeV, $a$=0.4$GeV^{-1}$, $c$= 0.1$GeV^{-1}$.

| Branching ratio | Theory $\xi$=0 $R_s$=0.0 $GeV^2$ | Theory $\xi$=0 $R_s$=0.1 $GeV^2$ | Theory $\xi$=1/3 $R_s$=0.1 $GeV^2$ | E691 Data |
|---|---|---|---|---|
| $B(D_s^+ \to K^+ \bar{K}^{*0})$ | 3.08 | 3.00 | 2.61 | 2.6±0.5 |
| $B(D_s^+ \to \rho^0 \pi^+)$ | 0.03 | 0.26 | 0.25 | <0.28 |
| $B(D_s^+ \to \phi \pi^+)$ | 3.99 | 4.25 | 3.75 | 3.5±0.8 |
| $\frac{B(D_s^+ \to K^+ \bar{K}^{*0})}{B(D_s^+ \to \phi \pi^+)}$ | 0.77 | 0.71 | 0.69 | 0.74±0.12±0.06 |
| $\frac{B(D_s^+ \to \rho^0 \pi^+)}{B(D_s^+ \to \phi \pi^+)}$ | 0.01 | 0.06 | 0.07 | <0.08 |
| $\frac{B(D_s^+ \to \bar{K}^0 K^{*+})}{B(D_s^+ \to K^+ \bar{K}^{*0})}$ | 0.43 | 0.35 | 0.24 | - |
| $\frac{B(D_s^+ \to \rho^+ \pi^0)}{B(D_s^+ \to \rho^0 \pi^+)}$ | 1.0 | 1.0 | 1.0 | - |
| $\frac{B(D_s^+ \to K^+ \bar{K}^{*0})}{B(D_s^+ \to \rho^0 \pi^+)}$ | 98.53 | 11.53 | 10.42 | - |

In Fig. 5 we have shown the allowed values of the parameters $a$ and $\Gamma_{11}$ needed to fit E-691 data on $D_s^+ \to VP$ for

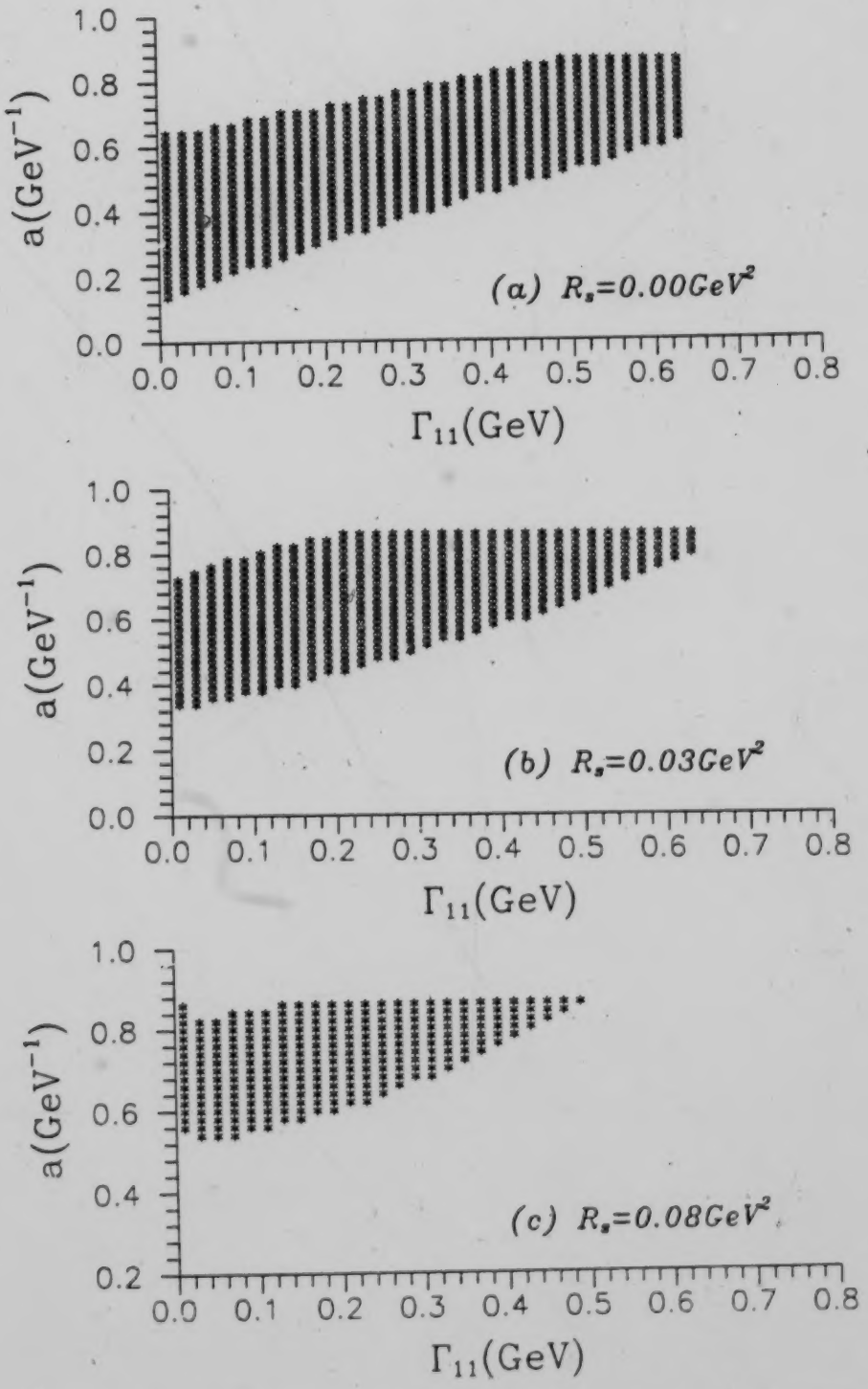


**Fig. 5** Fits to E-691 data[65] for $D_s^+ \to VP$ for the same parameters as in Fig. 4.

different values of annihilation parameter $R_s$. For these plots we have used $a_1/a_2=-2.0$ and $\xi=0$ and constrained parameter $c$ by $c=a/4$. We found no solutions for $R_s>0.1$ GeV$^2$ for $a_1/a_2=-2.0$ and $\xi=0$. Clearly the allowed size of the annihilation parameter is smaller than that allowed by ARGUS data.

For $\xi=1/3$ we found solutions to E-691 data for $-2.1\geq a_1/a_2\geq -2.9$. At $a_1/a_2=-2.9$ an annihilation parameter in the range (0.14-0.15)GeV$^2$ was needed to fit the data. In the range $-2.9\leq a_1/a_2\leq -2.5$, a finite annihilation parameter was necessary to fit the data. The value of $R_s$ at the two limiting points were: $R_s=(0.14\text{-}0.15)$ GeV$^2$ at $a_1/a_2=-2.9$ and $R_s=(0.01\text{-}0.13)$ GeV$^2$ at $a_1/a_2=-2.5$. For $a_1/a_2\geq -2.4$ an annihilation parameter was not required, though allowed by the data. For example E-691 data could be fit with $a_1/a_2=-2.4$ and $R_s$ in the range (0-0.13) GeV$^2$ while for $a_1/a_2=-2.1$ we needed $R_s$ in the range (0-0.06) GeV$^2$. In column 4 of Table 4 we have shown a particular fit, using $\xi=1/3$, to E-691 data. We return to a discussion of the allowed values of $a_1/a_2$ and $\xi$, at the end of the next section.

*Summary of the $D_s^+\to VP$ data fits*

In the above we have presented the results of a two-channel fit to Cabibbo-angle favored $D_s^+\to VP$ data from ARGUS and E-691. The fits to ARGUS data with $\xi=0$ were obtained for $a_1/a_2$ in the range: $-2.3\leq a_1/a_2\leq -1.8$ and to E-691 data in the range: $-2.7\leq a_1/a_2\leq -1.7$. The allowed range

of $a_1/a_2$ for $\xi$=1/3 was only slightly different.

In Table 5 we have tabulated the range of the annihilation parameter, $R_s$, needed by our model to fit the data. Evidently as the magnitude of $a_1/a_2$ increases, one requires in our model, a finite annihilation term. This annihilation term can be as big as (15-30)% of the spectator term for some decay modes.

**Table 5.** Range of annihilation parameter allowed by Cabibbo angle favoured $D_s^+ \to VP$ data.

| | Range of $R_s(GeV^2)$; $\xi$=0 | | Range of $R_s(GeV^2)$; $\xi$=1/3 | |
|---|---|---|---|---|
| $a_1/a_2$ | ARGUS data | E-691 data | ARGUS data | E-691 data |
| -2.0 | 0.05-0.17 | 0.00-0.10 | | No Solution |
| -2.1 | 0.09-0.18 | 0.00-0.11 | No Solution | 0.00-0.06 |
| -2.2 | 0.12-0.19 | 0.00-0.12 | 0.12-0.18 | 0.00-0.11 |
| -2.3 | 0.16-0.19 | 0.00-0.13 | 0.15-0.19 | 0.00-0.12 |
| -2.4 | No Solution | 0.00-0.13 | 0.19 | 0.00-0.13 |
| -2.5 | | 0.04-0.14 | No Solution | 0.01-0.13 |
| -2.6 | | 0.08-0.14 | | 0.04-0.14 |
| -2.7 | | 0.11-0.14 | | 0.07-0.15 |
| -2.8 | | No Solution | | 0.10-0.15 |
| -2.9 | | | | 0.14-0.15 |
| -3.0 | | | | No Solution |

The limit on $B(D_s^+ \to \rho^0\pi^+)$ serves to constrain the parameters of the model, in particular, the annihilation parameter, quite severely. Another measurement that will restrict the parameters of the model is $B(D_s^+ \to \bar{K}^0 K^{*+})$. A measurement of, or an upper limit on, this branching ratio would be helpful.

*Branching ratio for* $D_s^+ \to \omega\pi^+$

In our discussion above, we have not considered $D_s^+ \to \omega\pi^+$.

This mode is particularly interesting for the following reason. In a factorization model, there is no contribution from the spectator diagram for this mode. Although an annihilation contribution would appear to be possible at the quark level, it indeed vanishes;[22] the vector part of the $(\bar{u}d)$ current makes no contribution due to Conserved Vector Current (CVC) hypothesis and first class axial vector current cannot connect vacuum to $\omega\pi^+$ state which has even G-parity.

It has been argued[66] that a diagrammatic analysis[67] of two-body decays of $D^+$, $D^0$ and $D_s^+$ requires a significant annihilation term. Based on this it was predicted[66] that $B(D_s^+\to\omega\pi^+) \gtrsim B(D_s^+\to\phi\pi^+)$. Since $B(D_s^+\to\phi\pi^+) \approx 3\%$, it implies a significantly large branching ratio for $D_s^+\to\omega\pi^+$. The estimates of other models on $B(D_s^+\to\omega\pi^+)$ differ greatly. Blok and Shifman[29] include non-factorizable contributions, but ignore factorizable annihilation to calculate $B(D_s^+\to\omega\pi^+) = 0.3\%$. The question then arises: What should the magnitude of $B(D_s^+\to\omega\pi^+)$ be?

In absence of final state interactions, $B(D_s^+\to\omega\pi^+)$ should be zero. However, final state interactions can change the picture substantially; $\omega\pi^+$ could be generated by coupling to other final states. Since $\omega\pi^+$ has G=+1, it will couple only to G-even states, i.e., to $\phi\pi^+$ and $|K^*\bar{K}\rangle_{G=+1}$. However, $\phi\pi^+ \not\Leftrightarrow \omega\pi^+$ is disallowed by OZI rule. Hence, $\omega\pi^+$ will couple only to the symmetric $|K^*\bar{K}\rangle_S$ state. This interchannel coupling is achieved[22] by extending the G-even

2x2 **K**-matrix in eq.(IV.6) to a 3x3 matrix, thereby including the $\omega\pi^+$ mode, as follows:

$$\mathbf{K} = \begin{bmatrix} k_1 b & \sqrt{k_1 k_2}\, c & \sqrt{k_1 k_3}\, f \\ \sqrt{k_2 k_1}\, c & k_2 a & \sqrt{k_2 k_3}\, d \\ \sqrt{k_3 k_1}\, f & \sqrt{k_3 k_2}\, d & k_3 e \end{bmatrix} \qquad \text{(IV.33)}$$

with channel labels i=(1,2,3) belonging to $\phi\pi^+$, $|K^*\bar{K}\rangle_S$ and $\omega\pi^+$ respectively. The parameters $d$, $e$ and $f$ are also chosen to be energy independent (zero range approximation), $k_3$ is the c.m. momenta in the $\omega\pi^+$ channel. Since $\phi\pi^+ \nrightarrow \phi\pi^+$ and $\omega\pi^+ \nrightarrow \phi\pi^+$ transitions are disallowed by OZI rule, we set $b$ and $f$ equal to zero as an approximation. Clearly, this disallows the OZI-violating transitions in the lowest order in the **K**-matrix. The coupling in G=-1 states is retained as before. Our model has four parameters $a, c, d$ and $e$ in the G-even **K**-matrix and one parameter, $\Gamma_{11}$, in the G-odd **K**-matrix.

For $d, e=0$, $\omega\pi^+$ channel decouples from the other two channels and one gets $B(D_S^+ \nrightarrow \omega\pi^+)=0$. However, for non-zero $d$ & $e$, the number of parameters involved in the coupled channel problem is large and an exact branching ratio for $D_S^+ \nrightarrow \omega\pi^+$ cannot be predicted. We therefore vary the parameters of our model to determine the maximum possible $B(D_S^+ \nrightarrow \omega\pi^+)$, consistent with the ARGUS[64] and E691[65] data for the other coupled channels. We find that, for reasonable values of $d$ and $e$, it is possible to produce $B(D_S^+ \nrightarrow \omega\pi^+)$ upto 3%, keeping the other branching ratios (i.e., for $\bar{K}^{*0}K^+$, $\rho^0\pi^+$, $\phi\pi^+$

modes) within the experimental limits.

In our model, $D_s^+ \to \omega\pi^+$ is being generated via final state interactions and not directly from annihilation in $\omega\pi$ channel. We do, however, include an annihilation parameter in the $K^*\bar{K}$ amplitude, which feeds into the $\omega\pi^+$ final state. Note that the un-unitarized amplitude for $D_s^+ \to \omega\pi^+$ is zero.

A fit to ARGUS data requires that the annihilation parameter $R_S$ be non-zero, even if we demand $B(D_s^+ \to \omega\pi^+)=0$ (as was seen in the earlier discussion, which excluded $D_s^+ \to \omega\pi^+$ mode). Although fits to E691 data may be obtained for vanishing $R_S$, non-vanishing $R_S$ is also allowed by the data; larger $B(D_s^+ \to \omega\pi^+)$ being obtained for $R_S \neq 0$. The maximum value of $B(D_s^+ \to \omega\pi^+)$ consistent with a fit to ARGUS data requires an annihilation term $\simeq$ 40% of the spectator term in $D_s^+ \to K^{*+}\bar{K}^0$ and that for E691, $\simeq$ 25% of the spectator term. For E691 data, even with the annihilation parameter set equal to zero, final state interactions alone can generate $B(D_s^+ \to \omega\pi^+)$ upto about 2%.

In Table 6 we show a fit to the ARGUS data (for $\xi=0$ and $\xi=1/3$), where the various parameters are chosen such that $B(D_s^+ \to \omega\pi^+)$ is at its maximum value. Table 7 lists the same for E-691 data. We note that $B(D_s^+ \to \omega\pi^+)$ falls as $a_1/a_2$ increases in magnitude. Also, E-691 data, where $B(D_s^+ \to \bar{K}^{*0}K^+)$ is lower than in ARGUS data, allows a larger value of $B(D_s^+ \to \omega\pi^+)$ than the ARGUS data. This presumably results from more of $\bar{K}^{*0}K^+$ rate being siphoned off into $\omega\pi^+$ mode.

In summary, we find that in a factorization model,

**Table 6.** Fits to ARGUS data[64] for Cabibbo-angle favored $D_s^+ \to VP$ decays. The various parameters in the model are selected to maximize $B(D_s^+ \to \omega\pi^+)$ consistent with data. The parameters $d, e$ take values greater than $a, c$ and lie in the range (0.1-1)GeV$^{-1}$. The $R_s$ values are in GeV$^2$.

| Branching ratio(%) | Theory $\xi$=0 $R_s$=0.15 $a_1/a_2$ =-2.0 | Theory $\xi$=0 $R_s$=0.17 $a_1/a_2$ =-2.2 | Theory $\xi$=1/3 $R_s$=0.15 $a_1/a_2$ =-2.0 | Theory $\xi$=1/3 $R_s$=0.17 $a_1/a_2$ =-2.2 | ARGUS data |
|---|---|---|---|---|---|
| $B(D_s^+ \to \bar{K}^{*0}K^+)$ | 3.86 | 3.71 | 4.32 | 4.13 | 5.0±1.3 |
| $B(D_s^+ \to \rho^0\pi^+)$ | 0.59 | 0.56 | 0.66 | 0.63 | <0.77 |
| $B(D_s^+ \to \phi\pi^+)$ | 3.57 | 3.45 | 4.00 | 3.83 | 3.2±0.7±0.5 |
| $B(D_s^+ \to \omega\pi^+)$ | 1.66 | 0.71 | 1.86 | 0.83 | - |

**Table 7.** Fits to E-691 data[65] for Cabibbo angle favored $D_s^+ \to VP$ decays for the same conditions as specified for Table 6. The values in parentheses correspond to $R_s$=0.0GeV$^2$.

| Branching ratio(%) | Theory $\xi$=0 $R_s$=0.10 $a_1/a_2$ =-2.0 | Theory $\xi$=0 $R_s$=0.11 $a_1/a_2$ =-2.2 | Theory $\xi$=1/3 $R_s$=0.09 $a_1/a_2$ =-2.0 | Theory $\xi$=1/3 $R_s$=0.11 $a_1/a_2$ -2.2 | E-691 data |
|---|---|---|---|---|---|
| $B(D_s^+ \to \bar{K}^{*0}K^+)$ | 2.24 (2.30) | 2.11 (2.11) | 2.13 (2.57) | 2.10 (2.14) | 2.6±0.5 |
| $B(D_s^+ \to \rho^0\pi^+)$ | 0.27 (0.006) | 0.24 (0.004) | 0.25 (0.006) | 0.27 (0.005) | <0.28 |
| $B(D_s^+ \to \phi\pi^+)$ | 3.64 (3.76) | 3.43 (3.43) | 3.52 (4.21) | 3.43 (3.51) | 3.5±0.8 |
| $B(D_s^+ \to \omega\pi^+)$ | 2.48 (1.84) | 1.73 (0.89) | 2.75 (2.05) | 2.02 (1.15) | - |

where the quark level (spectator and weak annihilation) amplitude for $D_s^+ \to \omega\pi^+$ is zero, final state interactions can generate $B(D_s^+ \to \omega\pi^+)$ as large as ≈3%. An observation of a

signal at this level, will not necessarily constitute an evidence for an annihilation term in the decay amplitude for $D_s^+ \to \omega\pi^+$, at the quark level as suggested.[66]

A recent measurement[68] of the $D_s^+ \to \omega\pi^+$ mode by E-691 group, supports our claim. They set the limit: $B(D_s^+ \to \omega\pi^+) < 0.5\ B(D_s^+ \to \phi\pi^+)$, well within the maximum branching ratio limit obtained by us. A suitable choice of the parameters d and e can give branching ratio at this level, with or without annihilation parameter $R_s$.

In a revised version of ref.[66], the predictions of $B(D_s^+ \to \omega\pi^+)$ has been lowered[69] to $\frac{1}{10}\ B(D_s^+ \to \phi\pi^+)$.

**IV.4** Cabibbo-angle favored D→VP

Cabibbo-angle favored decays D→VP involve at least five coupled channels: $K\rho$, $K^*\pi$, $\bar{K}^0\phi$, $\bar{K}^0\omega$ and $\bar{K}^{*0}\eta$. The ununitarized amplitudes for these modes are evaluated to be (using eqs.(IV.20) & (IV.21)),

$$A(D^0 \to \bar{K}^0\rho^0) = \frac{G_F}{\sqrt{2}} \cos^2\theta_c \{a_2 \langle \bar{K}^0\rho^0|\bar{s}d|0\rangle\langle 0|\bar{u}c|D^0\rangle + a_2\langle \bar{K}^0|\bar{s}d|0\rangle\langle \rho^0|\bar{u}c|D^0\rangle\}$$

$$= \frac{G_F}{\sqrt{2}} \cos^2\theta_c \left\{ \frac{-a_2 R}{\sqrt{2}} + a_2\sqrt{2} f_K m_\rho \frac{h_{A0}(D\to\rho)}{1-q^2/m_D^2} \right\} (\varepsilon\cdot k)$$

$$A(D^0 \to K^-\rho^+) = \frac{G_F}{\sqrt{2}} \cos^2\theta_c \{a_1 \langle \rho^+|\bar{u}d|0\rangle\langle K^-|\bar{s}c|D^0\rangle + a_2\langle K^-\rho^+|\bar{s}d|0\rangle\langle 0|\bar{u}c|D^0\rangle\}$$

$$= \frac{G_F}{\sqrt{2}} \cos^2\theta_c \left\{ a_1 2 f_\rho m_\rho \frac{h_{F1}(D\to K)}{1-q^2/m_{D_s^*}^2} + a_2 R \right\} (\varepsilon\cdot k)$$

$$A(D^0 \to \bar{K}^{*0}\pi^0) = \frac{G_F}{\sqrt{2}} \cos^2\theta_c \{a_2 \langle \bar{K}^{*0}\pi^0|\bar{s}d|0\rangle\langle 0|\bar{u}c|D^0\rangle$$

$$+ a_2\langle\bar{K}^{*0}|\bar{s}d|0\rangle\langle\pi^0|\bar{u}c|D^0\rangle\}$$

$$= \frac{G_F}{\sqrt{2}}\cos^2\theta_c\left\{\frac{a_2R}{\sqrt{2}} + a_2\sqrt{2}f_{K^*}m_{K^*}\frac{h_{F1}(D\to\pi)}{1-q^2/m_{D^*}^2}\right\}(\varepsilon\cdot k)$$

$$A(D^0\to K^{*-}\pi^+) = \frac{G_F}{\sqrt{2}}\cos^2\theta_c\{a_1\langle\pi^+|\bar{u}d|0\rangle\langle K^{*-}|\bar{s}c|D^0\rangle$$

$$+ a_2\langle K^{*-}\pi^+|\bar{s}d|0\rangle\langle 0|\bar{u}c|D^0\rangle\}$$

$$= \frac{G_F}{\sqrt{2}}\cos^2\theta_c\left\{a_1 2f_\pi m_{K^*}\frac{h_{A0}(D\to K^*)}{1-q^2/m_{D_s}^2} - a_2R\right\}(\varepsilon\cdot k)$$

$$A(D^0\to\bar{K}^0\phi) = \frac{G_F}{\sqrt{2}}\cos^2\theta_c\{a_2\langle\bar{K}^0\phi|\bar{s}d|0\rangle\langle 0|\bar{u}c|D^0\rangle\}$$

$$= \frac{G_F}{\sqrt{2}}\cos^2\theta_c\, R(\varepsilon\cdot k)$$

$$A(D^0\to\bar{K}^{*0}\eta) = \frac{G_F}{\sqrt{2}}\cos^2\theta_c\{a_2\langle\bar{K}^{*0}\eta|\bar{s}d|0\rangle\langle 0|\bar{u}c|D^0\rangle$$

$$+ a_2\langle\bar{K}^{*0}|\bar{s}d|0\rangle\langle\eta|\bar{u}c|D^0\rangle\}$$

$$= \frac{G_F}{\sqrt{2}}\cos^2\theta_c\left\{a_2 3R + a_2 2f_{K^*}m_{K^*}\frac{h_{F1}(D\to\eta)}{1-q^2/m_{D^*}^2}\right\}\frac{(\varepsilon\cdot k)}{\sqrt{6}}$$

where we take $\eta$ to be pure octet,

$$A(D^0\to\bar{K}^0\omega) = \frac{G_F}{\sqrt{2}}\cos^2\theta_c\{a_2\langle\bar{K}^0\omega|\bar{s}d|0\rangle\langle 0|\bar{u}c|D^0\rangle$$

$$+ a_2\langle\bar{K}^0|\bar{s}d|0\rangle\langle\omega|\bar{u}c|D^0\rangle\}$$

$$= \frac{G_F}{\sqrt{2}}\cos^2\theta_c\left\{a_2R + a_2 2f_K m_\omega\frac{h_{A0}(D\to\omega)}{1-q^2/m_D^2}\right\}\frac{(\varepsilon\cdot k)}{\sqrt{2}}$$

$$A(D^+\to\bar{K}^{*0}\pi^+) = \frac{G_F}{\sqrt{2}}\cos^2\theta_c\{a_1\langle\pi^+|\bar{u}d|0\rangle\langle\bar{K}^{*0}|\bar{s}c|D^+\rangle$$

$$+ a_2\langle\bar{K}^{*0}|\bar{s}d|0\rangle\langle\pi^+|\bar{u}c|D^+\rangle\}$$

$$= \frac{G_F}{\sqrt{2}}\cos^2\theta_c\left\{a_1 2f_\pi m_{K^*}\frac{h_{A0}(D\to K^*)}{1-q^2/m_{D_s}^2}\right.$$

$$+ a_2 2f_{K^*} m_{K^*} \frac{h_{F1}(D\to\pi)}{1-q^2/m_{D^*}^2} \Big\}(\varepsilon\cdot k)$$

$$A(D^+\to\bar{K}^0\rho^+) = \frac{G_F}{\sqrt{2}} \cos^2\theta_c \{a_1 \langle\rho^+|\bar{u}d|0\rangle\langle\bar{K}^0|\bar{s}c|D^+\rangle$$

$$+ a_2\langle\bar{K}^0|\bar{s}d|0\rangle\langle\rho^+|\bar{u}c|D^{+0}\rangle\}$$

$$= \frac{G_F}{\sqrt{2}} \cos^2\theta_c \Big\{ a_1 2f_\rho m_\rho \frac{h_{F1}(D\to K)}{1-q^2/m_{D_s^*}^2}$$

$$+ a_2 2f_K m_\rho \frac{h_{A0}(D\to\rho)}{1-q^2/m_D^2} \Big\}(\varepsilon\cdot k)$$

...(IV.34)

Here, the annihilation is assumed to proceed via a $\bar{K}^0$-like resonance and SU(3) is used to relate the annihilation contributions of the various channels. A model involving all these five channels interacting in the final state would have too many free parameters to be useful. However, the problem can be simplified somewhat as follows. The ununitarized weak decay amplitudes for $D^0\to\bar{K}^0\omega$ and $\bar{K}^{*0}\eta$, are proportional to $a_2$ (class II amplitudes as described in chapter II), which is smaller than $a_1$ in magnitude. The $K^+\rho^-$ and $K^{*+}\pi^-$ modes have decay amplitudes proportional to $a_1$ (apart from the annihilation term) and are therefore large. Thus, it is not unrealistic to set up a three channel model involving $K\rho$, $K^*\pi$ and $\bar{K}^0\phi$ channels to see if $\bar{K}^0\phi$ channel can be fed[20] by the other two channels in a manner consistent with data. This we have attempted in the following.

In Cabibbo-angle favored D→VP decays, the final state can have I=1/2 in all the three channels $K\rho$, $K^*\pi$ and $\bar{K}^0\phi$,

while only two of these channels, $K\rho$ and $K^*\pi$, can have I=3/2. Hence in I=1/2 final state, we shall have a three-channel coupled problem while in I=3/2 state we have a two-channel coupled problem. We leave the decay amplitudes for $D^0 \to \bar{K}^0\omega$ and $\bar{K}^{*0}\eta$ un-unitarized.

We introduce the decay amplitudes $A^{K^*\pi}_{1/2}$, $A^{K^*\pi}_{3/2}$ and $A^{K\rho}_{1/2}$, $A^{K\rho}_{3/2}$ for decays to I=1/2 and 3/2 states as:

$$
\begin{aligned}
A^{K^*\pi}_{1/2} &= \frac{1}{\sqrt{3}} \{|\bar{K}^{*0}\pi^0> - \sqrt{2}|K^{*-}\pi^+>\} \\
A^{K^*\pi}_{3/2} &= \frac{1}{\sqrt{3}} \{|K^{*-}\pi^+> + \sqrt{2}|\bar{K}^{*0}\pi^0>\} \\
A^{K\rho}_{1/2} &= \frac{1}{\sqrt{3}} \{|\bar{K}^0\rho^0> - \sqrt{2}|K^-\rho^+>\} \\
A^{K\rho}_{3/2} &= \frac{1}{\sqrt{3}} \{|K^-\rho^+> + \sqrt{2}|\bar{K}^0\rho^0>\}
\end{aligned}
\qquad \text{(IV.35)}
$$

A K-like resonance can contribute to I=1/2 amplitude in the 'direct' channel. An unconfirmed K-like resonance $\bar{K}^0(1830)$, lies[10] very close to the D-meson mass and could influence D-decays into strange VP systems with I=1/2. Hence in I=1/2 final state we choose a resonance parameterization of the form given in eq.(IV.11) to unitarize the three decay amplitudes $D^0 \to K\rho$, $K^*\pi$ and $\bar{K}^0\phi$. We choose $m_R$=1830 and $\Gamma_R$=250 MeV. Using the constraints given in eqs. (IV.12) to (IV.14) we get down to two independent parameters.

In I=3/2 final state, $K^*\pi$ and $K\rho$ channels couple. Since there is no resonance in this isospin state, we use a non-resonant parameterization (eq.IV.6) with constant parameters *a*, *b* and *c*. We reduce the number of parameters down to two by imposing the constraint det**K**=0. This condi-

tion though not as intuitive here, as in the resonant case, still implies that $T_{ik} \propto a_{ik}$, where $a_{ik}$ is the scattering length for i→k.

Once the unitarized I=1/2, 3/2 amplitudes are evaluated, the unitarized physical amplitudes are determined as follows:

$$A^u(D^0 \to \bar{K}^{*0}\pi^0) = \frac{1}{\sqrt{3}} \{ \sqrt{2}\, A^{u,K^*\pi}_{3/2} + A^{u,K^*\pi}_{1/2} \}$$

$$A^u(D^0 \to K^{*-}\pi^+) = \frac{1}{\sqrt{3}} \{ A^{u,K^*\pi}_{3/2} - \sqrt{2}\, A^{u,K^*\pi}_{1/2} \}$$

$$A^u(D^0 \to \bar{K}^0\rho^0) = \frac{1}{\sqrt{3}} \{ \sqrt{2}\, A^{u,K\rho}_{3/2} + A^{u,K\rho}_{1/2} \}$$

$$A^u(D^0 \to K^-\rho^+) = \frac{1}{\sqrt{3}} \{ A^{u,K\rho}_{3/2} - \sqrt{2}\, A^{u,K\rho}_{1/2} \} \qquad \text{(IV.36)}$$

$$A^u(D^0 \to \bar{K}^0\phi) = A^{u,K\phi}_{1/2}$$

$$A^u(D^+ \to \bar{K}^{*0}\pi^+) = \sqrt{3}\, A^{u,K^*\pi}_{3/2}$$

$$A^u(D^+ \to \bar{K}^0\rho^+) = \sqrt{3}\, A^{u,K\rho}_{3/2}$$

To determine the fits to the experimental data, we followed the same procedure as in the two-channel case of $D_s^+ \to VP$, discussed in the previous section. We searched for solutions consistent with MARK III[6] data, both with and without the annihilation term. We found no solutions to the seven branching ratio measurements shown in the last column of Table 8. (By a 'solution', we mean theoretical predictions which fall within the experimental errors of all data being fit). We did however, come close to satisfying all of the MARK III data shown in Table 8. (By a 'near fit' or 'close to a solution' we mean theoretical predictions which

**Table 8.** Fits to MARK-III data (ref.6) for Cabibbo-angle favored D→VP in a three-channel model. Theory column with $\xi$=0, R=0 uses $a_1/a_2$=-2.0, $\Gamma_{11}$=0.135GeV, $\Gamma_{22}$=0.0, $\Gamma_{33}$=0.7 GeV, $a$=0.1GeV$^{-1}$, $b$=0.3GeV$^{-1}$; $\xi$=0, R=0.1GeV$^2$ column uses $a_1/a_2$=-2.0, $\Gamma_{11}$=0.0, $\Gamma_{22}$=0.128GeV, $\Gamma_{33}$=0.7GeV, $a$=0.8GeV$^{-1}$, $b$=0.5GeV$^{-1}$; $\xi$=1/3, R=0.1GeV$^2$ column uses $a_1/a_2$=-2.4, $\Gamma_{11}$=0.0, $\Gamma_{22}$=0.128GeV, $\Gamma_{33}$=0.7GeV, $a$=0.05GeV$^{-1}$, $b$=0.1GeV$^{-1}$.

| Branching ratio | Theory $\xi$=0 R=0.0 GeV$^2$ | Theory $\xi$=0 R=0.1 GeV$^2$ | Theory $\xi$=1/3 R=0.1 GeV$^2$ | MARK-III Data |
|---|---|---|---|---|
| $B(D^0\to K^-\rho^+)$ | 8.95 | 8.81 | 8.11 | 10.8±0.4±1.7 |
| $B(D^0\to \bar{K}^0\rho^0)$ | 1.10 | 0.62 | 0.88 | 0.75±0.09±0.47 |
| $B(D^0\to K^{*-}\pi^+)$ | 3.70 | 6.52 | 3.70 | 5.2±0.3±1.5 |
| $B(D^0\to \bar{K}^{*0}\pi^0)$ | 2.79 | 1.94 | 3.04 | 2.6±0.3±0.7 |
| $B(D^0\to \bar{K}^0\phi)$ | 0.5 | 0.57 | 0.45 | $0.86^{+0.50+0.31}_{-0.41-0.17}$ |
| $B(D^+\to \bar{K}^0\rho^+)$ | 10.04 | 10.85 | 8.61 | 6.9±0.8±2.3 |
| $B(D^+\to \bar{K}^{*0}\pi^+)$ | 1.11 | 1.69 | 1.72 | 5.9±1.9±2.5 |

fall within 2$\sigma$ of all data being fit). We wish to point out, that once $\xi$ and $a_1/a_2$ are chosen, our model has four parameters to describe the final state interactions. In columns 2 and 3 of Table 8 we have shown two of our best fits to MARK III data with $\xi$=0. The fit with $\xi$=0 and R=0 is consistent with six of the seven branching ratios but predicts $B(D^+\to\bar{K}^{*0}\pi^+)$ slightly below the least value allowed by data. On the other hand the fit with $\xi$=0 and R=0.1 GeV$^2$ predicts $B(D^+\to\bar{K}^0\rho^+)$ slightly above the maximum allowed value, while being consistent with the remaining six branching ratios. The fit with $\xi$=1/3 in column 4 of Table 8 uses $a_1/a_2$=-2.4 and an annihilation term R=0.1 GeV$^2$. In this

case $B(D^0 \to K^- \rho^+)$ is predicted slightly below the experimental measurement while the remaining six branching ratios are consistent with data.

We have purposely left out $B(D^0 \to \bar{K}^0 \omega)$ and $B(D^0 \to \bar{K}^{*0} \eta)$ from our discussion above. This is because we performed a three channel unitarization in I=1/2 state leaving these two channels out of the unitarization scheme. The un-unitarized amplitudes for $D^0 \to \bar{K}^0 \omega$ and $D^0 \to \bar{K}^{*0} \eta$ lead to the following branching ratios belonging to the three theory columns of Table 8 : $B(D^0 \to \bar{K}^0 \omega) = 0.65\%$ (for $\xi=0$, R=0), 1.55% ($\xi=0$, R=0.1 $GeV^2$) and 1.02% ($\xi=1/3$, R=0.1 $GeV^2$). The experimental number is: $B(D^0 \to \bar{K}^0 \omega) = (3.2 \pm 1.3 \pm 0.8)\%$. For $D^0 \to \bar{K}^{*0} \eta$ we get: $B(D^0 \to \bar{K}^{*0} \eta) = 0.35\%$ ($\xi=0$, R=0), 0.004% ($\xi=0$, R=0.1$GeV^2$) and 0.002% ($\xi=1/3$, R=0.1$GeV^2$). There are no measurements yet of this branching ratio. The un-unitarized branching ratio for $D^0 \to \bar{K}^0 \omega$ is consistent with data with a small annihilation parameter. Note however, that both $D^0 \to \bar{K}^0 \omega$ and $D^0 \to \bar{K}^{*0} \eta$ could be fed by the other three channels, $K\rho$, $K^* \pi$ and $\bar{K}^0 \phi$, in a 5-channel mixing scheme. In particular, even modest inter-channel couplings would effect $D^0 \to \bar{K}^{*0} \eta$ significantly since the un-unitarized amplitudes for $D^0 \to K^* \pi$ and $K\rho$ decays are large. A measurement of $B(D^0 \to \bar{K}^{*0} \eta)$ would be desirable.

Summarizing, in the above three-channel ($D^0 \to K\rho$, $K^* \pi$ and $\bar{K}^0 \phi$) calculation, we secured some 'near fits' to MARK-III data for $\xi=0$ and $\xi=1/3$. These 'near fits' were obtained both with and without a weak annihilation term. Clearly, it is possible to generate enough $B(D^0 \to \bar{K}^0 \phi)$ without a weak

annihilation term, though a finite annihilation term, about (15-20)% of the spectator term in $D^0 \to K^- \rho^+$, is not ruled out by data.

We now turn to a discussion of the role of the parameters $a_1$, $a_2$, $\xi$ and the annihilation parameter in both D and $D_s$ decays to VP modes. As we have commented earlier, a value of $a_1/a_2$ in the desired range of (-2.0 to -3.0) is secured with relative ease in perturbative QCD with $\xi=0$ and $\Lambda$ in range required by deep inelastic data. However for $\xi=1/3$ one has to use a higher value of $\Lambda$ ($\approx$500 MeV) to get $a_1/a_2$ in the desired range perturbatively. An alternate way to get $a_1/a_2$ in the desired range for $\xi=1/3$ would be by giving $c_+$ and $c_-$ non-perturbative contributions. However, in this case we loose control over the calculation of the parameters $a_1$ and $a_2$.

Once a value of $a_1/a_2$ is assumed, the value of $a_2$ is determined by eq.(IV.26). The value of $|a_2|$ so determined, though fairly insensitive to the value of $\xi$ (in the range $0 \leq \xi \leq 1/3$), tends to rise with $\xi$. For example, at $\xi=0$ and $a_1/a_2=-2.0$, one gets $|a_2|=0.6933$ while with $\xi=1/3$ and $a_1/a_2=-2.0$ one gets $|a_2|=0.7336$. This increase in $|a_2|$ raises the normalization of all the amplitudes listed in Table 1. This change in the amplitudes can be compensated by using a non-zero annihilation term. Thus if a solution could be found with $\xi=0$ and R=0, for a certain value of the ratio $a_1/a_2$, we could, in general, also find a solution with $\xi=1/3$ and $R\neq0$ for the same value of the ratio $a_1/a_2$. This is

evident from the calculations of this and the previous section (see Tables 3, 4 and 8).

In presenting our results in Tables 3, 4 and 8, we have usec $a_1/a_2$ =-2.0 for $\xi$=0 and $a_1/a_2$=-2.4 for $\xi$=1/3 for the simple reason that while $a_1/a_2$=-2.0 can be secured with relative ease in NLL perturbation theory with $\xi$=0, such is not the case for $\xi$=1/3. However, for $\xi$=1/3, one can get $a_1/a_2$ in the region of -2.5 with $\Lambda\simeq$0.5GeV and $\mu\simeq$1.2GeV.

## IV.5 Cabibbo-angle favored D,$D_s\to$VV

*D→VV*

Very little experimental data[68,70] is available for these modes so far. However, it is still interesting to examine the role of weak annihilation and final state interactions in these decays. The Cabibbo-angle favored VV modes for D decay are: $K^*\rho$ and $\bar{K}^{*0}\omega$. Note that $\bar{K}^{*0}\phi$ is kinematically disallowed. The amplitudes in the VV case are more complicated than in the PV case, as they involve a larger number of form-factors. Using eq.(IV.22) we have,

$$A(D^0\to K^{*-}\rho^+) = \frac{G_F}{\sqrt{2}}\cos^2\theta_c\{a_1\langle\rho^+|\bar{u}d|0\rangle\langle K^{*-}|\bar{s}c|D^0\rangle + a_2\langle K^{*-}\rho^+|\bar{s}d|0\rangle\langle 0|\bar{u}c|D^0\rangle\}$$

$$= \frac{G_F}{\sqrt{2}}\cos^2\theta_c\left\{\left(a_1\frac{2m_\rho f_\rho}{m_D+m_{K^*}}\frac{h_v(D\to K^*)}{1-q^2/m_1^2}+a_2R\right)\times\varepsilon_{\mu\nu\rho\sigma}\varepsilon_\rho^\mu\,\varepsilon_{K^*}^\nu\,P_D^\rho\,P_{K^*}^\sigma\right.$$

$$\left.+ia_1m_\rho f_\rho\left(\varepsilon_\rho.\varepsilon_{K^*}\,(m_D+m_{K^*})\frac{h_{A1}(D\to K^*)}{1-q^2/m_1^2}\right.\right.$$

$$- \frac{\varepsilon_{K^*}\cdot q}{(m_D+m_{K^*})}(P_D+P_{K^*})\cdot\varepsilon_\rho \frac{h_{A2}(D\to K^*)}{1-q^2/m_{1^+}^2}\Bigg)\Bigg\}$$

$$A(D^0\to\bar{K}^{*0}\rho^0) = \frac{G_F}{\sqrt{2}}\cos^2\theta_c\{a_2\langle\bar{K}^{*0}|\bar{s}d|0\rangle\langle\rho^0|\bar{u}c|D^0\rangle$$

$$+a_2\langle\bar{K}^{*0}\rho^0|\bar{s}d|0\rangle\langle 0|\bar{u}c|D^0\rangle\}$$

$$= \frac{G_F}{\sqrt{2}}\cos^2\theta_c\frac{a_2}{\sqrt{2}}m_{K^*}f_{K^*}$$

$$\times\Bigg\{\Bigg(\frac{2}{m_D+m_\rho}\frac{h_V(D\to\rho)}{1-q^2/m_{1^-}^2} - R\Bigg)\varepsilon_{\mu\nu\rho\sigma}\varepsilon_{K^*}^{\mu}\varepsilon_\rho^{\nu}P_D^{\rho}P_\rho^{\sigma}$$

$$i\Bigg(\varepsilon_\rho\cdot\varepsilon_{K^*}(m_D+m_\rho)\frac{h_{A1}(D\to\rho)}{1-q^2/m_{1^+}^2}$$

$$- \frac{\varepsilon_\rho\cdot q}{(m_D+m_\rho)}(P_D+P_\rho)\cdot\varepsilon_{K^*}\frac{h_{A2}(D\to\rho)}{1-q^2/m_{1^+}^2}\Bigg)\Bigg\}$$

$$A(D^0\to\bar{K}^{*0}\omega) = \frac{G_F}{\sqrt{2}}\cos^2\theta_c\{a_2\langle\bar{K}^{*0}|\bar{s}d|0\rangle\langle\omega|\bar{u}c|D^0\rangle$$

$$+ \quad a_2\langle\bar{K}^{*0}\omega|\bar{s}d|0\rangle\langle 0|\bar{u}c|D^0\rangle\}$$

$$= \frac{G_F}{\sqrt{2}}\cos^2\theta_c\frac{a_2}{\sqrt{2}}m_{K^*}f_{K^*}$$

$$\times\Bigg\{\Bigg(\frac{2}{m_D+m_\omega}\frac{h_V(D\to\omega)}{1-q^2/m_{1^-}^2} + R\Bigg)\varepsilon_{\mu\nu\rho\sigma}\varepsilon_{K^*}^{\mu}\varepsilon_\omega^{\nu}P_D^{\rho}P_\rho^{\sigma}$$

$$i\Bigg(\varepsilon_\omega\cdot\varepsilon_{K^*}(m_D+m_\omega)\frac{h_{A1}(D\to\omega)}{1-q^2/m_{1^+}^2}$$

$$- \frac{\varepsilon_\omega\cdot q}{(m_D+m_\omega)}(P_D+P_\omega)\cdot\varepsilon_{K^*}\frac{h_{A2}(D\to\omega)}{1-q^2/m_{1^+}^2}\Bigg)\Bigg\}$$

...(IV.37)

where, $m_{1^-}$ and $m_{1^+}$ are the vector and axial vector poles of the appropriate currents respectively. R is an annihilation

parameter.

The $K^*\rho$ state can have isospin 1/2 and 3/2, while $K^*\omega$ will have isospin 1/2 final state only. Hence we have a two coupled channel problem in I=1/2. The isospin decomposition of $K^*\rho$ is given by,

$$|I=1/2,\ I_3=1/2\rangle = \frac{1}{\sqrt{3}}[|\bar{K}^{*0}\rho^0\rangle - \sqrt{2}\ |K^{*-}\rho^+\rangle]$$
$$|I=3/2,\ I_3=1/2\rangle = \frac{1}{\sqrt{3}}[\sqrt{2}\ |\bar{K}^{*0}\rho^0\rangle + |K^{*-}\rho^+\rangle] \qquad \text{(IV.38)}$$

Again as in VP case, we may use the $\bar{K}^0(1830)$ resonance for coupling the I=1/2 states. The amplitudes written in eq.(IV.37) involve a P-wave (L=1) term and terms which are mixtures of S and D-waves. The $\bar{K}^0$ resonance will couple only to the P-wave (L=1) terms. Therefore as a first approximation, we will unitarize only this part of each of the amplitudes. In principle, there can be non-resonant scattering in the other partial waves, but we ignore them for the moment.

Using eq.(IV.10) and the condition det**K**=0, our resonant **K**-matrix is left with only one independent parameter. We vary this parameter and estimate the unitarized isospin 1/2 amplitudes for different values of annihilation parameter R.. The unitarized physical decay amplitudes will then have the form,

$$A^u(D^0\to K^{*-}\rho^+) = \sqrt{\frac{1}{3}}A^{O,K^*\rho}_{3/2,I} - \sqrt{\frac{2}{3}}A^{u,K^*\rho}_{1/2,I} + A^{O,K^{*-}\rho^+}_{II} + A^{O,K^{*-}\rho^+}_{III}$$

$$A^u(D^0\to \bar{K}^{*0}\rho^0) = \sqrt{\frac{2}{3}}A^{O,K^*\rho}_{3/2,I} + \sqrt{\frac{2}{3}}A^{u,K^*\rho}_{1/2,I} + A^{O,\bar{K}^{*0}\rho^0}_{II} + A^{O,\bar{K}^{*0}\rho^0}_{III}$$

$$A^u(D^0\to \bar{K}^{*0}\omega) = A^{O,K^*\omega}_{I} + A^{O,K^*\omega}_{II} + A^{O,K^*\omega}_{III}$$

...(IV.39)

where, the subscript I denotes the P-wave part while II and III denote parts that contain both S and D partial waves. The resulting branching ratios are listed in Table 9 for $a_1/a_2=-2.0$ and $\xi=0$. As is evident from Table 9, unitarization in P-wave only, does not alter the results very much. This is due to the fact that the dominant term in the un-unitarized amplitude is not the P-wave term.

**Table 9.** Theoretical branching ratios in percent for Cabibbo allowed D→VV decays, including a resonant coupling in the isospin 1/2, P-partial wave amplitudes. These have been evaluated at $a_1/a_2=-2.0$ and $\xi=0$. The range of values shown for each R, correspond to differing values of the parameter $\Gamma_{11}$.

| Mode | Theoretical Branching Ratio (%) | | |
|---|---|---|---|
| | $R=0.0GeV^2$ | $R=0.1GeV^2$ | $R=0.2GeV^2$ |
| $B(D^0\to\bar{K}^{*0}\omega)$ | 2.67-3.32 | 2.71-3.31 | 2.74-3.29 |
| $B(D^0\to K^{*-}\rho^+)$ | 24.3-26.3 | 25.2-26.4 | 25.6-26.5 |
| $B(D^0\to\bar{K}^{*0}\rho^0)$ | 3.26-3.46 | 3.37-3.47 | 3.38-3.48 |

Next we separate the S and D-partial wave amplitudes. This is achieved by rewriting the amplitudes in eqs.(IV.38) as, (see appendix B),

$$A(D^0\to K^{*-}\rho^+) = \frac{G_F}{\sqrt{2}}\cos^2\theta_C\left\{\left(a_1\frac{2m_\rho f_\rho}{m_D+m_{K^*}}\frac{h_V(D\to K^*)}{1-q^2/m_1^2}+a_2R\right)\right.$$

$$\times(-\sqrt{2}ikm_D)$$

$$\left.+ia_1m_\rho f_\rho\left((m_D+m_{K^*})\frac{h_{A1}(D\to K^*)}{1-q^2/m_1^2}\frac{1}{\sqrt{3}}(2-\frac{P_{K^*}\cdot P_\rho}{m_{K^*}m_\rho}\right)\right.$$

$$+ \frac{1}{(m_D+m_{K^*})} \frac{h_{A2}(D\to K^*)}{1-q^2/m_{1+}^2} \frac{2}{\sqrt{3}} \frac{k^2}{m_{K^*}m_\rho} m_D^2$$

$$+ (m_D+m_{K^*}) \frac{h_{A1}(D\to K^*)}{1-q^2/m_{1+}^2} \sqrt{\frac{2}{3}} \left(1 + \frac{P_{K^*}.P_\rho}{m_{K^*}\, m_\rho}\right)$$

$$- \frac{1}{(m_D+m_{K^*})} \frac{h_{A2}(D\to K^*)}{1-q^2/m_{1+}^2} \sqrt{\frac{2}{3}} \frac{2\, k^2 m_D^2}{m_{K^*}m_\rho}\Bigg)\Bigg\} -$$

$$A(D^0\to \bar{K}^{*0}\rho^0) = \frac{G_F}{\sqrt{2}} \cos^2\theta_c \frac{a_2}{\sqrt{2}} m_{K^*}\, f_{K^*}$$

$$\times \left\{\left(\left(\frac{2}{m_D+m_\rho} \frac{h_V(D\to\rho)}{1-q^2/m_{1-}^2} - R\right) \times (-\sqrt{2}ikm_D)\right.\right.$$

$$i\left(\left(m_D+m_\rho\right) \frac{h_{A1}(D\to\rho)}{1-q^2/m_{1+}^2} \frac{1}{\sqrt{3}} \left(2 - \frac{P_{K^*}.P_\rho}{m_{K^*}\, m_\rho}\right)\right.$$

$$+ \frac{1}{(m_D+m_\rho)} \frac{h_{A2}(D\to\rho)}{1-q^2/m_{1+}^2} \frac{2}{\sqrt{3}} \frac{k^2}{m_{K^*}m_\rho} m_D^2$$

$$+ (m_D+m_\rho) \frac{h_{A1}(D\to\rho)}{1-q^2/m_{1+}^2} \sqrt{\frac{2}{3}} \left(1 + \frac{P_{K^*}.P_\rho}{m_{K^*}\, m_\rho}\right)$$

$$\left.\left. - \frac{1}{(m_D+m_\rho)} \frac{h_{A2}(D\to\rho)}{1-q^2/m_{1+}^2} \sqrt{\frac{2}{3}} \frac{2\, k^2 m_D^2}{m_{K^*}m_\rho}\right)\right\}, \qquad \ldots(IV.40)$$

where k is the momentum of either of the vector particles produced in each mode. We then introduce a phase in the dominant D-wave terms and look at the variation of the amplitudes with this phase. The D-wave phase would be different in the two isospin states. Hence, the unitarized amplitudes will be given by,

$$A^{u}(D^{0}\to K^{*-}\rho^{+}) = A^{P,K^{*-}\rho^{+}} + A^{S,K^{*-}\rho^{+}} + \frac{1}{\sqrt{3}}A^{D,K^{*}\rho}_{3/2}\, e^{i\delta_3} - \sqrt{\frac{2}{3}}\, A^{D,K^{*}\rho}_{1/2}\, e^{i\delta_1}$$

$$A^{u}(D^{0}\to \bar{K}^{*0}\rho^{0}) = A^{P,\bar{K}^{*0}\rho^{0}} + A^{S,\bar{K}^{*0}\rho^{0}} + \sqrt{\frac{2}{3}}\, A^{D,K^{*}\rho}_{3/2}\, e^{i\delta_3} + \frac{1}{\sqrt{3}}A^{D,K^{*}\rho}_{1/2}\, e^{i\delta_1}\,. \qquad \ldots(IV.41)$$

A phase in the D-partial wave amplitude will not affect the $\bar{K}^{*0}\omega$ mode, as it has only one isospin state.

The results of the above calculation are presented in Table 10. A large variation in the $B(D^{0}\to K^{*-}\rho^{+})$ and $B(D^{0}\to \bar{K}^{*0}\rho^{0})$ is observed for differing phase values in the

**Table 10.** Theoretical branching ratios in percent for Cabibbo allowed D→VV decays, with a phase in the D-partial amplitudes evaluated for $a_1/a_2=-2.0$ and $\xi=0$.

| Phase in degrees | Theoretical branching ratios (%) R=0.0GeV$^2$ | | R=0.1GeV$^2$ | |
|---|---|---|---|---|
| | $K^{*-}\rho^{+}$ | $\bar{K}^{*0}\rho^{0}$ | $K^{*-}\rho^{+}$ | $\bar{K}^{*0}\rho^{0}$ |
| 0 | 27.91 | 3.77 | 27.23 | 3.57 |
| 30 | 27.00 | 4.68 | 26.32 | 4.48 |
| 60 | 24.52 | 7.17 | 23.83 | 6.97 |
| 90 | 21.12 | 10.57 | 20.44 | 10.36 |
| 120 | 17.72 | 13.96 | 17.04 | 13.76 |
| 150 | 15.24 | 16.45 | 14.55 | 16.25 |
| 180 | 14.33 | 17.36 | 13.64 | 17.16 |

D-partial wave of the amplitudes. In the above we did not mention the $D^{+}\to\bar{K}^{*0}\rho^{+}$ mode. This was due to the fact that this mode involves only one isospin (3/2) state. In the above unitarization scheme it's amplitude will remain

unaffected.

$D_s^+ \to VV$

The Cabibbo angle favored decay modes are: $\bar{K}^{*0}K^{*+}$, $\omega\rho^+$, $\phi\rho^+$ and $\rho^+\rho^0$. The un-unitarized amplitudes for these modes are evaluated using eqs.(IV.22),

$$A(D_s^+ \to \bar{K}^{*0}K^{*+}) = \frac{G_F}{\sqrt{2}} \cos^2\theta_c \{a_2 \langle \bar{K}^{*0}|\bar{s}d|0\rangle\langle K^{*+}|\bar{u}c|D_s^+\rangle + a_1 \langle \bar{K}^{*0}K^{*+}|\bar{u}d|0\rangle\langle 0|\bar{s}c|D_s^+\rangle\}$$

$$= \frac{G_F}{\sqrt{2}} \cos^2\theta_c \left\{\left(a_2 \frac{2m_{K^*} f_{K^*}}{m_{D_s}+m_{K^*}} \frac{h_v(D_s\to K^*)}{1-q^2/m_1^2} + a_1 R_s\right) \times \varepsilon_{\mu\nu\rho\sigma}\varepsilon^{\mu}_{\bar{K}^{*0}} \varepsilon^{\nu}_{K^{*+}} P^{\rho}_{D_s} P^{\sigma}_{K^{*+}} + ia_2 m_{K^*} f_{K^*}\left(\varepsilon_{\bar{K}^{*0}}\cdot\varepsilon_{K^{*+}} (m_{D_s}+m_{K^*}) \frac{h_{A1}(D_s\to K^*)}{1-q^2/m_1^2} - \frac{\varepsilon_{K^{*+}}\cdot q}{(m_{D_s}+m_{K^*})}(P_{D_s}+P_{K^{*+}})\cdot\varepsilon_{\bar{K}^{*0}} \frac{h_{A2}(D_s\to K^*)}{1-q^2/m_1^2}\right)\right\}$$

$$A(D_s^+ \to \omega\rho^+) = \frac{G_F}{\sqrt{2}} \cos^2\theta_c a_1 \langle \omega\rho^+|\bar{u}d|0\rangle\langle 0|\bar{s}c|D_s^+\rangle\}$$

$$= \frac{G_F}{\sqrt{2}} \cos^2\theta_c \; a_1\sqrt{2}R_s \; \varepsilon_{\mu\nu\rho\sigma}\varepsilon^{\mu}_{\omega} \; \varepsilon^{\nu}_{\rho^+} \; P^{\rho}_{D_s} P^{\sigma}_{\rho^+}$$

$$A(D_s^+ \to \phi\rho^+) = \frac{G_F}{\sqrt{2}} \cos^2\theta_c a_1 \langle \rho^+|\bar{u}d|0\rangle\langle \phi|\bar{s}c|D_s^+\rangle$$

$$= \frac{G_F}{\sqrt{2}} \cos^2\theta_c a_1 f_\rho m_\rho \left\{\left(\frac{2}{m_{D_s}+m_\phi} \frac{h_v(D_s\to\phi)}{1-q^2/m_1^2} \times \varepsilon_{\mu\nu\rho\sigma}\varepsilon^{\mu}_{\rho} \; \varepsilon^{\nu}_{\phi} \; P^{\rho}_{D_s} P^{\sigma}_{\phi}\right.\right.$$

$$+ i \left[ \varepsilon_\phi \cdot \varepsilon_\rho \ (m_{D_s} + m_\phi) \frac{h_{A1}(D_s \to \phi)}{1 - q^2/m_{1^+}^2} \right.$$

$$\left. \left. - \frac{\varepsilon_\phi \cdot q}{(m_{D_s} + m_\phi)} (P_{D_s} + P_\phi) \cdot \varepsilon_\rho \ \frac{h_{A2}(D_s \to \phi)}{1 - q^2/m_{1^+}^2} \right] \right\}$$

$$A(D_s^+ \to \rho^0 \rho^+) = 0. \qquad \ldots(IV.42)$$

SU(3) has been used to relate the annihilation terms of $\omega\rho^+$ and $\bar{K}^{*0}K^{*+}$. At the Cabibbo-allowed level, the spectator terms in $D_s$ decay must have final states that contain the s and $\bar{s}$ quarks. Hence in both $\omega\rho^+$ and $\rho^0\rho^+$ modes, spectator terms are absent. Further the vector current contribution to the annihilation terms are zero due to CVC. In the absence of second class currents, the axial vector current can contribute only to states with odd G-parity. Since $\rho^0\rho^+$ state has G=+1, its un-unitarized amplitude is then identically zero, while there is annihilation contribution to the G=-1 $\omega\rho^+$ state. Hence, the decays $D_s^+ \to \omega\rho^+$ and $D_s^+ \to \rho^0\rho^+$ are very interesting and experimental limits on these would be beneficial.

We couple the three G-odd states ($\bar{K}^{*0}K^{*+}$ has G=-1 in J=0 state). The G-even $\rho^0\rho^+$ state remains uncoupled. We thus expect the branching ratio for the $\rho^0\rho^+$ state to vanish. Regarding the experimental situation, the only two-body mode which has been measured[5] so far is that of $D_s^+ \to \bar{K}^{*0}K^{*+}$. Recently a value for $B(D_s^+ \to \phi\pi^0\pi^+)$ (presumably due to $\phi\rho^+$) has been reported.[68]

The $\bar{K}^{*0}K^{*+}$ and $\omega\rho^+$ modes can couple via a $\pi$-like resonance. Note that this resonant coupling is possible only in the P-wave. $\bar{K}^{*0}K^{*+}$ and $\phi\rho^+$ will only have non-resonant coupling (quark interchange diagrams). $\omega\rho^+ \leftrightarrow \phi\rho^+$ coupling is forbidden by OZI rule. We introduce non-resonant coupling in the dominant D-partial wave only, apart from the resonant coupling in the P-wave. The amplitudes are rewritten in a form, where the S and D-partial waves are separated (see Appendix B):

$$A(D_s^+ \to \bar{K}^{*0}K^{*+}) = \frac{G_F}{\sqrt{2}} \cos^2\theta_c \left\{ \left[ a_2 \frac{2m_{K^*} f_{K^*}}{m_{D_s}+m_{K^*}} \frac{h_V(D_s\to K^*)}{1-q^2/m_1^2} + a_1 R_s \right] \times (-\sqrt{2}ikm_{D_s}) \right.$$

$$+ ia_2 m_{K^*} f_{K^*} \left[ (m_{D_s}+m_{K^*}) \frac{h_{A1}(D_s\to K^*)}{1-q^2/m_1^2} \frac{1}{\sqrt{3}} \left(2 - \frac{P_{\bar{K}^{*0}} \cdot P_{K^{*+}}}{m_{K^*}^2}\right) \right.$$

$$+ \frac{1}{(m_{D_s}+m_{K^*})} \frac{h_{A2}(D_s\to K^*)}{1-q^2/m_1^2} \frac{2k^2}{\sqrt{3}m_{K^*}^2} m_{D_s}^2$$

$$+ (m_{D_s}+m_{K^*}) \frac{h_{A1}(D_s\to K^*)}{1-q^2/m_1^2} \sqrt{\frac{2}{3}} \left(1 + \frac{P_{\bar{K}^{*0}} \cdot P_{K^{*+}}}{m_{K^*}^2}\right)$$

$$\left. \left. - \frac{1}{(m_{D_s}+m_{K^*})} \frac{h_{A2}(D_s\to K^*)}{1-q^2/m_1^2} \sqrt{\frac{2}{3}} \frac{2k^2}{m_{K^*}^2} m_{D_s}^2 \right] \right\}$$

$$A(D_s^+ \to \phi\rho^+) = \frac{G_F}{\sqrt{2}} \cos^2\theta_c a_1 f_\rho m_\rho \left\{ \left[ \frac{2}{m_{D_s}+m_\phi} \frac{h_V(D_s\to\phi)}{1-q^2/m_1^2} \right. \right.$$

$$\times (-\sqrt{2}ikm_{D_s})$$

$$+i\Bigg[(m_{D_s}+m_\phi)\frac{h_{A1}(D_s\to\phi)}{1-q^2/m_{1+}^2}\frac{1}{\sqrt{3}}\left(2-\frac{P_\phi\cdot P_\rho}{m_\phi\cdot m_\rho}\right)$$

$$+\frac{1}{(m_{D_s}+m_\phi)}\frac{h_{A2}(D_s\to\phi)}{1-q^2/m_{1+}^2}\frac{2k^2}{\sqrt{3}m_\phi\cdot m_\rho}m_{D_s}^2$$

$$+(m_{D_s}+m_\phi)\frac{h_{A1}(D_s\to\phi)}{1-q^2/m_{1+}^2}\sqrt{\frac{2}{3}}\left(1+\frac{P_\phi\cdot P_\rho}{m_\phi\cdot m_\rho}\right)$$

$$-\frac{1}{(m_{D_s}+m_\phi)}\frac{h_{A2}(D_s\to\phi)}{1-q^2/m_{1+}^2}\sqrt{\frac{2}{3}}\frac{2k^2}{m_\phi\cdot m_\rho}m_{D_s}^2\Bigg]\Bigg\} \quad \ldots(IV.43)$$

Hence, in our problem, we have two coupled channels in each of the P and D-partial waves. The **K**-matrix for the P-wave has the resonant form of eq.(IV.7), while the non-resonant matrix coupling the D-wave amplitudes is given by eq.(IV.6). Note that $\omega\rho^+$ has only a P-wave amplitude. We vary the independent parameters of the corresponding **K**-matrices, to fit the known $B(D_s^+\to\bar{K}^{*0}K^{*+})$ and $B(D_s^+\to\phi\pi^0\pi^+)$, for various values of the annihilation parameter. This is done for both $\xi=0$ and $\xi=1/3$. The branching ratio for $D_s^+\to\bar{K}^{*0}K^{*+}$ restricts the range of R to be $\lesssim 0.6$ GeV$^2$.

We find that even for R=0, through final state interactions alone $B(D_s^+\to\omega\rho^+)$ can be $\simeq 0.13\%$. A higher value is obtained for $R\neq 0$. A measurement of this mode would be very useful. A fit to data is presented in Table 11. Regarding $B(D_s^+\to\phi\rho^+)$, we wish to point out that in absence of final state interactions, the un-unitarized amplitude yields a branching ratio of $\simeq 21\%$ (for $a_1=1.3$), which is much larger

than that deduced from the observation[68] of $\phi\pi^0\pi^+$ modes,

**Table 11.** Fits for Cabibbo allowed $D_s \to VV$ decays. Theory columns with $\xi=0$ use $a_1/a_2=-2.0$, $b=1.2\text{GeV}^{-1}$ and $c=2.6\text{GeV}^{-1}$ while that for $\xi=1/3$ use $a_1/a_2=-2.4$, $b=1.2\text{GeV}^{-1}$ and $c=2.4\text{GeV}^{-1}$. The values listed are for $\Gamma_{11}=0.31$ GeV, $\Gamma_{22}=0.66$ GeV.

| Branching ratio(%) | Theory $\xi=0$ | | Theory $\xi=1/3$ | | Data(%) |
|---|---|---|---|---|---|
| | $R_s=0.0$ GeV$^2$ | $R_s=0.10$ GeV$^2$ | $R_s=0.0$ GeV$^2$ | $R_s=0.1$ GeV$^2$ | |
| $B(D_s^+\to\bar{K}^{*0}K^{*+})$ | 7.31 | 6.94 | 6.45 | 6.21 | 8.1±4.2±2.8 |
| $B(D_s^+\to\omega\rho^+)$ | 0.10 | 1.90 | 0.06 | 1.78 | - |
| $B(D_s^+\to\phi\rho^+)$ | 12.2 | 12.2 | 11.8 | 11.8 | 8.4±4.1 |

$B(D_s\to\phi\pi^0\pi^+)/B(D_s\to\phi\pi^+)=2.4\pm1.0\pm0.5$. With inclusion of final state interactions, this value is satisfied, for $c \gtrsim 2.00\text{GeV}^{-1}$. Note that the solutions in Table 11, are obtained for $c>b$. Since, the $K^*K^* \Leftrightarrow \phi\rho$ coupling is via a quark interchange diagram (nonplanar), while $K^*K^* \Leftrightarrow K^*K^*$ coupling is planar, one would have expected $c<b$. One reason for this result could be that the form-factors appearing in the vector, vector amplitudes may not be reliable. Another possibility is that the $B(D_s\to\phi\rho^+)$ is itself large- but there is some cancellation, resulting in a small $\phi\pi\pi$ branching ratio. A measurement of $\phi\rho^+$ mode itself, could clarify the issue.

**IV.6** Cabibbo-suppressed D→VP modes

The possible modes of decay for D at the Cabibbo

-suppressed level are: $\rho\pi$, $\phi\pi$, $\omega\pi$, $\phi\eta$, $\omega\eta$, $\omega\eta'$, $\eta\rho$, $\eta'\rho$, $K^*K$. A few of these Cabibbo-suppressed D→VP decay modes have been measured.[6] Two of these modes are particularly interesting, $D^0\to K^{*0}\bar{K}^0$ and $D^+\to\rho^0\pi^+$. The amplitude for $D^0\to K^{*0}\bar{K}^0$ does not get a contribution from the spectator diagram. An upper limit on it's branching ratio exits.[6] The measured value[65] of $B(D^+\to\rho^0\pi^+)$ is $\simeq 0.2\%$. In the absence of final state interaction and weak annihilation the theoretical branching ratio is two orders of magnitude smaller.

We first consider the decays of the neutral D mesons. The un-unitarized amplitudes for the above modes are given by,

$$A(D^0\to\rho^-\pi^+) = \frac{-G_F}{\sqrt{2}}\cos\theta_c\sin\theta_c\{a_1\langle\pi^+|\bar{u}d|0\rangle\langle\rho^-|\bar{d}c|D^0\rangle + a_2\langle\rho^-\pi^+|\bar{d}d|0\rangle\langle 0|\bar{u}c|D^0\rangle\}$$

$$= \frac{-G_F}{\sqrt{2}}\cos\theta_c\sin\theta_c\left\{a_1 f_\pi 2m_\rho \frac{h_{A0}(D\to\rho)}{1-q^2/m_0^2} + a_2\frac{R}{\sqrt{2}}\right\}(\varepsilon\cdot k)$$

$$A(D^0\to\rho^+\pi^-) = \frac{-G_F}{\sqrt{2}}\cos\theta_c\sin\theta_c\{a_1\langle\rho^+|\bar{u}d|0\rangle\langle\pi^-|\bar{d}c|D^0\rangle + a_2\langle\pi^-\rho^+|\bar{d}d|0\rangle\langle 0|\bar{u}c|D^0\rangle\}$$

$$= \frac{-G_F}{\sqrt{2}}\cos\theta_c\sin\theta_c\left\{a_1 f_\rho 2m_\rho \frac{h_{F1}(D\to\pi)}{1-q^2/m_1^2} - a_2\frac{R}{\sqrt{2}}\right\}(\varepsilon\cdot k)$$

$$A(D^0\to\rho^0\pi^0) = \frac{-G_F}{\sqrt{2}}\cos\theta_c\sin\theta_c\{a_2\langle\rho^0|\bar{d}d|0\rangle\langle\pi^0|\bar{u}c|D^0\rangle + a_2\langle\pi^0|\bar{d}d|0\rangle\langle\rho^0|\bar{u}c|D^0\rangle + a_2\langle\rho^0\pi^0|\bar{d}d|0\rangle\langle 0|\bar{u}c|D^0\rangle\}$$

$$= \frac{G_F}{\sqrt{2}} \cos\theta_c \sin\theta_c a_2 \left\{ f_\pi m_\rho \frac{h_{A0}(D\to\rho)}{1-q^2/m_0^2} + f_\rho m_\rho \frac{h_{F1}(D\to\pi)}{1-q^2/m_1^2} \right\} (\varepsilon\cdot k)$$

$$A(D^0\to\omega\pi^0) = \frac{-G_F}{\sqrt{2}} \cos\theta_c \sin\theta_c (a_2 \langle\omega|\bar{d}d|0\rangle\langle\pi^0|\bar{u}c|D^0\rangle + a_2\langle\pi^0|\bar{d}d|0\rangle\langle\omega|\bar{u}c|D^0\rangle)$$

$$= \frac{-G_F}{\sqrt{2}} \cos\theta_c \sin\theta_c a_2 \left\{ f_\omega m_\omega \frac{h_{F1}(D\to\pi)}{1-q^2/m_1^2} - f_\pi m_\omega \frac{h_{A0}(D\to\omega)}{1-q^2/m_0^2} \right\} (\varepsilon\cdot k)$$

$$A(D^0\to\phi\pi^0) = \frac{G_F}{\sqrt{2}} \cos\theta_c \sin\theta_c a_2 \langle\phi|\bar{s}s|0\rangle\langle\pi^0|\bar{u}c|D^0\rangle$$

$$= \frac{G_F}{\sqrt{2}} \cos\theta_c \sin\theta_c a_2 \sqrt{2} f_\phi m_\phi \frac{h_{F1}(D\to\pi)}{1-q^2/m_1^2} (\varepsilon\cdot k)$$

$$A(D^0\to\phi\eta) = \frac{G_F}{\sqrt{2}} \cos\theta_c \sin\theta_c \, a_2 \langle\phi|\bar{s}s|0\rangle\langle\eta|\bar{u}c|D^0\rangle$$

$$= \frac{G_F}{\sqrt{2}} \cos\theta_c \sin\theta_c \, a_2 2 f_\phi m_\phi \frac{h_1(D\to\eta)}{1-q^2/m_1^2} \times \left(\frac{\cos\theta_p}{\sqrt{2}} - \sin\theta_p\right) \frac{(\varepsilon\cdot k)}{\sqrt{3}}$$

where $\theta_p$ is the pseudoscalar mixing angle (see Chapter V),

$$A(D^0\to\omega\eta) = \frac{-G_F}{\sqrt{2}} \cos\theta_c \sin\theta_c (a_2 \langle\omega|\bar{d}d|0\rangle\langle\eta|\bar{u}c|D^0\rangle + a_2\langle\eta|\bar{d}d|0\rangle\langle\omega|\bar{u}c|D^0\rangle - a_2\langle\eta|\bar{s}s|0\rangle\langle\omega|\bar{u}c|D^0\rangle)$$

$$= \frac{-G_F}{\sqrt{2}} \cos\theta_c \sin\theta_c a_2 \left\{ \left( f_\omega m_\omega \frac{h_{F1}(D\to\eta)}{1-q^2/m_1^2} + f_\eta m_\omega \frac{h_{A0}(D\to\omega)}{1-q^2/m_0^2} \right) \right.$$

$$\times \left(\frac{\cos\theta_p}{\sqrt{2}} - \sin\theta_p\right)\sqrt{\frac{2}{3}}$$

$$+ f_\eta^- m_\omega \frac{h_{A0}(D\to\omega)}{1-q^2/m_{0-}^2} \left(\sqrt{2}\cos\theta_p + \sin\theta_p\right)\sqrt{\frac{2}{3}}\Bigg\}(\varepsilon\cdot k)$$

where $f_{\eta'}$, $f_\eta^-$ are the decay constants corresponding to the non-strange and strange currents respectively (Appendix A),

$$A(D^0\to\omega\eta') = \frac{-G_F}{\sqrt{2}}\cos\theta_c\sin\theta_c\{a_2\langle\omega|\bar{d}d|0\rangle\langle\eta'|\bar{u}c|D^0\rangle$$

$$+ a_2\langle\eta'|\bar{d}d|0\rangle\langle\omega|\bar{u}c|D^0\rangle - a_2\langle\eta'|\bar{s}s|0\rangle\langle\omega|\bar{u}c|D^0\rangle\}$$

$$= \frac{-G_F}{\sqrt{2}}\cos\theta_c\sin\theta_c a_2\Bigg\{\Bigg(f_\omega m_\omega \frac{h_{F1}(D\to\eta')}{1-q^2/m_{1-}^2} + f_{\eta'} m_\omega \frac{h_{A0}(D\to\omega)}{1-q^2/m_{0-}^2}\Bigg)$$

$$\times \left(\frac{\sin\theta_p}{\sqrt{2}} - \cos\theta_p\right)\sqrt{\frac{2}{3}}$$

$$+ f_{\eta'}^- m_\omega \frac{h_{A0}(D\to\omega)}{1-q^2/m_{0-}^2} \left(\sqrt{2}\sin\theta_p - \cos\theta_p\right)\sqrt{\frac{2}{3}}\Bigg\}(\varepsilon\cdot k)$$

$$A(D^0\to\rho^0\eta) = \frac{-G_F}{\sqrt{2}}\cos\theta_c\sin\theta_c\{a_2\langle\rho^0|\bar{d}d|0\rangle\langle\eta|\bar{u}c|D^0\rangle$$

$$+ a_2\langle\eta|\bar{d}d|0\rangle\langle\rho^0|\bar{u}c|D^0\rangle - a_2\langle\eta|\bar{s}s|0\rangle\langle\rho^0|\bar{u}c|D^0\rangle\}$$

$$= \frac{-G_F}{\sqrt{2}}\cos\theta_c\sin\theta_c a_2\Bigg\{\Bigg(-f_\rho m_\rho \frac{h_{F1}(D\to\eta)}{1-q^2/m_{1-}^2} + f_\eta m_\rho \frac{h_{A0}(D\to\rho)}{1-q^2/m_{0-}^2}\Bigg)$$

$$\times \left(\frac{\cos\theta_p}{\sqrt{2}} - \sin\theta_p\right)\sqrt{\frac{2}{3}}$$

$$+ f_\eta^- m_\rho \frac{h_{A0}(D\to\rho)}{1-q^2/m_{0-}^2} \left(\sqrt{2}\cos\theta_p + \sin\theta_p\right)\sqrt{\frac{2}{3}}\Bigg\}(\varepsilon\cdot k)$$

$$A(D^0\to\rho^0\eta') = \frac{-G_F}{\sqrt{2}}\cos\theta_c\sin\theta_c\{a_2\langle\rho^0|\bar{d}d|0\rangle\langle\eta'|\bar{u}c|D^0\rangle$$

$$+ a_2\langle\eta'|\bar{d}d|0\rangle\langle\rho^0|\bar{u}c|D^0\rangle - a_2\langle\eta'|\bar{s}s|0\rangle\langle\rho^0|\bar{u}c|D^0\rangle\}$$

$$= \frac{-G_F}{\sqrt{2}} \cos\theta_c \sin\theta_c a_2 \Big\{ \Big( -f_\rho m_\rho \frac{h_{F1}(D\to\eta')}{1-q^2/m_1^2} + f_{\eta'} m_\rho \frac{h_{A0}(D\to\rho)}{1-q^2/m_0^2} \Big)$$

$$\times \Big( \frac{\sin\theta_p}{\sqrt{2}} - \cos\theta_p \Big) \sqrt{\frac{2}{3}}$$

$$+ f_\eta m_\rho \frac{h_{A0}(D\to\rho)}{1-q^2/m_0^2} \Big( \sqrt{2}\sin\theta_p - \cos\theta_p \Big) \sqrt{\frac{2}{3}} \Big\} (\varepsilon\cdot k)$$

$$A(D^0\to K^+K^{*-}) = \frac{G_F}{\sqrt{2}} \cos\theta_c \sin\theta_c \{ a_1 \langle K^+|\bar{u}s|0\rangle\langle K^{*-}|\bar{s}c|D^0\rangle$$

$$+ a_2 \langle K^+K^{*-}|\bar{s}s|0\rangle\langle 0|\bar{u}c|D^0\rangle \}$$

$$= \frac{G_F}{\sqrt{2}} \cos\theta_c \sin\theta_c \Big\{ a_1 2 f_K m_{K^*} \frac{h_{A0}(D\to K^*)}{1-q^2/m_0^2} + a_2 \frac{R}{\sqrt{2}} \Big\} (\varepsilon\cdot k)$$

$$A(D^0\to K^{*+}K^-) = \frac{G_F}{\sqrt{2}} \cos\theta_c \sin\theta_c \{ a_1 \langle K^{*+}|\bar{u}s|0\rangle\langle K^-|\bar{s}c|D^0\rangle$$

$$+ a_2 \langle K^{*+}K^-|\bar{s}s|0\rangle\langle 0|\bar{u}c|D^0\rangle \}$$

$$= \frac{G_F}{\sqrt{2}} \cos\theta_c \sin\theta_c \Big\{ a_1 2 f_{K^*} m_{K^*} \frac{h_{F1}(D\to K)}{1-q^2/m_1^2} - a_2 \frac{R}{\sqrt{2}} \Big\} (\varepsilon\cdot k)$$

$$A(D^0\to K^0\bar{K}^{*0}) = \frac{-G_F}{\sqrt{2}} \cos\theta_c \sin\theta_c \{ a_2 \langle K^0\bar{K}^{*0}|\bar{d}d|0\rangle\langle 0|\bar{u}c|D^0\rangle$$

$$- a_2 \langle K^0\bar{K}^{*0}|\bar{s}s|0\rangle\langle 0|\bar{u}c|D^0\rangle \}$$

$$= \frac{G_F}{\sqrt{2}} \cos\theta_c \sin\theta_c \sqrt{2} a_2 R \, (\varepsilon\cdot k)$$

$$A(D^0\to K^{*0}\bar{K}^0) = -\frac{G_F}{\sqrt{2}} \cos\theta_c \sin\theta_c \sqrt{2} a_2 R \, (\varepsilon\cdot k)$$

...(IV.44)

The annihilation in $\rho\pi$'s is assumed to proceed via a $\pi$-like resonance whereas in $K^*K$'s through an $\eta$-like or $\pi$-like resonance. The annihilation contribution in these modes is related by SU(3). No resonance with appropriate quantum

numbers is available for the annihilation to proceed in the other channels (note a vector resonance cannot contribute).

Since the weak current has I=1/2 and 3/2 pieces, the isospin of the final states can be 0, 1 or 2. Strong coupling conserves G-parity and isospin. We therefore list the states that contribute to the different isospins for each G-parity separately,

$$\begin{aligned} G=-1: \quad & I=0 \ \rho\pi,\ \phi\eta,\ \omega\eta,\ \omega\eta',\ K^*K \\ & I=1 \ \rho\pi,\ K^*K \\ & I=2 \ \rho\pi \qquad\qquad (IV.45) \\ G=+1 \quad & I=0 \ K^*K \\ & I=1 \ \omega\pi,\ \phi\pi,\ \eta\rho,\ \eta'\rho,\ K^*K\ . \end{aligned}$$

In G=-1, I=1, $\rho\pi$ states can couple to $K^*K$'s through a $\pi$-like resonance. In G=-1, I=0, $\rho\pi \leftrightarrow K^*K$, $K^*K \leftrightarrow \omega\eta/\omega\eta'$ and $\rho\pi \leftrightarrow \omega\eta/\omega\eta'$ ($K^*K \leftrightarrow \phi\eta$) can couple via a $\bar{u}u$ (or $\bar{s}s$) resonance. An isospin zero, G=-1 resonance will be $\omega$-like (or $\phi$-like for $\bar{s}s$). However, a vector resonance cannot contribute to final state interactions in D→VP modes. Note that $\phi\eta \leftrightarrow \omega\eta/\omega\eta'$ coupling will be nonresonant and that $\rho\pi \leftrightarrow \phi\eta$ is disallowed by OZI. Again in G=+1, $\omega\pi$ coupling to $\eta\rho$, $\eta'\rho$ and $K^*K$'s can only be via a $\bar{u}u$ resonance. It must have G=+1, I=1, i.e., $\rho$-like, which again is disallowed. We shall ignore the non-resonant couplings and consider only the resonant coupling of $K^*K$ and $\rho\pi$ in G=-1, I=1 isospin state, as very little experimental data is available on all the other decay modes.

We thus need to first construct eigen-states of

G-parity and isospin for $K^*K$'s. For the $K^*\bar{K}$ states, where the particle and antiparticle doublets are given by

$$K^* = \begin{pmatrix} K^{*+} \\ K^{*0} \end{pmatrix} \qquad \text{and} \qquad \bar{K} = \begin{pmatrix} \bar{K}^0 \\ -K^- \end{pmatrix}$$

the isospin 1 and 0 states are given by

$$|I=1,\ I_3=0\rangle_I = -\frac{1}{\sqrt{2}}|K^{*+}K^-\rangle + \frac{1}{\sqrt{2}}|K^{*0}\bar{K}^0\rangle$$
$$|I=0,\ I_3=0\rangle_I = -\frac{1}{\sqrt{2}}|K^{*+}K^-\rangle - \frac{1}{\sqrt{2}}|K^{*0}\bar{K}^0\rangle \qquad \text{(IV.46)}$$

Similarly for $K\bar{K}^*$ states (i.e., particle pseudoscalar, antiparticle vector),

$$|I=1,\ I_3=0\rangle_{II} = -\frac{1}{\sqrt{2}}|K^+K^{*-}\rangle + \frac{1}{\sqrt{2}}|K^0\bar{K}^{*0}\rangle$$
$$|I=0,\ I_3=0\rangle_{II} = -\frac{1}{\sqrt{2}}|K^+K^{*-}\rangle - \frac{1}{\sqrt{2}}|K^0\bar{K}^{*0}\rangle \qquad \text{(IV.47)}$$

The combined isospin states are:

$$|1,0\rangle_s = \frac{1}{2}\{|K^{*0}\bar{K}^0\rangle + |K^0\bar{K}^{*0}\rangle - (|K^{*+}K^-\rangle + |K^+K^{*-}\rangle)\} \qquad G=+1$$
$$|1,0\rangle_A = \frac{1}{2}\{|K^{*0}\bar{K}^0\rangle - |K^0\bar{K}^{*0}\rangle - |K^{*+}K^-\rangle + |K^+K^{*-}\rangle\} \qquad G=-1$$
$$|0,0\rangle_s = -\frac{1}{2}\{|K^{*0}\bar{K}^0\rangle + |K^0\bar{K}^{*0}\rangle + |K^{*+}K^-\rangle + |K^+K^{*-}\rangle\} \qquad G=-1$$
$$|0,0\rangle_A = \frac{1}{2}\{-|K^{*0}\bar{K}^0\rangle + |K^0\bar{K}^{*0}\rangle - |K^{*+}K^-\rangle + |K^+K^{*-}\rangle\} \qquad G=+1$$
$$\ldots\text{(IV.48)}$$

As indicated, these are states of definite G-parity.

The isospin decomposition for the $\rho\pi$ states is given by,

$$A_0^{\rho\pi} = \frac{1}{\sqrt{3}}\{|\rho^+\pi^-\rangle + |\rho^-\pi^+\rangle + |\rho^0\pi^0\rangle\}$$
$$A_1^{\rho\pi} = \frac{1}{\sqrt{2}}\{|\rho^+\pi^-\rangle - |\rho^-\pi^+\rangle\} \qquad \text{(IV.49)}$$
$$A_2^{\rho\pi} = \frac{1}{\sqrt{6}}\{|\rho^+\pi^-\rangle + |\rho^-\pi^+\rangle - 2|\rho^0\pi^0\rangle\}$$

Hence, we couple $A_1^{\rho\pi}$ and the $|1,0\rangle_A$ $K^*K$ state via a resonant K-matrix given in eq.(IV.7) with $m_R$=1770MeV and $\Gamma_R$=300MeV.

The unitarized physical amplitudes are obtained as follows,

$$A^u(D^0\to\rho^+\pi^-) = \frac{1}{\sqrt{6}} A_2^{0,\rho\pi} + \frac{1}{\sqrt{2}} A_1^{u,\rho\pi} + \frac{1}{\sqrt{3}} A_0^{0,\rho\pi}$$

$$A^u(D^0\to\rho^-\pi^+) = \frac{1}{\sqrt{6}} A_2^{0,\rho\pi} - \frac{1}{\sqrt{2}} A_1^{u,\rho\pi} + \frac{1}{\sqrt{3}} A_0^{0,\rho\pi}$$

$$A^u(D^0\to\rho^0\pi^0) = A^0(D^0\to\rho^0\pi^0)$$

$$A^u(D^0\to K^{*+}K^-) = -\frac{1}{2}\{A^{0,K^*K}_{I=1,G=1} + A^{u,K^*K}_{I=1,G=-1} + A^{0,K^*K}_{I=0,G=-1} + A^{0,K^*K}_{I=0,G=+1}\}$$

$$A^u(D^0\to K^{*0}\bar{K}^0) = \frac{1}{2}\{A^{0,K^*K}_{I=1,G=1} + A^{u,K^*K}_{I=1,G=-1} - A^{0,K^*K}_{I=0,G=-1} - A^{0,K^*K}_{I=0,G=+1}\}$$

$$A^u(D^0\to K^0\bar{K}^{*0}) = \frac{1}{2}\{A^{0,K^*K}_{I=1,G=1} - A^{u,K^*K}_{I=1,G=-1} - A^{0,K^*K}_{I=0,G=-1} + A^{0,K^*K}_{I=0,G=+1}\}$$

$$A^u(D^0\to K^+K^{*-}) = -\frac{1}{2}\{A^{0,K^*K}_{I=1,G=1} - A^{u,K^*K}_{I=1,G=-1} + A^{0,K^*K}_{I=0,G=-1} - A^{0,K^*K}_{I=0,G=+1}\}$$

...(IV.50)

Next we consider the corresponding $D^+$ decay modes. The un-unitarized amplitudes for the modes being coupled are :

$$A(D^+\to\rho^0\pi^+) = \frac{-G_F}{\sqrt{2}} \cos\theta_c\sin\theta_c\{a_1\langle\pi^+|\bar{u}d|0\rangle\langle\rho^0|\bar{d}c|D^+\rangle + a_1\langle\pi^+\rho^0|\bar{u}d|0\rangle\langle 0|\bar{d}c|D^0\rangle + a_2\langle\rho^0|\bar{d}d|0\rangle\langle\pi^+|\bar{u}c|D^+\rangle\}$$

$$= \frac{G_F}{\sqrt{2}} \cos\theta_c\sin\theta_c\left\{a_1\sqrt{2}f_\pi m_\rho \frac{h_{A0}(D\to\rho)}{1-q^2/m_0^2} - a_1 R + a_2\sqrt{2}f_\rho m_\rho \frac{h_{F1}(D\to\pi)}{1-q^2/m_1^2}\right\}(\varepsilon\cdot k)$$

$$A(D^+\to\rho^+\pi^0) = \frac{-G_F}{\sqrt{2}} \cos\theta_c\sin\theta_c\{a_1\langle\rho^+|\bar{u}d|0\rangle\langle\pi^0|\bar{d}c|D^+\rangle + a_1\langle\rho^+\pi^0|\bar{u}d|0\rangle\langle 0|\bar{d}c|D^0\rangle + a_2\langle\pi^0|\bar{d}d|0\rangle\langle\rho^+|\bar{u}c|D^+\rangle\}$$

$$= \frac{G_F}{\sqrt{2}} \cos\theta_c \sin\theta_c \left\{ a_1 \sqrt{2} f_\rho m_\rho \frac{h_{F1}(D\to\pi)}{1-q^2/m_1^2} + a_1 R \right.$$

$$\left. + a_2 \sqrt{2} f_\pi m_\rho \frac{h_{A0}(D\to\rho)}{1-q^2/m_0^2} \right\} (\varepsilon\cdot k)$$

$$A(D^+\to K^{*+}\bar{K}^0) = \frac{G_F}{\sqrt{2}} \cos\theta_c \sin\theta_c \{ a_1 \langle K^{*+}|\bar{u}s|0\rangle\langle\bar{K}^0|\bar{s}c|D^0\rangle$$

$$- a_1 \langle K^{*+}\bar{K}^0|\bar{u}d|0\rangle\langle 0|\bar{d}c|D^0\rangle \}$$

$$= \frac{G_F}{\sqrt{2}} \cos\theta_c \sin\theta_c \left\{ a_1 2 f_{K^*} m_{K^*} \frac{h_{F1}(D\to K)}{1-q^2/m_1^2} - a_1 \frac{R}{\sqrt{2}} \right\} (\varepsilon.k)$$

$$A(D^+\to K^+\bar{K}^{*0}) = \frac{G_F}{\sqrt{2}} \cos\theta_c \sin\theta_c \{ a_1 \langle K^+|\bar{u}s|0\rangle\langle\bar{K}^{*0}|\bar{s}c|D^0\rangle$$

$$- a_1 \langle K^+\bar{K}^{*0}|\bar{u}d|0\rangle\langle 0|\bar{d}c|D^0\rangle \}$$

$$= \frac{G_F}{\sqrt{2}} \cos\theta_c \sin\theta_c \left\{ a_1 2 f_K m_{K^*} \frac{h_{A0}(D\to K^*)}{1-q^2/m_0^2} + a_1 \frac{R}{\sqrt{2}} \right\} (\varepsilon.k)$$

...(IV.51)

The $I=1$, $G=-1$ amplitude for $\rho\pi$ and $K^*K$ states resulting from the $D^+$ decays can in principle be related to the corresponding $D^0$ decay states. These could then be used to evaluate the branching ratio for $D^+\to\rho^0\pi^+$ and $D^+\to K^+\bar{K}^{*0}$. Since there are experimental values available for these modes, this could further constrain the parameters of the **K**-matrix. However, unlike the Cabibbo-allowed VP decays, the relation between $D^0$ and $D^+$ decay amplitudes in the Cabibbo-suppressed decays is more involved. Note that Cabibbo-suppressed $D^+$ decays can get contributions from both spectator and annihilation graphs.

The isospin decomposition for $\rho\pi$ modes in $D^+$decay may

be written as,

$$|\rho^0\pi^+> = -\frac{1}{\sqrt{2}}A_2'^{\rho\pi} + \frac{1}{\sqrt{2}}A_1'^{\rho\pi}$$
$$|\rho^+\pi^0> = -\frac{1}{\sqrt{2}}A_2'^{\rho\pi} - \frac{1}{\sqrt{2}}A_1'^{\rho\pi} \qquad \text{(IV.52)}$$

The isospin 2 part of the amplitude arises only from the $\Delta I=3/2$ term of the Hamiltonian. Also, it contributes only to spectator diagrams. Hence, $A_2'^{\rho\pi}$ can be related to $A_2^{\rho\pi}$ simply through the Wigner-Eckart theorem,

$$A_2'^{\rho\pi} = \sqrt{\frac{3}{2}}\, A_2^{\rho\pi} \ . \qquad \text{(IV.53)}$$

To relate $A_1'^{\rho\pi}$ and $A_1^{\rho\pi}$ is not so straightforward as the isospin 1 amplitude gets contribution from both $\Delta I=1/2$ and $\Delta I=3/2$ parts of the Hamiltonian. Further, the spectator and annihilation terms of the $D^0$ and $D^+$ amplitudes arise from different terms in the Hamiltonian. The spectator part of $A_1^{\rho\pi}$ gets contribution from $a_1(\bar{u}d)(\bar{d}c)$ part of the Hamiltonian, the corresponding contribution to $A_1'^{\rho\pi}$ comes from $a_1(\bar{u}d)(\bar{d}c)$ as well as from $a_2(\bar{d}d)(\bar{u}c)$. Similarly, the contribution to the annihilation part in $A_1^{\rho\pi}$ comes from $a_2(\bar{d}d)(\bar{u}c)$ while that for $A_1'^{\rho\pi}$ from $a_1(\bar{u}d)(\bar{d}c)$. Hence we may write,

$$A(D^0\to\rho^0\pi^+) = -\frac{1}{\sqrt{2}}xA_2^{\rho\pi} + \frac{1}{\sqrt{2}}\{yA_1^{\rho\pi}(\text{spect.}) + y'A_1^{\rho\pi}(\text{ann.})\}$$
$$\ldots(\text{IV.54})$$

where x , y and y' are determined by equating the above to the amplitude for this mode written directly from the Hamiltonian to obtain,

$$x=\sqrt{\frac{3}{2}}, \qquad y=\frac{1}{\sqrt{2}} - \frac{1}{\sqrt{2}}\frac{a_2}{a_1} \qquad \text{and} \qquad y'=-\sqrt{2}\,\frac{a_1}{a_2}.$$

The value of x is the same as obtained in eq.(IV.53).

The $K^*K$ states in $D^+$ decay can occur only in isospin one final state. The G=-1 and G=+1 combinations of these states are given by,

$$A'^{K^*K}_{I=1,G=-1} = \frac{1}{\sqrt{2}}(|K^{*+}\bar{K}^0> - |K^+\bar{K}^{*0}>)$$
$$A'^{K^*K}_{I=1,G=+1} = \frac{1}{\sqrt{2}}(|K^{*+}\bar{K}^0> + |K^+\bar{K}^{*0}>) \qquad \text{(IV.55)}$$

These can also be related to the isospin one, G even and odd states resulting from $D^0$ decays, by following the same procedure described above for the $\rho\pi$ states, i.e., we may write,

$$A'^{K^*K}_{I=1,G=-1} = zA^{K^*K}_{I=1,G=-1}(\text{spect.}) + z'A^{K^*K}_{I=1,G=-1}(\text{ann.})$$
$$A'^{K^*K}_{I=1,G=+1} = zA^{K^*K}_{I=1,G=+1}(\text{spect.}) + z'A^{K^*K}_{I=1,G=+1}(\text{ann.}) \qquad \text{...(IV.56)}$$

Equating the above to the amplitude obtained directly from the Hamiltonian, we get, $z=-\sqrt{2}$ and $z'=\sqrt{2}a_1/a_2$.

Since the $D^0$ and $D^+$ amplitudes are not simply related, we cannot just use the unitarized $D^0$ amplitudes determined, to evaluate the unitarized $D^+$ amplitudes. However, we can use the same **K**-matrix to separately couple the $\rho\pi$, $K^*K$ (I=1, G=-1) states resulting from $D^+$ decay (final state interactions are assumed to occur through a $\pi^+(1770)$ resonance). The unitarized amplitudes for the observable $D^+$ decay modes are therefore given by,

$$A^u(D^+\to\rho^0\pi^+) = -\frac{1}{\sqrt{2}}A_2'^{o,\rho\pi} + \frac{1}{\sqrt{2}}A_1'^{u,\rho\pi}$$

$$A^u(D^+\to\rho^+\pi^0) = -\frac{1}{\sqrt{2}}A_2'^{0,\rho\pi} - \frac{1}{\sqrt{2}}A_1'^{u,\rho\pi}$$

$$A^u(D^+\to K^{*+}\bar{K}^0) = \frac{1}{\sqrt{2}}\left[A'^{u,K^*K}_{I=1,G=-1} + A'^{0,K^*K}_{I=1,G=+1}\right]$$

$$A^u(D^+\to K^+\bar{K}^{*0}) = \frac{1}{\sqrt{2}}\left[A'^{u,K^*K}_{I=1,G=+1} - A'^{0,K^*K}_{I=1,G=-1}\right]$$

...(IV.56)

**Table 12.** Branching ratios for Cabbibo-suppressed D→VP decays. Theory column with $\xi$=0 uses: $a_1/a_2$=-2.0, R=0.13GeV$^2$, $\Gamma_{11}$=0.173GeV & $\Gamma_{22}$=0.655GeV, while that for $\xi$=1/3 uses: $a_1/a_2$=-2.4, R=0.10GeV$^2$, $\Gamma_{11}$=0.104GeV & $\Gamma_{22}$=0.698GeV

| Mode | Theoretical Branching Ratio(%) | | Mark III Data |
|---|---|---|---|
| | $\xi$=0 | $\xi$=1/3 | |
| $B(D^0\to\rho^+\pi^-)$ | 1.041 | 0.927 | |
| $B(D^0\to\rho^-\pi^+)$ | 0.165 | 0.179 | |
| $B(D^0\to\rho^0\pi^0)$ | 0.126 | 0.083 | |
| $B(D^0\to K^{*+}K^-)$ | 0.643 | 0.565 | |
| $B(D^0\to K^{*-}K^+)$ | 0.199 | 0.215 | |
| $B(D^0\to K^{*+}K^-_{+c.c.})$ | 0.842 | 0.780 | 0.8±0.5 |
| $B(D^0\to K^{*0}\bar{K}^0)$ | 0.068 | 0.034 | |
| $B(D^0\to\bar{K}^{*0}K^0)$ | 0.068 | 0.034 | |
| $B(D^0\to K^{*0}\bar{K}^0_{+c.c.})$ | 0.136 | 0.068 | <0.55 |
| $B(D^+\to\rho^0\pi^+)$ | 0.242 | 0.121 | 0.20±0.08±0.03 |
| $B(D^+\to\rho^+\pi^0)$ | 1.598 | 1.526 | |
| $B(D^+\to K^+\bar{K}^{*0})$ | 0.668 | 0.669 | 0.44±0.20±0.11 |
| $B(D^+\to K^{*+}\bar{K}^0)$ | 1.328 | 1.174 | |

Note that the K-matrix being the same, the $D^+$ branching ratios will constrain the parameters of our model. We therefore leave $\Gamma_{11}$ and $\Gamma_{22}$ as independent parameters.

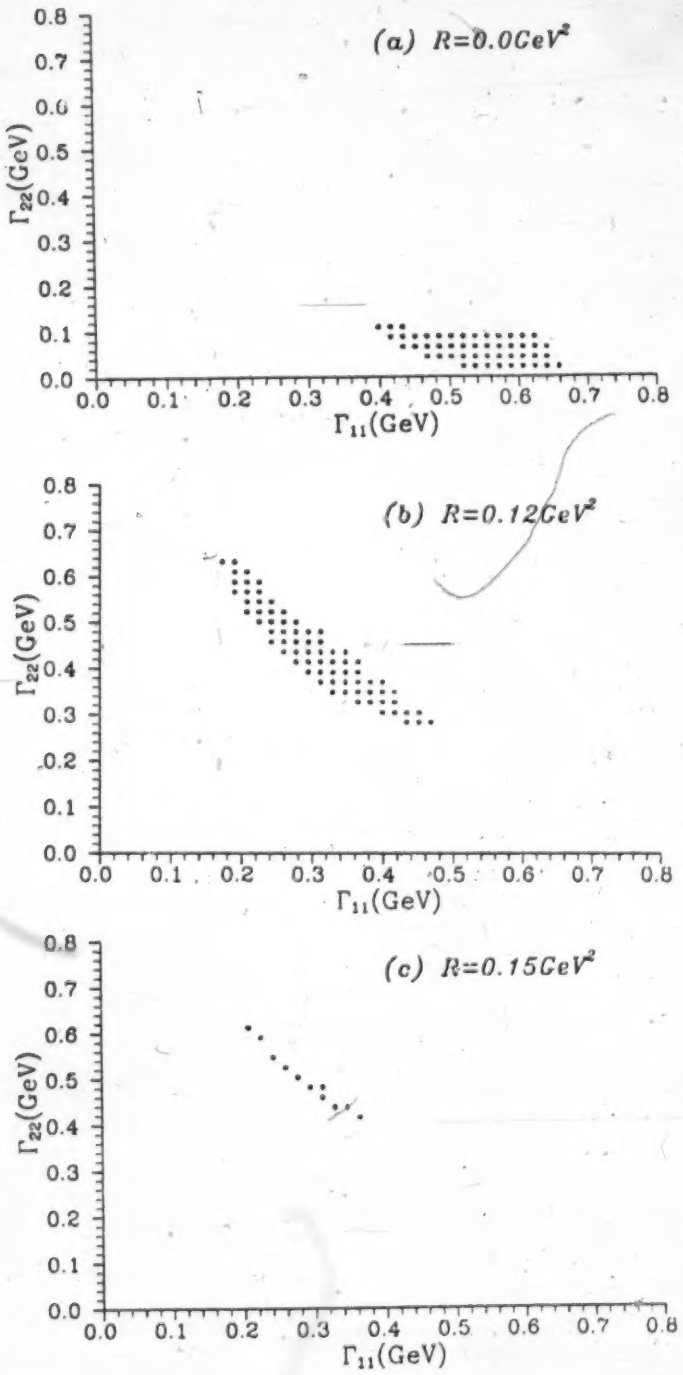


**Fig. 6** Fits to data[6] for Cabibbo suppressed D→VP decays. Allowed region is marked in $\Gamma_{11}$-$\Gamma_{22}$ space for different values of the annihilation parameters R. We have used $a_1/a_2$=-2.0 and $\xi$=0

Typical fits to data are shown in Table 12. We were able to obtain fits to data for both zero and non-zero values of the annihilation parameter R. The limit on $B(D^0 \to K^{*0}\bar{K}^0 + c.c)$ restricts the range of R, which is specified for the different $a_1/a_2$ values in Table 13. In Fig. 6(a), we show

**Table 13.** Range of R allowed in the Cabibbo suppressed D→VP decays.

| $a_1/a_2$ | $\xi=0$ ($GeV^2$) | $\xi=1/3$ ($GeV^2$) |
|---|---|---|
| -2.0 | 0.0-0.16 | 0.0-0.01 |
| -2.0 | 0.0-0.20 | 0.0-0.02 and 0.10-0.14 |
| -2.4 | 0.0-0.21 | 0.0-0.19 |

the allowed range of the parameters $\Gamma_{11}$ and $\Gamma_{22}$ for R=0. As R is raised to $0.12GeV^2$, a bigger range of $\Gamma_{11}$ and $\Gamma_{22}$ is allowed (Fig. 6(b)). Further increase in the R value, reduces this range, as is shown in Fig. 6(c). We would also like to point out that in the above model, it is possible to fit the $B(D^+ \to \rho^0\pi^+)$; the un-unitarized amplitude did not satisfy the observed value as pointed out earlier.

## V. OTHER APPROACHES TO STUDY HEAVY FLAVOR DECAYS

In the last chapter we presented a model calculation for various nonleptonic two-body exclusive decays of D, $D_s$ mesons. We now briefly describe some of the other theoretical approaches[27-29] to these decays and point out their successes and shortcomings.

First, in comparing our procedure to that of Bauer, Stech and Wirbel (BSW),[27] we would like to point that the two approaches are similar, as both are based on the assumption of factorization and use identical form-factors in the weak amplitudes. However, the BSW approach does not include a satisfactory treatment of final state interactions. Further, they retain only the spectator diagrams, while weak annihilation is ignored. From a fit to data, they conclude that the color mismatch factor $\xi$, is zero. Since $\xi$ represents the impact of low energy strong interactions, i.e., soft gluon effects etc., one would hardly expect to find a universal value of $\xi$. The phenomenological fit of Bauer et al., can perhaps be justified within the framework of the $1/N_c$ approach, which is discussed in the following section.

### V.1 $1/N_c$ approach

't Hooft[71] has shown that QCD simplifies considerably when one assumes that quarks have a large number $N_c$ of colors. In particular the physics of mesons becomes rather

simple. A meson is represented solely by its valence quark content and the meson decay amplitudes can be written as the product of quark currents. In the large $N_c$ limit, a $1/N_c$ expansion could be used to obtain approximate solutions in QCD. The diagrammatic rules in the $1/N_c$ approach are as follows: A quark is represented by a line and a gluon by two lines as shown in Fig. 7(a). Furthermore, quark-gluon and meson-quark vertices are represented as shown in figs. 7(b) and (c) respectively. The color factors are then assigned as follows,

(i) a factor $N_c$ for each closed quark loop,

(ii) a factor $1/\sqrt{N_c}$ for each quark-gluon vertex and

(iii) a factor $1/\sqrt{N_c}$ for each meson-quark vertex.

Buras, Gerard and Ruckl[28] have used this approach to evaluate non-leptonic weak decay amplitudes for the charmed mesons. They start with the usual operator product expansion for the matrix element of the effective weak Hamiltonian, (assuming factorization of short and long distance effects),

$$\langle AB|H_W^{eff}|M\rangle = \sum_i C_i \langle AB|O_i|M\rangle \qquad (V.1)$$

where A, B are the final state mesons resulting from the decay of the meson M; $C_i$'s are the Wilson coefficient functions which include the short distance QCD corrections and $O_i$ are local operators (see Chapter II). The proposal then is to expand the hadronic matrix elements $\langle AB|O_i|M\rangle$ in $1/N_c$,

$$\langle AB|O_i|M\rangle = \sqrt{N_c}\{\, a_i + b_i/N_c + O(1/N_c^2) \,\} \qquad (V.2)$$

where $a_i$ and $b_i$ are $N_c$-independent numerical expansion

coefficients, which are in principle calculable in QCD. Since the relevant expansion parameter is $1/N_c$ and not $\alpha_s$, the coefficients $a_i$ and $b_i$ include contributions from all orders in $\alpha_s$. This exhibits the non-perturbative character of the expansion. Weak interaction effects to first order can be included in the $1/N_c$ approach by adding the following prescription to the rules given above:

(i) a factor $C_1$ for a charged current interaction (Fig.7d)

(ii) a factor $C_2$ for a neutral current interaction (Fig.7e).

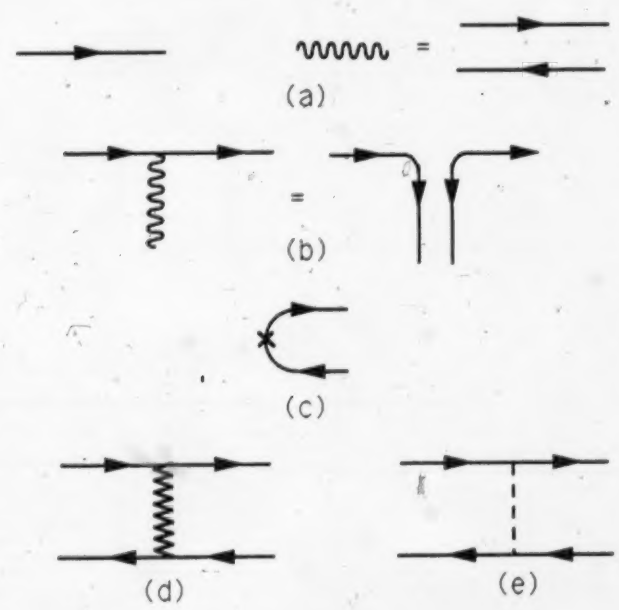


**Fig. 7** Diagrammatic rules in the 1/N approach.

The diagrams contributing to a given matrix element are then found by connecting the decaying meson M in all possible ways with the mesons A and B using quark lines, soft gluon lines and a single weak interaction line (charged or neutral). These diagrams are depicted in Figs. 8(a) and

(b). There are two types of leading order diagrams,

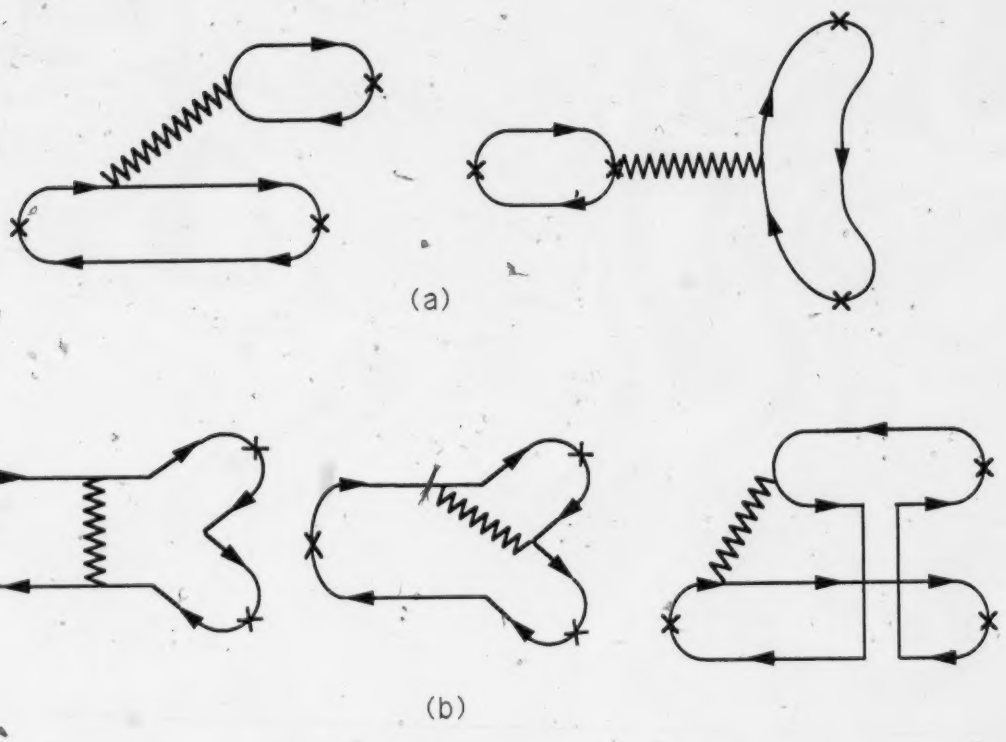


**Fig. 8** Leading and next-to-leading charged current diagrams contributing to two-body decays. Analogous diagrams exist for effective neutral current interactions.

contributing to $a_i$ of eq.(V.2), namely, one of the spectator and one of the annihilation type. At the next to leading level, there are three kinds of diagrams: a spectator diagram, a weak annihilation diagram and diagrams involving final state interactions. We note that all the leading order diagrams are factorizable into simpler diagrams by cutting the weak line. The non-leading spectator and annihilation diagrams have factorizable and non-factorizable pieces. The factorizable part can be extracted through a Fierz transfor-

mation. For example (see Fig.9):

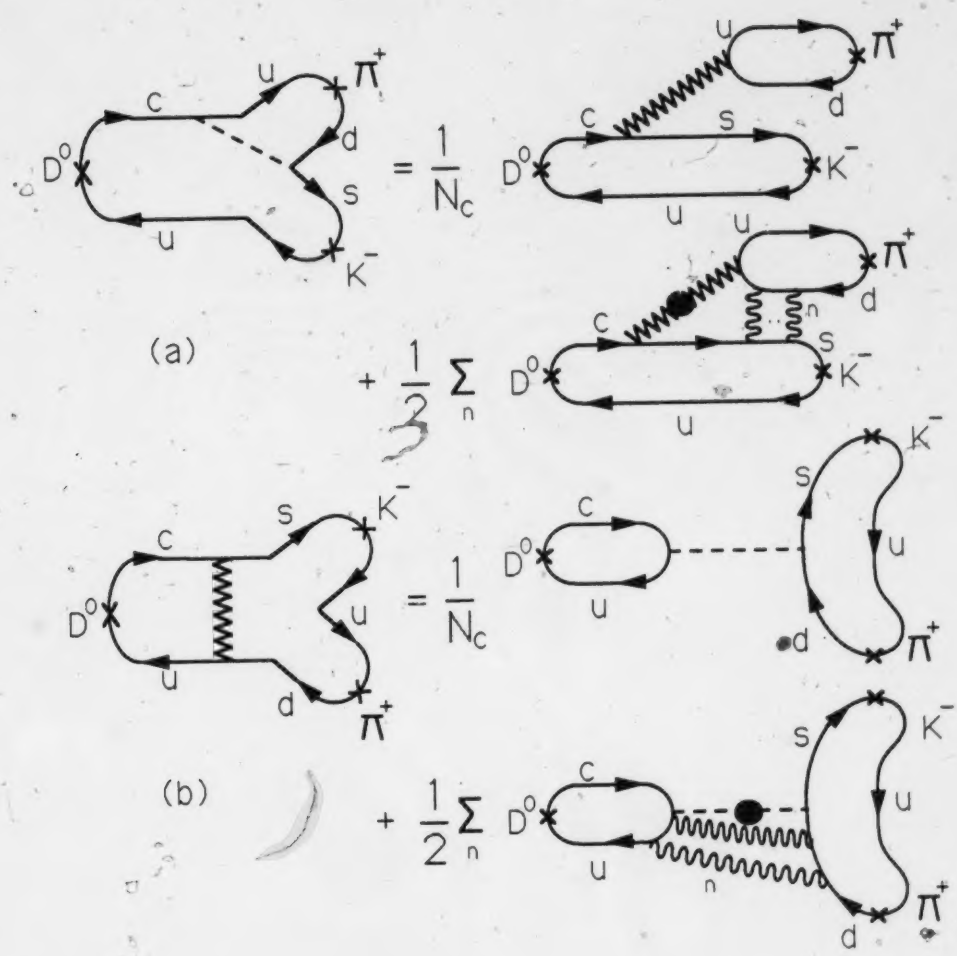


**Fig. 9** Diagrammatic relations which follow from Fierz identity and color algebra.

$$\langle\pi^+K^-|(\bar{u}c)_L(\bar{s}d)_L|D^0\rangle = \frac{1}{N_c}\langle\pi^+|(\bar{u}d)_L|0\rangle\langle K^-|(\bar{s}c)_L|D^0\rangle + \frac{1}{2}\langle\pi^+K^-|(\bar{u}\lambda_a d)_L(\bar{s}\lambda^a c)_L|D^0\rangle,$$

$$\langle\pi^+K^-|(\bar{u}d)_L(\bar{s}c)_L|D^0\rangle = \frac{1}{N_c}\langle\pi^+K^-|(\bar{s}d)_L|0\rangle\langle 0|(\bar{u}c)_L|D^0\rangle$$

$$+ \frac{1}{2}\langle \pi^+ K^- | (\bar{s}\lambda_a d)_L (\bar{u}\lambda^a c)_L | D^0 \rangle . \quad \ldots (V.3)$$

Buras et al.,[28] determine the weak amplitudes for various D, $D_s$ decays by retaining only the leading $1/N_c$ terms. Note that this is equivalent to taking $\xi=0$ in the factorization model. Although weak annihilation diagrams also occur at the leading level, they are neglected due to helicity suppression. This approach provides a reasonable fit to the data, but there are some obvious discrepancies. For example, $B(D^0 \to \bar{K}^0 \phi)$, $B(D^0 \to K^+K^-)/B(D^0 \to \pi^+\pi^-)$ typically come out too small. The predictions for class I transitions overshoot the experimental numbers.

In summary, the $1/N_c$ approach is compact and self-consistent, since it is based on just one basic assumption, namely ignoring terms that are non-leading in $1/N_c$. The assumption is however purely adhoc. $1/N_c$ is by no means small in the real world. Although the approach provides a simple tool, it does not advance our theoretical understanding, unless at least the first non-leading corrections are computed. Strong interaction final state effects being of non-leading order are neglected, yet there is clear experimental evidence[6] for their significance in D meson decays.

The evaluation of non-factorizable part of the amplitudes, which are ignored in the $1/N_c$ approach, requires explicit use of QCD. Such a calculation is possible in the framework of QCD sum rules, discussed in the following

section.

## V.2 QCD Sum Rules

*Summary of Sum Rule technique*

The idea[72] of the QCD sum rules is to make use of the simplicity of QCD in the perturbative regime to gain information on the bound state structure of hadrons, where perturbation theory cannot be applied. The starting point for the QCD sum rule approach is the correlation function between n currents, where the currents carry the quantum numbers of the hadrons one wants to study. For example consider the two-point function,

$$\int d^4x\, e^{iq.x} \langle 0|T(j_\mu(x) j_\nu(0))|0\rangle = \Pi_{\mu\nu}(q^2) \qquad (V.4)$$

where $j_\mu(x)$ is a vector/axial vector current and T denotes the time ordered product. For large $q^2$, or in the short distance region, one assumes an operator product expansion[43] (OPE) for the time ordered product:

$$\int d^4x\, e^{iq.x} \langle 0|T(j_\mu(x) j_\nu(0))|0\rangle = \sum_k C^k_{\mu\nu}(Q^2) O_k \qquad (V.5)$$

where $Q^2=-q^2$, $O_k$ are local operators constructed from quark or gluon fields. The Wilson coefficients $C^k(Q^2)$ depend on the process under study, i.e., the Lorentz structure and the quantum numbers of the currents. The operators in eq. (V.5) are ordered by increasing dimension and the coefficients fall off with corresponding powers in $1/Q^2$. Therefore, the operators with lowest dimension dominate the expansion at large $Q^2$. The coefficients $C^k(Q^2)$ can be calculated perturbatively. Non-perturbative effects are introduced by allowing

for non-vanishing vacuum expectation values of the operators $O_k$:

$$<0|O_k|0> \neq 0.$$

These matrix elements are treated as free parameters which can be fitted in one physical reaction and can then be used in all other processes, since they are process independent by definition.

Next one invokes analyticity to write a dispersion relation for the polarization function,

$$\Pi(Q^2) = \frac{1}{\pi}\int \frac{Im\Pi(s)}{(s+Q^2)}\, ds. \qquad (V.6)$$

The imaginary part of the polarization operator is determined by a sum over discrete spectrum of resonances and a continuum above the appropriate threshold $s_c$,

$$\Pi(Q^2) = \sum_k \frac{m_k^2 f_k^2}{m_k^2+Q^2} + \frac{1}{\pi}\int_{s_c}^{\infty} \frac{Im\Pi(s)}{(s+Q^2)}\, ds, \qquad (V.7)$$

where $f_k$ is the decay constant of the meson of mass $m_k$. In order to pick out only the lowest resonance in the above, one defines the $n^{th}$ moment of $\Pi(q^2)$:

$$\Pi_n(Q^2) = \frac{1}{n!}\left(-\frac{d}{dQ^2}\right)^n \Pi(Q^2)|_{Q^2=Q_0^2}$$

$$= \sum_k \frac{m_k^2 f_k^2}{(m_k^2+Q_0^2)^{n+1}} + \frac{1}{\pi}\int_{s_c}^{\infty} \frac{Im\Pi(s)\,ds}{(s+Q_0^2)^{n+1}}. \qquad (V.8)$$

The above technique also gets rid of the unknown subtraction constants in the dispersion relation. Note that large $Q^2$ must be chosen in order to terminate the OPE by first few terms, however large $Q^2$ sacrifices the enhancement of low-lying poles in the dispersion integral. The remedy is to

operate the sum rule by

$$L_M = \left[ \lim_{Q^2\to\infty,\ n\to\infty} \right] \frac{1}{n!} (Q^2)^{n+1} \left[ -\frac{d}{dQ^2} \right]^n \qquad (V.9)$$

where the ratio $Q^2/n=M^2$ is fixed, to obtain the Borel transformed sum rule.

*Application of Sum Rule approach to D-decays*

QCD sum rules have been applied to study the decays of charmed mesons into two light mesons by Blok and Shifman.[29] They analyzed the four-point correlator:

$$\Pi_{\mu\nu}(Q_1,Q_2;q^2) = \int d^4x\, d^4y\, d^4z\, e^{i(Q_2.x+q.y)} \times \langle 0|T\{j_{A\mu}(y)\, j_{B\nu}(x)\, j_D(0)\, H_W(z)\}|0\rangle \qquad (V.10)$$

where $j_D$ is a quark current with the quantum numbers of a charmed meson with momentum $Q_1$; $j_A$ and $j_B$ are the quark currents corresponding to the particles A and B, which are formed in the decay of the charmed meson and carry momenta q and $Q_2$ respectively. $H_W(z)$ is the weak Hamiltonian. The correlator in eq.(V.10) is depicted in Fig. 10. They work in

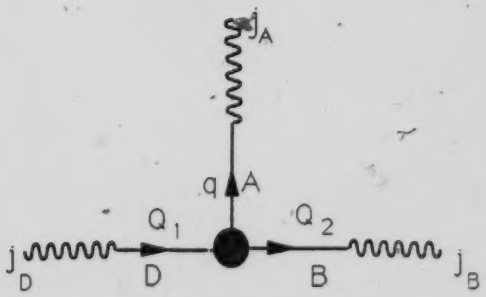


**Fig. 10** Four point correlator, shaded blob stands for the amplitude of the weak decay of the charmed mesons into two light mesons.

the chiral limit: $m_u=m_d=m_s=0$. Thus, the light pseudoscalar mesons have zero mass, and the vector mesons all have equal

masses, $m_\rho$. The value of the vector meson decay constant used is $f_\rho \simeq 200$MeV. In the case of the $\eta'$ meson $m_{\eta'}=0.96$GeV, $f_{\eta'}=100$MeV is used.

There exist three bare diagrams which give a contribution to the polarization operator. They are depicted in Fig. 11. The diagram of Fig.11 (a) represents the weak annihilation mechanism while diagrams in Figs. 11(b) and (c) correspond to spectator processes. Actual graphs are obtained from these bare diagrams by adding gluons and/or cutting some quark or gluon line to include the effect of non-vanishing vacuum expectation values in the OPE. If the added gluon lines are located entirely inside the triangle or the external loop, the diagram corresponds to a factorizable amplitude, while if the gluon lines connect the triangle and the external loop, the diagram is clearly non-factorizable.

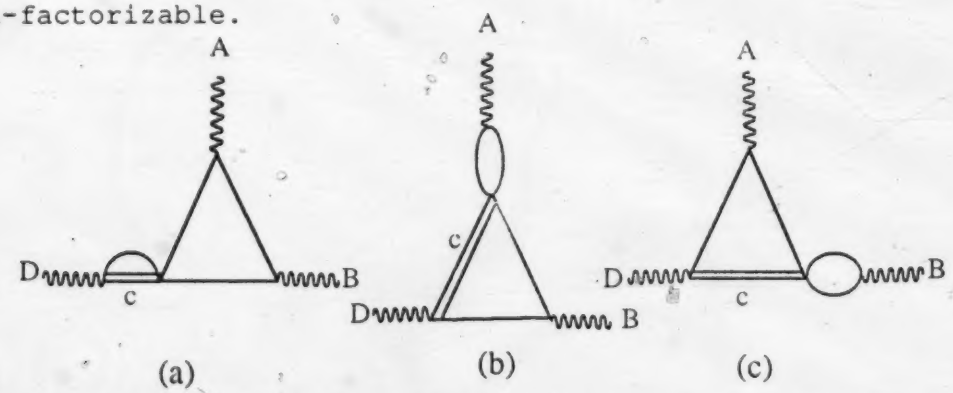


**Fig. 11** The skeleton diagrams in the QCD sum rules for two particle D meson decays. The wavy lines denote external currents producing mesons from vacuum.

Corresponding to the decay D→AB, where A is a light pseudoscalar meson and B is a pseudoscalar or vector meson, the phenomenological side of the sum rule is determined in

terms of the meson masses and decay constants. A double Borel transformation with the parameters $M^2$ and $M'^2$ is applied to suppress the contributions from the excited states in the D-meson channel and in the channel connected with B. To account for the contribution of higher resonances in the channel connected with the light meson A, in which a Borel transformation is not applied, a special choice is made, for the spectral density in this channel. Only one further resonance, corresponding to the $A_1$ meson is added, by assuming the following form for the form-factor $F_\pi(Q^2)$,

$$F_\pi(Q^2) = 1 - \frac{Q^2}{(m_{A_1}^2 + Q^2)} \qquad \text{(V.11)}$$

The sum rule for the amplitude then has the form,

$$f_T(M^2, M'^2, Q^2) = \frac{T\, f_D (m_D^2/m_c) f_A f_B F_\pi(Q^2)}{Q^2} \exp\left[-\left(\frac{m_D^2}{M^2} + \frac{m_B^2}{M'^2}\right)\right]. \qquad \text{...(V.12)}$$

In order to diminish contributions from diagrams other than that for, the decay D→AB, the above is differentiated w.r.t. $1/M^2$ to obtain:

$$-\frac{1}{m_D^2}\frac{d}{d(1/M^2)}\left[\frac{f_T(M^2, M'^2, Q^2)}{f_A f_B f_D m_D^2/m_c}\right]\exp\left(\frac{m_D^2}{M^2} + \frac{m_B^2}{M'^2}\right) = \frac{T F_\pi(Q^2)}{Q^2} \qquad \text{...(V.13)}$$

$f_T(M^2, M'^2, Q^2)$ can be decomposed into the sum of two terms,

$$f_T(M^2, M'^2, Q^2) = f_f(M^2, M'^2, Q^2) + f_n(M^2, M'^2, Q^2) \qquad \text{(V.14)}$$

where $f_f(M^2, M'^2, Q^2)$ corresponds to the factorizable diagrams, i.e., diagrams where the two blocks are not connected by anything except by the four fermion vertex; the function $f_n(M^2, M'^2, Q^2)$ corresponds to the sum of all other

diagrams. A sum rule, similar to eq.(V.13) may be written for the factorizable amplitude $f_f(M^2,M'^2,Q^2)$. The non-factorizable amplitudes are then determined through a sum rule obtained by subtracting the sum rule for the factorizable part from the sum rule for the full decay amplitude,

$$-\frac{1}{m_D^2}\frac{d}{d(1/M^2)}\left[\frac{f_n(M^2,M'^2,Q^2)}{f_A f_B f_D m_D^2/m_c}\right]\exp\left(\frac{m_D^2}{M^2}+\frac{m_B^2}{M'^2}\right)=\frac{T_n F_\pi(Q^2)}{Q^2} \qquad \ldots(V.14)$$

where $T_n = T - T_f$.

The operator product expansion is then used for $f_n(M^2,M'^2,Q^2)$:

$$f_n(M^2,M'^2,Q^2) = \alpha_1 G_1(M^2,M'^2,Q^2) + \alpha_2 G_2(M^2,M'^2,Q^2) + \alpha_3 G_3(M^2,M'^2,Q^2) \qquad (V.15)$$

where the coefficients $\alpha_1, \alpha_2$ and $\alpha_3$ are constants and depend on the specific decay mode. $G_1(M^2,M'^2,Q^2)$, $G_2(M^2,M'^2,Q^2)$ and $G_3(M^2,M'^2,Q^2)$ are the functions corresponding to the diagrams in Fig.11a,b & c, which receive contributions from the operators of dimension 5 and 6. Note that quark condensate $\langle\bar{\psi}\psi\rangle_0$ and the vacuum average $\langle G^2\rangle_0$ will contribute only to the factorizable part of the amplitude. Operators of dimension greater than six are ignored.

For each of the functions $G_1$, $G_2$ and $G_3$, the parameters $M_1$, $M_2$ and $M_3$ fix the corresponding parts of the amplitude $T_n$. For each group of decays, $D,D_s \to PP$, $D,D_s \to PV$ and $D,D_s \to P\eta'$, it is sufficient to consider three sum rules which determine these parameters. They are determined by requiring the left hand side of the sum rule to depend weakly on the Borel parameters $M^2$ and $M'^2$ and that, the contribution of the

continuum and the higher power corrections to the sum rule be small in the desired region.

Once these parameters are determined the non-factorizable amplitudes for all the decay modes can be evaluated. The factorizable pieces are evaluated in the usual fashion, using $\xi=1/3$. It is found that, in some of the decay modes, the factorizable terms of order $1/N_c$ approximately cancel with the non-factorizable contributions. The dynamical analysis of Blok and Shifman may thus provide a 'theoretical foundation' for the rule of neglecting $1/N_c$ contributions to the amplitudes which has been found in the phenomenological approach of Bauer et al.[27] and assumed in the work of Buras et al.[28]

In summary Blok and Shifman's treatment[27] represents a theoretical improvement in the sense that it allows the inclusion of non-factorizable contributions to the amplitudes. They generate $B(D^0\to\bar{K}^0\phi)\simeq 1.3\%$, purely from non-factorizable weak annihilation. However, final state interaction effects which are known to be significant, have not been incorporated in their scheme.

*Effect of Final State Interactions on Blok and Shifman's Amplitudes*

To see the effect of final state scattering on the amplitudes given by Blok and Shifman, we proceed as follows. The various decay amplitudes are decomposed into the different isospin parts. In the presence of a phase in each of the isospins, the ratio of the decay rates of any two

modes - $R_{00}$ or $R_{0+}$ etc., (to be described below), can be expressed in terms of the ratio of the isospin amplitudes, r, and the phase difference $\delta$. One can thus plot this ratio ($R_{00}$, or $R_{0+}$) as a function of r, for various phase difference values. Since the experimental values for $R_{00}$, $R_{0+}$ are known, one can determine the range of r and $\delta$ allowed by the data. The r value determined for Shifman's amplitudes of course corresponds to zero phase. First we check whether that value is allowed by the data. Next, for that same r value, we determine whether inclusion of a phase would be consistent with the experimental results. Note that we are introducing final state interactions only through a phase in each of the isospin amplitudes, thus its effects will be important only in decay modes with more than one isospin state.

The technique described above is applied to the following decay modes:

1. $K^*\pi$ - In the presence of phases $\delta_3$ and $\delta_1$ in the isospin states 3/2 and 1/2 respectively, we may write the decay amplitudes as,

$$A(D^0\to\bar{K}^{*0}\pi^0) = \frac{1}{\sqrt{3}}\left(\sqrt{2}A^{K^*\pi}_{3/2}\, e^{i\delta_3} + A^{K^*\pi}_{1/2}\, e^{i\delta_1}\right)$$

$$A(D^0\to K^{*-}\pi^+) = \frac{1}{\sqrt{3}}\left(A^{K^*\pi}_{3/2}\, e^{i\delta_3} - \sqrt{2}A^{K^*\pi}_{1/2}\, e^{i\delta_3}\right) \qquad \text{(V.16)}$$

$$A(D^+\to\bar{K}^{*0}\pi^+) = \sqrt{3}A^{K^*\pi}_{3/2}\, e^{i\delta_3}$$

Hence we have,

$$R_{00}(K^*\pi) = \frac{\Gamma(D^0\to\bar{K}^{*0}\pi^0)}{\Gamma(D^0\to K^{*-}\pi^+)} = \frac{2(r^{K^*\pi})^2+1+2\sqrt{2}r^{K^*\pi}\cos\delta^{K^*\pi}}{(r^{K^*\pi})^2+2-2\sqrt{2}r^{K^*\pi}\cos\delta^{K^*\pi}}$$

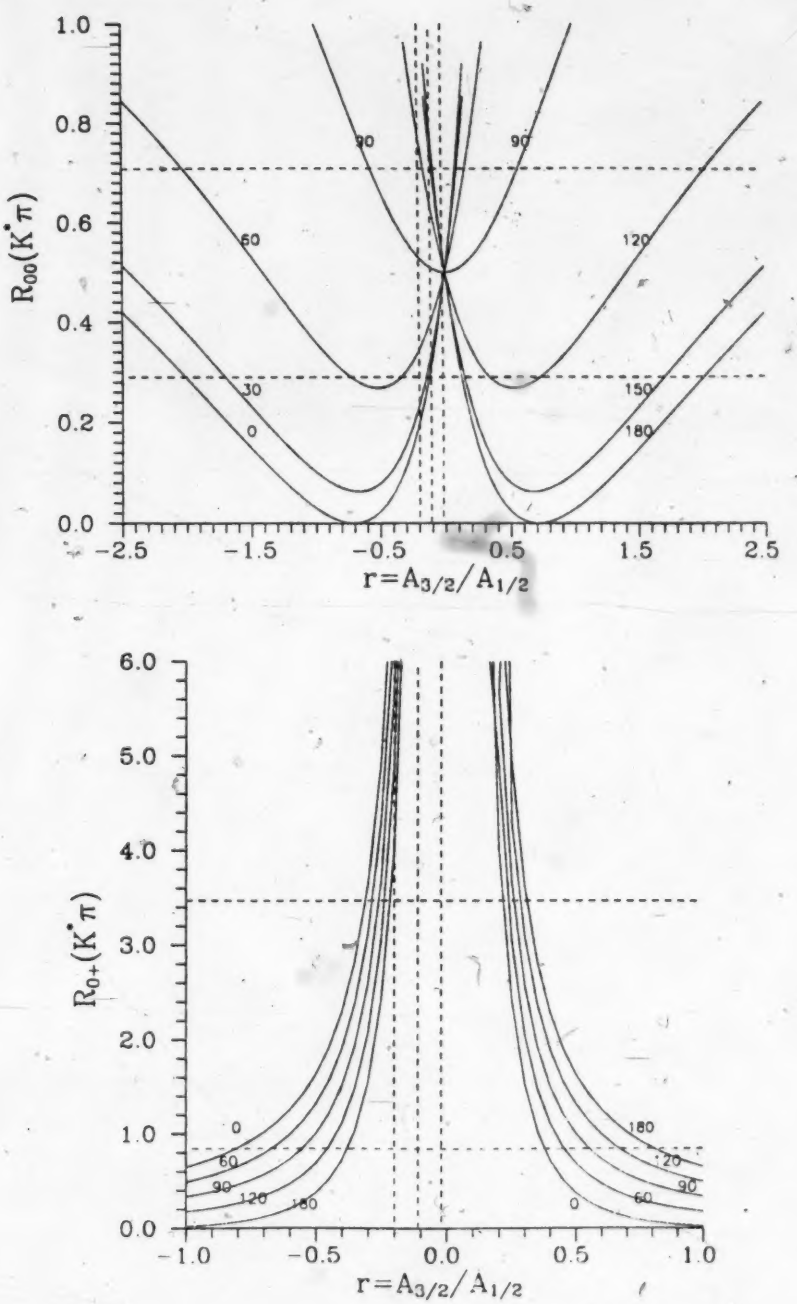


**Fig. 12(a).** The ratios $R_{00}(K^*\pi)$ and $R_{0+}(K^*\pi)$ vs $r^{K^*\pi}$, for various phase difference values. The dashed horizontal lines correspond to the experimental limits; the dashed vertical lines correspond to the theoretical ratio $r^{K^*\pi}$ with errors.

and (V.17)

$$R_{0+}(K^*\pi) = \frac{\Gamma(D^0\to K^{*-}\pi^+)}{\Gamma(D^+\to \bar{K}^{*0}\pi^+)} = \frac{1}{(3r^{K^*\pi})^2}[(r^{K^*\pi})^2+2-2\sqrt{2}r^{K^*\pi}\cos\delta^{K^*\pi}]$$

where, $r^{K^*\pi} = A^{K^*\pi}_{3/2}/A^{K^*\pi}_{1/2}$ and $\delta^{K^*\pi}=\delta_3-\delta_1$.

The experimental branching ratios[6] for the $K^*\pi$ modes imply that,

$$R_{00}(K^*\pi) = \frac{B(D^0\to\bar{K}^{*0}\pi^0)}{B(D^0\to K^{*-}\pi^+)} = 0.500\pm0.208$$

and $$R_{0+}(K^*\pi) = \frac{B(D^0\to K^{*-}\pi^+)\tau_{D^+}}{B(D^+\to\bar{K}^{*0}\pi^+)\tau_{D^0}} = 2.157\pm1.314. \quad (V.18)$$

For zero phases,

$$r^{K^*\pi} = \frac{A^{K^*\pi}_{3/2}}{A^{K^*\pi}_{1/2}} = \frac{\sqrt{2}A(D^0\to\bar{K}^{*0}\pi^0)+A(D^0\to K^{*-}\pi^+)}{A(D^0\to\bar{K}^{*0}\pi^0)-\sqrt{2}A(D^0\to K^{*-}\pi^+)}. \quad (V.19)$$

Using Blok and Shifman's amplitudes:

$$A(D^0\to\bar{K}^{*0}\pi^0) = \frac{G_F}{\sqrt{2}}\cos^2\theta_c\left\{\left(C_2+\frac{C_1}{3}\right)f_+^K\, 2m_\rho f_\rho + C_1(R_1-R_3)\right\}\frac{(e\cdot q)}{\sqrt{2}}$$

$$= -(1.171\pm0.166)\times10^{-6}(e\cdot q), \text{ and}$$

$$A(D^0\to K^{*-}\pi^+) = \frac{G_F}{\sqrt{2}}\cos^2\theta_c\left\{m_D\left(C_1+\frac{C_2}{3}\right)g_+f_\pi - (C_1R_1+C_2R_2)\right\}(e\cdot q)$$

$$= (2.118\pm0.276)\times10^{-6}(e\cdot q), \quad (V.20)$$

we get $$r^{K^*\pi} = -0.111\pm0.088. \quad (V.21)$$

Note that we have estimated the errors in the amplitudes using the theoretical uncertainties (as given in ref.29) in the various parameters.

2. $K\rho$ - The isospin decomposition of these amplitudes is similar to that of $K^*\pi$, hence we have identical relations for $R_{00}$ and $R_{0+}$. The observed branching ratios for the $K\rho$

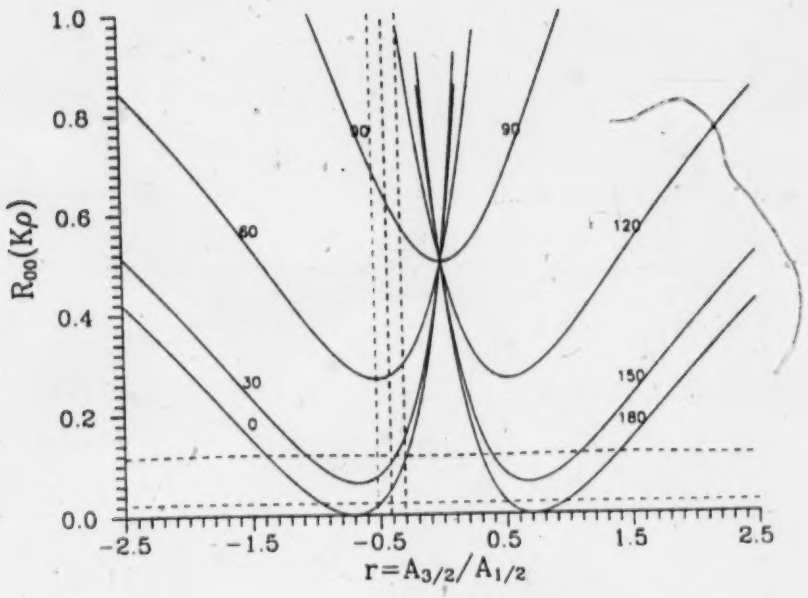


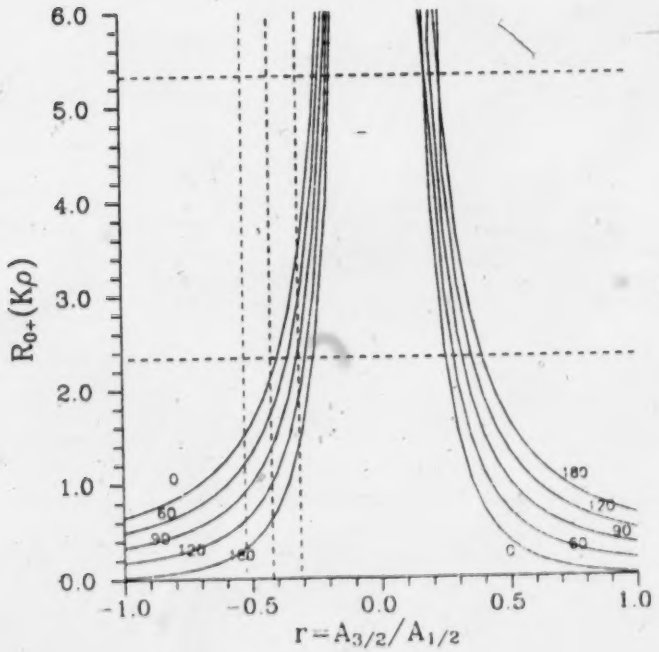


**Fig. 12(b).** The ratios $R_{00}(K\rho)$ and $R_{0+}(K\rho)$ vs $r^{\gamma\rho}$, for various phase difference values. The dashed horizontal lines correspond to the experimental limits; the dashed vertical lines correspond to the theoretical ratio $r^{\gamma\rho}$ with errors.

modes imply that,

$$R_{00}(K\rho) = \frac{B(D^0\to\bar{K}^0\rho^0)}{B(D^0\to K^-\rho^+)} = 0.069\pm0.046$$

and $$R_{0+}(K\rho) = \frac{B(D^0\to K^-\rho^+)\,\tau_{D^+}}{B(D^+\to\bar{K}^0\rho^+)\,\tau_{D^0}} = 3.831\pm1.494. \qquad (V.22)$$

Again, $r^{K\rho}$ is given by a relation similar to that in eq. (V.19). Blok and Shifman's amplitudes for these modes are given by,

$$A(D^0\to\bar{K}^0\rho^0) = \frac{G_F}{\sqrt{2}}\cos^2\theta_c\left\{m_D\left(C_2+\frac{C_1}{3}\right)g_+ f_\pi + C_1(R_1-R_2)\right\}\frac{(e\cdot q)}{\sqrt{2}}$$

$$= -(5.392\pm1.501)\times10^{-7} \text{ and}$$

$$A(D^0\to K^-\rho^+) = \frac{G_F}{\sqrt{2}}\cos^2\theta_c\left\{\left(C_1+\frac{C_2}{3}\right)f_+^K\, 2m_\rho f_\rho - (C_1R_1+C_2R_3)\right\}(e\cdot q)$$

$$= (2.416\pm0.313)\times10^{-6}. \qquad (V.23)$$

Hence, $$r^{K\rho} = -(0.418\pm0.108). \qquad (V.24)$$

3. $K\pi$ - The isospin decomposition is again similar. The experimental branching ratios imply,

$$R_{00}(K\pi) = \frac{B(D^0\to\bar{K}^0\pi^0)}{B(D^0\to K^-\pi^+)} = 0.452\pm0.123$$

and $$R_{0+}(K\pi) = \frac{B(D^0\to K^-\pi^+)\;\tau_{D^+}}{B(D^+\to\bar{K}^0\pi^+)\;\tau_{D^0}} = 3.212\pm0.703. \qquad (V.25)$$

The theoretical amplitudes are,

$$A(D^0\to\bar{K}^0\pi^0) = \frac{G_F}{\sqrt{2}}\cos^2\theta_c\left\{\left(C_2+\frac{C_1}{3}\right)f_+^K\, m_D^2 f_\pi + C_1(M_1-M_3)\right\}\frac{1}{\sqrt{2}}$$

$$= -(1.295\pm0.238)\times10^{-6} \text{ and}$$

$$A(D^0\to K^-\pi^+) = \frac{G_F}{\sqrt{2}}\cos^2\theta_c\left\{m_D^2\left(C_1+\frac{C_2}{3}\right)f_+^K f_\pi - (C_1M_1+C_2M_2)\right\}$$

$$= (3.078\pm0.430)\times10^{-6}, \qquad (V.26)$$

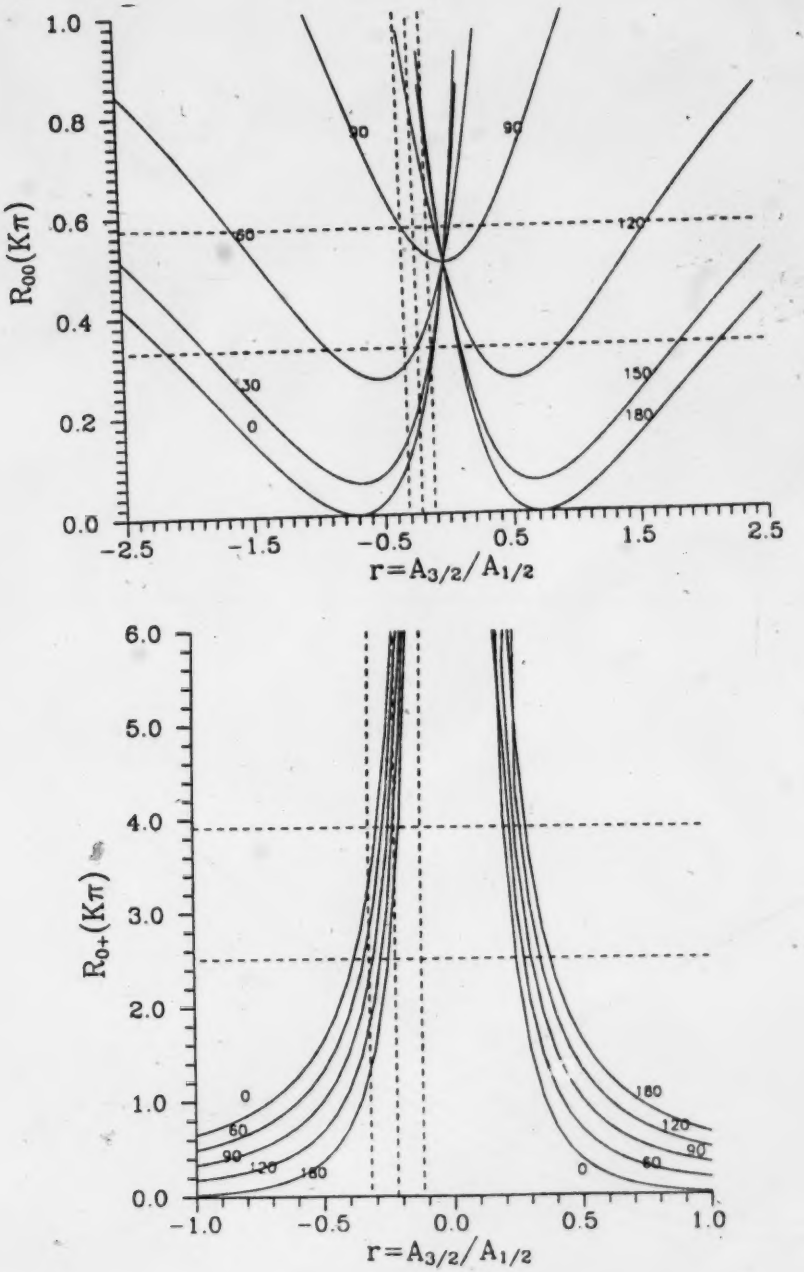


**Fig. 12(c).** The ratios $R_{00}(K\pi)$ and $R_{0+}(K\pi)$ vs $r^{K\pi}$, for various phase difference values. The dashed horizontal lines correspond to the experimental limits; the dashed vertical lines correspond to the theoretical ratio $r^{K\pi}$ with errors.

giving the following value,

$$r^{K\pi} = -(0.221\pm0.100). \qquad (V.27)$$

4. $\pi\pi$ - The $\pi\pi$ states can be in isospin 0 or 2. The decomposition is given by,

$$\begin{aligned} A(D^0\to\pi^+\pi^-) &= \frac{1}{\sqrt{3}}\left(\sqrt{2}A_0^{\pi\pi}\, e^{i\delta_0^{\pi\pi}} + A_2^{\pi\pi}\, e^{i\delta_2^{\pi\pi}}\right) \\ A(D^0\to\pi^0\pi^0) &= \frac{1}{\sqrt{3}}\left(A_0^{\pi\pi}\, e^{i\delta_0^{\pi\pi}} - \sqrt{2}A_2^{\pi\pi}\, e^{i\delta_2^{\pi\pi}}\right) \qquad (V.28) \\ A(D^+\to\pi^0\pi^+) &= \sqrt{3}A_2^{\pi\pi}\, e^{i\delta_2^{\pi\pi}} \end{aligned}$$

Therefore,

$$R_{00}(\pi\pi) = \frac{\Gamma(D^0\to\pi^+\pi^-)}{\Gamma(D^0\to\pi^0\pi^0)} = \frac{2(r^{\pi\pi})^2+1+2\sqrt{2}r^{\pi\pi}\cos\delta^{\pi\pi}}{(r^{\pi\pi})^2+2-2\sqrt{2}r^{\pi\pi}\cos\delta^{\pi\pi}} \qquad (V.29)$$

and

$$R_{0+}(\pi\pi) = \frac{\Gamma(D^0\to\pi^+\pi^-)}{\Gamma(D^+\to\pi^0\pi^+)} = \frac{1}{9}\left[2(r^{\pi\pi})^2+1+2\sqrt{2}r^{\pi\pi}\cos\delta\right]$$

where,

$$r^{\pi\pi} = \frac{A_0^{\pi\pi}}{A_2^{\pi\pi}} \quad \text{and} \quad \delta^{\pi\pi} = \delta_0-\delta_2.$$

For zero phases, $r^{\pi\pi}$ can be determined as,

$$r^{\pi\pi} = \frac{A_0^{\pi\pi}}{A_2^{\pi\pi}} = \frac{\sqrt{2}A(D^0\to\pi^+\pi^-) + A(D^0\to\pi^0\pi^0)}{A(D^0\to\pi^+\pi^-) - \sqrt{2}A(D^0\to\pi^0\pi^0)} \qquad (V.30)$$

The experimental branching ratios for these modes imply the following limits,

$$R_{00} > 0.467 \quad \text{and} \quad R_{0+} > 0.714. \qquad (V.31)$$

In Blok and Shifman's approach we have,

$$A(D^0\to\pi^0\pi^0) = \frac{G_F}{\sqrt{2}}\cos\theta_C\sin\theta_C\left\{\left(C_1+\frac{C_2}{3}\right)f_+^K\, m_D^2 f_\pi + C_1(M_1-M_2)\right\}$$

$$= -(4.232\pm0.778)\times10^{-8} \text{ and}$$

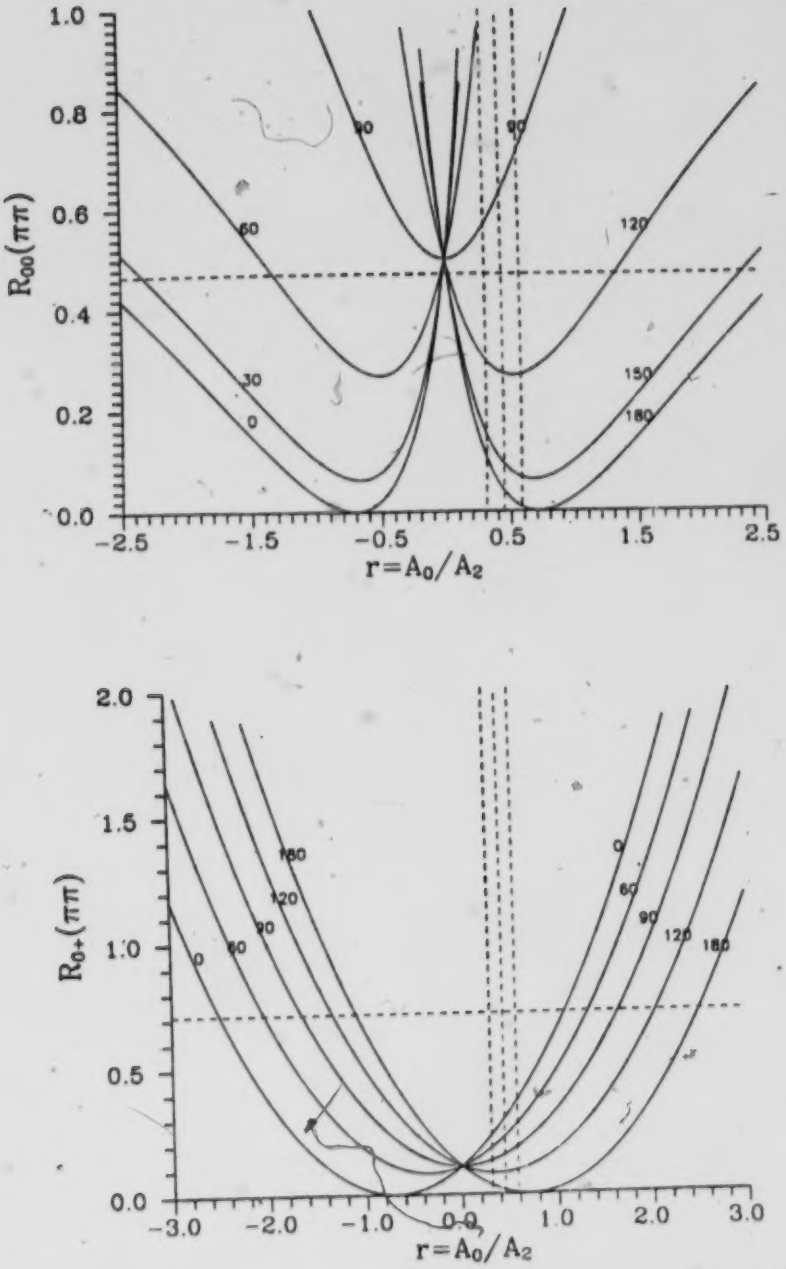


**Fig. 12(d).** The ratios $R_{00}(\pi\pi)$ and $R_{0+}(\pi\pi)$ vs $r^{\pi\pi}$, for various phase difference values. The dashed horizontal lines correspond to the experimental limits; the dashed vertical lines correspond to the theoretical ratio $r^{\pi\pi}$ with errors.

$$A(D^0\to\pi^+\pi^-) = \frac{G_F}{\sqrt{2}}\cos\theta_c\sin\theta_c\left\{m_D^2\left(C_1+\frac{C_2}{3}\right)f_+^K f_\pi - (C_1M_1+C_2M_2)\right\}$$

$$= (7.112\pm0.993)\times10^{-7}, \qquad (V.32)$$

giving the following value,

$$r^{\pi\pi} = 0.445\pm0.133. \qquad (V.33)$$

5. $K\bar{K}$ - In this case isospin 0 and 1 amplitudes are involved,

$$A(D^0\to K^+K^-) = \frac{1}{\sqrt{2}}\left(A_0^{K\bar{K}}\, e^{i\delta_0^{KK}} + A_1^{K\bar{K}}\, e^{i\delta_1^{KK}}\right)$$

$$A(D^0\to K^0\bar{K}^0) = \frac{1}{\sqrt{2}}\left(A_0^{K\bar{K}}\, e^{i\delta_0^{KK}} - A_1^{K\bar{K}}\, e^{i\delta_1^{KK}}\right) \qquad (V.34)$$

$$A(D^+\to\bar{K}^0K^+) = \sqrt{2}A_1^{\pi\pi}\, e^{i\delta_1^{KK}}$$

Hence we have,

$$R_{00}(KK) = \frac{\Gamma(D^0\to K^+K^-)}{\Gamma(D^0\to K^0\bar{K}^0)} = \frac{1+(r^{KK})^2+2\cos\delta^{KK}}{1+(r^{KK})^2-2\cos\delta^{KK}}$$

and (V.35)

$$R_{0+}(KK) = \frac{\Gamma(D^0\to K^+K^-)}{\Gamma(D^+\to\bar{K}^0K^+)} = \frac{1+(r^{KK})^2+2\cos\delta^{KK}}{(2r^{KK})^2},$$

where $r^{KK} = \dfrac{A_1^{KK}}{A_0^{KK}}$ and $\delta^{KK} = \delta_1-\delta_0$.

The observed branching ratios imply that,

$$R_{00}(KK) = 2.550\pm2.607 \quad \text{and} \quad R_{0+}(KK) = 1.236\pm0.522.$$

For zero phases we have,

$$r^{KK} = \frac{A_1^{KK}}{A_0^{KK}} = \frac{A(D^0\to K^+K^-) - A(D^0\to K^0\bar{K}^0)}{A(D^0\to K^+K^-) + A(D^0\to K^0\bar{K}^0)}. \qquad (V.36)$$

Since the amplitude for $D^0\to K^0\bar{K}^0$ is zero in Blok and Shifman's approach, thus

$$r^{KK} = 1.$$

The resulting plots for the above decay modes (1-5) are shown in Figs. 12(a)-(e) respectively. The allowed values of

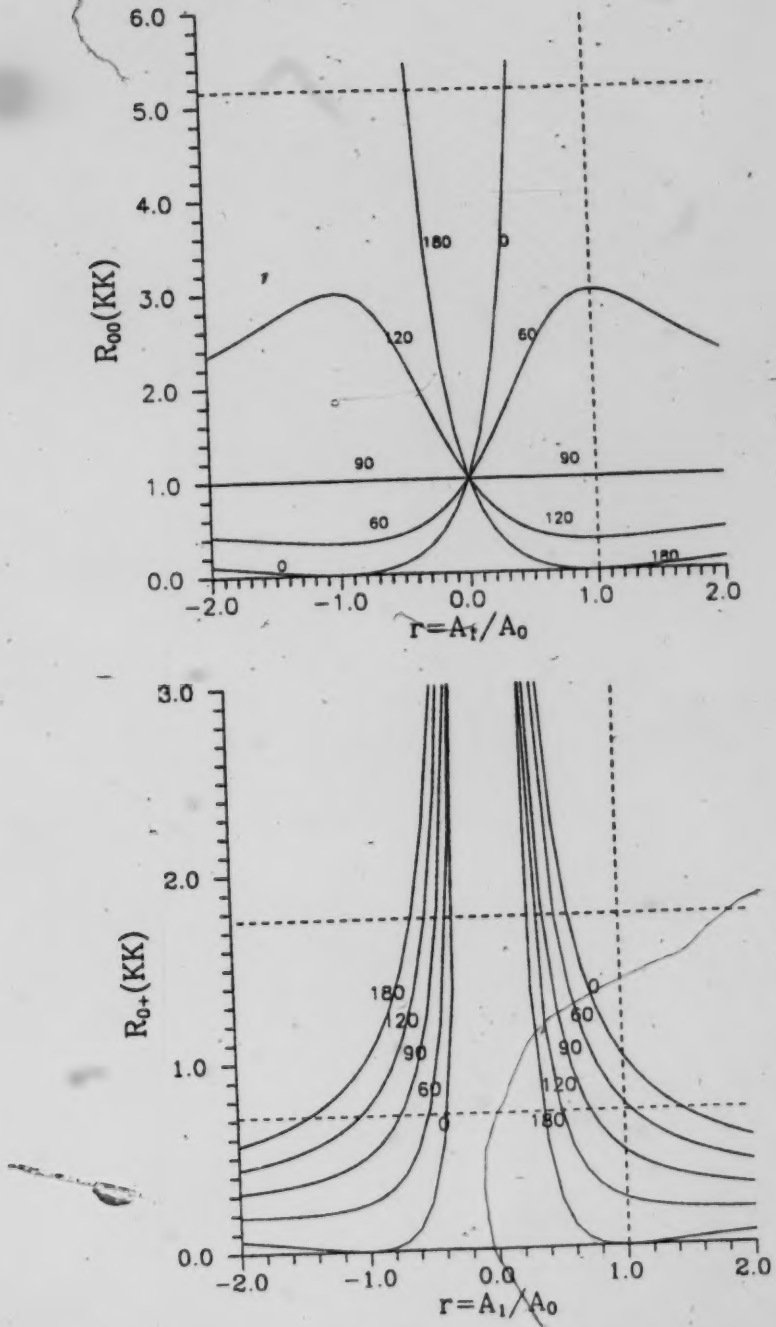


**Fig. 12(e).** The ratios $R_{00}(KK)$ and $R_{0+}(KK)$ vs $r^{KK}$, for various phase difference values. The dashed horizontal lines correspond to the experimental limits; the dashed vertical lines correspond to the theoretical ratio $r^{KK}$ with errors.

the phase differences corresponding to each of the ratios plotted, are listed in Table 14. It is seen that a reasonable agreement between theory and experiment[5,6] is achieved for most decays. However, there are certain discrepancies. In particular, $B(D^0\to K^{*-}\pi^+)/B(D^+\to\bar{K}^{*0}\pi^+)$ and $B(D^0\to\pi^+\pi^-)/B(D^+\to\pi^0\pi^+)$ do not agree with the data, for any value of the phase included in the amplitudes.

**Table 14.** The range of phase values that Blok and Shifman's (ref.29) amplitudes can accomodate, being consistent with data.

| Ratio of Amplitudes | phase value allowed |
|---|---|
| $R_{00}(K^*\pi)$ | 0-180° |
| $R_{0+}(K^*\pi)$ | no allowed value |
| $R_{00}(K\rho)$ | ~0-30° |
| $R_{0+}(K\rho)$ | 0-90° |
| $R_{00}(K\pi)$ | ~0-110° |
| $R_{0+}(K\pi)$ | 0-180° |
| $R_{00}(\pi\pi)$ | ~0-100° |
| $R_{0+}(\pi\pi)$ | no allowed value |
| $R_{00}(KK)$ | ~45-180° |
| $R_{0+}(KK)$ | 0-60° |

To investigate the role of non-factorizable contributions vs. the factorizable part we look at some of the amplitudes in more detail. For example, in the amplitude for $D^+\to\bar{K}^{*0}\pi^+$,

$$A(D^+\to\bar{K}^{*0}\pi^+) = \frac{G_F}{\sqrt{2}}\cos^2\theta_c\left\{\left(C_2+\frac{C_1}{3}\right)f_+^K\, 2m_\rho f_\rho + m_D\left(C_1+\frac{C_2}{3}\right)g_+ f_\pi \right.$$

$$\left. - (C_1R_3+C_2R_2)\right\}(e\cdot q),$$

the relative magnitudes of the factorizable term and the non-factorizable term are,

$$A_f(D^+\to\bar{K}^{*0}\pi^+) = 0.160 \quad \text{and} \quad A_n(D^+\to\bar{K}^{*0}\pi^+) = -0.101.$$

Also, the $D^+\to \bar{K}^0\rho^+$ amplitude,

$$A(D^+\to\bar{K}^0\rho^+) = \frac{G_F}{\sqrt{2}}\cos^2\theta_c\left\{m_D\left(C_2+\frac{C_1}{3}\right)g_+ f_\pi + \left(C_1+\frac{C_2}{3}\right)f_+^K\, 2m_\rho f_\rho - (C_1R_2+C_2R_3)\right\}(e\cdot q),$$

is composed of the following factorizable and non-factorizable parts,

$$A_f(D^+\to\bar{K}^0\rho^+) = 0.162 \quad \text{and} \quad A_n(D^+\to\bar{K}^0\rho^+) = +0.049\ .$$

**Table 15.** Factorizable and non-factorizable parts (columns 5 and 6) of amplitudes obtained in the Sum Rule approach. Branching ratios given in columns 2 and 3 are in percent.

| Mode | B.R. in Sum Rule Approach | Expt. B.R. | Comment | Fact. Part | Non fact. Part |
|---|---|---|---|---|---|
| $B(D^+\to\bar{K}^0\rho^+)$ | 14 | 6.9±2.4 | high | +0.162 | +0.049 |
| $B(D^+\to\bar{K}^{*0}\pi^+)$ | 0.8 | 5.9±3.1 | low | +0.160 | -0.101 |
| $B(D^0\to K^{*-}\pi^+)$ | 8.6 | 5.2±1.5 | high | +0.158 | +0.133 |
| $B(D^0\to K^-\rho^+)$ | 14.8 | 10.8±1.8 | high | +0.159 | +0.089 |
| $B(D^0\to\pi^+\pi^-)$ | 0.28 | 0.14± | high | +0.132 | +0.149 |

A comparison with the data[6] reveals that $B(D^+\to\bar{K}^{*0}\pi^+)$ is smaller than the experimental value and $B(D^+\to\bar{K}^0\rho^+)$ is larger than the observed value. Since, the non-factorizable term in the $\bar{K}^{*0}\pi^+$ mode reduces the net amplitude and that for $\bar{K}^0\rho^+$, enhances it, it is plausible that the non-factorizable amplitudes have been overestimated in the sum rule approach.

A similar pattern emerges in some of the other decay modes which are listed in Table 15.

In conclusion, the above models can explain the experimental data with reasonable success. However, there are many discrepancies, which could perhaps be accounted for by proper inclusion of final state interaction effects. The BSW model attempts to include these effects but they have rather adhoc treatment of final state interactions. Moreover, they justify their $\xi=0$ rule using the $1/N_c$ approach; simultaneous inclusion of final state interactions (non-leading in $1/N_c$) is however then, inconsistent.

There is one more entirely different approach,[67] which is based on diagrammatic classification of the weak decay processes which has not been discussed above. We will briefly refer to this approach, in the next chapter.

## VI. THE DECAY MODES $D_s^+ \to \eta\pi^+$ AND $D_s^+ \to \eta'\pi^+$.

A lot of interest has been generated by the modes $D_s^+ \to \eta\pi^+$ and $D_s^+ \to \eta'\pi^+$. Mark II[5,32] has observed surprisingly large branching ratios for these modes, $B(D_s^+ \to \eta\pi^+)/B(D_s^+ \to \phi\pi^+) = 3.0 \pm 1.1$ and $B(D_s^+ \to \eta'\pi^+)/B(D_s^+ \to \phi\pi^+) = 4.8 \pm 2.1$. Mark III had also reported[30] $B(D_s^+ \to \eta\pi^+)/B(D_s^+ \to \phi\pi^+) = 2.5 \pm 0.8 \pm 0.8$ and $B(D_s^+ \to \eta\pi^+)/B(D_s^+ \to \bar{K}^0 K^+) = 2.3 \pm 0.7 \pm 0.8$. The recent Mark III analysis[31] results only in upper limits: $B(D_s^+ \to \eta\pi^+)/B(D_s^+ \to \phi\pi^+) < 2.5$ and $B(D_s^+ \to \eta'\pi^+)/B(D_s^+ \to \phi\pi^+) < 1.9$. One would like to know whether it is at all possible to obtain the large Mark II branching ratios for the $D_s^+ \to \eta\pi^+$ and $D_s^+ \to \eta'\pi^+$ modes in a theoretical framework.

### VI.1 $\eta$-$\eta'$ Mixing

The decays into modes involving the $\eta$ and $\eta'$ are complicated by mixing in the pseudoscalar sector. The SU(3) basis states are:

the octet, $$|\eta_8\rangle = \frac{1}{\sqrt{6}}|u\bar{u}+d\bar{d}-2s\bar{s}\rangle$$

and the singlet, $$|\eta_0\rangle = \frac{1}{\sqrt{3}}|u\bar{u}+d\bar{d}+s\bar{s}\rangle \ .$$

Assuming orthogonal mixing for the physical states $\eta$ and $\eta'$, we have,

$$\begin{aligned} |\eta\rangle &= \eta_8 \cos\theta_p - \eta_0 \sin\theta_p \\ |\eta'\rangle &= \eta_8 \sin\theta_p + \eta_0 \cos\theta_p \ . \end{aligned} \qquad \text{(VI.1)}$$

In terms of a quark basis, the above may be written as:

$$|\eta\rangle = X_\eta \frac{1}{\sqrt{2}}|u\bar{u}+d\bar{d}\rangle + Y_\eta |s\bar{s}\rangle$$

$$|\eta'> = X_{\eta'} \frac{1}{\sqrt{2}}|u\bar{u}+d\bar{d}> + Y_{\eta'} |s\bar{s}>,$$

where,
$$X_{\eta} = Y_{\eta'} = \sqrt{\frac{1}{3}} \cos\theta_p - \sqrt{\frac{2}{3}} \sin\theta_p$$
$$Y_{\eta} = -X_{\eta'} = -\sqrt{\frac{2}{3}} \cos\theta_p - \sqrt{\frac{1}{3}} \sin\theta_p .$$

...(VI.2)

The quadratic Gell-Mann-Okubo mass formula[73] yields a value of $\theta_p \simeq -10^\circ$, while the mass formula which is linear in the masses gives $\theta_p \simeq -23^\circ$. In the past, two-photon experiments gave,[74] $\theta_p \simeq -11^\circ$. Recent measurements employing a different technique seem to indicate[74] $\theta_p \simeq -19^\circ$. This value is also in agreement with the data from $J/\psi \to \eta(\eta')\gamma$.

The above mixing scheme can be extended to include mixing of the pseudoscalars (isosinglets) and gluonic bound states. Defining,

$$|N> \equiv \frac{1}{\sqrt{2}} |u\bar{u}+d\bar{d}> , \quad |S> \equiv |s\bar{s}> \quad \text{and} \quad |G> \equiv |\text{gluonium}>,$$

the $\eta$ and $\eta'$ states in this generalized mixing scheme[75] are written as,

$$|\eta> = X_{\eta}|N> + Y_{\eta}|S> + Z_{\eta}|G>$$
$$|\eta'> = X_{\eta'}|N> + Y_{\eta'}|S> + Z_{\eta'}|G> \qquad \text{(VI.3)}$$

with the normalization $X_i^2+Y_i^2+Z_i^2=1$, $i=\eta,\eta'$. A significant gluonic admixture in a state is possible only if $Z_i^2 = 1-X_i^2-Y_i^2 > 0$. $\eta$ is well understood as an SU(3) flavor octet with a small quarkonium singlet admixture, and does not have much room for a significant gluonium admixture. However, information on $\eta'$ is incomplete[75] without a significant constraint on it's $s\bar{s}$ content.

## VI.2 Factorization Approach

In the following we have looked at the predictions[76] for the $D_s^+ \to \eta\pi^+$ and $\eta'\pi^+$ modes, using an orthogonal mixing scheme. To estimate the amplitudes we used two factorization models, one due to Bauer, Stech and Wirbel[27] (BSW) and the second due to Kamal and Sinha[77] (KS).

Following the method of BSW, we obtain the following decay amplitudes (using eqs.(IV.17) & (IV.18)),

$$A(D_s^+\to\eta\pi^+) = \frac{G_F}{\sqrt{2}}\cos^2\theta_c a_1 \langle\pi^+|\bar{u}d|0\rangle\langle\eta|\bar{s}c|D_s^+\rangle$$
$$= \frac{G_F}{\sqrt{2}}\cos^2\theta_c a_1 i f_\pi (m_{D_s}^2 - m_\eta^2)\frac{h_0(D_s\to\eta)}{1-m_\pi^2/m_{0^+}^2}\sqrt{\frac{2}{3}}\left(\cos\theta_p + \frac{\sin\theta_p}{\sqrt{2}}\right)$$

$$A(D_s^+\to\eta'\pi^+) = \frac{G_F}{\sqrt{2}}\cos^2\theta_c a_1 \langle\pi^+|\bar{u}d|0\rangle\langle\eta'|\bar{s}c|D_s^+\rangle$$
$$= \frac{-G_F}{\sqrt{2}}\cos^2\theta_c a_1 i f_\pi (m_{D_s}^2 - m_{\eta'}^2)\frac{h_0(D_s\to\eta')}{1-m_\pi^2/m_{0^+}^2}$$
$$\times \frac{1}{\sqrt{3}}(\cos\theta_p - \sqrt{2}\sin\theta_p)$$

$$A(D_s^+\to K^+\bar{K}^0) = \frac{G_F}{\sqrt{2}}\cos^2\theta_c a_2 \langle\bar{K}^0|\bar{s}d|0\rangle\langle K^+|\bar{u}c|D_s^+\rangle$$
$$= \frac{-G_F}{\sqrt{2}}\cos^2\theta_c a_2 i f_K (m_{D_s}^2 - m_K^2)\frac{h_0(D_s\to K)}{1-m_K^2/m_{0^+}^2} \quad . \qquad \ldots(VI.4)$$

Note that annihilation plays no role in the above decays. This is a consequence of CVC hypothesis in the $(\bar{u}d)$ sector. The amplitude for $D_s^+\to\phi\pi^+$ mode is given by,

$$A(D_s^+\to\phi\pi^+) = \frac{G_F}{\sqrt{2}}\cos^2\theta_c a_1 2m_\phi f_\pi \frac{h_{A0}(D_s\to\phi)}{1-m_\pi^2/m_{0^-}^2}(\varepsilon\cdot k),$$

(as given in eq.(IV.29)). This amplitude is included to compare the theoretical predictions with the experimental

results which are normalized to $B(D_s^+ \to \phi\pi^+)$.

In the KS model, the $\langle P|J_\mu|I\rangle$ hadronic matrix element is written as,

$$\langle P_i|J_j^\mu|I_k\rangle = f_{ijk}[f_+(q^2)(P_I+P_P)_\mu + f_-(q^2)(P_I-P_P)_\mu$$

where I and P are the initial and final pseudoscalar mesons respectively. In the case of $D_s^+ \to \eta\pi^+, \eta'\pi^+, \bar{K}^0K^+$, the form-factors $f_-(m_\pi^2)$ and $f_-(m_K^2)$ are neglected since they are multiplied by $m_\pi^2$ and $m_K^2$ respectively. In this model SU(4) symmetry is used to generate the form-factors $f_+(q^2)$ and $f_-(q^2)$. Hence using,

$$f_+(m_\pi^2) \approx f_+(m_K^2) \approx f_+(0) = 1,$$

the relevant PP amplitudes in the KS model are:

$$A(D_s^+ \to \eta\pi^+) = \frac{G_F}{\sqrt{2}}\cos^2\theta_c a_1 f_\pi (m_{D_s}^2 - m_\eta^2)\ \frac{2}{\sqrt{3}}\left(\cos\theta_P + \frac{\sin\theta_P}{\sqrt{2}}\right)$$

$$A(D_s^+ \to \eta'\pi^+) = \frac{-G_F}{\sqrt{2}}\cos^2\theta_c a_1 f_\pi (m_{D_s}^2 - m_{\eta'}^2)\ \sqrt{\frac{2}{3}}\left(\cos\theta_P - \sqrt{2}\sin\theta_P\right)$$

$$A(D_s^+ \to K^+\bar{K}^0) = \frac{-G_F}{\sqrt{2}}\cos^2\theta_c a_2 \sqrt{2} f_K (m_{D_s}^2 - m_K^2).$$

...(VI.5)

The decay constants in the KS model are defined through,

$$\langle P|J_\mu|0\rangle = -i\sqrt{2} f_P k_\mu,$$

and the values of $f_\pi$ and $f_K$ used are 93 and 120 MeV. To calculate the $D_s \to \phi\pi^+$ amplitude (or any P→PV amplitude), the KS model uses the fact that only the axial vector current can contribute. Partially conserved axial current (PCAC) hypothesis is then employed to determine these amplitudes. Hence, in this model,

$$\langle P|J_\mu|0\rangle\langle V|A^\mu|I\rangle = -i\sqrt{2} f_P k_\mu \langle V|A^\mu|I\rangle$$

$$= -\sqrt{2} f_P \langle V|\partial_\mu A^\mu|I\rangle .$$

The amplitude for $D_s \to \phi\pi^+$ is therefore given by,

$$A(D_s^+ \to \phi\pi^+) = \frac{G_F}{\sqrt{2}} \cos^2\theta_c a_1 2\sqrt{2} f_\pi f_{D_s} g_{VPP}(\varepsilon\cdot k),$$

where the $V_i \to P_j P_k$ coupling constant is introduced via the vertex,

$$g_{ijk} = i f_{ijk} \varepsilon\cdot(P_j - P_k) g_{VPP}.$$

**Table 16.** Rates (in $10^{10}$ $sec^{-1}$) and the ratios of rates for various decays in KS and BSW models

| Mode | KS model (ref.77) | | BSW model (ref.27) | |
|---|---|---|---|---|
| | $\theta_p = -11^\circ$ | $\theta_p = -19^\circ$ | $\theta_p = -11^\circ$ | $\theta_p = -19^\circ$ |
| $\Gamma(D_s^+ \to \eta'\pi^+)$ | $5.64a_1^2$ | $7.11a_1^2$ | $2.87a_1^2$ | $3.63a_1^2$ |
| $\Gamma(D_s^+ \to \eta\pi^+)$ | $9.11a_1^2$ | $6.50a_1^2$ | $4.89a_1^2$ | $3.50a_1^2$ |
| $\Gamma(D_s^+ \to \phi\pi^+)$ | $4.83a_1^2$ | | $4.67a_1^2$ | |
| $\Gamma(D_s^+ \to \bar{K}^0 K^+)$ | $30.91a_2^2$ | | $12.76a_2^2$ | |
| $\frac{\Gamma(D_s^+ \to \eta'\pi^+)}{\Gamma(D_s^+ \to \eta\pi^+)}$ | 0.62 | 1.09 | 0.59 | 1.04 |
| $\frac{\Gamma(D_s^+ \to \eta\pi^+)}{\Gamma(D_s^+ \to \phi\pi^+)}$ | 1.89 | 1.35 | 1.05 | 0.75 |

In Table 16, we have summarized the results of our calculations for different relevant rates. These rates depend on the QCD coefficients $a_1$ and $a_2$ and the $\eta$-$\eta'$ mixing angle. We have used $\theta_p = -11^\circ$ and $\theta_p = -19^\circ$. As the magnitude of the mixing angle is increased, $\Gamma(D_s^+ \to \eta\pi^+)$ decreases and $\Gamma(D_s^+ \to \eta'\pi^+)$ increases. For a mixing angle of $\approx -19^\circ$ we find,

as is seen from Table 16, that both KS and BSW models give $B(D_s^+\to\eta'\pi^+)/B(D_s^+\to\eta\pi^+)\approx$ 1. However, since the effect of a larger (and negative) mixing angle is to lower the rate for $D_s^+\to\eta\pi^+$, $B(D_s^+\to\eta\pi^+)/B(D_s^+\to\phi\pi^+)$ for $\theta_p=-19^\circ$ is lower than that for $\theta_p=-11^\circ$. In Table 17 we list the branching ratios for the above modes. We have shown three numbers in this table for each branching ratio. They correspond to NLL calculated $a_1$ and $a_2$, with $\xi=0$, for QCD parameters (in GeV), $(\mu_c,\Lambda)$ = (1.5,0.1), (1.5,0.2) and (1.5,0.3).

**Table 17.** Branching ratios (in %) for various decays of the KS and BSW models. The three entries (a,b,c) are obtained with $(\mu,\Lambda)=(1.5.0.1),(1.5,0.2),(1.5,0.3)$, respectively.

| Mode | KS model | | BSW model | | Experiment[ref] |
|---|---|---|---|---|---|
| | $\theta_p=-11^\circ$ | $\theta_p=-19^\circ$ | $\theta_p=-11^\circ$ | $\theta_p=-19^\circ$ | |
| $B(D_s^+\to\eta'\pi^+)$ | 3.43[a] | 4.33 | 1.74 | 2.20 | $16.8\pm7.73$[32] |
| | 3.70[b] | 4.67 | 1.81 | 2.38 | |
| | 4.09[c] | 5.16 | 2.07 | 2.62 | $<6.65$[31] |
| $B(D_s^+\to\eta\pi^+)$ | 5.55 | 3.96 | 2.97 | 2.12 | $10.5\pm4.13$[32] |
| | 5.98 | 4.25 | 3.20 | 2.29 | |
| | 6.61 | 4.72 | 3.54 | 2.53 | $<8.75$[31] |
| $B(D_s^+\to\phi\pi^+)$ | 2.94 | | 2.84 | | $3.5\pm0.5$[6] |
| | 3.17 | | 3.06 | | $2.0\pm1.0$[5] |
| | 3.50 | | 3.39 | | |
| $B(D_s^+\to\bar{K}^0K^+)$ | 1.96 | | 0.81 | | $3.22\pm1.40$[5] |
| | 2.79 | | 1.15 | | |
| | 4.01 | | 1.69 | | |

The results of tables 16 & 17 can be summarized as follows. $B(D_s^+\to\phi\pi^+)$ is predicted to be consistent with data in both the KS and BSW models. $B(D_s^+\to\bar{K}^0K^+)$, in the KS model is consistent with data with QCD coefficients calculated with $\mu$=1.5 GeV and $\Lambda$ in the range (0.1-0.3) GeV. In the BSW

model this branching ratio is predicted to be too low for $\Lambda$=0.1 and 0.2 GeV, but is consistent with data for $\Lambda$=0.3 GeV. $B(D_S^+\to\eta\pi^+)$ is consistent with the Mark III limits in both models. The Mark II $B(D_S\to\eta\pi^+)$ is barely satisfied by the KS model for $\theta_p=-11^\circ$ at $\mu$=1.5 GeV, $\Lambda$=0.3GeV. Neither the KS, nor the BSW model, can give $B(D_S\to\eta'\pi^+)$ consistent with the Mark II measurement.

In the standard $\eta$-$\eta'$ mixing formalism the two ratios $B(D_S^+\to\eta\pi^+)/B(D_S^+\to\phi\pi^+)$ and $B(D_S^+\to\eta'\pi^+)/B(D_S^+\to\phi\pi^+)$ pull in opposite directions as a function of the mixing angle $\theta_p$, that is, raising the magnitude of $\theta_p$ has the effect of lowering the first ratio and raising the second. Thus, if

$$\begin{aligned} B(D_S^+\to\eta\pi^+)/B(D_S^+\to\phi\pi^+) &\gtrsim 1.5 \\ B(D_S^+\to\eta'\pi^+)/B(D_S^+\to\eta\pi^+) &\gtrsim 1.0 \end{aligned} \qquad \ldots(VI.6)$$

the standard orthogonal mixing model will have difficulty in explaining the data. The Mark II data[32] indicate that the first ratio in eq.(VI.6) is about 3 and that the second ratio in eq.(VI.6) is about 1.6. This implies $B(D_S^+\to\eta'\pi^+)$ is about 17%; as is evident from Table 17 such a large branching ratio poses a problem for standard orthogonal $\eta$-$\eta'$ mixing model. The branching ratio for $D_S^+\to\eta'\pi^+$ could be enhanced by using a larger mixing angle, however, in that case $B(D_S^+\to\eta\pi^+)$ will drop to unacceptably low values.

If eq.(VI.6) is true and the standard orthogonal mixing for $\eta$ and $\eta'$ runs into trouble with $D_S^+\to\eta\pi^+$ and $D_S^+\to\eta'\pi^+$ data, one would seek to reconcile the data with theory in one or more of the ways discussed below.

The models we have discussed use factorization of the hadronic decay amplitude. One may suspect factorization, yet factorization appears to work reasonably well[22,27] in other hadronic decays of charm. Further, we note that even in the QCD sum rule approach[29] which includes non-factorizable amplitudes, the $B(D_s^+\to\eta\pi^+)$ and $B(D_s^+\to\eta'\pi^+)$ are much below the Mark II values. The assumption of factorization itself is then unlikely to be the reason for discrepancy. One could also suspect nonperturbative contributions to the QCD coefficients. However, both the decay amplitudes for $D_s^+\to\eta\pi^+$ and $D_s^+\to\eta'\pi^+$ involve the same combination of QCD coefficients. Hence, the relative normalization of the two rates should remain unaffected by nonperturbative effects.

Earlier analysis[78] of Mark III data on $J/\psi$ decays, which had neglected double Okubo-Zweig-Iizuka rule violating[79] (DOZI) amplitudes, in terms of a generalized mixing, had concluded that there was a significant gluonium content in $\eta'$. Their analysis had yielded

$$|X_\eta|=0.63\pm0.06, \qquad |Y_\eta|=0.83\pm0.13$$
$$|X_{\eta'}|=0.36\pm0.05, \qquad |Y_{\eta'}|=0.72\pm0.12\ . \tag{VI.7}$$

Haber and Perrier analysis[80] gave similar results. The above set is consistent with $Z_\eta=0$ but allows $|Z_{\eta'}|=0.59\pm0.09$.

A recent analysis[81] of Mark III $J/\psi$ data, with the inclusion of DOZI amplitudes, concludes that if DOZI amplitudes are about 15% of OZI -violating amplitudes then there is no room for gluonium in $\eta'$ and one can satisfactorily explain $J/\psi$ decay data using the standard orthogonal

$\eta$-$\eta'$ mixing scheme with $\theta_P \approx -19^\circ$. Howeyer, if the orthogonality condition is dropped, the normalization condition appears to be oversubscribed[81]: $X^2_{\eta'}+Y^2_{\eta'} = 1.44\pm0.26$. Thus, if DOZI amplitudes are at the level of 15% of the OZI-violating amplitudes, $Z_{\eta'}\approx 0$. However, if DOZI amplitudes are considerably smaller, then $Z_{\eta'}$ is allowed to be nonzero and one could enhance the rate for $D_s^+\to\eta'\pi^+$ while leaving the rate for $D_s^+\to\eta\pi^+$ unaffected. Note that such a mechanism would also enhance the rates for $D_s^+\to$(gluonium)$\pi^+$.

In Tables 16 & 17, we have used the un-unitarized amplitudes to calculate the decay rates for the various modes. In principle, the three channels $\bar{K}^0K^+$, $\eta\pi^+$ and $\eta'\pi^+$ could mix through final state interactions. All these channels involve a single isospin state, I=1. The only scalar resonance with I=1, G=-1 and J=0 appears[10] to be $a_0(980)$ well below the $D_s^+$ mass. A coupled three-channel calculation, using the resonant parameterization (eq.IV.11) was performed. $a_0$ cannot decay to $\eta'\pi^+$, being kinematically disallowed; we thus constrain the parameters $\Gamma_{11}$ and $\Gamma_{22}$ by the relation, $k_1\Gamma_{11} + k_2\Gamma_{22} = \Gamma_R m_R$. The ratio $B(a_0\to\bar{K}^0K^+)/B(a_0\to\eta\pi^+) = \Gamma_{11}/\Gamma_{22}$ and the parameter $\Gamma_{33}$ are varied and the corresponding unitarized amplitudes determined. One set of branching ratios calculated using such unitarized amplitudes is given in Table 18. Thus, final state interactions do not play a significant role in these modes. This was to be expected, since the resonance activity occurs well below the $D_s^+$ mass; the effect of final state interactions will then be

simply to rotate the amplitudes leaving the magnitude of the amplitudes largely unaffected. However, since the final states involve only a single isospin amplitude, the phase of the amplitude is irrelevant.

**Table 18.** Branching ratios(%) using un-unitarized and unitarized amplitudes. We use $a_1/a_2=-2.3$ and $\Gamma_{11}/\Gamma_{22}=1.0$. Note that unitarization has negligible effect.

| Mode | B.R. using un-unitarized amplitudes | B.R. using unitarized amplitudes |
|---|---|---|
| $B(D_S^+\to\bar{K}^0K^+)$ | 1.95519 | 1.95544 |
| $B(D_S^+\to\eta\pi^+)$ | 3.59369 | 3.59340 |
| $B(D_S^+\to\eta'\pi^+)$ | 2.10410 | 2.10410 |

We would like to point out that the penguin diagrams play no role in $D_S^+\to\eta\pi^+$ and $\eta'\pi^+$ decays. Hence, indeed if the branching ratios of $D_S^+\to\eta\pi^+$ and $\eta'\pi^+$ are large, they pose a problem for the standard orthogonal $\eta$-$\eta'$ mixing model with a mixing angle in the region of $\theta_p\simeq-19^\circ$.

**VI.3** A Nonet Symmetry breaking model

$B(D_S^+\to\eta'\pi^+)$ larger than $B(D_S^+\to\eta\pi^+)$ inspite of the phase space suppression, may also suggest that the decay amplitudes involving an SU(3) flavor singlet and a flavor octet pseudoscalar ($0^-$) meson in the final state are larger than the ones involving two SU(3) flavor octet $0^-$ mesons. In the standard approaches there is a tacit assumption of nonet symmetry i.e., the flavor singlet and octet couple the same

way. We discuss here a scheme[82] where nonet symmetry is explicitly broken and explore it's consequences.

The charm lowering Hamiltonian has the form,

$$H(\Delta c=-1)=\frac{1}{2}\{J^{\mu}, J^{\dagger}_{\mu}\}$$
$$=\frac{1}{2}\left[\{\bar{s}c,\bar{u}d\}\cos^2\theta_c + \sin\theta_c\cos\theta_c(\{\bar{s}c,\bar{u}s\}-\{\bar{d}c,\bar{u}d\}) - \sin^2\theta_c\{\bar{d}c,\bar{u}s\}\right]. \quad \ldots(VI.8)$$

The Hamiltonian thus involves a product of charm-changing and charm-conserving currents, which transform[83] as elements of the representations [3] (or [$3^*$]) and [8] respectively. In general $[8]\otimes[3]=[3^*]\oplus[6]\oplus[15^*]$. The [6] and [$15^*$] are antisymmetric and symmetric under the exchange of the quark fields respectively. The [$3^*$] does not contribute to the above Hamiltonian.

The general structure of the charm lowering decay amplitude for decay into two SU(3) flavor octet $0^-$ mesons ($P_8$) may be written as,[84]

$$A(\text{charm}\to P_8P_8) = c(P^n_kP^m_nP^l)\ H^k_{[lm]} + d(P^n_kP^m_nP^l)\ H^k_{\{lm\}} + e(P^nP^l_nP^m_k)\ H^k_{\{lm\}} \quad \ldots(VI.9)$$

where $P^l$ is the C=1 triplet ($D^0$, $D^+$, $D_s^+$) and $P^m_n$ is the pseudoscalar octet. $H^k_{[lm]}$ represents the weak spurion belonging to the 6-dimensional representation of SU(3) and $H^k_{\{lm\}}$ to the $15^*$-dimensional representation. For Cabibbo-angle favored decays, $H^k_{lm} \equiv H^2_{13}$ and for Cabibbo-angle suppressed decays, $H^k_{lm} \equiv H^3_{13}-H^2_{12}$. In the above it is assumed that the decay amplitudes are SU(3) symmetric, hence they

involve only three parameters c, d and e. All QCD correction factors are absorbed in these coefficients. The indices in eq.(VI.9) run from 1 to 3.

If the final state involves an SU(3) flavor singlet and an octet the most general form of the decay amplitude is,

$$A(\text{charm}\to P_0 P_8) = (P_0 P_k^l P^m)(a\, H^k_{[lm]} + b\, H^k_{\{lm\}}), \qquad \text{(VI.10)}$$

where $P_0$ is the pseudoscalar singlet; a and b are two parameters. In the limit of nonet symmetry we have a=c and b=d, e=0. The antisymmetric terms in the Hamiltonian are enhanced relative to the symmetric terms, implying sextet dominance.[83] We would thus anticipate that $|c|>(|d|,|e|)$ and $|a|>|b|$.

For Cabibbo-allowed (CA) modes eq.(VI.9) may be written as,

$$\begin{aligned} A^{CA}(\text{charm}\to P_8 P_8) &= c(P_2^n P_n^3 P^1 - P_2^n P_n^1 P^3) + d(P_2^n P_n^3 P^1 + P_2^n P_n^1 P^3) \\ &\quad + e(P^n P_n^1 P_2^3 + P^n P_n^3 P_2^1) \\ &= D^0\left\{\pi^+ K^- (c+d+e) + \pi^0 \bar{K}^0 \left(\frac{-\sqrt{3}(c+d)+e}{\sqrt{6}}\right)\right. \\ &\quad \left. + \eta_8 \bar{K}^0 \left(\frac{-(c+d)+e}{\sqrt{6}}\right)\right\} \\ &\quad + D^+\left\{\pi^+ \bar{K}^0 2e\right\} + D_s^+\left\{\pi^+ \eta_8 \left(\frac{2(d-c-e)}{\sqrt{6}}\right)\right. \\ &\quad \left. + \bar{K}^0 K^+ (-c+d+e)\right\}, \end{aligned} \qquad \text{...(VI.11)}$$

and eq.(VI.10) has the form,

$$\begin{aligned} A^{CA}(\text{charm}\to P_0 P_8) &= a(P_0 P_2^1 P^3 - P_0 P_2^3 P^1) + b(P_0 P_2^1 P^3 + P_0 P_2^3 P^1) \\ &= \sqrt{\frac{2}{3}}\left\{D_s^+ \pi^+ \eta_0 (a+b) + D^0 \bar{K}^0 \eta_0 (-a+b)\right\}. \end{aligned} \qquad \text{(VI.12)}$$

In Cabibbo-suppressed (CS) decays, the $H^2_{12}$ piece for decay

to two octets gives,

$$A^{(cs)}(\text{charm}\to P_8 P_8) = c(P_2^n P_n^2 P^1 - P_2^n P_n^1 P^2) + d(P_2^n P_n^2 P^1 + P_2^n P_n^1 P^2) + e(P^n P_n^1 P_2^2 + P^n P_n^2 P_2^1)$$
$$- D^0\left\{\pi^+\pi^-(c+d+e) + \pi^0\pi^0(c+d-e) + \bar{K}^0K^0(c+d) + \eta_8\eta_8\left(\frac{c+d+e}{3}\right) - \pi^0\eta_8\frac{(c+d)}{\sqrt{3}}\right\}$$
$$+ D^+\left\{\bar{K}^0K^+(-c+d) + \pi^+\eta_8\left(\frac{2(-c+d+e)}{\sqrt{6}}\right) - \pi^+\pi^0\sqrt{2}e\right\}$$
$$+ D_s^+\left\{K^+\eta_8\frac{e}{\sqrt{2}} + K^0\pi^+e - \pi^0K^+\frac{e}{\sqrt{2}}\right\},$$

...(VI.13a)

while the contribution from the $H_{13}^3$ piece is,

$$A^{cs}(\text{charm}\to P_8 P_8) = c(P_3^n P_n^3 P^1 - P_3^n P_n^1 P^3) + d(P_3^n P_n^3 P^1 + P_3^n P_n^1 P^3) + e(P^n P_n^1 P_3^3 + P^n P_n^3 P_3^1)$$
$$- D^0\left\{K^+K^-(c+d+e) + K^0\bar{K}^0(c+d) + \eta_8\eta_8\left(\frac{4(c+d)-2e}{3}\right) - \pi^0\eta_8\frac{e}{\sqrt{3}}\right\} + D^+\left\{\bar{K}^0K^+e - \pi^+\eta_8\sqrt{\frac{2}{3}}\,e\right\}$$
$$+ D_s^+\left\{K^+\pi^0\left(\frac{-c+d}{\sqrt{2}}\right) + K^+\eta_8\left(\frac{c-d-4e}{\sqrt{6}}\right) + K^0\pi^+(-c+d)\right\}.$$

...(VI.13b)

The Cabibbo-suppressed amplitude involving a singlet and octet has the general form,

$$A^{cs}(\text{charm}\to P_0 P_8) = P_0\{a(P_3^1P^3 - P_3^3P^1) + b(P_3^1P^3 + P_3^3P^1)\} - P_0\{a(P_2^1P^2 - P_2^2P^1) + b(P_2^1P^2 + P_2^2P^1)\}$$
$$- \sqrt{\frac{2}{3}}\left\{D_s^+K^+\eta_0(a+b) - D^+\pi^+\eta_0(a+b) + D^0\pi^0\eta_8\left(\frac{b-a}{\sqrt{2}}\right) - D^0\eta_8\eta_0\sqrt{\frac{3}{2}}(b-a)\right\}.$$

...(VI.14)

Using eqs.(VI.11-VI.14) we can evaluate the amplitudes for

**Table 19.** Un-unitarized decay amplitudes obtained from eqs. (VI.11-VI.14). We have defined A=a+b, B=a-b, C=c+d, D=c-d.

| Mode | Amplitude |
|---|---|
| Cabibbo-angle favored: | |
| $D^0 \to K^- \pi^+$ | C+e |
| $\to \bar{K}^0 \pi^0$ | $(-C+e)/\sqrt{2}$ |
| $\to \eta \bar{K}^0$ | $(e-C)\ \cos\theta_p/\sqrt{6} + 2B\ \sin\theta_p/\sqrt{6}$ |
| $\to \eta' \bar{K}^0$ | $(e-C)\ \sin\theta_p/\sqrt{6} - 2B\ \cos\theta_p/\sqrt{6}$ |
| $D^+ \to \bar{K}^0 \pi^+$ | 2e |
| $D_S^+ \to \pi^+ \pi^0$ | 0 (forbidden by isospin) |
| $\to \bar{K}^0 K^+$ | e-D |
| $\to \eta \pi^+$ | $-2(D+e)\ \cos\theta_p/\sqrt{6} - 2A\ \sin\theta_p/\sqrt{6}$ |
| $\to \eta' \pi^+$ | $-2(D+e)\ \sin\theta_p/\sqrt{6} + 2A\ \cos\theta_p/\sqrt{6}$ |
| Cabibbo-angle suppressed: multiply by $\tan\theta_C$ | |
| $D^0 \to \pi^+ \pi^-$ | C+e |
| $\to \pi^0 \pi^0$ | C-e |
| $\to K^+ K^-$ | -C-e |
| $\to K^0 \bar{K}^0$ | 0 |
| $\to \eta \pi^0$ | $(e-C)\ \cos\theta_p/\sqrt{3} - B\ \sin\theta_p/\sqrt{3}$ |
| $\to \eta' \pi^0$ | $(e-C)\ \sin\theta_p/\sqrt{3} + B\ \cos\theta_p/\sqrt{3}$ |
| $\to \eta\eta$ | $(e-C)\ \cos^2\theta_p + B\ \sin 2\theta_p$ |
| $\to \eta'\eta$ | $(e-C)\ \sin 2\theta_p/2 - B\ \cos 2\theta_p$ |
| $D^+ \to \pi^+ \pi^0$ | $-\sqrt{2}e$ |
| $\to K^+ \bar{K}^0$ | -D-e |
| $\to \eta \pi^+$ | $-2(D-2e)\ \cos\theta_p/\sqrt{6} - 2A\ \sin\theta_p/\sqrt{6}$ |
| $\to \eta' \pi^+$ | $-2(D-2e)\ \sin\theta_p/\sqrt{6} + 2A\ \cos\theta_p/\sqrt{6}$ |
| $D_S^+ \to K^+ \pi^0$ | $(D-e)/\sqrt{2}$ |
| $\to K^0 \pi^+$ | D+e |
| $\to K^+ \eta$ | $(5e-D)\ \cos\theta_p/\sqrt{6} + 2A\ \sin\theta_p/\sqrt{6}$ |
| $\to K^+ \eta'$ | $(5e-D)\ \sin\theta_p/\sqrt{6} - 2A\ \cos\theta_p/\sqrt{6}$ |

the decay of $D^0$, $D^+$ and $D_s^+$ into two pseudoscalar mesons. In Table 19, we have listed these amplitudes for both the Cabibbo-allowed and Cabibbo-suppressed modes.

To explore the predictions of our model we need to determine the five parameters a,b,c,d and e. We express all the decay amplitudes in terms of more convenient parameters: A=a+b, B=a-b, C=c+d, D=c-d and e. Using experimental data[5] we determine these parameters under the assumption that final state interactions simply rotate the amplitudes and not significantly change their magnitudes. In the case of modes involving only one isospin, the absolute value of the amplitudes (which determine the branching ratios) do not involve any phases. The effect of final state interactions will therefore be important only in the amplitudes involving more than one isospin state.

Thus, for example, in case of $D^0\to K^-\pi^+$, $\bar{K}^0\pi^0$ and $D^+\to\bar{K}^0\pi^+$, the unitarized amplitudes will have the form,

$$\begin{aligned} A^u(D^0\to\bar{K}^0\pi^0) &= \frac{1}{\sqrt{3}}\left(\sqrt{2}A_{3/2}^{K\pi}\, e^{i\delta_3} + A_{1/2}^{K\pi}\, e^{i\delta_1}\right) \\ A^u(D^0\to K^-\pi^+) &= \frac{1}{\sqrt{3}}\left(A_{3/2}^{K\pi}\, e^{i\delta_3} - \sqrt{2}A_{1/2}^{K\pi}\, e^{i\delta_3}\right) \qquad \text{(VI.15)} \\ A^u(D^+\to\bar{K}^0\pi^+) &= \sqrt{3}A_{3/2}^{K\pi}\, e^{i\delta_3}\ . \end{aligned}$$

Using the un-unitarized amplitudes for these modes given in Table 19, the unitarized amplitudes are given by,

$$\begin{aligned} A^u(D^0\to\bar{K}^0\pi^0) &= \frac{2\sqrt{2}e}{3}\, e^{i\delta_3} - \frac{(3C+e)}{3\sqrt{2}}\, e^{i\delta_1} \\ A^u(D^0\to K^-\pi^+) &= \frac{2e}{3}\, e^{i\delta_3} + \frac{(3C+e)}{3}\, e^{i\delta_3} \qquad \text{(VI.16)} \\ A^u(D^+\to\bar{K}^0\pi^+) &= 2e\, e^{i\delta_3}\ . \end{aligned}$$

The parameter e can be determined directly from the

$B(D^+\to\bar{K}^0\pi^+)$. To evaluate C, we proceed as follows. First we note that,

$$\left|\frac{A^u_{1/2}}{A^u_{3/2}}\right| = |R\, e^{i\delta}| = R \qquad \text{(VI.17)}$$

where $\delta=(\delta_1-\delta_3)$. R and $\delta$ can therefore be determined using the experimental branching ratios and have the values,[6]

$$R=3.67\pm0.27 \text{ and } \delta=(103\pm11)^\circ \qquad \text{(VI.18)}$$

or $$R=-(3.67\pm0.27) \text{ and } \delta=(77\pm11)^\circ.$$

Either choice of R and $\delta$ would fit $D\to K\pi$ data, but the two solutions have different implications on the other two body modes. Also, since

$$R = \left|\frac{A^u_{1/2}}{A^u_{3/2}}\right| = \frac{A^o_{1/2}}{A^o_{3/2}} = \frac{(-C+e) - 2(C+e)}{\sqrt{2}(C+e) + \sqrt{2}(-C+e)} \qquad \text{(VI.19)}$$

we have the relation

$$C/e = -(2\sqrt{2}\ R+1)/3 \qquad \text{(VI.20)}$$

Knowing C and e, the branching ratios $B(D^0\to\bar{K}^0\eta)$ and $B(D_s^+\to\bar{K}^0K^+)$ are used to determine B and D respectively. The parameter A is then varied to predict all other branching ratios. From the parameter set we select only those solutions that are consistent with sextet dominance, i.e., those solutions which give (a+b) and (a-b) of the same sign and so also (c+d) and (c-d). We further restricted the parameter set by requiring that the calculated values of $B(D^0\to\eta'\bar{K}^0)$ satisfies the limit given by the data.[5] We use $\theta_p=-19^\circ$. The parameter A is also required to satisfy the experimental data[31,32] on $B(D_s^+\to\eta\pi^+)$ and $B(D_s^+\to\eta'\pi^+)$.

In Table 20 , we give the predictions corresponding to

**Table 20.** Solution sets for |A|, |B|, |C|, |D| and |e| satisfying selection criteria (see text) in units of $10^{-6}$GeV and Branching ratios in percent. Mark III limits: $B(D_s^+\to\eta\pi^+)<2.5B(D_s^+\to\phi\pi^+)$ and $B(D_s^+\to\eta'\pi^+)<1.9B(D_s^+\to\phi\pi^+)$ are used to restrict the parameter |A|.

| | $B(D_s^+\to\phi\pi^+)=3.5\pm0.5$ | | $B(D_s^+\to\phi\pi^+)=2.0\pm1.0$ | | |
|---|---|---|---|---|---|
| | Set I | Set II | Set I | Set II | |
| \|A\| | <3.00 | <4.00 | <2.00 | <3.00 | |
| \|B\| | 4.08±1.52 | 1.30±1.55 | 4.08±1.52 | 1.30±1.55 | |
| \|C\| | 2.24±0.36 | 2.72±0.42 | 2.24±0.36 | 2.72±0.42 | |
| \|D\| | 3.09±0.52 | 1.66±0.52 | 2.51±0.59 | 1.08±0.59 | |
| \|e\| | 0.72±0.10 | 0.72±0.10 | 0.72±0.10 | 0.72±0.10 | |
| Mode | Branching ratio | | | | Data |
| $D^0\to\bar{K}^0\eta$ | 1.60±0.72 | 1.60±0.72 | 1.60±0.72 | 1.60±0.72 | input |
| $D^0\to\bar{K}^0\eta'$ | 3.64±2.90 | 0.13±0.55 | 3.64±2.90 | 0.13±0.55 | <2.7 |
| $D^0\to\eta\pi^0$ | $<1.69\times10^{-3}$ | .089±.041 | $<1.69\times10^{-3}$ | .089±.041 | <0.9 |
| $D^0\to\eta'\pi^0$ | 0.17±0.11 | <0.11 | 0.17±0.11 | <0.11 | |
| $D^0\to\eta\eta$ | 0.45±0.23 | 0.45±0.23 | 0.45±0.23 | 0.45±0.23 | <1.2 |
| $D^0\to\eta'\eta$ | 0.19±0.16 | $<1.88\times10^{-3}$ | 0.19±0.16 | $<1.88\times10^{-3}$ | |
| $D^+\to\eta\pi^+$ | <0.22 | <0.64 | <0.12 | <0.46 | |
| $D^+\to\eta'\pi^+$ | <0.52 | <1.07 | <0.26 | <0.65 | |
| $D_s^+\to\bar{K}^0K^+$ | 3.22±1.40 | 3.22±1.40 | 1.84±1.19 | 1.84±1.19 | input |
| $D_s^+\to\eta K^+$ | $<2.13\times10^{-3}$ | <0.33 | <0.01 | <0.25 | |
| $D_s^+\to\eta'K^+$ | <0.13 | <0.13 | <0.07 | <0.07 | |

the limits on $B(D_s^+\to\eta\pi^+)$ and $B(D_s^+\to\eta'\pi^+)$ given by Mark III.[31] We find two sets of solutions. The parameters obtained in set I exhibit nonet symmetry breaking (|a|>|c|,|b|>|d|),

while those in set II show approximate nonet symmetry. We have done the calculations using both $B(D_s^+ \to \phi\pi^+) = 3.5\%$ (ref.6)

**Table 21.** Solution sets for |A|, |B|, |C|, |D| and |e| satisfying selection criteria (see text) in units of $10^{-6}$GeV and Branching ratios in percent. Mark II values $B(D_s^+ \to \eta\pi^+) = (3.0\pm1.1)B(D_s^+ \to \phi\pi^+)$ and $B(D_s^+ \to \eta\pi^+) = (4.8\pm2.1)B(D_s^+ \to \phi\pi^+)$ are used to restrict the parameter |A|.

| | $B(D_s^+ \to \phi\pi^+) = 2.0\pm1.0$ | | |
|---|---|---|---|
| | Set I | Set II | |
| \|A\| | 2.00-3.50 | 7.00-7.25 | |
| \|B\| | 4.08±1.52 | 1.30±1.55 | |
| \|C\| | 2.24±0.36 | 2.72±0.42 | |
| \|D\| | 2.51±0.59 | 1.08±0.59 | |
| \|e\| | 0.72±0.10 | 0.72±0.10 | |
| Mode | Branching ratio | | Data |
| $D^0 \to \bar{K}^0\eta$ | 1.60±0.72 | 1.60±0.72 | input |
| $D^0 \to \bar{K}^0\eta'$ | 3.64±2.90 | 0.13±0.55 | <2.7 |
| $D^0 \to \eta\pi^0$ | $<1.69\times10^{-3}$ | .089±.041 | <0.9 |
| $D^0 \to \eta'\pi^0$ | 0.17±0.11 | <0.11 | |
| $D^0 \to \eta\eta$ | 0.45±0.23 | 0.45±0.23 | <1.2 |
| $D^0 \to \eta'\eta$ | 0.19±0.16 | $<1.88\times10^{-3}$ | |
| $D^+ \to \eta\pi^+$ | 0.00-0.03 | 0.00-0.007 | |
| $D^+ \to \eta'\pi^+$ | 0.18-0.65 | 2.29-2.71 | |
| $D_s^+ \to \bar{K}^0K^+$ | 1.84±1.19 | 1.84±1.19 | input |
| $D_s^+ \to \eta K^+$ | 0.00-0.02 | 0.34-0.48 | |
| $D_s^+ \to \eta' K^+$ | 0.06-0.20 | 0.51-0.60 | |

and the new $B(D_s^+ \to \phi\pi^+)=2\%$ observed by CLEO.[5] Since Mark III[31] only provides upper limits on $B(D_s^+ \to \eta\pi^+)$ and $B(D_s^+ \to \eta'\pi^+)$, the parameter A is allowed to have a wide range. We plot $B(D_s^+ \to \eta\pi^+)$ vs $B(D_s^+ \to \eta'\pi^+)$, in Figs. 13(a) and (b), for the two sets of solutions obtained. Once either branching ratio is known, the other can be read off from this plot. We find no solutions corresponding to Mark II data[32] with $B(D_s^+ \to \phi\pi^+)=3.5\%$. Solutions to Mark II data with $B(D_s^+ \to \phi\pi^+)=2.0\%$ are given in Table 21. Here both the solutions sets exhibit nonet symmetry breaking.

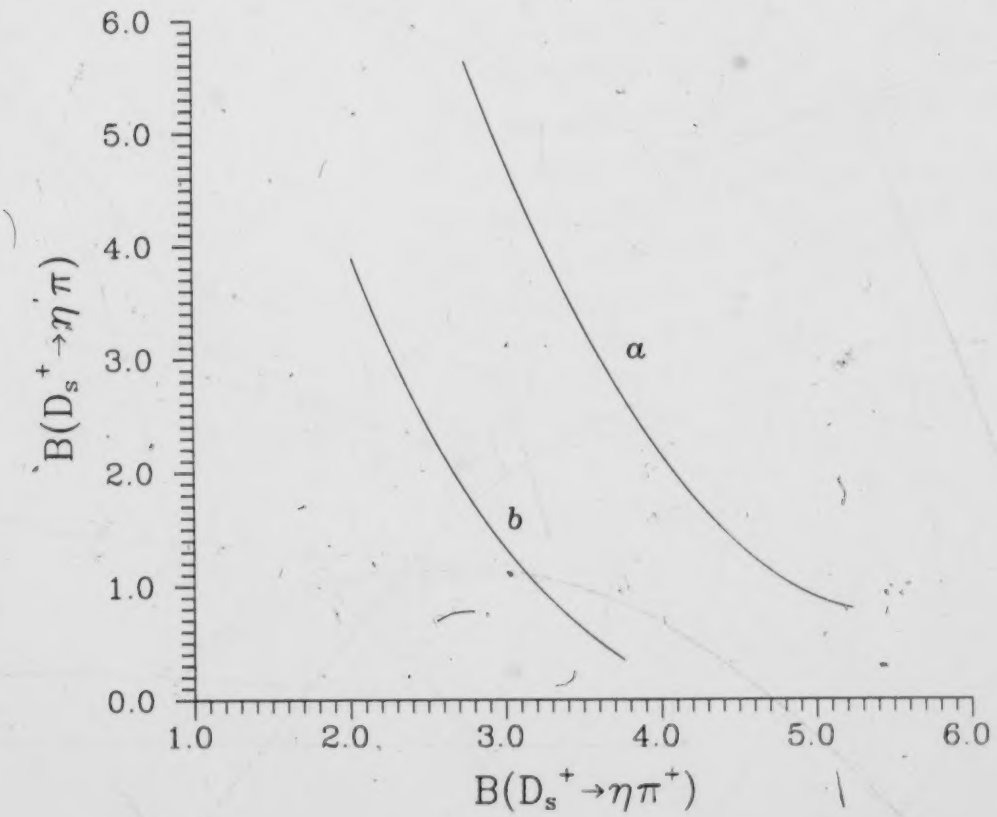


**Fig. 13(a)** $B(D_s^+ \to \eta'\pi^+)$ vs. $B(D_s^+ \to \eta\pi^+)$ for solution set I satisfying Mark III data. Curve *a* corresponds to $B(D_s^+ \to \phi\pi^+)$ $=(3.5\pm0.5)\%$ while the cuve *b* is for $B(D_s^+ \to \phi\pi^+) = (2.0\pm1.0)\%$

From Tables 20 & 21, we see that the theoretical predictions for $D^0 \to \eta\eta$ and $D^0 \to \eta\pi^0$ satisfy the experimental limits.[84] We predict branching ratios for only those modes that involve a single isospin in the final state. The rates for $D^0 \to \pi^+\pi^-$ and $D^0 \to K^+K^-$ depend[21] strongly on the interference between the two isospin amplitudes involved.

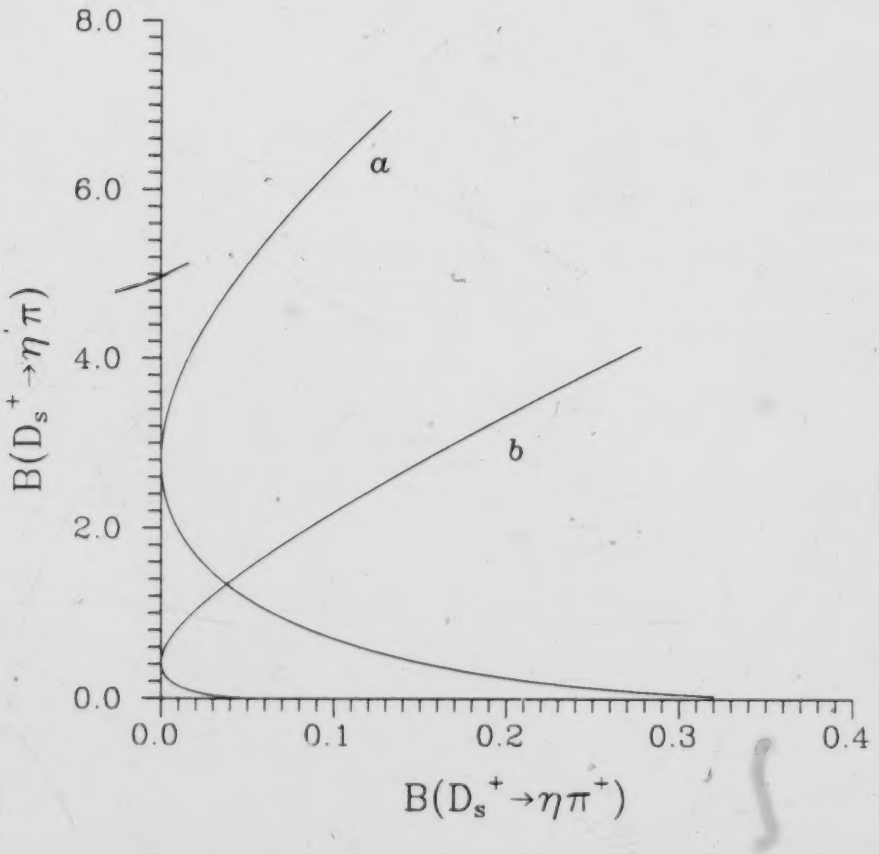


**Fig. 13(b)** $B(D_s^+ \to \eta'\pi^+)$ vs. $B(D_s^+ \to \eta\pi^+)$ for solution set II satisfying Mark III data. Curve *a* corresponds to $B(D_s^+ \to \phi\pi^+) = (3.5 \pm 0.5)\%$ while the cuve *b* is for $B(D_s^+ \to \phi\pi^+) = (2.0 \pm 1.0)\%$

We would like to point out that the nonet-symmetry breaking is equivalent to the inclusion of hairpin contri-

butions.[86] These diagrams are OZI suppressed and are nonleading in $1/N_c$ and have the property that they contribute only to decays with a meson containing an SU(3) flavor singlet component, hence breaking the nonet symmetry. In the absence of hairpin contributions, Chau and Cheng predict,[86]

$$B(D_s^+ \to \eta' \pi^+) \sim 1\% \ , \quad B(D_s \to \bar{K}^0 \eta') \sim 1\% .$$

Any deviation from this prediction is a signal of the importance of hairpin contributions in $D_s \to PP$ decays, in their model. (They had a second solution set $B(D_s^+ \to \eta' \pi^+) \sim 0.2\%$, $B(D_s \to \bar{K}^0 \eta') \sim 7\%$, which has already been ruled out by the data.)

In conclusion the results of this and the previous section may be summarized as follows. In a factorization approach large $B(D_s^+ \to \eta\pi^+)$ and $B(D_s^+ \to \eta'\pi^+)$ cannot be explained in a orthogonal $\eta$-$\eta'$ mixing scheme. A gluonium content in $\eta'$ could enhance the $B(D_s^+ \to \eta'\pi^+)$ significantly. A nonet symmetry breaking model can accommodate both $B(D_s^+ \to \eta\pi^+)$ and $B(D_s^+ \to \eta'\pi^+)$ as measured by Mark II, only with the restriction $B(D_s^+ \to \phi\pi^+) = 2\%$. The solutions here depict larger couplings to the singlet as compared to the octet.

## VII. FINAL STATE INTERACTIONS IN TWO-BODY B DECAYS

The next heavy flavor beyond charm is bottom. The decays of the bottom mesons should be simpler to understand due to the heavier b quark mass, as nonperturbative effects would be less important. There is much less experimental data available for exclusive B-meson decays, than that for the charmed mesons. However, both ARGUS[47] and CLEO[47] have reconstructed a small sample of exclusive decays, which allows us a preliminary glimpse into the weak decays of the b quark system.

The decays of B mesons arise largely from b→c transitions, yielding final states containing $D^0$, $D^+$, their vector partners and charmonium $J/\psi$. The $D_s$ fraction is expected to be small, since it's spectator amplitude depends on the KM matrix elements $|V_{cb}||V_{us}|$. B decays to non-charmed and non-strange states are of great interest since they involve the mixing angle $|V_{ub}|$, and hence could be used to estimate this unknown parameter.

Although B mesons lie much beyond the resonance region, nonresonant final state scattering could still be present. One would like to estimate the effect of these final state interactions. Of particular interest here, is the effect of final state interactions in the two body modes $\pi\pi$ and $\rho\pi$. Any theoretical uncertainties in the amplitudes for these modes will be reflected in the value of $|V_{ub}|$ extracted from

them.

**VII.1** Phases from isospin relations

We consider the dominant PP and PV decay modes: $B\to D\pi$, $D\rho$, $D^*\pi$. Each of them involve two isospin amplitudes. We introduce a phase in each of the isospin states. The known experimental branching ratios (or limits on branching ratios) are then used to check if at all, any nonvanishing phases in the amplitudes are allowed by the data. In this section, our procedure is independent of any other theoretical uncertainties in the un-unitarized amplitudes themselves. The ratios of two decay modes in any channel ($R_{00}$, $R_{0-}$) defined below, depend only on the ratio (r) of the two isospin (un-unitarized) amplitudes and on the phase difference ($\delta$) between them. We plot the ratios $R_{00}$ and $R_{0-}$ as a function of r for various $\delta$ values. (A similar procedure was followed in section V.2)

The unitarized amplitudes for the $D\pi$ states may be written as,

$$\begin{aligned} A^u(\bar{B}^0\to D^0\pi^0) &= \frac{1}{\sqrt{3}}\left(\sqrt{2}A^{D\pi}_{3/2}e^{i\delta_3} - A^{D\pi}_{1/2}e^{i\delta_1}\right) \\ A^u(\bar{B}^0\to D^+\pi^-) &= \frac{1}{\sqrt{3}}\left(A^{D\pi}_{3/2}e^{i\delta_3} + \sqrt{2}A^{D\pi}_{1/2}e^{i\delta_3}\right) \qquad \text{(VII.1)} \\ A^u(B^-\to D^0\pi^-) &= \sqrt{3}A^{D\pi}_{3/2}\,e^{i\delta_3}\,. \end{aligned}$$

Hence we have,

$$R_{00}(D\pi) = \frac{\Gamma(\bar{B}^0\to D^0\pi^0)}{\Gamma(\bar{B}^0\to D^+\pi^-)} = \frac{2(r^{D\pi})^2+1-2\sqrt{2}\,r^{D\pi}\cos\delta^{D\pi}}{(r^{D\pi})^2+2+2\sqrt{2}\,r^{D\pi}\cos\delta^{D\pi}}$$

and (VII.2)

$$R_{0^-}(D\pi) = \frac{\Gamma(\bar{B}^0 \to D^+\pi^-)}{\Gamma(B^- \to D^0\pi^-)} = \frac{1}{(3r^{D\pi})^2}[(r^{D\pi})^2 + 2 + 2\sqrt{2}\, r^{D\pi}\cos\delta^{D\pi}],$$

where, $r^{D\pi} = A^{D\pi}_{3/2}/A^{D\pi}_{1/2}$ and $\delta^{D\pi} = \delta_3 - \delta_1$. [8]

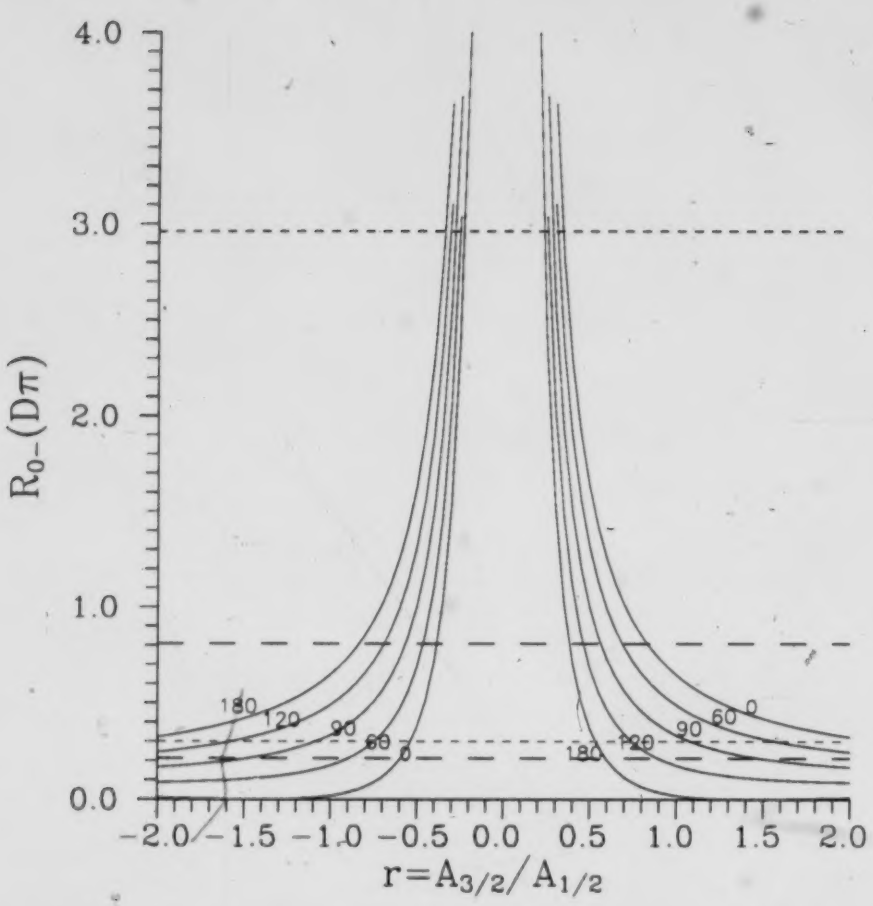


**Fig. 14(a)** $R_{0^-}(D\pi)$ vs. $r^{D\pi}$ . The short dashed lines indicate limits from ARGUS data, while the long dashed lines correspond to the CLEO limits

The experimental branching ratios for the $D\pi$ modes imply that,

$$R_{0^-}(D\pi) = \frac{B(\bar{B}^0 \to D^+\pi^-)}{B(B^- \to D^0\pi^-)} = 1.632 \pm 1.331 \quad \text{ARGUS data}^{87}$$

$$= 0.511 \pm 0.298 \quad \text{CLEO data}^{47},$$

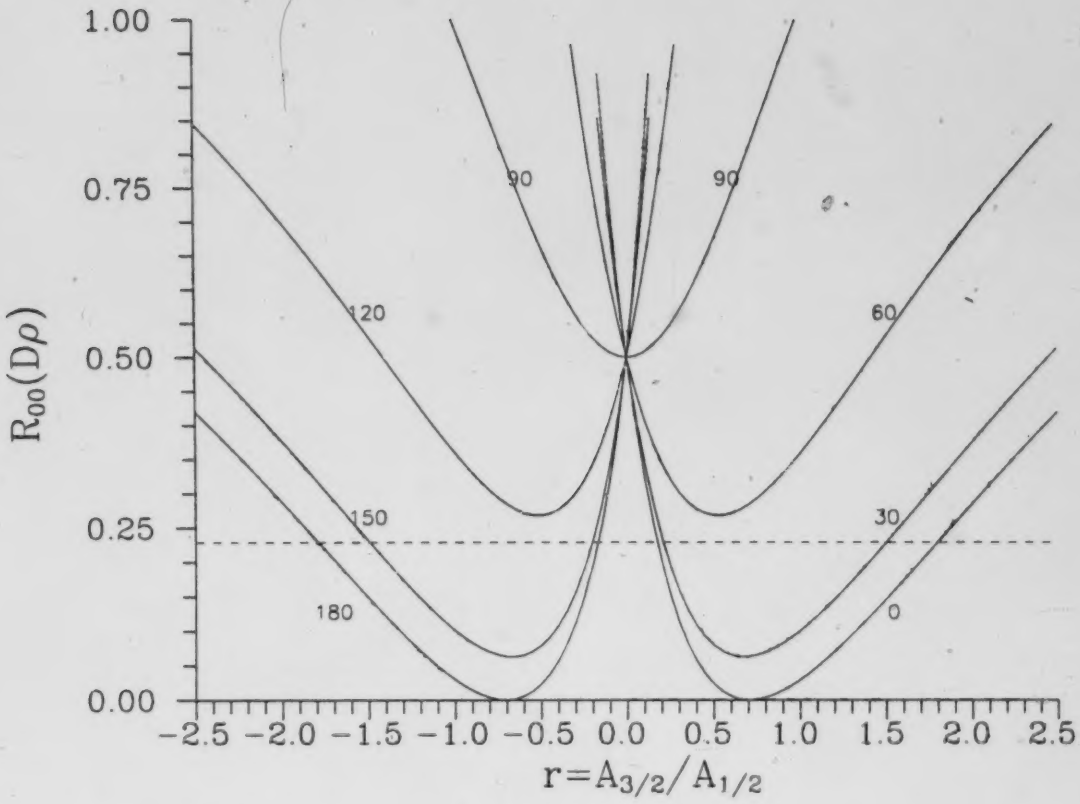


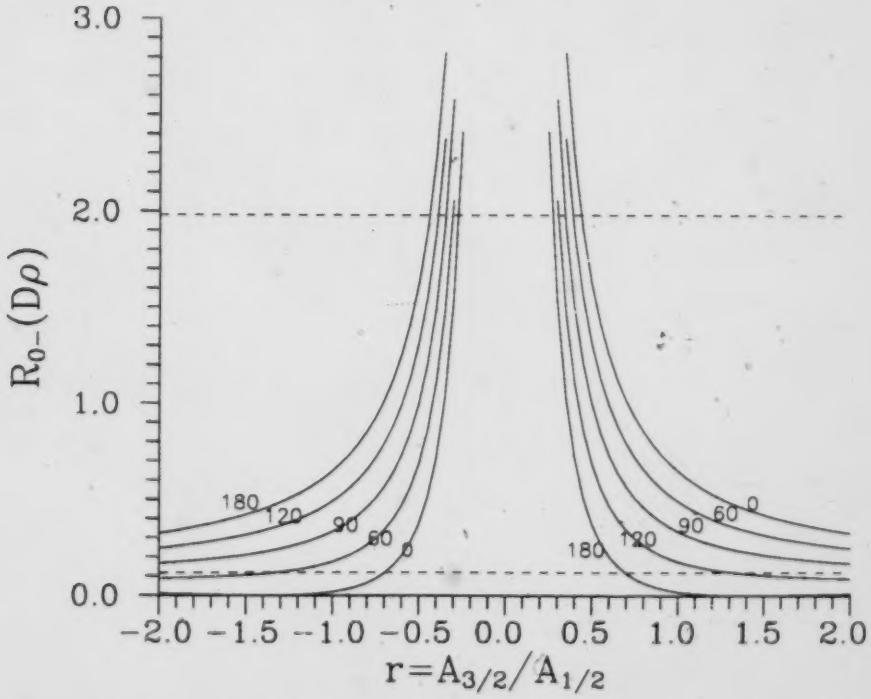


**Figs. 14(b)** and **(c)** $R_{00}(D\rho)$ and $R_{0-}(D\rho)$ vs. $r^{D\rho}$. The dashed lines indicate limits from ARGUS data.

while $R_{00}$ is unknown. The plot in Fig.14(a), indicates that the data so far allows all values ($0^\circ$-$180^\circ$) for the phase $\delta$. A measurement of $B(\bar{B}^0 \to D^0\pi^0)$ would help in restricting this phase.

Relations similar to eqs.(VII.1) and (VII.2) exist for the $D\rho$ and $D^*\pi$ modes. The experimental data implies that,

$$R_{0-}(D\rho) = \frac{B(\bar{B}^0 \to D^+\rho^-)}{B(B^- \to D^0\rho^-)} = 1.048 \pm 0.932$$

and $$R_{00}(D\rho) = \frac{B(\bar{B}^0 \to D^0\rho^0)}{B(\bar{B}^0 \to D^+\rho^-)} < 0.229 ,$$

while only the branching ratio for the $\bar{B}^0 \to D^{*+}\pi^-$ is known. From Figure 14(b) & (c), we can see that the allowed phase in the $D\rho$ amplitudes is $\sim(0^\circ$-$45^\circ)$.

As is evident from the above, there are not enough data as yet to extract a model independent conclusive evidence regarding final state interactions in the two-body B decays.

## VII.2 Theoretical amplitudes and the resulting phases

The un-unitarized amplitudes for bottom decays are generated through the following Hamiltonian,

$$\begin{aligned} H_{NL}^{eff}(\Delta b=-1) = \frac{G_F}{\sqrt{2}}\Big[ & V_{cb}V_{ud}^*\{a_1(\bar{c}b)(\bar{d}u)+a_2(\bar{c}u)(\bar{d}b)\} \\ & + V_{ub}V_{ud}^*\{a_1(\bar{u}b)(\bar{d}u)+a_2(\bar{u}u)(\bar{d}b)\} \\ & + V_{cb}V_{us}^*\{a_1(\bar{c}b)(\bar{s}u)+a_2(\bar{c}u)(\bar{s}b)\} \\ & + V_{ub}V_{us}^*\{a_1(\bar{u}b)(\bar{s}u)+a_2(\bar{u}u)(\bar{s}b)\} \\ & + V_{cb}V_{cs}^*\{a_1(\bar{c}b)(\bar{s}c)+a_2(\bar{c}c)(\bar{s}b)\} \\ & + V_{ub}V_{cs}^*\{a_1(\bar{u}b)(\bar{s}c)+a_2(\bar{u}c)(\bar{s}b)\} \end{aligned}$$

$$+ V_{cb}V_{cd}^{*}\{a_1(\bar{c}b)(\bar{d}c)+a_2(\bar{c}c)(\bar{d}b)\}$$
$$+ V_{ub}V_{cd}^{*}\{a_1(\bar{u}b)(\bar{d}c)+a_2(\bar{u}c)(\bar{d}b)\}\Big] . \quad \ldots(VII.3)$$

where, $(\bar{q}_1 q_2)$ represent the left-handed hadronic currents. The short distance QCD correction coefficients $c_+$ and $c_-$ can be determined using an NLL formula similar to eq.(IV.28), scaled down to the bottom mass scale. The values obtained are listed in Table 22. We also tabulate the corresponding values of the parameters $a_1$ and $a_2$, for both $\xi=0$ and $\xi=1/3$.

**Table 22.** NLL values of QCD coefficients for $\mu=4.5$ GeV.

| $\Lambda$(GeV) | $c_+$ | $c_-$ | $a_1/a_2$ | | $a_2$ | |
|---|---|---|---|---|---|---|
| | | | $\xi=0$ | $\xi=1/3$ | $\xi=0$ | $\xi=1/3$ |
| $m_t$=50 GeV | | | | | | |
| 0.1 | 0.866 | 1.342 | -4.633 | 7.900 | -0.238 | 0.130 |
| 0.2 | 0.844 | 1.413 | -3.967 | 11.272 | -0.285 | 0.092 |
| 0.3 | 0.828 | 1.472 | -3.572 | 16.984 | -0.322 | 0.061 |
| $m_t$=100 GeV | | | | | | |
| 0.1 | 0.869 | 1.330 | -4.777 | 7.502 | -0.230 | 0.136 |
| 0.2 | 0.848 | 1.340 | -4.086 | 10.367 | -0.275 | 0.100 |
| 0.3 | 0.832 | 1.454 | -3.676 | 14.843 | -0.311 | 0.070 |

To estimate $\xi$, $a_1$ and $a_2$ are determined using the observed branching ratios for the decay modes, $B^- \to \psi K^-$ and $B^- \to D^0\pi^-$. We do not expect these modes to have any appreciable final state interaction effects, since these amplitudes involve only one isospin state. Also, annihilation diagrams if present, will not contribute to these modes. The amplitude for $B^- \to \psi K^-$ depends only on the parameter $a_2$, while $B^- \to D^0\pi^-$ involves both $a_1$ and $a_2$. The un-unitarized amplitude

for $B^- \to \psi K^-$ is given by (using eq.(IV.20)),

$$A(B^- \to J/\psi K^-) = \frac{G_F}{\sqrt{2}} V_{cb}V_{cs}^* a_2 \langle J/\psi|\bar{c}c|0\rangle\langle K^-|\bar{s}b|B^-\rangle$$

$$= \frac{G_F}{\sqrt{2}} V_{cb}V_{cs}^* a_2 f_\psi m_\psi^2 \frac{h_{F1}(B\to K)}{1-m_\psi^2/m_{1^-}^2},$$

which yields the decay rate,

$$\Gamma(B^- \to J/\psi K^-) = a_2^2\ (0.8503\times 10^{10})\,\text{sec}^{-1}.$$

Since $B(B^- \to \psi K^-) = (0.07\pm 0.02)\times 10^{-2}$, we have,

$$a_2 = \pm\ (0.287\pm 0.041)\times 10^{-6}\ \text{sec}^{1/2}\ \tau_B^{-1/2} \qquad \text{(VII.4)}$$

$$= \pm\ (0.264\pm 0.025).$$

We shall use this value of $a_2$, to determine $a_1/a_2$ from the mode $B^- \to D^0\pi^-$. The amplitude for this mode is given by,

$$A(B^- \to D^0\pi^-) = \frac{G_F}{\sqrt{2}} V_{cb}V_{ud}^* \{a_1\langle\pi^-|\bar{d}u|0\rangle\langle D^0|\bar{c}b|B^-\rangle$$

$$+ a_2\langle D^0|\bar{c}u|0\rangle\langle\pi^-|\bar{d}b|B^-\rangle\}$$

$$= \frac{G_F}{\sqrt{2}} V_{cb}V_{ud}^* \left\{a_1(-if_\pi)(m_B^2-m_D^2)\frac{h_{F0}(B\to D)}{1-m_\pi^2/m_{0^+}^2}\right.$$

$$\left. + a_2(-if_D)(m_B^2-m_\pi^2)\frac{h_{F0}(B\to\pi)}{1-m_D^2/m_{0^+}^2}\right\}. \qquad \text{(VII.5)}$$

This gives, $\Gamma(B^- \to D^0\pi^-) = 0.395\times 10^{10} a_2^2 (a_1/a_2+0.75)^2\,\text{sec}^{-1}$. Using eq.(VII.4) and equating the calculated branching ratio of the above mode to the experimental value, we get the following for $a_1/a_2$,

$a_1/a_2 = -(4.552\pm 0.876)$ or $(3.052\pm 0.876)$ CLEO data,[47]

$a_1/a_2 = -(3.167\pm 1.029)$ or $(1.667\pm 1.029)$ ARGUS data.[47] (VII.6)

Note that the negative values of the ratio $a_1/a_2$ and $a_2$ (in eqs.(VII.4 and VII.6)), satisfying both CLEO and ARGUS data are consistent with the NLL calculations for $\xi=0$. Of course,

this '$\xi$=0 rule' can only be verified when the branching ratios of many more channels have been measured.

The un-unitarized amplitudes for the $D\pi$, $D\rho$, $D^*\pi$, $\pi\pi$ and $\rho\pi$ modes are (using eqs. (IV.17)-(IV.21)):

$$A(\bar{B}^0\to D^0\pi^0) = \frac{G_F}{\sqrt{2}} V_{cb}V_{ud}^* a_2 \langle D^0|\bar{c}u|0\rangle\langle\pi^0|\bar{d}b|\bar{B}^0\rangle$$
$$= \frac{G_F}{\sqrt{2}} V_{cb}V_{ud}^* a_2 \frac{(-if_D)}{\sqrt{2}}(m_B^2-m_\pi^2)\frac{h_{F0}(B\to\pi)}{1-m_D^2/m_{0^+}^2}$$

$$A(\bar{B}^0\to D^+\pi^-) = \frac{G_F}{\sqrt{2}} V_{cb}V_{ud}^* a_1 \langle\pi^-|\bar{d}u|0\rangle\langle D^+|\bar{c}b|\bar{B}^0\rangle$$
$$= \frac{G_F}{\sqrt{2}} V_{cb}V_{ud}^* a_1 (-if_\pi)(m_B^2-m_D^2)\frac{h_{F0}(B\to D)}{1-m_\pi^2/m_{0^+}^2}$$

$$A(\bar{B}^0\to D^0\rho^0) = \frac{G_F}{\sqrt{2}} V_{cb}V_{ud}^* a_2 \langle D^0|\bar{c}u|0\rangle\langle\rho^0|\bar{d}b|\bar{B}^0\rangle$$
$$= \frac{G_F}{\sqrt{2}} V_{cb}V_{ud}^* a_2 \sqrt{2}f_D m_\rho \frac{h_{A0}(B\to\rho)}{1-m_D^2/m_{0^-}^2}$$

$$A(\bar{B}^0\to D^+\rho^-) = \frac{G_F}{\sqrt{2}} V_{cb}V_{ud}^* a_1 \langle\rho^-|\bar{d}u|0\rangle\langle D^+|\bar{c}b|\bar{B}^0\rangle$$
$$= \frac{G_F}{\sqrt{2}} V_{cb}V_{ud}^* a_1 2f_\rho m_\rho \frac{h_{F1}(B\to D)}{1-m_\rho^2/m_{1^-}^2}$$

$$A(B^-\to D^0\rho^-) = \frac{G_F}{\sqrt{2}} V_{cb}V_{ud}^* \{a_1\langle\rho^-|\bar{d}u|0\rangle\langle D^0|\bar{c}b|B^-\rangle$$
$$+ a_2\langle D^0|\bar{c}u|0\rangle\langle\rho^-|\bar{d}b|B^-\rangle\}$$
$$= \frac{G_F}{\sqrt{2}} V_{cb}V_{ud}^* \left\{a_1 2f_\rho m_\rho \frac{h_{F1}(B\to D)}{1-m_\rho^2/m_{1^-}^2} + a_2 2f_D m_\rho \frac{h_{A0}(B\to\rho)}{1-m_D^2/m_{0^-}^2}\right\}$$

$$A(\bar{B}^0\to D^{*0}\pi^0) = \frac{G_F}{\sqrt{2}} V_{cb}V_{ud}^* a_2 \langle D^{*0}|\bar{c}u|0\rangle\langle\pi^0|\bar{d}b|\bar{B}^0\rangle$$
$$= \frac{G_F}{\sqrt{2}} V_{cb}V_{ud}^* a_2 \sqrt{2}f_{D^*}m_{D^*}\frac{h_{F1}(B\to\pi)}{1-m_{D^*}^2/m_{1^-}^2}$$

$$A(\bar{B}^0\to D^{*+}\rho^-) = \frac{G_F}{\sqrt{2}} V_{cb}V_{ud}^* a_1 \langle\pi^-|\bar{u}d|0\rangle\langle D^{*+}|\bar{c}b|\bar{B}^0\rangle$$

$$= \frac{G_F}{\sqrt{2}} V_{cb}V_{ud}^* a_1 2 f_\pi m_{D^*} \frac{h_{A0}(B\to D^*)}{1-m_\pi^2/m_{0^-}^2}$$

$$A(\bar{B}^0\to\pi^0\pi^0) = \frac{G_F}{\sqrt{2}} V_{ub}V_{ud}^* a_2 \langle\pi^0|\bar{u}u|0\rangle\langle\pi^0|\bar{d}b|\bar{B}^0\rangle$$

$$= \frac{G_F}{\sqrt{2}} V_{ub}V_{ud}^* a_2 \frac{(-if_\pi)}{\sqrt{2}}(m_B^2-m_\pi^2)\frac{h_{F0}(B\to\pi)}{1-m_\pi^2/m_{0^+}^2}$$

$$A(\bar{B}^0\to\pi^+\pi^-) = \frac{G_F}{\sqrt{2}} V_{ub}V_{ud}^* a_1 \langle\pi^-|\bar{d}u|0\rangle\langle\pi^+|\bar{u}b|\bar{B}^0\rangle$$

$$= \frac{G_F}{\sqrt{2}} V_{ub}V_{ud}^* a_1 (-if_\pi)(m_B^2-m_\pi^2)\frac{h_{F0}(B\to\pi)}{1-m_\pi^2/m_{0^+}^2}$$

$$A(B^-\to\pi^0\pi^-) = \frac{G_F}{\sqrt{2}} V_{ub}V_{ud}^* \{a_1\langle\pi^-|\bar{d}u|0\rangle\langle\pi^0|\bar{u}b|B^-\rangle$$

$$+ a_2\langle\pi^0|\bar{u}u|0\rangle\langle\pi^-|\bar{d}b|B^-\rangle\}$$

$$= \frac{G_F}{\sqrt{2}} V_{ub}V_{ud}^* (-if_\pi)(m_B^2-m_\pi^2)\frac{h_{F0}(B\to\pi)}{1-m_\pi^2/m_{0^+}^2}\frac{(a_1+a_2)}{\sqrt{2}}$$

$$A(\bar{B}^0\to\rho^0\pi^0) = \frac{G_F}{\sqrt{2}} V_{ub}V_{ud}^* a_2\{\langle\pi^0|\bar{u}u|0\rangle\langle\rho^0|\bar{d}b|\bar{B}^0\rangle$$

$$+ \langle\rho^0|\bar{u}u|0\rangle\langle\pi^0|\bar{d}b|\bar{B}^0\rangle\}$$

$$= \frac{G_F}{\sqrt{2}} V_{ub}V_{ud}^* a_2\left\{f_\pi m_\rho \frac{h_{A0}(B\to\rho)}{1-m_\pi^2/m_{0^-}^2} + m_\rho f_\rho \frac{h_{F1}(B\to\pi)}{1-m_\rho^2/m_{1^-}^2}\right\}$$

$$A(\bar{B}^0\to\rho^+\pi^-) = \frac{G_F}{\sqrt{2}} V_{ub}V_{ud}^* a_1 \langle\pi^-|\bar{d}u|0\rangle\langle\rho^+|\bar{u}b|\bar{B}^0\rangle$$

$$= \frac{G_F}{\sqrt{2}} V_{cb}V_{ud}^* a_1 2 f_\pi m_\rho \frac{h_{A0}(B\to\rho)}{1-m_\pi^2/m_{0^-}^2}$$

$$A(\bar{B}^0\to\rho^-\pi^+) = \frac{G_F}{\sqrt{2}} V_{ub}V_{ud}^* a_1 \langle\rho^-|\bar{d}u|0\rangle\langle\pi^+|\bar{u}b|\bar{B}^0\rangle$$

$$= \frac{G_F}{\sqrt{2}} V_{ub}V_{ud}^* a_1 2 f_\rho m_\rho \frac{h_{F1}(B\to\pi)}{1-m_\rho^2/m_{1^-}^2}$$

$$A(B^-\to\rho^0\pi^-) = \frac{G_F}{\sqrt{2}} V_{ub}V_{ud}^* \{a_1\langle\pi^-|\bar{d}u|0\rangle\langle\rho^0|\bar{u}b|B^-\rangle$$

$$+ a_2\langle\rho^0|\bar{u}u|0\rangle\langle\pi^-|\bar{d}b|B^-\rangle\}$$

$$= \frac{G_F}{\sqrt{2}} V_{ub}V_{ud}^{*}\sqrt{2}\left\{a_1 f_\pi m_\rho \frac{h_{A0}(B\to\rho)}{1-m_\pi^2/m_{0^-}^2} + a_2 f_\rho m_\rho \frac{h_{F1}(B\to\pi)}{1-m_\rho^2/m_{1^-}^2}\right\}$$

$$A(B^-\to\rho^-\pi^0) = \frac{G_F}{\sqrt{2}} V_{ub}V_{ud}^{*}\{a_1\langle\rho^-|\bar{d}u|0\rangle\langle\pi^0|\bar{u}b|B^-\rangle$$

$$+ a_2\langle\pi^0|\bar{u}u|0\rangle\langle\rho^-|\bar{d}b|B^-\rangle\}$$

$$= \frac{G_F}{\sqrt{2}} V_{ub}V_{ud}^{*}\sqrt{2}\left\{a_1 f_\rho m_\rho \frac{h_{F1}(B\to\pi)}{1-m_\rho^2/m_{1^-}^2} + a_2 f_\pi m_\rho \frac{h_{A0}(B\to\rho)}{1-m_\pi^2/m_{0^-}^2}\right\}. \quad \ldots(VII.7)$$

In the above we have neglected the contribution from the annihilation diagrams. These are expected[8] to be less important in B decays.

The amplitudes for the $D\pi$ modes given above are used in eq.(VII.1). The unitarized amplitudes squared, for the physical $D\pi$ modes are then given by,

$$|A^u(\bar{B}^0\to D^0\pi^0)|^2 = \frac{1}{3}\{2(A_{3/2}^{D\pi})^2+(A_{1/2}^{D\pi})^2-2\sqrt{2}A_{3/2}^{D\pi}A_{1/2}^{D\pi}\cos\delta\}$$

$$|A^u(\bar{B}^0\to D^+\pi^-)|^2 = \frac{1}{3}\{(A_{3/2}^{D\pi})^2+2(A_{1/2}^{D\pi})^2+2\sqrt{2}A_{3/2}^{D\pi}A_{1/2}^{D\pi}\cos\delta\}$$

$$|A^u(B^-\to D^0\pi^-)|^2 = 3(A_{3/2}^{D\pi})^2 \quad \ldots(VII.8)$$

with similar relations for the $D\rho$ and $D^*\pi$ modes. Note that this method is more restrictive, as individual branching ratios are used (not just the ratios); on the other hand, it depends on the theoretical amplitudes calculated. We give the resulting branching ratios for the $D\pi$, $D\rho$ and $D^*\pi$ modes in Table 23 (a), (b) and (c) respectively. The ARGUS branching ratio[87] for $B^-\to D^0\pi^-$ is not satisfied by the theoretical amplitude; note that this value is independent of the phase in the amplitude.

From Table 23, we deduce the phase values for the Dπ, Dρ and $D^*\pi$ modes, that are consistent with the data.[47] We evaluate the amplitudes for $a_1$ and $a_2$ calculated at $\mu$=4.5 GeV. The CLEO branching ratio for $\bar{B}^0 \to D^+\pi^-$ requires a phase

**Table 23(a).** Branching ratios of the Dπ modes (in %) for various phase values. The ARGUS branching ratios for these modes are, $B(\bar{B}^0 \to D^+\pi^-) = 0.31 \pm 0.16$ and $B(B^- \to D^0\pi^-) = 0.19 \pm 0.12$ while CLEO reports, $B(\bar{B}^0 \to D^+\pi^-) = 0.24 \pm 0.11$ and $B(B^- \to D^0\pi^-) = 0.47 \pm 0.17$. The three values for each phase correspond to $a_1$ and $a_2$ calculated at $\Lambda$=0.1, 0.2 and 0.3 GeV respectively.

| Phase in degrees | $B(\bar{B}^0 \to D^+\pi^-)$ | $B(\bar{B}^0 \to D^0\pi^0)$ | $B(B^- \to D^0\pi^-)$ |
|---|---|---|---|
| 0 | 0.623 | 0.014 | 0.389 |
| | 0.601 | 0.011 | 0.395 |
| | 0.575 | 0.008 | 0.404 |
| 30 | 0.590 | 0.046 | |
| | 0.569 | 0.042 | |
| | 0.544 | 0.038 | |
| 60 | 0.502 | 0.134 | |
| | 0.482 | 0.129 | |
| | 0.459 | 0.123 | |
| 90 | 0.381 | 0.255 | |
| | 0.364 | 0.248 | |
| | 0.343 | 0.239 | |
| 120 | 0.260 | 0.376 | |
| | 0.245 | 0.366 | |
| | 0.228 | 0.355 | |
| 150 | 0.172 | 0.465 | |
| | 0.158 | 0.453 | |
| | 0.143 | 0.440 | |
| 180 | 0.139 | 0.497 | |
| | 0.126 | 0.485 | |
| | 0.112 | 0.471 | |

of $\gtrsim 100^\circ$, $\sim(95^\circ\text{-}170^\circ)$ and $\sim(90^\circ\text{-}160^\circ)$, corresponding to $\Lambda$=0.1, 0.2 and 0.3 GeV respectively. The branching ratios

for the Dρ modes are consistent with the data for a phase in the approximate range (0°-55°). The ARGUS branching ratio of $B^- \to D^{*+}\pi^-$ can be satisfied for all the phases (0°-180°) at Λ=0.1 GeV, ~(0°-160°) at Λ=0.2 GeV and allows a phase of ~(0°-120°) at Λ=0.3 GeV. CLEO value for this mode can be

**Table 23(b)**, Branching ratios of the Dρ modes (in %) for various phase values. The ARGUS branching ratios for these modes are, $B(\bar{B}^0 \to D^+\rho^-) = 2.2 \pm 1.5$, $B(B^- \to D^0\rho^-) = 2.1 \pm 1.2$ and $B(\bar{B}^0 \to D^0\rho^0) < 0.3$. The three values for each phase correspond to $a_1$ and $a_2$ calculated at Λ=0.1, 0.2 and 0.3 GeV respectively.

| Phase in degrees | $B(\bar{B}^0 \to D^+\rho^-)$ | $B(\bar{B}^0 \to D^0\rho^0)$ | $B(B^- \to D^0\rho^-)$ |
|---|---|---|---|
| 0 | 1.609 | 0.007 | 1.321 |
| | 1.553 | 0.006 | 1.300 |
| | 1.486 | 0.004 | 1.278 |
| 30 | 1.518 | 0.098 | |
| | 1.464 | 0.094 | |
| | 1.401 | 0.089 | |
| 60 | 1.270 | 0.346 | |
| | 1.223 | 0.335 | |
| | 1.169 | 0.321 | |
| 90 | 0.931 | 0.685 | |
| | 0.894 | 0.664 | |
| | 0.852 | 0.639 | |
| 120 | 0.592 | 1.024 | |
| | 0.565 | 0.993 | |
| | 0.534 | 0.956 | |
| 150 | 0.343 | 1.273 | |
| | 0.324 | 1.234 | |
| | 0.302 | 1.189 | |
| 180 | 0.253 | 1.364 | |
| | 0.236 | 1.322 | |
| | 0.217 | 1.274 | |

fitted with a phase (30°-120°), at Λ=(0.1, 0.2) GeV and (0°-105°) for Λ=0.3GeV.

**Table 23(c)**. Branching ratios of the $D^*\pi$ modes (in %) for various phase values. The known ARGUS branching ratio is $B(\bar{B}^0 \to D^{*+}\pi^-) = 0.35 \pm 0.22$ while CLEO reports, $B(\bar{B}^0 \to D^{*+}\pi^-) = 0.33 \pm 0.11$. The three values for each phase correspond to $a_1$ and $a_2$ calculated at $\Lambda = 0.1$, 0.2 and 0.3 GeV respectively.

| Phase in degrees | $B(\bar{B}^0 \to D^{*+}\pi^-)$ | $B(\bar{B}^0 \to D^{*0}\pi^0)$ | $B(B^- \to D^{*0}\pi^-)$ |
|---|---|---|---|
| 0 | 0.473 | 0.020 | 0.238 |
| | 0.456 | 0.016 | 0.249 |
| | 0.437 | 0.011 | 0.263 |
| 30 | 0.450 | 0.043 | |
| | 0.433 | 0.038 | |
| | 0.414 | 0.033 | |
| 60 | 0.387 | 0.105 | |
| | 0.371 | 0.100 | |
| | 0.353 | 0.095 | |
| 90 | 0.302 | 0.191 | |
| | 0.287 | 0.185 | |
| | 0.269 | 0.178 | |
| 120 | 0.217 | 0.276 | |
| | 0.202 | 0.270 | |
| | 0.185 | 0.262 | |
| 150 | 0.154 | 0.339 | |
| | 0.140 | 0.332 | |
| | 0.124 | 0.324 | |
| 180 | 0.131 | 0.362 | |
| | 0.117 | 0.354 | |
| | 0.102 | 0.346 | |

We would like to point out that in the above calculation, we have neglected the annihilation contribution in the amplitudes, which though expected[8] to be small may not vanish. Particularly, the presence of a heavy (charm) quark in the final state could result in smaller helicity suppression. Also, in these decays, the theoretical un-unitarized amplitudes depend on the overlap between

wavefunctions of a very heavy and a light meson, errors in such a calculation may be large.[7] Hence, the large phase deduced for the $D\pi$ modes may not necessarily exist.

We apply the above procedure to the $\pi\pi$ and $\rho\pi$ modes as well. These will then be used to set limits on $|V_{ub}|$. The isospin decomposition for the $\pi\pi$ modes is given by,

$$A(\bar{B}^0\to\pi^+\pi^-) = \frac{1}{\sqrt{3}}\,(A_2^{\pi\pi} + \sqrt{2}A_0^{\pi\pi})$$

$$A(\bar{B}^0\to\pi^0\pi^0) = \frac{1}{\sqrt{3}}\,(\sqrt{2}A_2^{\pi\pi} - A_0^{\pi\pi}) \qquad \text{(VII.9)}$$

$$A(B^-\to\pi^0\pi^-) = \sqrt{\frac{3}{2}}\,A_2^{\pi\pi}\ .$$

Using the above and the un-unitarized amplitudes given in eq.(VII.7), we get the following unitarized amplitude squared,

$$|A^u(\bar{B}^0\to\pi^0\pi^0)|^2 = \frac{1}{3}\,\{2(A_2^{\pi\pi})^2 + (A_0^{\pi\pi})^2 - 2\sqrt{2}A_2^{\pi\pi}\,A_0^{\pi\pi}\cos\delta\}$$

$$|A^u(\bar{B}^0\to\pi^+\pi^-)|^2 = \frac{1}{3}\,\{(A_2^{\pi\pi})^2 + 2(A_0^{\pi\pi})^2 + 2\sqrt{2}A_2^{\pi\pi}A_0^{\pi\pi}\cos\delta\} \qquad \text{(VII.10)}$$

$$|A^u(B^-\to\pi^0\pi^-)|^2 = 3/2\,(A_2^{\pi\pi})^2\ .$$

**Table 24(a).** Upper limits for $|V_{ub}|$ and predictions for branching ratios, $B(\bar{B}^0\to\pi^0\pi^0)$ and $B(B^-\to\pi^0\pi^-)$ (in %), for various phase values using $B(\bar{B}^0\to\pi^+\pi^-)<0.9\times10^{-2}$ (%).

| Phase in degrees | $\lvert V_{ub}\rvert$ | $B(\bar{B}^0\to\pi^0\pi^0)$ | $B(B^-\to\pi^0\pi^-)$ |
|---|---|---|---|
| 0 | 0.0102 | 0.35E-03 | 0.23E-02 |
| 30 | 0.0105 | 0.83E-03 | 0.25E-02 |
| 60 | 0.0113 | 0.24E-02 | 0.28E-02 |
| 90 | 0.0128 | 0.57E-02 | 0.37E-02 |
| 120 | 0.0152 | 0.0116 | 0.51E-02 |
| 150 | 0.0181 | 0.0203 | 0.73E-02 |
| 180 | 0.0196 | 0.0256 | 0.86E-02 |

The upper limit[47] on $B(\bar{B}^0 \to \pi^+\pi^-)$, is used to obtain limits on $|V_{ub}|$. The limits on $|V_{ub}|$ obtained corresponding to the different phase values are listed in Table 24(a). We also give the predictions for the $B(\bar{B}^0 \to \pi^0\pi^0)$ for each of these phases. A measurement of this mode would be useful.

Similarly, the unitarized amplitudes for the decay modes $B^- \to \rho^0\pi^-$ and $B^- \to \rho^-\pi^0$ can be written in the form,

$$A(B^- \to \rho^0\pi^-) = \frac{1}{\sqrt{2}} \left(A_2^{\rho\pi} e^{i\delta_2^{\rho\pi}} + A_1^{\rho\pi} e^{i\delta_1^{\rho\pi}}\right)$$
$$A(B^- \to \rho^-\pi^0) = \frac{1}{\sqrt{2}} \left(A_2^{\rho\pi} e^{i\delta_2^{\rho\pi}} - A_1^{\rho\pi} e^{i\delta_1^{\rho\pi}}\right) . \qquad \text{(VII.11)}$$

**Table 24(b).** Upper limits for $|V_{ub}|$ and predictions for the branching ratio, $B(B^- \to \rho^-\pi^0)$ (in %), for various phase values using $B(B^- \to \rho^0\pi^-) < 1.5\times10^{-2}$ (%).

| Phase in degrees | $\lvert V_{ub}\rvert$ | $B(B^- \to \rho^-\pi^0)$ |
|---|---|---|
| 0 | 0.0521 | 0.235 |
| 30 | 0.0370 | 0.111 |
| 60 | 0.0241 | 0.039 |
| 90 | 0.0181 | 0.015 |
| 120 | 0.0151 | 0.583E-02 |
| 150 | 0.0136 | 0.203E-02 |
| 180 | 0.0132 | 0.096E-02 |

The unitarized amplitude for $B^- \to \rho^0\pi^-$, where the $A_2^{\rho\pi}$ and $A_1^{\rho\pi}$ are given in terms of the un-unitarized amplitudes of eq.(VII.7), is used to obtain the limit on $|V_{ub}|$. These values are listed in Table 24(b). The $\bar{B}^0 \to \rho\pi$ modes will involve three isospin states, 0,1 and 2. In the above scheme, these amplitudes would require at least one additional phase. These modes are therefore not very useful due to lack of

sufficient data.

The upper limits on $|V_{ub}|$ deduced from the $\pi\pi$ modes vary from 0.01 to 0.02, corresponding to the phase values 0° to 180°. The $B(B^- \to \rho^0 \pi^-)$ gives a larger upper limit on $|V_{ub}|$. It might be noted that the semileptonic decays of B, provide a more stringent limit on $|V_{ub}|$ at this time. In future, when more data becomes available, the effect of final state interactions and other theoretical uncertainties in the B two body nonleptonic decay modes may be resolved.

## VIII. SUMMARY AND CONCLUSIONS

Recent increase in the amount of experimental data on exclusive hadronic decays of charmed mesons has improved our understanding of the heavy quark decay mechanism. Analysis of quasi-two-body modes have stressed the importance of final state interactions in D, $D_s$ decays.

We have incorporated the effect of final state interactions in hadronic D, $D_s$ decays by performing coupled multichannel calculations. This is achieved through a **K**-matrix formalism. If a resonance of appropriate quantum numbers lies close to the decaying meson, the **K**-matrix is parameterized in the single resonance approximation. Non-resonant parameterization is used otherwise. Note that a resonance close to the D and $D_s$ mass could also provide a dynamical mechanism for enhancement of the weak annihilation amplitude, even in the absence of final state interactions. We have included weak annihilation as a parameter in the un-unitarized decay amplitudes.

In Cabibbo-allowed $D_s \to VP$ sector, we studied the modes: $D_s^+ \to \phi\pi^+$, $K^{*+}\bar{K}^0$, $K^+\bar{K}^{*0}$, $\rho\pi^+$. Isospin and G-parity considerations, reduce the coupling in these states to a pair of two coupled channel problems. In this interchannel mixing scheme, even the small branching ratio allowed for $D_s^+ \to \rho^0\pi^+$ (where only an annihilation graph exists) can be satisfied with a non-zero annihilation parameter in the amplitude. In

particular fits to E691 data were consistent with an annihilation term of the order of (15-30)% of the spectator term, although annihilation was not required by the data. ARGUS data on the other hand required a non-zero annihilation term, which was generally larger than that needed to fit E691 data. Fits were obtained for both $\xi=0$ and $\xi=1/3$. The above calculation was extended to include the $D_s^+ \to \omega\pi^+$ mode. The un-unitarized amplitude for this mode is zero. This mode could however be fed by the $K^*K$, G=+1 channel. $\omega\pi^+$ mode can be produced at the level of the experimental limit, keeping the rest of the branching ratios consistent with the data.

For Cabibbo-angle favored D→VP decays, we performed a three coupled channel calculation, where the $K^*\pi$, $K\rho$ and $\bar{K}^0\phi$ channels were coupled in I=1/2 state. In I=3/2 state only $K^*\pi$ and $K\rho$ channels were coupled. We secured some 'nearfits' to Mark III data for $\xi=0$ and $\xi=1/3$. These nearfits were obtained both with and without a weak annihilation term. Clearly it is possible to generate enough $B(D^0 \to \bar{K}^0\phi)$ without a weak annihilation term, though a finite annihilation ~(15-20)% of spectator term in $D^0 \to K^-\rho^+$ is not ruled out by data.

As for D, $D_s$→VV decays, only a few of the modes have been measured so far. These can be explained through final state interactions in our model. A coupled channel calculation for the Cabibbo-suppressed $D \to K^*K$ and $\rho\pi$ modes in isospin 1 and G-odd state was also performed. Fits to data could be obtained for both zero and non-zero annihilation. In particular the $D^+ \to \rho^0\pi^+$ branching ratio could be fitted,

whereas its un-unitarized amplitude yielded a branching ratio much below the observed value.

The other approaches to heavy flavor decays were also examined. Although quite successful in fits to data, none of these include a satisfactory treatment of final state interactions. In particular, the QCD sum rule approach, which presents a theoretical improvement, as it incorporates non-factorizable pieces of the weak amplitudes, fails to allow for final state interactions. We see the effect of final state rescattering through introduction of phases to some of the amplitudes obtained in this approach.

Surprisingly large branching ratios of the $D_s^+ \to \eta\pi^+$, $\eta'\pi^+$ were reported by Mark II. It is difficult to obtain these branching ratios in a factorization model with orthogonal mixing scheme. A nonet symmetry breaking model can accommodate large $\eta\pi^+$ and $\eta'\pi^+$ branching ratios, only for $B(D_s \to \phi\pi^+) \simeq 2\%$.

The effect of phases in the hadronic decay amplitudes of B-meson were studied as well. An estimation of the KM element $|V_{ub}|$ obtained from non-charmed and non-strange hadronic decays, could differ with such a phase in the amplitudes.

In summary, we were able to perform an effective coupled multichannel calculation to account for final state interactions in two body hadronic charm decays. Weak annihilation though not expected to be dominant, could be ~(15-30)% of the spectator amplitude, depending on the decay mode. A complete analysis of B meson decays would be possible

in the near future, when more data is available.

## REFERENCES


1. For reviews see H. Fritzsch and P. Minkowski, Phys. Rep. 73, 67 (1981);
   L. B. Okun, *Leptons and Quarks*, North Holland Amsterdam 1982.
2. S. L. Glashow, Nucl. Phys. **22**, 579 (1961);
   A. Salam and J. C. Ward, Phys. Lett. 13, 168 (1964);
   S. Weinberg, Phys. Rev. Lett 19, 1264 (1967).
3. C. Quigg, *Gauge Theories of Strong, Weak and Electromagnetic interactions*, Benjamin Cummings, 1983.
4. D. J. Gross and F. Wilczek, Phys. Rev. Lett 30, 1343 (1973); Phys. Rev. D8, 3633 (1973); D9, 980 (1974);
   H. D. Politzer, Phys. Rev. Lett. 30, 1346 (1973); Phys. Rep. 14C, 129 (1974).
5. G. Gladding, Charm decay results, Invited review talk at Int. Symp. on Heavy Quark Physics, Cornell Univ., Ithaca, N.Y. 1989.
6. D. Hitlin, in the *Proceedings of the Banff Summer School*, Banff 1988, ed. A. N. Kamal and F. C. Khanna, World Scientific, Singapore 1989.
7. I. Bigi., Nonleptonic decay models, Invited review talk at Int. Symp. on Heavy Quark Physics, Cornell Univ., Ithaca, N.Y. 1989;
   M. Wirbel, Prog. Part. and Nucl. Phys. 21, 33 (1988);
   F. Gilman, Invited talks at the Heavy Flavor Phys. Symp., Beijing, China 1988;
   M. A. Shifman, in *Proceedings of Int. Symp. on Lepton and Photon Interactions at High Energies*, Hamburg, W. Germany, ed. R. Ruckl and W. Bartel [Nucl. Phys. B, Proc. Suppl. 3 (1988)];
   A. N. Kamal, in *Proceedings of the XXIV Int. Conf. on High Energy Phys.*, Munich 1988, ed. by R. Kotthaus and J. Kuhn, Springer, Berlin 1988.
8. R. Rückl, Weak decays of heavy flavors, Habilitation-

sschrift submitted to the Univ. of Munich, CERN preprint (1983).

9. A. De Rújula, H. Georgi and S. L. Glashow, Phys. Rev. D12, 147 (1975);
N. Isgur, G. Karl, Phys. Rev. D18, 4187 (1978); *ibid*, D19, 2653 (1979);
T. Appelquist, R. M. Barnett and K. Lane, Ann. Rev. Nucl. Part. Sci. 28, 387 (1978);
E. Eichten et. al., Phys. Rev. Lett. 34, 369 (1975); Phys. Rev. D17, 3090 (1978).
10. Particle Data Group, Phys. Lett. 204B (1988).
11. M. Kobayashi and T. Maskawa, Prog. Theor. Phys. 49, 652 (1973).
12. M. K. Gaillard and B. W. Lee, Phys. Rev. Lett. 33, 108 (1974);
G. Altarelli and L. Maiani, Phys. Lett. 52B, 351 (1974).
13. G. Altarelli, G. Curci, G. Martinelli and S. Petrarca, Phys. Lett. 99B, 141 (1981); Nucl. Phys. B187, 461 (1981).
14. J. Ellis, M. K. Gaillard, B. W. Lee and J. L. Rosner, Rev. Mod. Phys. 47, 227 (1975);
J. Ellis, M. K. Gaillard and D. V. Nanopoulos, Nucl. Phys. B100, 313 (1975);
N. Cabibbo and L. Maiani, Phys. Lett. 73B, 418 (1978).
15. D. Fakirov and B. Stech, Nucl. Phys. B133, 315 (1978).
16. A. N. Kamal, Phys. Rev. D33, 1344 (1986).
17. M. Wirbel, B. Stech and M. Bauer, Z. Phys. C29, 637 (1985).
18. H. Lipkin, Phys. Rev. Lett. 44, 710 (1980);
A. N. Kamal and E. D. Cooper, Z. Phys. C8, 67 (1981).
19. C. Sorensen, Phys. Rev. D23, 2618 (1981); *ibid* 2976.
20. J. F. Donoghue, Phys. Rev. D33, 1516 (1986).
21. A. N. Kamal and R. Sinha, Phys. Rev. D36, 3510 (1987).
22. A. N. Kamal, N. Sinha and R. Sinha, Z. Phys. C41, 207 (1988); Phys. Rev. D39, 3503 (1989).
23. M. Bander, D Silverman and A. Soni, Phys. Rev. Lett. 44,

7 (1980);
H. Fritzsch and P. Minkowski, Phys. Lett. 90B, 455 (1980).

24. H. Harari, *Hadronic Interactions of Electrons and Photons*, Academic Press 1971.
25. R. Feynman, *Symmetries in Elementary Particle Physics*, Erice 1964, ed. A. Zichichi, Acamdemic Press 1965;
O. Hann and B. Stech, Nucl. Phys. B22, 488 (1970).
26. R. H. Dalitz, *Strange Particles and Strong Interactions*, Oxford Univ. Press 1962.
27. M. Bauer, B. Stech and M. Wirbel, Z. Phys. C34, 103 (1987).
28. A. J. Buras, J. M. Gérard and R. Rückl, Nucl. Phys. B268, 16 (1986).
29. B. Yu Blok and M. A. Shifman, Sov. J. Nucl. Phys. 45, 1 (1987); *ibid*, 301; *ibid*, 522.
30. Mark III Collaboration, I. E. Stockdale, Intl. Symp. on the Production and Decay of Heavy Flavors, Stanford 1987.
31. Mark III Collaboration, P. Kim, talk at Int. Symp. on Heavy Quark Physics, Cornell Univ., Ithaca, N.Y. 1989.
32. G. Wormser et. al.,Phys. Rev. Lett. 61, 1057 (1988).
33. R. S. Orr, in *Proceedings of the Second Lake Louise Winter Institute on New Frontiers in Particle Phys.*, World Scientific, Singapore 1987.
34. N. Cabibbo, Phys. Rev. Lett. 10, 531 (1963).
35. E. D. Commins and P. H. Bucksbaum, *Weak Interactions of Leptons and quarks*, Cambridge Univ. Press 1983.
36. S. M. Bilenky and B. Pontecorvo, Phys. Rep. C41, 225 (1978); see also ref.10.
37. E. S. Abers and B. W. Lee, Phys. Rep. 9C, 1 (1973).
38. G. 't Hooft, Nucl. Phys. B33, 173 (1971); B35, 167 (1971).
39. J. Goldstone, Nuovo Cim. 19, 154 (1961).
40. P. W. Higgs, Phys. Rev. Lett. 13, 508 (1964); Phys. Rev. 145, 1156 (1967).
41. S. L. Glashow, J. Iliopoulos and L. Maiani, Phys. Rev.

D2, 1285 (1970).
42. M. Fierz, Z. Phys. 104, 553 (1937).
43. K. G. Wilson, Phys. Rev. 179, 1499 (1969).
44. E. C. G. Stückelberg And A. Petermann, Helv. Phys. Acta. 26, 499 (1953);
M. Gell-Mann and F. E. Low, Phys. Rev. 95, 1300 (1954);
G. C. Callan, Phys. Rev. D2, 1541 (1970);
K. Symanzik, Comm. Math. Phys. 18, 227 (1970).
45. B. Guberina, S. Nussinov, R. D. Peccei and R. Rückl, Phys. Lett. 89B, 111 (1979);
Y. Koide, Phys. Rev. D20, 1739 (1979);
T. Kobayashi and N. Yamazaki, Prog. Theor. Phys. 65, 775 (1981).
46. K. Shizuya, Phys. Lett. 100B, 79 (1981); 105B, 406 (1981).
47. K. Schubert, B decay results, Invited review talk at Int. Symp. on Heavy Quark Physics, Cornell Univ., Ithaca, N.Y. 1989.
48. A. N. Kamal, J. Phys. G: Nucl. Phys. 12, L43 (1986).
49. M. Lusignole and A. Pugliese, Universita di Roma preprint 515 (1986);
F. Hussain and A. N. Kamal, Alberta Thy-17-86.
50. I. I. Bigi and M. Fukugita, Phys. Lett. 91B, 121 (1980).
51. N. I. Muskhelishvili. Trud. Tblin. Mat. Inst. 10, 1 (1958); *Singular integral equations*, Edited by J. Radok, Noordhoff, Groningen 1958;
R. Omnés, Nuovo Cimento 8, 316 (1958).
52. J. D. Jackson, in *Dispersion relations*, edited by G. R. Screaton, Oliver and Boyd, Edinburgh, Scotland 1961; Nuovo Cimento 34, 1644 (1964);
J. Gillespie, *Final state interactions*, Holden-Day, San Francisco, CA. 1964;
G. Barton, *Dispersion techniques in field theory*, Benjamin, New York NY. 1965.
53. Y. Iwamura, Prog. Theor. Phys. (Kyoto) 56, 1812 (1976);
Y. Iwamura, S. Kurihara and Y. Takahashi, Prog. Theor.

Phys. (Kyoto) 58, 1669 (1977);
A. N. Kamal, Can. J. Phys. 57, 1815 (1979) and references therein.

54. F. Zachariasen and C. Zemch, Phys. Rev. 128, 849 (1962).
55. J. Bjorken, Phys. Rev. Lett. 4, 473 (9160);
G. Chew and S. Mandelstam, Phys. Rev. 119, 467 (1960).
56. J. Bjorken and M. Nauenberg, Phys. Rev. 121, 1250 (1961).
57. H. J. Kreuzer and A. N. Kamal, Phys. Rev. D6, 1638 (1972).
58. L. Castillejo, R. H. Dalitz and F. J. Dyson, Phys. Rev. 101, 453 (1956).
59. R. G. Newton, *Scattering theory of waves and particles*, 2 nd ed. Berlin, Heidelberg, New York: Springer 1982.
60. M. H. Ross, G. L. Shaw, Ann. Phys. (NY) 9, 391 (1960); *ibid* 13, 147 (1961).
61. See for example R. Cahn and P. Landshoff, Nucl. Phys. B266, 451 (1986).
62. The constraint $c_+^2 c_- = 1$, is strictly valid only in the leading log approximation. In the next to leading log approximation it is violated by less than 3%. See ref. 13.
63. S. Okubo, Phys. Lett. 5, 165 (1963);
G. Zweig, CERN Report 8419/TH412 (1964) unpublished;
I. Iizuka, K. Okada, O. Shito, Prog. Theor. Phys. 35, 1061 (1966);
G. Zweig, In *Symmetries in elementary particle physics*, A. Zichichi (ed.), New York Academic Press 1965.
64. H. Albrecht et al., Phys. Lett. 153B, 343 (1985); *ibid* 179B, 398 (1986); *ibid*, 195B, 102 (1987).
65. J. Anjos et al., Phys. Rev. Lett. 60, 897 (1988).
66. L. L. Chau and H. Y. Cheng, in *Proceedings of the XXIV International Conference on High Energy Physics*, Munich, West Germany, 1988, edited by R. Kotthaus and J. Kuhn, Springer, Berlin 1988.

67. L. L. Chau, Phys. Rep. 95, 1 (1983); L. L. Chau and H. Y. Cheng, Phys. Rev. D36, 137 (1987).
68. Mark III Collaboration, G. Punkar, talk at Int. Symp. on Heavy Quark Physics, Cornell Univ., Ithaca, N.Y. 1989.
69. L. L. Chau and H. Y. Cheng, Univ. of California, Davis, Report No. UCD-88-12 (unpublished).
70. F. De Jongh, talk at Int. Symp. on Heavy Quark Physics, Cornell Univ., Ithaca, N.Y. 1989.
71. G. 't Hooft, Nucl. Phys. B72, 461 (1974); *ibid*, B75, 461 (1974).
72 M. A. Shifman, A. I. Vanshtein and V. I. Zakharov, Nucl. Phys. B147, 385 (1979); *ibid*, 488 (1979).
73. S. Okubo, Prog. Theor. Phys. 27, 949 (1962); M. Gell-Mann, Phys. Rev. 125, 1067 (1962).
74. F. J. Gilman and R. Kauffman, Phys. Rev. D36, 2761 (1987).
75. J. L. Rosner, Phys. Rev. D27, 1101 (1983).
76. A. N. Kamal N. Sinha and R. Sinha, Phys. Rev. D38, 1612 (1988).
77. A. N. Kamal and S. N. Sinha, Report No. Alberta Thy-1886 (unpublished). The method is described in ref.16.
78. Mark III Collaboration, R. M. Baltrusaitis et al., Phys. Rev. D32, 2833 (1985).
79. S. S. Pinsky, Phys. Rev. D31, 1753 (1985).
80. H. E. Haber and J. Perrier, Phys. Rev. D32, 2961 (1985).
81. Mark III Collaboration, D. Coffman et al., Report No. SLAC-PUB-4424, 1988 (unpublished).
82. A. N. Kamal N. Sinha and R. Sinha, Jou. Phy. G. 15, L63 (1989).
83. M. B. Einhorn and C. Quigg Phys. Rev. D12, 2015 (1975).
84. A. N. Kamal and R. Verma, Phys. Rev. D35, 3515 (1987).
85. Crystal Ball, R. A. Partridge, Ph.D. Thesis, California Institute of Technology (1984).
86. X. Y. Li, X. Q. Li and P. Wang, AS-ITP-87-007 (1987); X. Y. Li and S. F. Tuan, DESY preprint 83-078

(unpublished);
L. L. Chau and H. Y. Cheng, U. C. D.-88-18 (1988), in *Proceedings of the XXIV Int. Conf. on High Energy Phys.*, Munich, West Germany 1988, edited by R. Kotthaus and J. Kuhn (Springer, Berlin 1988).

87. ARGUS Collaboration, H. Albrecht et al.,Phys. Lett. B215, 424 (1988).

88. S. Gasiorowicz, *Elementary Particle Physics*, Wiley New York 1966.

89. M. Jacob and G. C. Wick, Annals Phys. 7, 404 (1959); M. L. Goldberger and K. M. Watson, *Collision Theory*, Wiley New York 1964.

## APPENDIX A

We list the values of overlap factors, pole masses and decay constants used in the estimation of un-unitarized amplitudes as given in ref.[27].

Overlap factors for D→P,V and B→P,V transitions

| Decay | $h_{F1}=h_{F0}$ | $h_V$ | $h_{A1}$ | $h_{A2}$ | $h_{A3}-h_{A0}$ |
|---|---|---|---|---|---|
| D→K | 0.762 | | | | |
| D→π | 0.692 | | | | |
| D→η | 0.681 | | | | |
| D→η′ | 0.655 | | | | |
| $D\to K^*$ | | 1.226 | 0.880 | 1.147 | 0.733 |
| D→ρ | | 1.225 | 0.775 | 0.923 | 0.669 |
| D→ω | | 1.236 | 0.772 | 0.920 | 0.669 |
| $D_s\to\eta$ | 0.723 | | | | |
| $D_s\to\eta'$ | 0.704 | | | | |
| $D_s\to K^*$ | | 1.250 | 0.717 | 0.853 | 0.634 |
| $D_s\to\phi$ | | 1.319 | 0.820 | 1.076 | 0.700 |
| B→D | 0.690 | | | | |
| B→K | 0.379 | | | | |
| B→π | 0.333 | | | | |
| B→η | 0.307 | | | | |
| B→η′ | 0.254 | | | | |
| $B\to D^*$ | | 0.705 | 0.651 | 0.686 | 0.623 |
| B→ρ | | 0.329 | 0.283 | 0.283 | 0.281 |

Values of pole masses (in GeV)

| Current | $m(0^-)$ | $m(1^-)$ | $m(0^+)$ | $m(1^+)$ |
|---|---|---|---|---|
| $\bar{d}c$ | 1.87 | 2.01 | 2.47 | 2.42 |
| $\bar{s}c$ | 1.97 | 2.11 | 2.60 | 2.53 |
| $\bar{u}b$ | 5.27 | 5.32 | 5.78 | 5.71 |
| $\bar{s}b$ | 5.38 | 5.43 | 5.89 | 5.82 |
| $\bar{c}b$ | 6.30 | 6.34 | 6.80 | 6.73 |

Values of decay constants (in MeV)

| Weak Current | Particle | $f_p$ | Weak Current | Particle | $f_v$ |
|---|---|---|---|---|---|
| $\bar{u}d$ | $\pi^-$ | 133 | $\bar{u}d$ | $\rho^-$ | 221 |
| $\bar{d}s$ | $\bar{K}^0$ | 162 | $\bar{d}s$ | $K^{-*0}$ | 221 |
| $\bar{d}d$ | $\eta$ | 68 | $\bar{d}d$ | $\omega$ | 156 |
| $\bar{s}s$ | $\eta$ | 92 | $\bar{s}s$ | $\phi$ | 233 |
| $\bar{d}d$ | $\eta'$ | 65 | $\bar{c}c$ | $J/\psi$ | 382 |
| $\bar{s}s$ | $\eta'$ | 96 | $\bar{u}c$ | $D^{*0}$ | 221 |
| $\bar{u}c$ | $D^0$ | 162 | | | |
| $\bar{s}c$ | $D_s^+$ | 162 | | | |

## APPENDIX B

In order to separate the S, P, D partial waves in the amplitudes for the decay of a pseudoscalar (I, of mass $m_I$) to two vector mesons, we first consider the helicities of the final VV states. In the center of mass frame, these final states move along the same axis but in opposite directions. We choose this to be the z-axis. The momenta of these vectors are therefore given by,

$$P_1 = (E_1, 0, 0, k) \quad \text{and} \quad P_2 = (E_2, 0, 0, -k) \qquad (B.1)$$

where $E_1$ and $E_2$ are the energies of the mesons 1 and 2 of masses $m_1$ and $m_2$ respectively. The helicity polarization vectors of meson 1 are then written as,[88]

$$\varepsilon_1^\mu(\pm 1,\ \theta=0) = \mp \frac{1}{\sqrt{2}} \begin{pmatrix} 0 \\ 1 \\ \pm i \\ 0 \end{pmatrix}, \qquad \varepsilon_1^\mu(0,\ \theta=0) = \begin{pmatrix} k/m_1 \\ 0 \\ 0 \\ E_1/m_1 \end{pmatrix}.$$

while those for the meson 2 are,

$$\varepsilon_2^\mu(\pm 1,\ \theta=\pi) = \mp \frac{1}{\sqrt{2}} \begin{pmatrix} 0 \\ -1 \\ \pm i \\ 0 \end{pmatrix}, \qquad \varepsilon_2^\mu(0,\ \theta=\pi) = \begin{pmatrix} k/m_2 \\ 0 \\ 0 \\ -E_2/m_2 \end{pmatrix}. \qquad \ldots(B.2)$$

The amplitudes in the P→VV decays involve the following type of terms:

(i) $\varepsilon_1^\mu \varepsilon_{2\mu}$, (ii) $\varepsilon_{\mu\nu\rho\sigma} \varepsilon_1^\mu\ \varepsilon_2^\nu\ P_1^\rho\ P_2^\sigma$ and (iii) $\varepsilon_1 \cdot P_2\ \varepsilon_2 \cdot (P_1 + P_I)$.

We evaluate each of these terms corresponding to different helicities of the two vector states. Using eq.(B.2), for the $\varepsilon_1^\mu \varepsilon_{2\mu}$ term we have,

$$\varepsilon_1^\mu \varepsilon_{2\mu} = 1 \qquad \text{for } \lambda_1=1,\ \lambda_2=1$$

$$= 1 \qquad \text{for } \lambda_1=-1,\ \lambda_2=-1$$

$$= \frac{k^2}{m_1 m_2} + \frac{E_1 E_2}{m_1 m_2} \qquad \text{for } \lambda_1=0,\ \lambda_2=0$$

...(B.3)

For momenta $P_1$ and $P_2$ specified by eq.(B.1), the $\varepsilon_{\mu\nu\rho\sigma}\varepsilon_1^\mu\ \varepsilon_2^\nu\ P_1^\rho\ P_2^\sigma$ term may be written as,

$$\varepsilon_{\mu\nu\rho\sigma}\varepsilon_1^\mu\ \varepsilon_2^\nu\ P_1^\rho\ P_2^\sigma = \varepsilon_{\mu\nu03}\varepsilon_1^\mu\ \varepsilon_2^\nu\ E_1(-k) + \varepsilon_{\mu\nu30}\varepsilon_1^\mu\ \varepsilon_2^\nu\ k\ E_2$$

$$= km_1(\varepsilon_1^1\ \varepsilon_2^2 - \varepsilon_1^2\ \varepsilon_2^1).$$

Hence, we have,

$$\varepsilon_{\mu\nu\rho\sigma}\varepsilon_1^\mu\ \varepsilon_2^\nu\ P_1^\rho\ P_2^\sigma = ikm_1 \qquad \text{for } \lambda_1=1,\ \lambda_2=1$$

$$= -ikm_1 \qquad \text{for } \lambda_1=-1,\ \lambda_2=-1 \qquad \text{(B.4)}$$

$$= 0 \qquad \text{for } \lambda_1=0,\ \lambda_2=0.$$

The $\varepsilon_1\cdot P_2\ \varepsilon_2\cdot(P_1+P_1)$ term in the VV amplitudes may be rewritten as,

$$\varepsilon_1\cdot P_2\ \varepsilon_2\cdot(P_1+P_1) = 2\ \varepsilon_1\cdot P_2\ \varepsilon_2\cdot P_1, \qquad \text{since, } \varepsilon_2\cdot P_2=0.$$

$$= 2\ [\varepsilon_1^0\ E_2 + \varepsilon_1^3\ k][\varepsilon_2^0\ E_1 - \varepsilon_2^3\ k],$$

which will be non-vanishing only for $\lambda_1=0$ and $\lambda_2=0$ and is given by,

$$\varepsilon_1\cdot P_2\ \varepsilon_2\cdot(P_1+P_1) = \frac{2k^2}{m_1 m_2}\ m_1^2 \qquad \lambda_1=0,\ \lambda_2=0. \qquad \text{(B.5)}$$

Using the above, for each of the terms (i), (ii) and (iii), we can determine the S, P, D partial amplitudes as follows. The states with helicities $\lambda_1$ and $\lambda_2$ can be connected to the states of definite angular momentum and spin through the following relation,[89]

$$|J,\lambda_1,\lambda_2\rangle = \sum_{L,S}\left(\frac{2L+1}{2J+1}\right)^{1/2} C\begin{matrix} S_1 & S_2 & S \\ \lambda_1 & -\lambda_2 & \lambda \end{matrix} C\begin{matrix} L & S & J \\ 0 & \lambda & \lambda \end{matrix} |JLS\rangle \qquad \text{(B.6)}$$

where, $\lambda=\lambda_1-\lambda_2$, C's denote Clebsch-Gordon coefficients. For the pseudoscalar decaying into two vectors, the final states

must have J=0; also $S_1$ and $S_2$ must be 1. The second Clebsch-Gordon coefficient in the above implies that $\lambda$ must be zero for J=0, i.e., $\lambda_1=\lambda_2$. Also, J=0 implies that L=S and since, $S=1\oplus 1$, $L=S\leq 2$. The allowed helicity states may thus be written as,

$$a)\ |J=0,\lambda_1=1,\lambda_2=1\rangle = \frac{1}{\sqrt{3}}|000\rangle - \frac{1}{\sqrt{2}}|011\rangle + \frac{1}{\sqrt{6}}|022\rangle$$

$$b)\ |J=0,\lambda_1=0,\lambda_2=0\rangle = -\frac{1}{\sqrt{3}}|000\rangle + \sqrt{\frac{2}{3}}|022\rangle$$

$$c)\ |J=0,\lambda_1=-1,\lambda_2=-1\rangle = \frac{1}{\sqrt{3}}|000\rangle + \frac{1}{\sqrt{2}}|011\rangle + \frac{1}{\sqrt{6}}|022\rangle \qquad \ldots(B.7)$$

where the |JLS> states on the RHS, in the spectroscopic notation are:

$$|000\rangle = {}^1S_0\ , \qquad |011\rangle = {}^3P_0 \quad \text{and} \quad |022\rangle = {}^5D_0.$$

Using eqs.(B.3) & (B.7), we have the following relations for the term (i):

$$\begin{aligned} \frac{1}{\sqrt{3}}A_S - \frac{1}{\sqrt{2}}A_P + \frac{1}{\sqrt{6}}A_D &= 1 \\ \frac{1}{\sqrt{3}}A_S + \frac{1}{\sqrt{2}}A_P + \frac{1}{\sqrt{6}}A_D &= 1 \qquad (B.8) \\ -\frac{1}{\sqrt{3}}A_S + \sqrt{\frac{2}{3}}A_D &= \frac{k^2}{m_1m_2} + \frac{E_1E_2}{m_1m_2}\ , \end{aligned}$$

where $A_S$, $A_P$ and $A_D$ represent the L=0, 1 and 2 partial wave amplitudes and are given by,

$$A_S = \frac{1}{\sqrt{3}}\left\{2 - \frac{E_1E_2+k^2}{m_1m_2}\right\} \quad A_P=0 \ \&\ A_D=\sqrt{\frac{2}{3}}\left\{1 + \frac{E_1E_2+k^2}{m_1m_2}\right\} \qquad (B.9)$$

For the $\varepsilon_{\mu\nu\rho\sigma}\varepsilon_1^{\mu}\,\varepsilon_2^{\nu}\,P_1^{\rho}\,P_2^{\sigma}$ term, eqs.(B.4) & (B.7) imply that,

$$A_S = A_D = 0 \text{ and } A_P = -i\sqrt{2}km_I \qquad (B.10)$$

Finally, for the term $\varepsilon_1 \cdot P_2\ \varepsilon_2 \cdot (P_1+P_I)$, eqs. (B.5) & (B.7) yield the following partial wave amplitudes,

$$A_S = -\frac{2}{\sqrt{3}}\frac{k^2}{m_1 m_2} m_I^2 , \quad A_P = 0 \quad \& \quad A_D = 2\sqrt{\frac{2}{3}}\frac{k^2}{m_1 m_2} m_I^2 . \qquad \text{(B.11)}$$

A decay amplitude of the form,

$$A_{VV}(I \to V_1 V_2) = \frac{2m_{V2} f_{V2}}{m_I + m_{V1}} \varepsilon_{\mu\nu\rho\sigma}\, \varepsilon_2^{\mu} \varepsilon_1^{\nu}\, P_I^{\rho}\, P_{V1}^{\sigma} V(q^2)$$
$$+ i m_{V2} f_{V2} \left\{ \varepsilon_1 \cdot \varepsilon_2 (m_I + m_{V1}) A_1(q^2) - \frac{\varepsilon_1 \cdot q}{(m_I + m_{V1})} (P_I + P_{V1}) \cdot \varepsilon_2 A_2(q^2) \right\}$$

may therefore be rewritten as,

$$A_{VV}(I \to V_1 V_2) = \frac{2m_{V2} f_{V2}}{m_I + m_{V1}} V(q^2)\ (-i\sqrt{2} k m_I) \qquad \leftarrow \text{P-wave}$$
$$+ i m_{V2} f_{V2} \left[ (m_I + m_{V1}) A_1(q^2) \frac{1}{\sqrt{3}} \left\{ 2 - \frac{E_1 E_2 + k^2}{m_1 m_2} \right\} \right.$$
$$\leftarrow \text{S-wave}$$
$$+ \frac{A_2(q^2)}{(m_I + m_{V1})} \frac{2}{\sqrt{3}} \frac{k^2}{m_1 m_2} m_I^2$$
$$(m_I + m_{V1}) A_1(q^2) \sqrt{\frac{2}{3}} \left\{ 1 + \frac{E_1 E_2 + k^2}{m_1 m_2} \right\}$$
$$\leftarrow \text{D-wave}$$
$$\left. - \frac{A_2(q^2)}{(m_I + m_{V1})} 2\sqrt{\frac{2}{3}} \frac{k^2}{m_1 m_2} m_I^2 \right] \qquad \ldots \text{(B.12)}$$

It may be noted that $k^2 + E_1 E_2 = P_1 \cdot P_2$.